CHALMERS TEKNISKA HÖGSKOLA

CHALMERS UNIVERSITY OF TECHNOLOGY
GÖTEBORG
SWEDEN

ON FLOCCULATION EFFICIENCY IN WATER TREATMENT

BY

CLAES HERNEBRING

Chalmers University of Technology
Department of Sanitary Engineering
Dissertation no 4
Göteborg 1981

CHALMERS UNIVERSITY OF TECHNOLOGY
Department of Sanitary Engineering
Dissertation no 4

ON FLOCCULATION EFFICIENCY IN WATER TREATMENT

by

Claes Hernebring

Göteborg 1981

To three of the Ma:s

It is awkward with an x and y
that are shining forth from many things

Nils Ferlin

TABLE OF CONTENTS

1 BACKGROUND

1.1 Introduction and scope of the study

In Sweden approximately half of the water consumed consists of surface water, which ordinary needs treatment of some kind before consumption.

The predominant treatment process is coagulation - flocculation by means of a hydrolysed metal salt, in practice almost exclusively aluminium sulphate. The yearly amount of surface water chemically treated in Sweden is about $450 \cdot 10^6$ m^3. Annual investment costs for treatment facilities can be estimated to $80 \cdot 10^6$ SEK/year. Methods to assure that these resources are used effectively are, of course, of greatest interest.

The fact that the quality of the treated water may have an impact on human health, is also a motive to ascertain the safety and effectiveness of the treatment process.

The surface waters used in Sweden are frequently only slightly affected by industrial or municipal waste water. They can be classified as low-turbidity waters, containing humic substances causing some colour.

In figure 1-1 a typical water treatment plant using chemical treatment is shown:

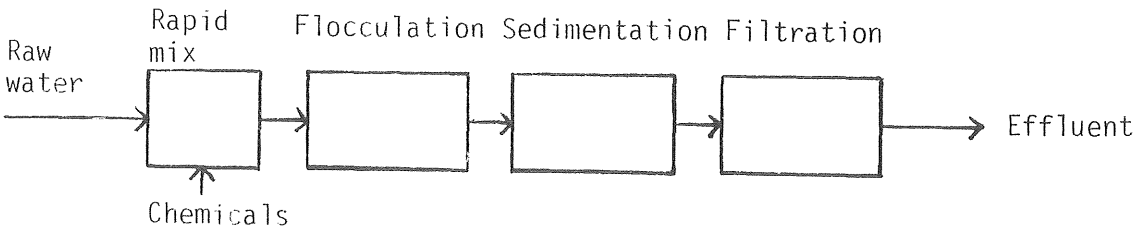

Fig 1-1. Flow diagram for a typical water treatment plant

The purpose of the treatment considered here, is to remove particulate matter in suspended or colloidal form from the raw water. A chemical (usually aluminium sulphate) is mixed into the water, forming precipitates including particles present in the raw water. Thus a separation of the raw water impurities is made possible.

There are essentially four basic units, that affect the solid-liquid separation: The mixing of chemicals into the raw water, the flocculation, the sedimentation and the filtration units. The main attention in this study is laid upon the flocculation-sedimentation processes.

The objective of this study is to provide data and procedures for an appropriate design and the optimal operation of a conventional chemical water treatment plant, particularly the flocculation operation.

The methods encountered in the literature for the estimation of the effects of various flocculation conditions on a practical sedimentation result, are limited. Numerous flocculation theories exist founded on probable flocculation mechanisms, but water plant operator have no use of them since the theories regularly cannot predict the sedimentation properties of the floc suspension. On the other hand there exist empirical relationships with that capability, however with limited theoretical sense.

This treatise is meant to be an attempt to overcome the gap between theory and practice in this respect. Firstly, a description of changes in settling properties is developed, from which it is relatively simple to make conclusions concerning the response of the practical sedimentation result to various flocculation conditions. Then a mathematical model is developed, where the particle size distribution is taken into account. Such a theory is of greatest interest as a means to understand the flocculation process and to be able to study it more systematically.

The waters studied are natural waters containing mainly humic substances, with low turbidity (little affected by industrial or municipal waste water) and used for consumption after chemical treatment. In order to avoid scale effects, most studies concerning flocculation are carried out in pilot-plant or full-scale treatment plants.

The flocculation is performed in agitated tanks. The subsequent separation steps sedimentation and filtration are studied, where sedimentation attracted most attention. Only coagulation with aluminium sulphate is considered.

Processes as adsorption and disinfection are not treated in this thesis.

1.2 Terminology

Some confusion exists about the terms "flocculation" and "coagulation", which sometimes are used synonymously, sometimes to denote different steps in describing the process of creating aggregates of particles which can easily be separated from the water.

Fiessinger (1978) presented one usual way of designating the different steps of particle aggregation (Table 1-1). The particles involved are often colloidal, resisting aggregation by their surface charge. The surface potential has to be decreased in some way (particle destabilization) before two particles can become so close that they get attached.

After destabilization, particles can come into contact by their differential motion caused by Brownian motion, velocity gradients or differential settling. The latter step is usually referred to as the particle transport step.

The reagent causing the particle destabilization is usually dissolved to form a feed solution which is dispersed and mixed into the water. In contact with water, the chemical reacts, forming products active in destabilization of particles.

In Table 1-1, the term coagulation is used for the destabilization step, and flocculation means particle collision and growth. The perikinetic flocculation is governed by molecular motion, and the orthokinetic flocculation is induced by velocity gradients in the fluid.

As an alternative terminology, the term "microflocculation" has been introduced, to characterize the step between "true" coagulation and "true" flocculation.

Table 1-1. Terminology associated with aggregation of colloidal particles. Fiessinger (1978)

<table>
<tr><th>STEPS</th><th>PHENOMENA</th><th colspan="3">TERMINOLOGY (general)</th></tr>
<tr><td>1. REAGENT FORMATION</td><td>1.1 Preparation: dissolution, ionisation, polymerisation ...</td><td colspan="3">Dilution</td></tr>
<tr><td></td><td>1.2 Introduction: dispersion, diffusion. Contact reagent-particle.</td><td colspan="3">Flash-mixing</td></tr>
<tr><td></td><td>1.3 Reaction with water: ionisation, hydrolysis, polymerisation. Formation of metal-hydroxo complexes with Al and Fe salts.</td><td colspan="3">Hydrolysis</td></tr>
<tr><td>2. PARTICLE DESTABILISATION</td><td>2.1 Compression of the electrical double layer by non hydrolysing counter ions.</td><td rowspan="4">Coagulation</td><td>Coagulation</td><td rowspan="6">Aggregation</td></tr>
<tr><td></td><td>2.2 Reduction of surface potential through chemisorption of hydrolysing metal ions or surface active substances (chemical reactions).</td><td rowspan="3">Micro flocculation</td></tr>
<tr><td></td><td>2.3 Enmeshment in a precipitate (sweep flocculation).</td></tr>
<tr><td></td><td>2.4 Interparticle bridging through specific adsorption of coagulant or flocculant (polymeric) species. Mutual aggregation.</td></tr>
<tr><td>3. PARTICLE TRANSPORT (collisions)</td><td>3.1 Brownian motion (thermal diffusion). For particles of size < 1 µm.</td><td>Perikinetic flocculation</td></tr>
<tr><td></td><td>3.2 Fluid (velocity gradients G).</td><td rowspan="2">Orthokinetic flocculation</td><td rowspan="2">Flocculation</td></tr>
<tr><td></td><td>3.3 Particles (differential) motion: e.g. settling, flotation.</td></tr>
<tr><td>4. SEPARATION</td><td>Sedimentation, flotation, filtration ...</td><td colspan="3"></td></tr>
</table>

Packham (1977) defined flocculation as "that part of the process ... in which the size of the aggregates of destabilized particles is increased as a result of some kind of agitation", which is in close agreement with the definition above. However, the term "coagulation" is used by Packham to denote the overall aggregation process.

It is also possible to find authors who use "flocculation" as a general term, Ives (1978a).

LaMer (1964) uses the terms flocculation and coagulation to distinguish between two different types of particle destabilization; coagulation for the reduction of electrostatic repulsive forces and flocculation for bridging of particles by water soluble polymers. Which one of these definitions is the most appropriate for the aggregation of colloidal matter by aluminium or iron salts in water treatment is not obvious.

The present author will adopt the view of Packham. Thus coagulation is used to denote the overall particle aggregation process, and flocculation means growth of particles by means of agitation.

2 COAGULATION

2.1 Coagulation with hydrolysed Al

Water treatment by the use of aluminium and ferric salts is a well known practice and investigations concerning the nature of the precipitation process have been carried out since the 19th century. In spite of this there do not exist adequate theories to predict treatment results. In practice one has to rely on the method known as the jar test. The lack of a consistent theory is, of course, to great extent due to the nature of impurities in the raw water, which can vary within vast limits.

A brief summary of concepts encountered in literature is given below, mainly based on reviews made by Packham (1962 a, b, 1963), Hall and Packham (1965), AWWA Committee Report (Singley *et.al.*, 1971), Fiessinger (1977, 1978), and Packham and Sheiham (1977).

2.1.1 Colloid stability

Many substances encountered in natural waters are present in the form of particles of the size of 0.005 to 0.2 µm, with the physicochemical properties characteristic for colloids. The ability of a substance (not in true solution) to remain permanently in the water, is usually in this context thought to be associated with colloid stability.

Usually a surface charge develops, caused by e.g. dissociation of functional groups on the surface or by adsorption (Lyklema, 1978). The surface charge has great significance for the stability because of the large specific surface area of the colloid particles.

In the vicinity of the colloid particle in a solution, ions with a charge opposite to the surface charge (counter ions) will accumulate to accomplish electroneutrality.

Helmholz (1879) developed a theory based on the concept of two surface charges separated by a distance, which could be treated as an electric condensor. Gouy (1910) and Chapman (1913) introduced the effect of the diffusion of counter-ions out from the surface caused by their concentration gradient. As a result a diffuse double layer is developed. Stern (1924) combined a fixed layer of counter-ions with the diffuse double layer. The mathematical treatment of these models, however, are beyond the scope of this study and reference is therefore made to the authors mentioned above.

The extent of the electric double layer is affected by the ionic-strength in the bulk of the solution, and together with the absolute value of the charge on the particle surface, it will determine the size of the repulsive forces when two particles get close to each other. In the immediate vicinity of the particle, attractive forces caused by atomic interactions, London - van der Waal forces, are predominant. The electric double layer thus causes an energy barrier to be over-come before aggregation can take place.

In an electric field the charged particle will move together with a part of the electric double layer. From electrophoretic mobility measurements (velocity of the particle per unit of field strength) property called zeta-potential can be calculated, see e.g. Riddik (1961). The zeta-potential can be interpreted as a measure of the energy barrier and the colloid stability.

O'Melia (1972) distinguished between four mechanisms to destabilize a colloid.

1 Compression of the double layer. By adding an electrolyte the ionic strength of the solution will be increased and the volume of the electric double layer will be reduced. This may cause the energy barrier resisting aggregation to diminish. Another way to compress the electric double layer is to increase the valence of the counter-ions, as expressed in the Schulze-Hardy rule for the critical concentration of coagulants.

2 Adsorption and charge neutralization. If, for example, surface active substances with a charge opposite to the surface charge is adsorbed, the primary charge can be partly or completely neutralized.

3 Enmeshment in a precipitate ("sweep coagulation"). When high concentrations of a coagulant is used causing precipitations of e.g. a metal hydroxide, the colloid particles can be absorbed into the precipitate, or even serve as precipitation nuclei. The latter effect can result in an inverse relationship between particle concentration and critical dosage of coagulant.

4 Bridging by polymers. When polymers (synthetic or metal hydrolysis products) are used for coagulation, the long polymer chains are thought to create particle aggregates by bridging between particles.

All these mechanisms of destabilization of a colloid (in addition, there are also other mechanisms proposed) are to varying extent usually considered to be effective when aluminium is used as a coagulant. For further discussion it is referred to Section 2.3.

In some cases it is possible to overdose the coagulant, thus causing the colloid to be restabilized by e.g. charge reversal.

2.1.2 Hydrolysis of aluminium

The hydrolysis of aluminium yields a variety of hydrolysis products capable of affecting the colloid stability.

The Al^{3+}-ion in aqueous solution is strongly hydrated, surrounded by six water molecules in an octahedral configuration, which may be represented as $Al(H_2O)_6^{3+}$. The hydrolysis of this ion yields the following dissociation steps, if coordinated water molecules are omitted:

$$Al^{3+} \rightleftarrows Al(OH)^{2+} \rightleftarrows Al(OH)_2^{+} \rightleftarrows Al(OH)_3 \rightleftarrows Al(OH)_4^{-} \qquad (2\text{-}1)$$

Between each step a proton is released as stated in eq (2-2)

$$Al(H_2O)_6^{3+} \rightleftarrows Al(H_2O)_5(OH)^{2+} + H^{+} \qquad (2\text{-}2)$$

The relative amount of the spieces according to eq (2-1) is depending on the pH of the solution and the various equilibrium constants. The amount of dissolved aluminium in equilibrium is governed by the solubility of aluminium hydroxide. In the range pH 6 - 7, a maximum amount of the uncharged $Al(OH)_3$ is produced, which is forming a gelatinous precipitate.

At higher and lower pH-values the precipitate may redissolve because of forming of aluminate and positively charged hydroxocomplexes, respectively. In the pH-interval 6-7 less than 10^{-6} M aluminium is dissolved; thus an analysed residual of about 0.01 mg Al^{3+}/l is to be expected. As nearly all of the added aluminium will form $Al(OH)_3$ the overall acid-base reaction can be written:

$$\begin{aligned} Al^{3+} + 3H_2O &\rightleftarrows Al(OH)_3 + 3H^+ \\ 3H^+ + 3HCO_3^- &\rightleftarrows 3H_2CO_3 \end{aligned} \qquad (2\text{-}3)$$

At the hydrolysis the H^+-ions released will be netralized as far as possible by the alkalinity. In natural waters the alkalinity almost exclusively is determined by the HCO_3^--ion. Eq (2-3) is valid as a basis for pH-calculations (by means of the carbonic acid equilibrium equations) if the alkalinity of the water is sufficient, otherwise a base has to be added.

In addition to the monomeric ions in eq (2-1), polycations as a result of polymerization like $Al_8(OH)_{20}^{4+}$ or $Al_7(OH)_{17}^{4+}$ has been proposed (Brosset, 1952, 1954, Matijevic *et.al.*, 1961). These ions are thought to be more effective in coagulation than the monomers.

Sullivan and Singley (1968), however, state that the hydrolysis of aluminium could be explained on the basis of mononuclear species.

Usually a solution of Al-sulphate is prepared before addition to the water. The concentration is often ca. 5% by weight. Fiessinger (1976, 1978) and Bersillon *et.al.* (1978) report that polymerisation in the stock Al-solution could be accomplished by adding a certain amount of OH^--ions prior to addition to the water. The coagulant achieved in this way is claimed to be more effective than a simple aluminium-sulphate solution.

Other anoins present may intervene in the polymerization process and result in different chemical properties of the precipitate. Especially phosphate is reported to lower the optimum pH-value for turbidity removal. Sulphate have the effect of broadening optimum pH-interval (Hanna and Rubin, 1970).

Baylis (1937) reported that increasing alkalinity (added as calcium carbonate, magnesium carbonate or sodium bicarbonate) decreased the necessary coagulation time and broadened the pH range over which coagulation was obtained.

Letterman *et.al.* (1979) present results of jar test concerning the influence of the initial bicarbonate ion concentration on the efficiency of turbidity removal. A marked improvement in residual turbidity was measured, from 25 to 2 FTU, as the bicarbonate ion concentration was increased from 20 to 90 mg/l. An increase in initial bicarbonate concentration from 35 to 70 mg/l permitted a decrease in the necessary alum dose for constant residual turbidity from 40 to 6 mg/l. The effects of anions as bicarbonate and sulphate were found not to be additive.

2.2 Characterization of the raw water

Natural waters contain dissolved organic and inorganic substances, colloidal matter of organic or inorganic orgin, and also coarse suspended matter. The main attention here will be given the colloidal matter and for practical purposes it is convenient to apply the definition used by Packham (1962). He distinguishes between colloidal matter causing turbidity and that giving rise to colour.

The turbidity is caused by mainly clay minerals, the colour is associated with what is usually called humic substances. The distinction is useful not only because the different origins of the colloids; the optimum conditions and mechanisms for removal have been shown to be different as well (see Section 2.3).

2.2.1 Aquatic humus

Humic substances are the dominant part of organic matter in natural waters. They consist of a complex mixture of organic compounds of natural orgin, principally from plant residues. The humic content in the water that causes a yellowish-brown colour is the water extractable fraction of soil humus, also called fulvic acid. According to Gjessing (1976) the differences in physical and chemical properties between humus in soil and humus in water are relatively small. Different fractions of the humic substances are often classified according to their solubility in acids and bases. The relevance has been discussed of differentiating between fulvic acid (soluble both in acids and in basis) or humic acid (soluble in bases but not in acids). The humic substances are acid, with a molecule weight of 10^2-10^5 (Pierrou, 1977).

The precise molecular constitution is uncertain. Available evidence suggest that humic substances are formed in the soil by polymerization of phenolic units derived from bacterial synthesis or breakdown of lignin. E.g. alcoholic OH, phenolic OH, carboxylic acid and quinonoid groupings have been domonstrated (Hall and Packham, 1965, Gjessing, 1976).

Humic and fulvic acids are considered to be harmless, from public health point of view. However, they are able to form stable complexes with heavy metals and can adsorb pesticides. Chlorination is shown to form chlorinated by-products, a numerous amount of compounds has been detected, e.g. chloroform (Rook, 1974).

2.2.2 Analytical methods

The methods briefly described here are simple and common in water treatment practice. For more extensive description of analytical methods see Gjessing (1976).

Because of the complicated structure of the humic substances the analytical methods for quantitative determination are unspecific, a summary measure is obtained, maybe reflecting different constituents to varying extent.

Colour

Colour determination can be made with a comparator, where the colour of the water is compared to solutions of colour forming substances of known concentration. The reference solution for the colour determination is a platinum cobalt chloride solution. A photometer can be used for absorbance measurements at a specific wavelength. The platinum cobolt solution has an absorbance maximum near 430 nm.

Colour measurements reported later in this chapter were carried out at the wavelength 436 nm. The results are given as the absorbance with a 4 cm cell. The relation between the absorbance reading and the unit mg Pt/l was found to be

$$E_{436}^{4\ cm} \cdot 1.2 \cdot 10^{3} = \quad \text{mg Pt/l} \qquad (2\text{-}4)$$

where $E_{436}^{4\ cm}$ is absorbance at 436 nm, 4 cm cell.

Unfortunately the absorbance of visible light is greatly affected by the turbidity of the samples. Even after filtering the samples, the turbidity could vary to a great extent. A rough indication of the influence of turbidity was obtained by mixing turbidity and colour standard solutions and simultaneously recording the turbidity and the absorbance. The solutions were prepared according to Swedish Standards, a platinum cobalt chloride solution and a standard formazin turbidity solution, respectively. In the mixtures the colour ranged from 0-100 mg Pt/l and the turbidity from 0-10 FTU. The expression in eq (2-5) was found to approximate the obtained result rather well:

$$\Delta E_{436}^{4\ cm} = \Delta FTU \cdot 1.3 \cdot 10^{-2} \qquad (2\text{-}5)$$

where $\Delta E_{436}^{4\ cm}$ is the difference in absorbance measurement caused by the change ΔFTU (formazin turbidity units) of turbidity.

Permanganate number

Traditionally in Europe, oxidation with potassium permanganate (heating under acid conditions) has been used as a quantitative method. This method will be denoted COD_{Mn} and results given in mg reduced $KMnO_4$ per litre. The oxidation of the organic content hereby, is not complete. Gjessing (1976) reports that not more than 30-35% of the humic substances is converted to CO_2. Though questionable for that reason, the method has been used since the 19th century, and is still used as a routine analysis.

UV-absorbance

Humic substances have no observable absorption maximum neither in the visible nor in the UV-range. Nevertheless absorption measurements around the wavelength 250-260 nm have been shown to be useful as a measure of the content of humic substance (e.g. Schilling, 1975). Dobbs *et.al.* (1972) have reported useful correlation between ultraviolet absorbance (at 254 nm) and TOC for numerous aqueous systems. Dobbs also studied the influence of turbidity. A relationship according to eq (2-6) was established:

$$\Delta E_{254}^{5\ cm} = \Delta JTU \cdot K \qquad (2\text{-}6)$$

The constant K in eq (2-6) varied depending on how the character of the particles causing the turbidity varied. By filtering sewage effluents K 0.045 was obtained. By adding different amounts of colloidal silica and bentonite the values 0.06 and 0.13, respectively, were measured.

2.3 Removal of humic substances

2.3.1 Coagulation mechanisms and stoichiometry

Stumm and O'Melia (1968) discussed different modes of destabilization of colloids and their relation to phenomena as e.g. the possibility of overdosing (restabilization). Stumm and O'Melia also used the term stoichiometry. The latter concept can be applied if there exists a quantative relationship between the necessary coagulant dose and the concentration of the colloid. Stumm and O'Melia used the surface area of colloids as a "concentration" measure. Results were presented where colloidal silicia was coagulated with hydrolysed Al(III) and Fe(III).

A destabilization according to the double-layer-theory would imply the absence of chemical interaction and adsorption. A coagulant dose in excess would have no effect and the required dosage would be virtually independent of colloid concentration. According to the chemical bridging model, optimal destabilization is reached when approximately half of the colloid surface area is covered. Thus a linear relationship between coagulant dose and surface area is to be expected, and restabilization due to complete surface coverage is possible.

If hydrolysed metal ions are adsorbed on the colloid surface, restabilization accompanied by charge reversal can occur. Stoichiometry is possible but does not always occur, according to Stumm and O'Melia.

The mechanism of sweep coagulation, where an excess of coagulant is forming insoluble hydroxide, is stated not to be stoichiometric.

Packham (1963) discussed the mechanisms of turbid water clarification. He found that the coagulation of dilute suspensions of clay particles was almost independent of the chemical nature of the particles. Aluminium sulphate was most efficient under conditions leading to rapid precipitation of aluminium hydroxide with pH around 7. The required dosage was inversely proportional to clay concentration. Packham emphasized the role of insuluble hydrolysis products in the coagulation. The function of the metal hydroxide was to provide a large number of particles and thereby increase the particle aggregation rate.

Licskó (1976), however, states the importance of polynuclear metal hydroxide complexes in the removal of turbidity from a natural colloid dispersion extracted from the River Danube. He demonstrated that the metal hydroxide sols are adsorbed on the discrete colloid particles and not the latter on the large flocs. "Aged" flocs are no more capable of appreciably affecting the stability of colloidal dispersion. The importance of a rapid and uniform distribution of the coagulant is stressed upon, otherwise the possibility exist that a considerable portion of colloid particles will not be embedded in the flocs. Because of insufficient data given by Licskó, it is not clear to what extent organic matter in the natural water is contributing to the result obtained (see below).

The mechanisms involved in the removal of humic substances are clearly different from those involved in turbidity removal. Hall and Packham (1965) presented results that do not seem to be in accordance with any of the destabilization mechanisms presented above. The required coagulant dose was found to be roughly proportional to the concentration of humic or fulvic acids. Optimum pH-range for removal of humic substances was pH 5 - 6. The presence of clay had little effect on the removal of fulvic acids. On the other hand, the presence of fulvic acids lowered the optimum pH for turbidity removal and increased the required coagulant dose. Hall and Packham concluded that the removal of humic substances, contrary to turbidity removal, may be explained by a process of chemical precipitation. The effect of phosphate to lower the optimum pH has been explained by the interaction of the phosphate ion in the coordination sphere of the aluminium ion. If humic substances behave in the same way, a precipitation of aluminium humate could account for observed results.

The suggested mechanism imply some kind of a stoichiometric relationship between coagulant dose and the concentration of humic substances. Besides a restabilization of the colloids when the dosage is increased would not be plausible. Results in accordance with this general view will be presented later in this chapter. However, Schilling (1975), reported results that are interpreted as a restabilization effect, when the dosage of aluminium sulphate is increased over a certain limit. The experiments were carried out whit waters containing high concentration of humic acids.

The view of Hall and Packham is summarized as follows:

"The extent to which humic substances are removed in coagulation is determined by the availability of the appropriate basic aluminium ion and the extent and type of ionization on the humic acid molecule. As the appropriate acid group of humic acid appears to be incompletely dissociated at pH 5, colour removal is limited at lower pH-values by both these factors. As the pH is increased, colour removal reaches an optimum and then declines, owing to the ionization of other groups (probably of phenolic character) on the humic acid molecule that can form a soluble complex with aluminium, thereby reducing precipitation. This effect can be overcome by increasing the coagulant dose, but at a certain aluminium ion activity the hydroxide precipitates, preventing further colour removal.

... in the presence of humic substances the coagulant dose for turbidity removal is increased ... owing to the fact that aluminium hydroxide cannot precipitate until most of the humic matter has been complexed."

Narkis and Rebhun (1975) and Klute *et.al.* (1979) found that when coagulation of clay was accomplished by a polyelectrolyte, the presence of humic substances increased the required dosage. The polyelectrolyte first reacted with the acid groups of the humic substances; not until after complete reaction with the humates, coagulation of the inorganic colloids could take place. The organic matter thus served as a coagulation inhibitor.

Narkis and Rebhun (1977) reports a linear relationship between alum dosage and content of humic acids at low humic acid concentrations. The chemical interaction with the humic acid was postulated to involve trivalent aluminium hydroxo complexes. A stoichiometric relationship was also found by van Breemen *et.al.* (1979), Haff (1978).

Black *et.al.* (1963), in coagulation experiments with ferric sulphate, conclude that the pH for maximum colour removal can be predicted from the colour of the raw water alone. The minimum dose of ferric sulphate required, at that pH to give acceptable colour, is essentially found to be a linear function of raw-water colour.

Haberer and Normann (1976) report increased removal efficiency of organic matter by a two stage process: coprecipitation with $CaCO_3$ after lime addition (pH 10,5) and subsequent coagulation at pH 6 with ferric chloride.

Overath *et.al.* (1979) improved the purification efficiency for a given amount of ferric chloride by adding an acid. The waters used were highly buffered (ca. 2,7 mmol HCO_3^-/l) and reported results are only effects of adjusting the pH.

Helenius (1972) gives examples of stoichiometric relationships used in practice to determine the required dosage of aluminium sulphate. Some rules of thumb are presented in eqs (2-7) to (2-9).

$$D = 0.8 \ldots 1.0 \cdot R_K \tag{2-7}$$

$$D = 0.3 \cdot R_f + 0.1 \cdot R_S + 15 \tag{2-8}$$

$$D = 0.7 \cdot R_f + 15 \tag{2-9}$$

where D is ppm aluminium sulphate

R_K is the raw water COD_{Mn}, mg $KMnO_4$/l

R_S is the raw water turbidity, mg SiO_2/l (1 FTU ~2 mg SiO_2/l, Hedberg, 1976)

R_f is the raw water colour, mg Pt/l

Helenius made a statistical analysis of applied aluminium suphate dosage at 14 Swedish and 14 Finnish water works. Examples of obtained regression equations are given in eqs (2-10) to (2-12)

$$D = 16 + 0.45\ R_K + 0.24\ R_f \tag{2-10}$$

$$D = 17 + 0.68\ R_K \tag{2-11}$$

$$D = 23 + 0.48\ R_f \tag{2-12}$$

2.3.2 Experiments

Coagulation tests on a laboratory scale were carried out at 20 Swedish water treatment plants. The results are shown in fig 2.2 to 2.41.

The scope of these experiments was to achieve comparable results from each water treatment plant, in order to answer the question how the treatment result was affected by coagulant dose and pH. The intention was to establish a "base-line" to which the actual treatment result at the plant could be related. In addition, some general insight was thought to be gained, for example, if there is any measurable property in the raw water, that can account for different optimum coagulation conditions. A standardized jar test procedure was developed. The experiments were carried out from the middle of March to the middle of June 1979.

2.3.2.1 Jar-test procedure

The experiments were performed in 2-litre jars (see fig 3.30), which were placed in a water-bath with a flow through of tap water. In that way a constant temperature was maintained during the coagulation-sedimentation process. The receptacle had room for eight 2 l beakers simultaneously.

During intense mixing the required amount of pH-adjusting chemical (NaOH or HCl) was added and after that the dose of aluminium sulphate. The flocculation scheme according to table 2-1 was started after that chemicals had been added to all jars. G-values in table 2-1 are calculated according to eq (3-100) (a temperature of $5^{o}C$ is assumed).

Table 2-1. Flocculation pattern in laboratory experiments.

Duration (minutes)	2	4	8	16
G-value (s^{-1})	200	140	60	10

After the flocculation time (30 min), stirrers were removed and the flocs were allowed to settle for 1 h.

2.3.2.2 Analyses

During flocculation, pH was checked (pH-meter Radiometer PHM52b, pH-electrode Ingold 421-88) and floc turbidity was measured (Hach Turbidimeter 2100 A).

After sedimentation samples were taken at 15 cm depth for turbidity measurement. The remaining water was filtered through a paper filter (Munktell 00 52-80-150). The first appr. 100 ml were discarded, appr. 500 ml filtrate were used for analyses. Turbidity measurements and absorbance measurements at 254 nm and 436 nm were carried out immediately. For absorbance measurements a Beckman photometer DB-G, usually equipped with a 4 cm cell, was used. No pH-adjustment of the samples was made before absorbance measurements. The colour of a humic water is sometimes said to be affected by pH. Some preliminary test were made, however, and the addition of a buffer solution virtually had no effect on the measurement within the actual pH-interval (5.5-7.5).

Samples for the analysis of aluminium and COD_{Mn} were transported to the laboratory. The latter samples were preserved by adding 5 ml 25 % H_2SO_4 to 100 ml of water. The analyses were performed within a week.

Aluminium was analysed photometrically, reagent: Alizarin S, according to Deutsche Einheitsverfahren zur Wasseruntersuchung, Chapter E9. For practical reasons only concentrations below 1 mg Al/l was quantitatively determined.

2.3.2.3 Chemical dose

Three different doses of aluminium sulphate were applied for each raw water, usually the dose at the water treatment plant and in addition with a higher and a lower dose, $\pm$ 10 ppm aluminium sulphate. A feed solution of 20 g Al-sulphate/l was renewed each day from a stock solution of 200 g Al-sulphate/l. The chemical for pH-adjustment was added in such amounts that the pH-value after aluminium sulphate addition was calculated to vary between pH 5-5.5 in the first jar up to appr. pH 7.5 in the eighth. For a rough estimate of required dosage of pH-adjusting chemicals fig 2.1 was used, where the pH of the raw water (pH_0) and the desired coagulation pH (pH_s) determine the value of (L-A)/B.

A is the number of acid equivalents added with the aluminium sulphate dose. The value of A for the aluminium sulphate used (Boliden aluminium sulphate, 17-18% Al_2O_3) was found to be less than the theoretical value based on the aluminium content. By titration the following relationship was established

$$A = \text{dose aluminium sulphate (mg/l)} \cdot 0.85/100 \text{ (meqv } H^+/l) \quad (2\text{-}13)$$

B is the alkalinity of the raw water, approximated by titration with HCl to pH 4.3 (Grohman, 1975). L is the dosage of pH-adjusting chemical to be calculated from the actual value of (L-A)/B. The result is obtained in meqv OH^-/l. A negative L means addition of an acid.

The curves are based on the assumptions that hydrogencarbonate (HCO_3^-) is the main (and only) buffering ion, that the first dissociation constant for carbonic acid is $pK_1 = 6.5$ and that no carbonate is added with the pH-adjusting chemical. The diagram was designed to simplify determination of the dose of pH-adjusting chemical. It was only necessary to carry out one acid titration, down to pH 4.3. The doses could then easily be calculated by means of fig 2.1. Usually the values were reasonably correct. This can be seen in the figures that follow: the eight pH_s values in fig 2.1 were those aimed at, the values that was actually obtained are presented in fig 2.2 to 2.41. However great differences sometimes occurred for the most acid and alkaline pH-values.

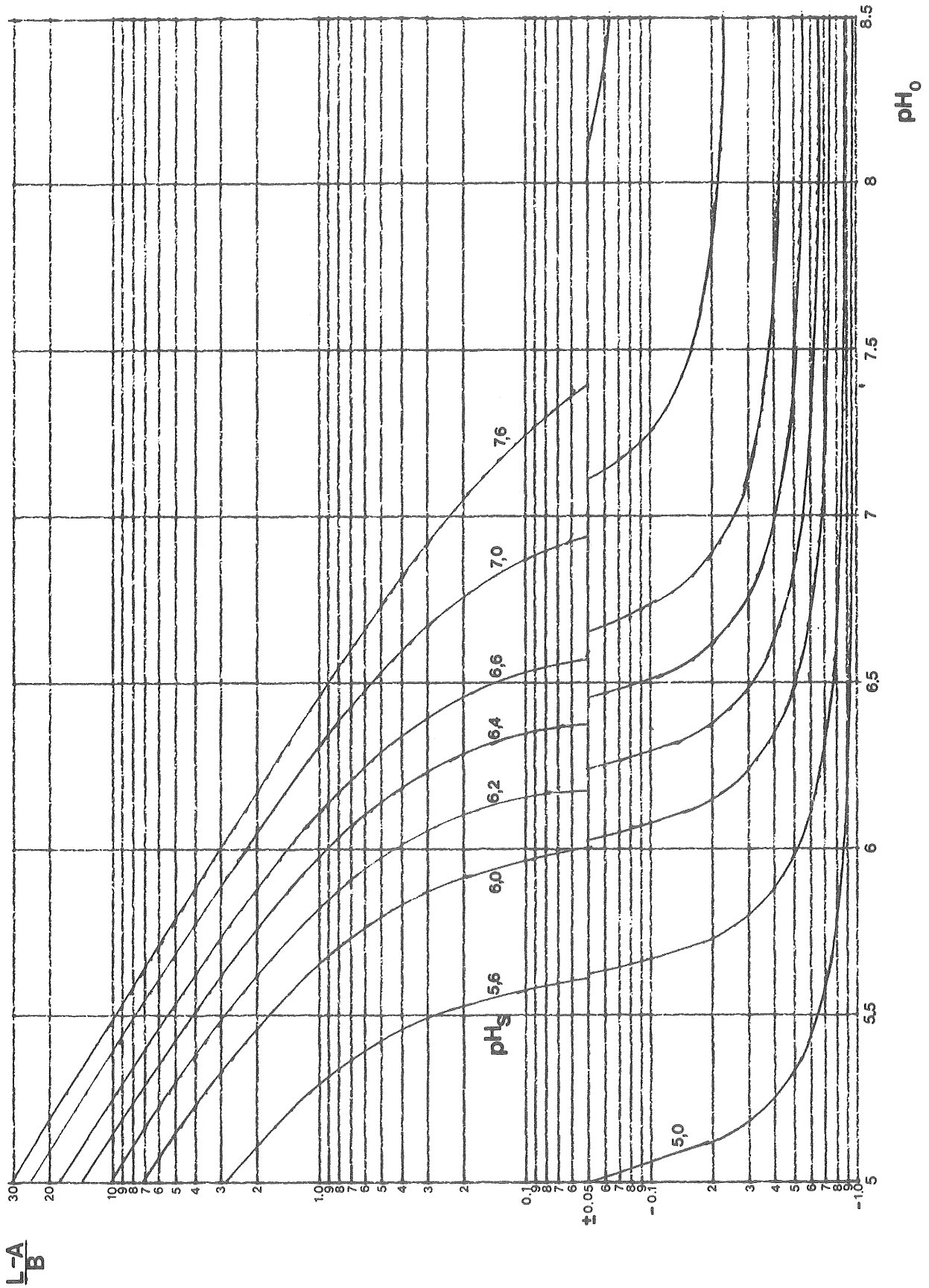

Fig 2.1. Curves for approximative calculation of required addition of pH-adjusting chemicals.

2.3.2.4 Raw water properties

Some characteristics of the various raw waters are given in table 2-2. The values are only representative for the days, usually two, when jar tests were carried out at the water treatment plant. The values in the table may differ slightly from those given in the diagrams, because the former are based on analyses on unfiltered raw waters. In fig 2.2 to 2.41 the results obtained are compared to filtered raw water (when the filtrate is considered).

Table 2-2. Some characteristics of the raw waters

	Raw water source L = Lake R = River	pH	Turbidity, FTU	$E^{4\ cm}_{254}$	$E^{4\ cm}_{436}$	COD_{Mn}, mg $KMnO_4$/l	Alkalinity, m eqv/l	Temperature °C
Borås	Öresjö (L)	7,4	0,46	1,5	0,060	30	0,62	2,0
Grängesberg	Norra Hörken (L)	6,5	0,24	0,60	0,034	19	0,10	6,0
Göteborg, Lackarebäck	Delsjön (L) transited from Göta Älv (R)	7,4	0,45	0,66	-	23	0,25	5,0
Hofors	Hammardammen (L)	6,8	0,70	0,84	0,056	27	0,18	13,5
Helsingborg	Ringsjön (L)	7,6	1,1	0,93	0,054	35	1,8	3,8
Härnösand	Bondsjön (L)	6,4	0,93	1,0	0,079	30	0,23	6,0
Karlshamn	Långasjön (L)	6,0	0,57	0,90	0,056	24	0,11	2,0
Kramfors	Sjöbysjön (L)	6,7	0,71	1,40	0,096	40	0,13	15,0
Lidköping	Vänern (L)	7,4	1,1	0,75	0,044	26	0,29	4,0
Lilla Edet	Göta Älv (R)	7,1	4,4	1,2	0,095	34	0,26	1,0
Mariestad	Vänern (L)	7,6	1,5	0,83	0,055	26	0,36	5,0
Mjölby	Svartån (R)	7,5	1,2	1,39	0,083	36	0,72	12,0
Mölndal	Långasjön (L)	6,2	0,64	0,70	0,040	24	0,13	1,0
Mönsterås	Lillån (R)	5,8	2,5	3,1	0,216	93	0,14	6,0
Morrköping	Motala Ström (R)	7,9	4,2	1,2	0,134	34	0,77	9,0
Nässjö	Spexhultasjön (L)	6,5	0,30	1,2	0,055	32	0,23	2,0
Säffle	Vänern (L)	6,6	3,4	0,74	0,084	23	0,15	4,0
Västervik	Hjorten (L)	6,7	2,9	0,72	0,070	24	0,35	5,0
Uddevalla	Köperödsjön(L) transited from Bäveån (R)	6,3	2,3	1,3	0,091	33	0,24	2,0
Åmål	Vänern (L)	7,2	1,7	0,71	0,050	25	0,23	2,0

2.3.2.5 Treatment of results

The concentration of humic substances is measured by the parameters COD_{Mn}, $E_{254}^{4\ cm}$ and $E_{436}^{4\ cm}$. The residuals after filtration are expressed as percentage of the raw water value. It is assumed that the residual as a function of the pH-value can be described with an expression of the form:

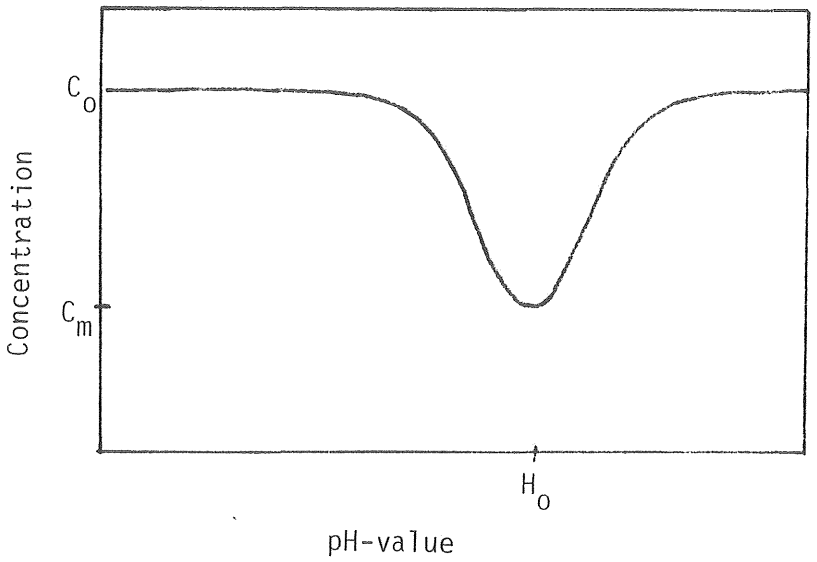

$$\frac{C_o - C}{C_o - C_m} = e^{-(K \cdot (H - H_o))^2} \qquad (2\text{-}14)$$

where C_o is the raw water concentration
C is the concentration at the pH-value H
C_m is the minimum observed concentration

If the assumption is correct, data can be linearized by the calculation:

$$\pm\sqrt{\ln\left(\frac{C_o - C_m}{C_o - C}\right)} = K \cdot (H - H_o) \qquad (2\text{-}15)$$

The sign is

- \- for $pH < H_m$
- \+ for $pH > H_m$

where H_m is the pH-value where minimum concentration (C_m) is observed.

Through the method of least squares the constants K and H_o are determined. H_o then not necessarily becomes equal to H_m.

In the case of turbidity and residual coagulant after filtration, there is no way of expressing removal efficiency as a part of a raw water value. Therefore, for simplicity, a quadratic function is fitted to the data obtained:

$$C = (K_1 \cdot (H - H_o))^2 + C_m \qquad (2\text{-}16)$$

For each measure of organic content the result as a function of the coagulant dose is summarized in four curves: minimum residual, amount removed, the percentage removal and characteristic pH-interval. The latter is calculated as 0.2/K, K according to eq (2-14) and describes how the result will change if the pH around the minimum value is changed. The mathematical meaning of this value, in relation to the calculated curve, is the pH-interval where the minimum value is exceeded with less than the amount $0.01 \cdot (C_o - C_{min})$. The optimum pH-value ($H_o$) is indicated at the top of this part of the figure.

Concerning residual aluminium and the filtrate turbidity, the minimum residual at varying coagulant dose is presented together with the variation of a characteristic pH-interval. In this case the interval is calculated as $2 \cdot \sqrt{0.1}/K_1$, K_1 according to eq (2-16). The expression in this case corresponds to the pH-interval, within which the minimum value is not exceeded with more than 0.1 units (mg Al/l and FTU, respectively).

The calculated pH-intervals are just meant to be a means of comparison within each variable and to give a general measure of the pH-dependence. The two modes of calculating the characteristic pH-interval are arbitrarily chosen for convenience; a covariation between the two is probable, but their relative magnitude is of no significance.

Besides the analyses mentioned (after filtration), there are two other pH-depending relationships shown in the figures for each set of jar tests: the floc turbidity and the removal efficiency by sedimentation. The latter is expressed as the residual (percentage of initial floc turbidity) in a sample taken at 15 cm depth after 1 h of sedimentation. The type of curve represented in eq (2-14) is fitted to the data points. The sedimentation properties are treated in the same way as the data representing residual organic substance. The floc turbidity is assumed to be described by a Gaussian curve added on the raw water turbidity. On the acid and basic side, respectively, the curves thus approaches the raw water turbidity.

The interrelation of COD_{Mn}-values and $E_{254}^{4\ cm}$ of corresponding samples achieved in each set of jar tests is summarized in a diagram.

The schematic method applied here to fit curves of a predetermined type to the data has some inherent inaccuracy. The number of values is limited and the location of a maximum or minimum value may be very uncertain, especially if it is determined by means of values located only on one side of the extreme value (!). This is sometimes the case, unfortunately. Each test has just been carried out once. These curves must naturally be looked upon critically. Performance for other coagulant doses and for other parameters with the same dose is helpful when determining the reliability of such a curve.

The location (and magnitude) of a minimum value can also be uncertain due to experimental errors. If, for example two equal minimum values are detected, maybe with a slightly higher value in between, the calculation pattern demands a decision which is to be regarded as the minimum value. Regularly in such cases, the value corresponding to the lowest pH is chosen, which may introduce some bias. Some curves, however, may look more arbitrary than they really are. As e.g., aluminium only was measured quantitatively in concentrations less than 1,0 mg Al/l, there may be points, not present in the figure, on which considerations concerning possible location of the curve is based. Any practical way to represent analytical results such as > 1 mg/l, in a figure, was not found.

For simplicity, symmetry around the pH-value representing the minimum or maximum value has been assumed. Sometimes this is obviously not the case. For example, residual aluminium usually shows a more rapid increase on the acid side than on the alkaline. It was thought, however, that the limited number of data did not justify a more sophisticated curve-fitting. The rough method proposed here, is believed to give enough information for the present purpose.

Fig 2-2. Results from coagulation tests at Borås water treatment plant

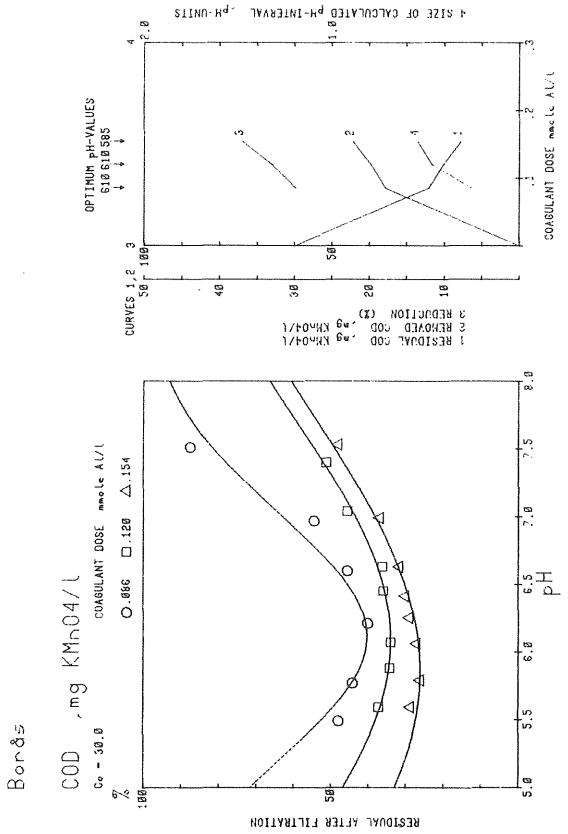

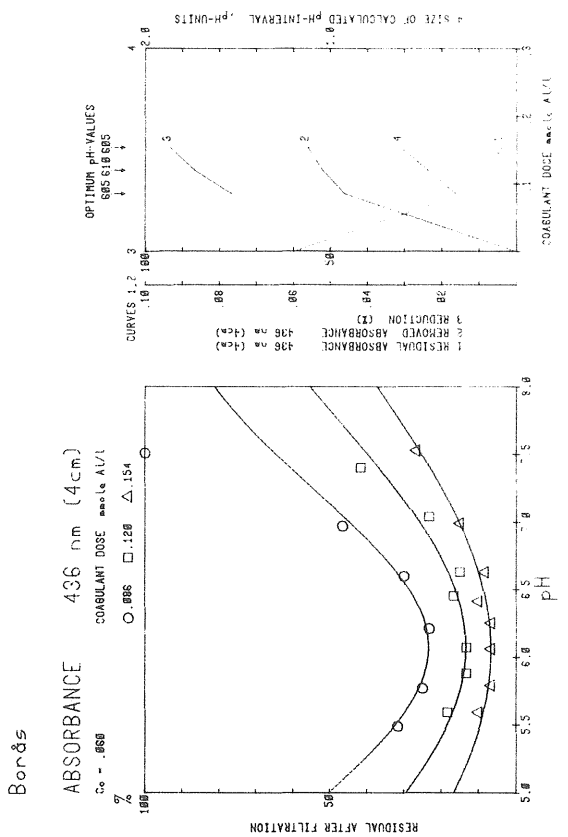

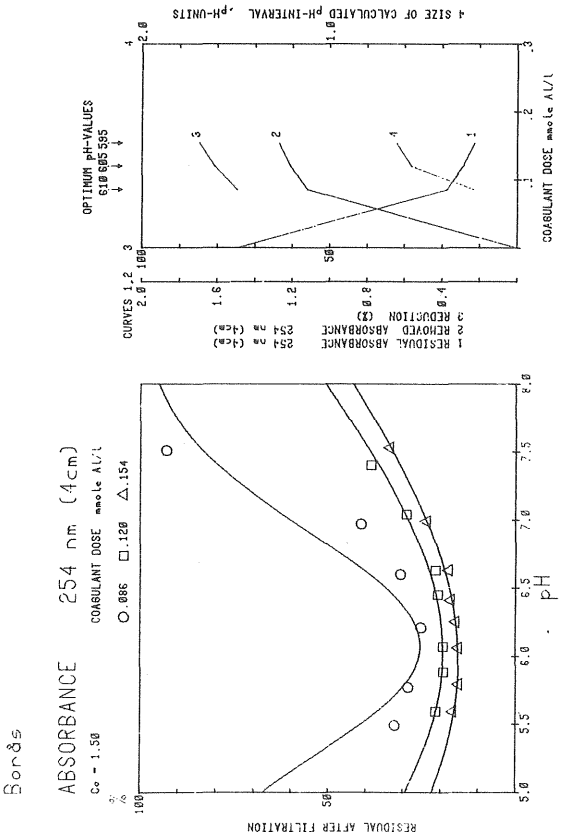

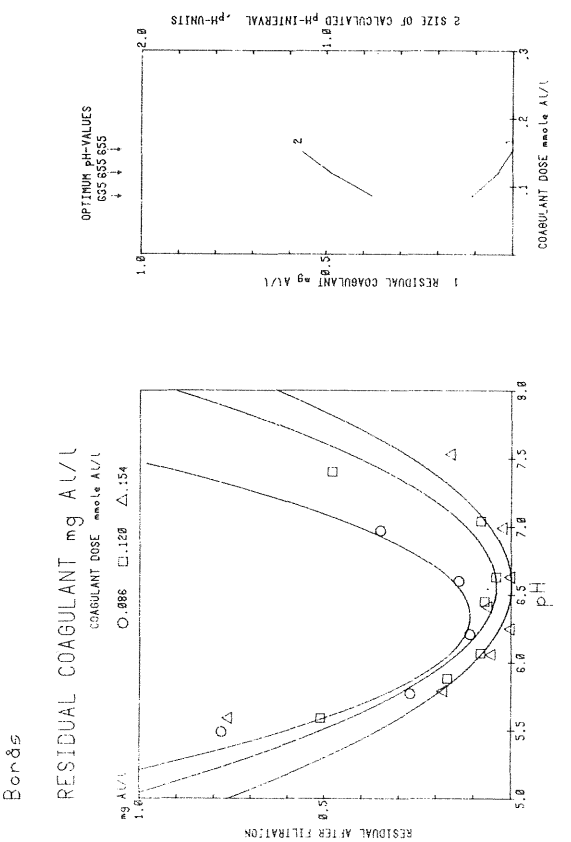

Fig 2-3. Results from coagulation tests at Borås water treatment plant (contd)

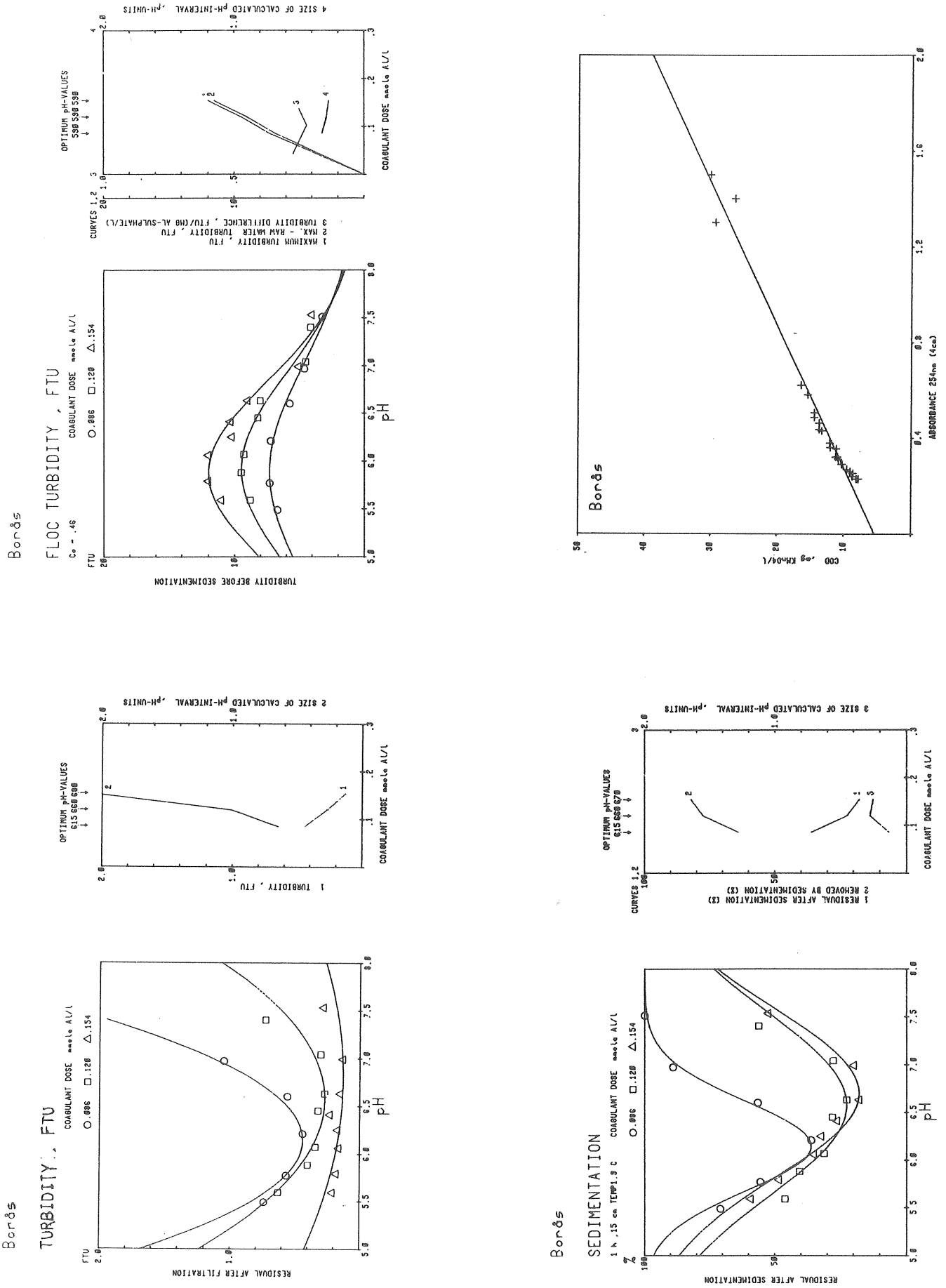

Fig 2-4. Results from coagulation tests at Grängesberg water treatment plant

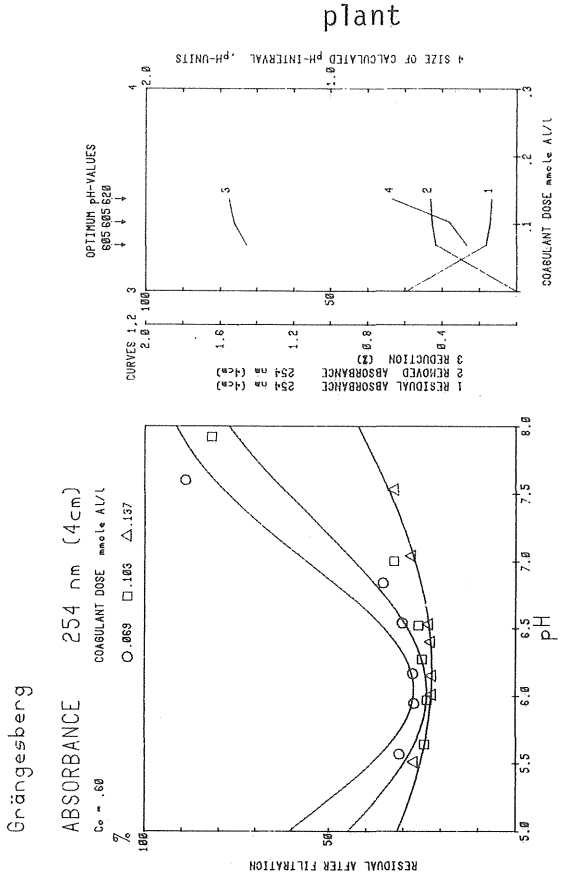

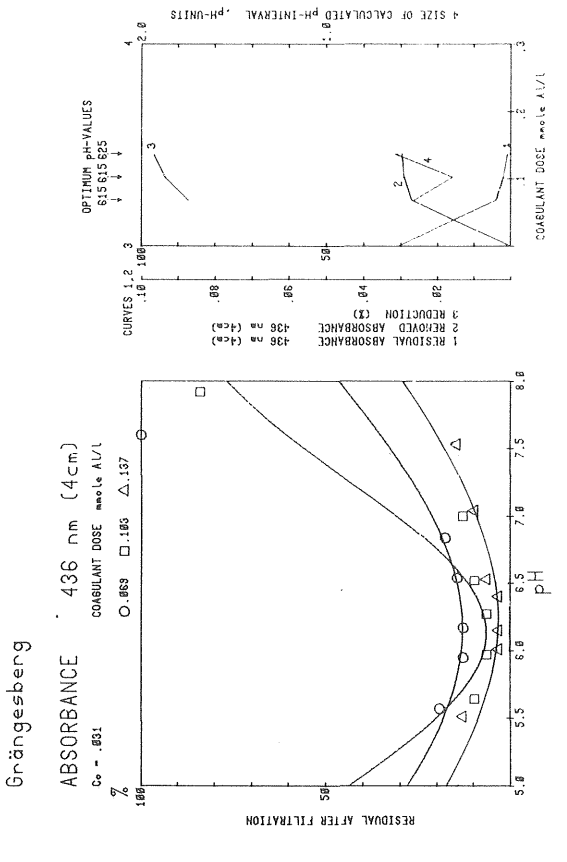

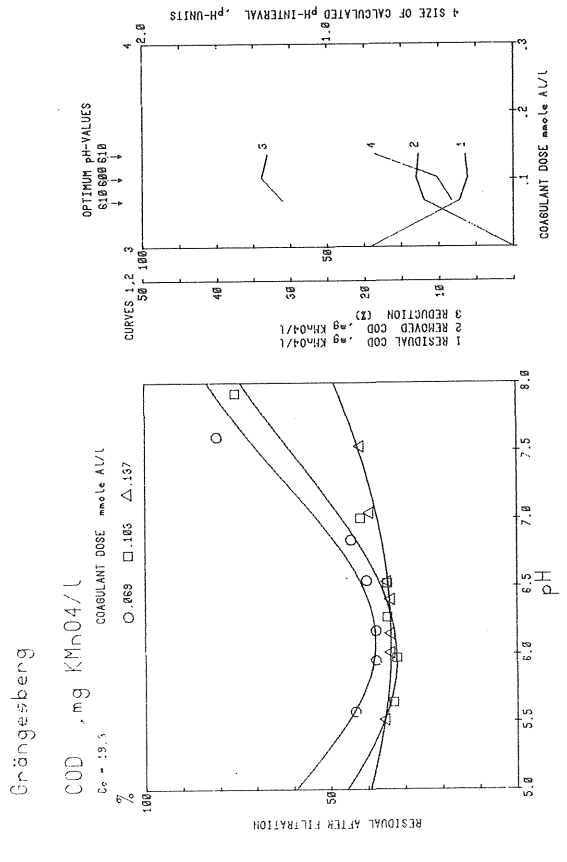

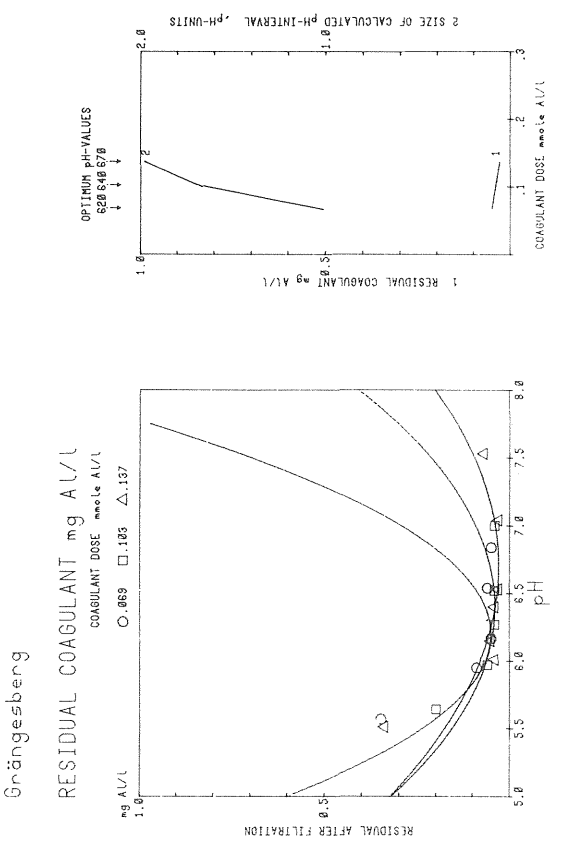

Fig 2-5. Results from coagulation tests at Grängesberg water treatment plant (contd)

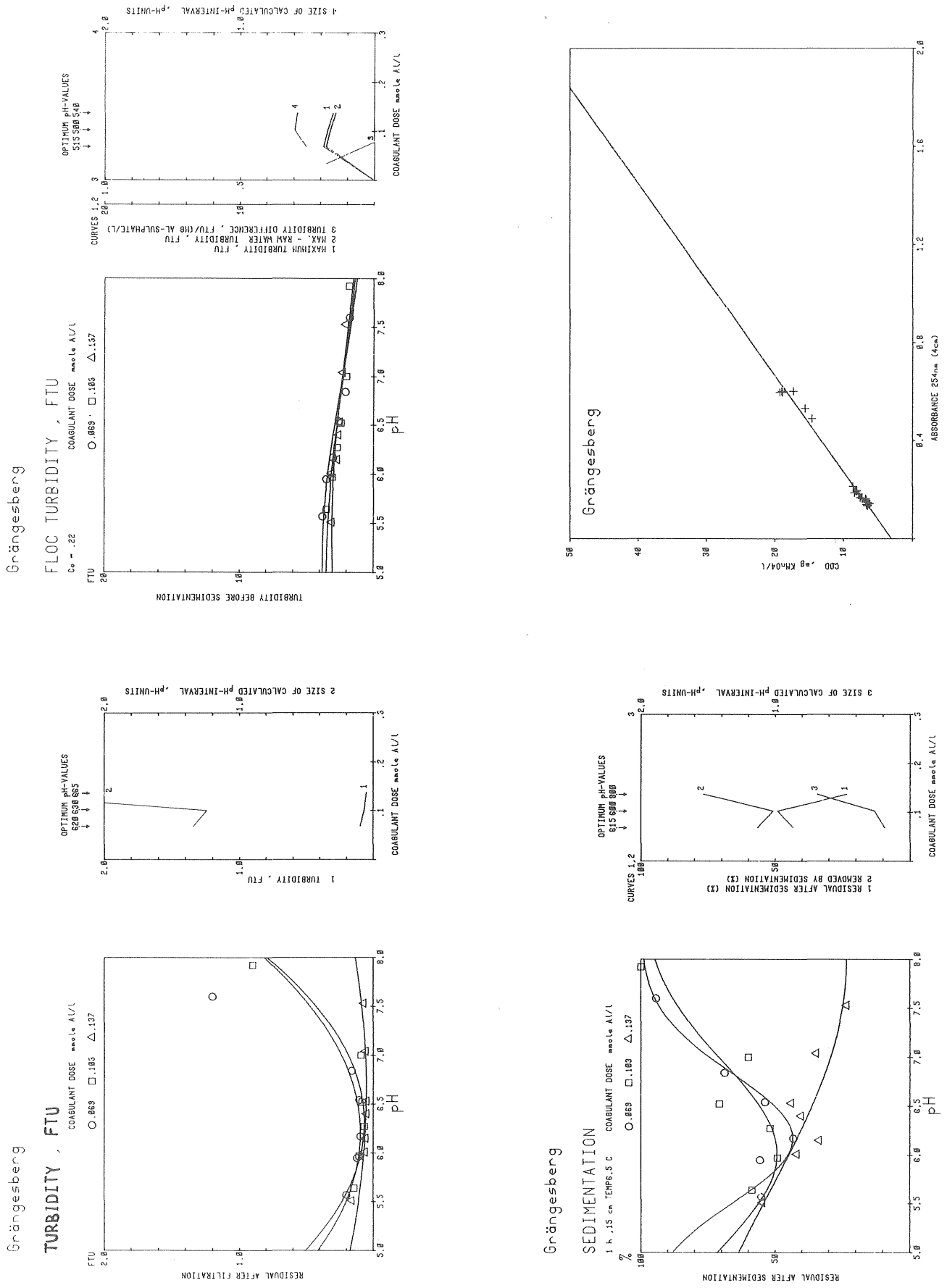

Fig 2-6. Results from coagulation tests at Göteborg (Lackarebäck) water treatment plant

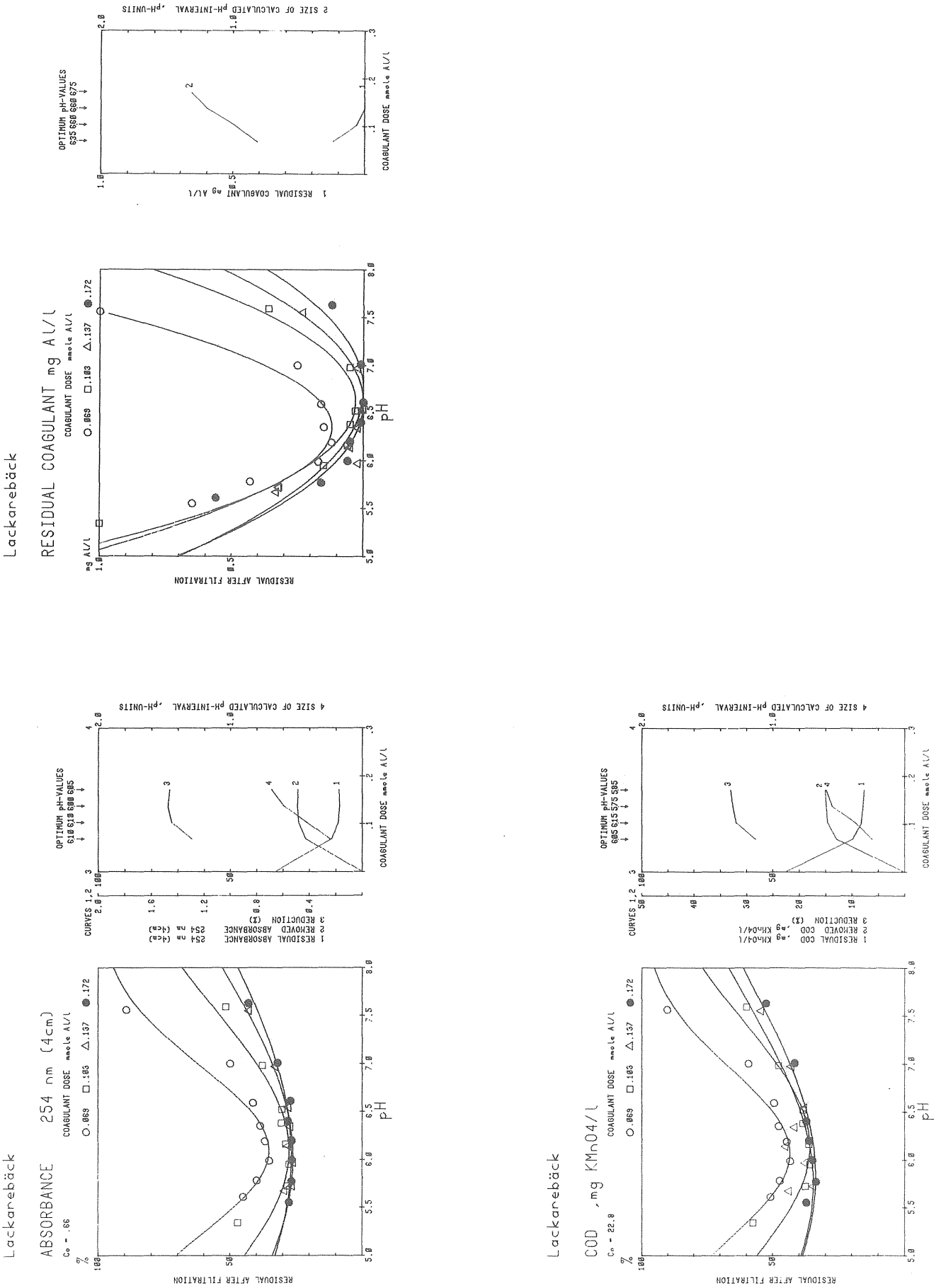

Fig 2-7. Results from coagulation tests at Göteborg (Lackarebäck) water treatment plant (contd)

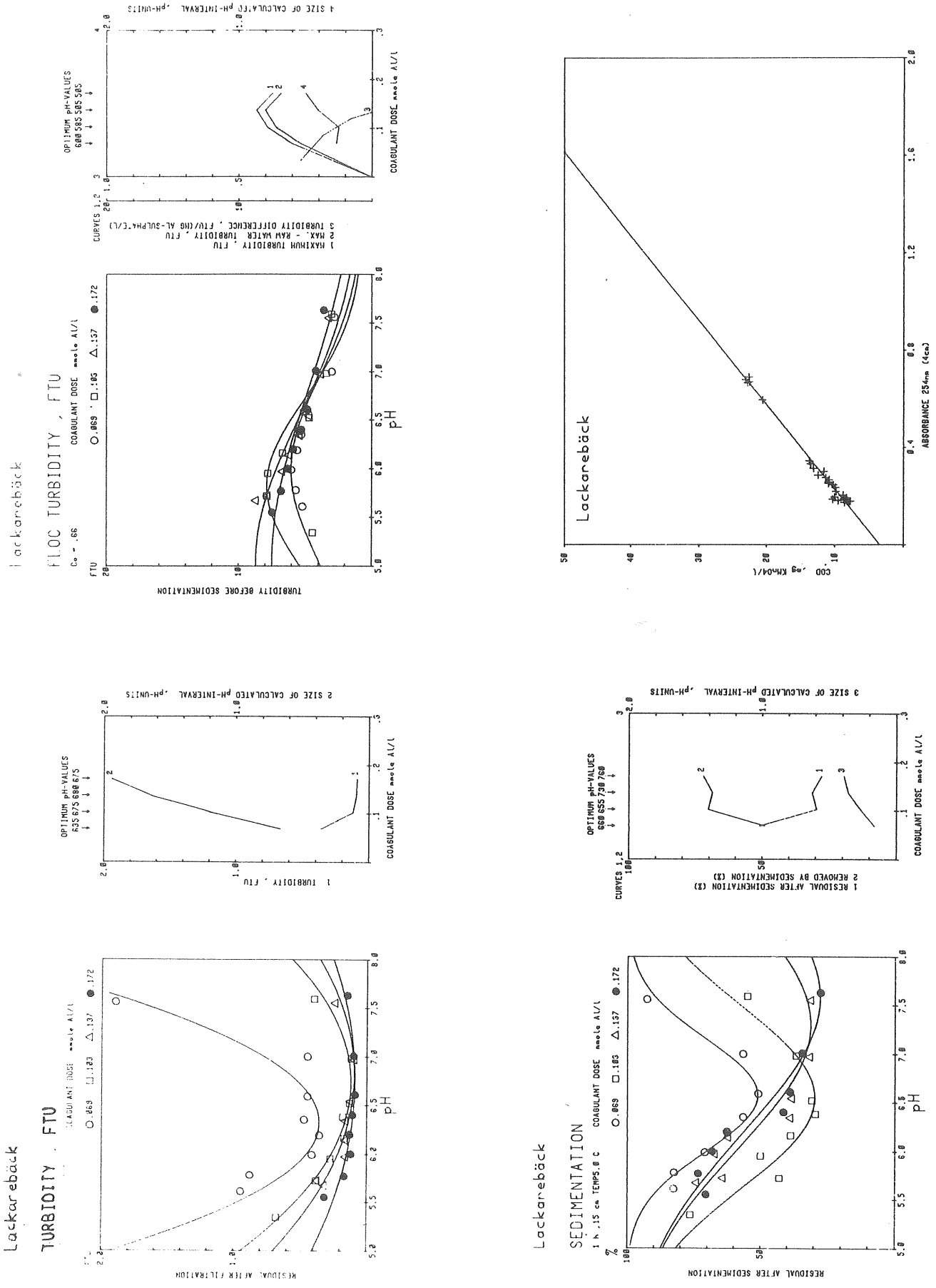

Fig 2-8. Results from coagulation tests at Hofors water treatment plant

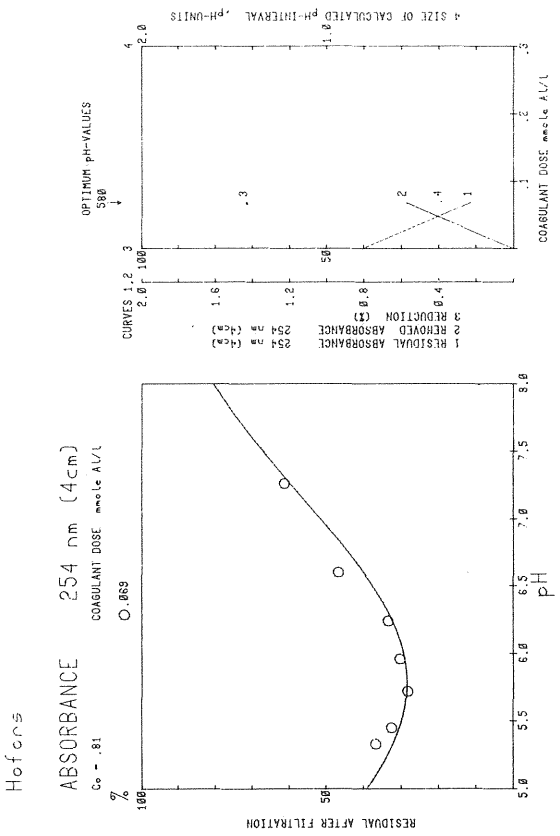

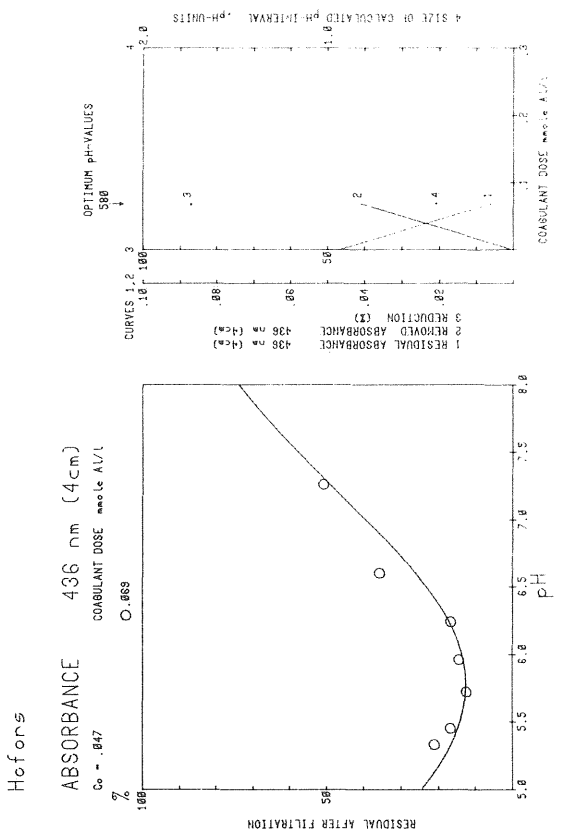

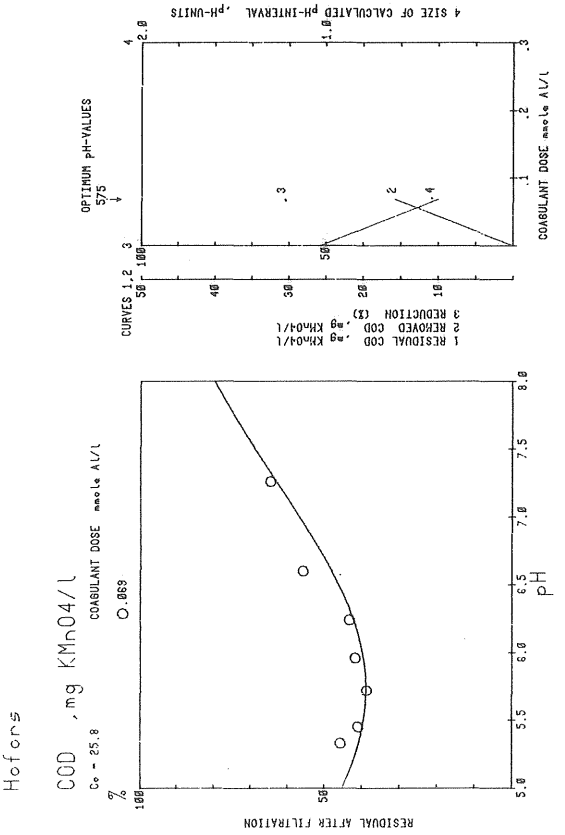

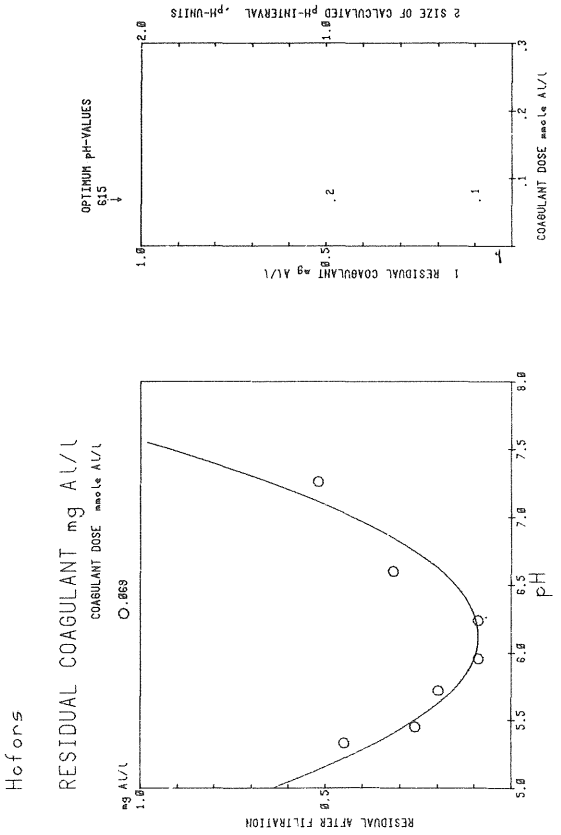

Fig 2-9. Results from coagulation tests at Hofors water treatment plant (contd)

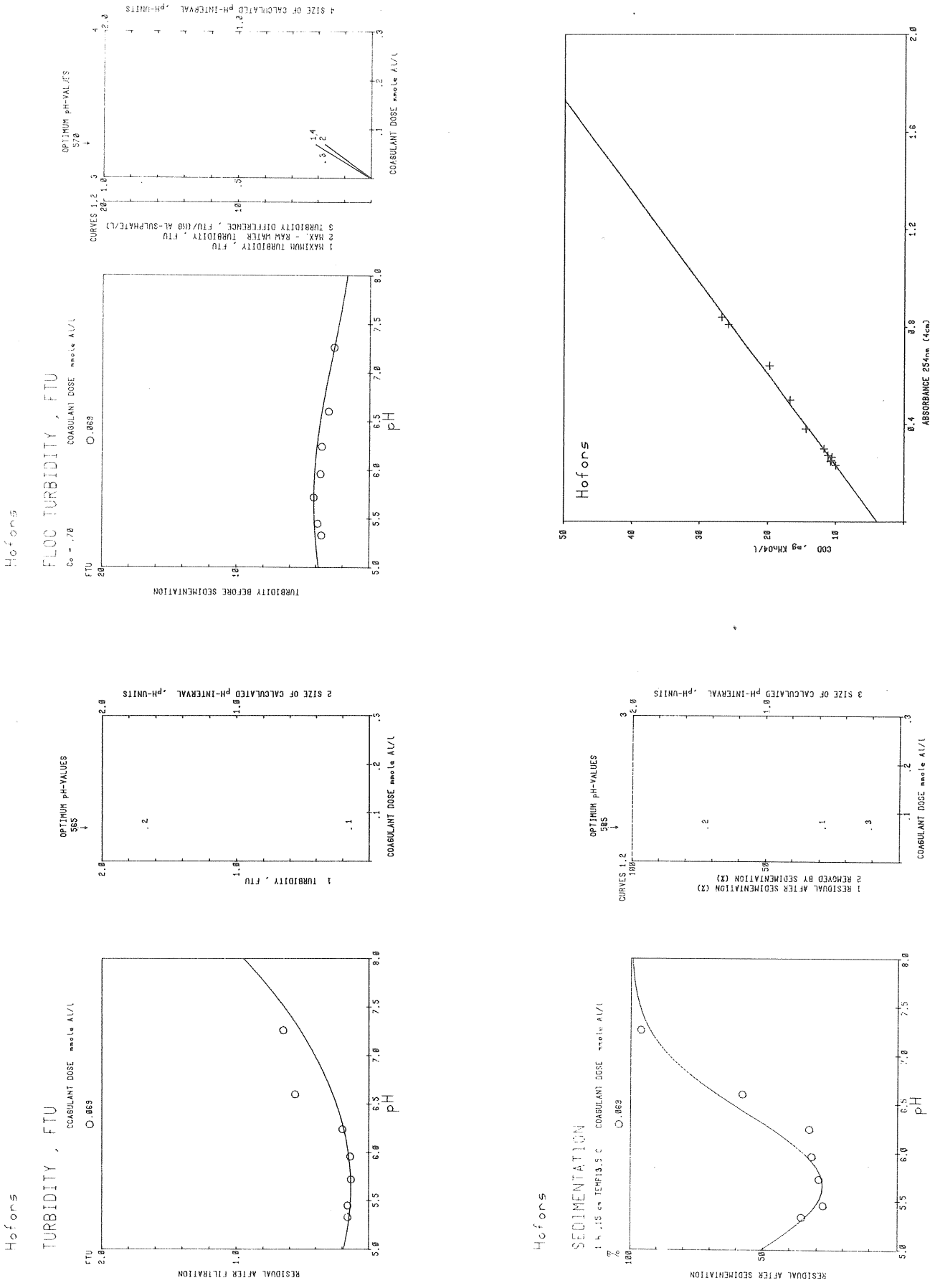

Fig 2-10. Results from coagulation tests at Helsingborg (Ringsjön) water treatment plant

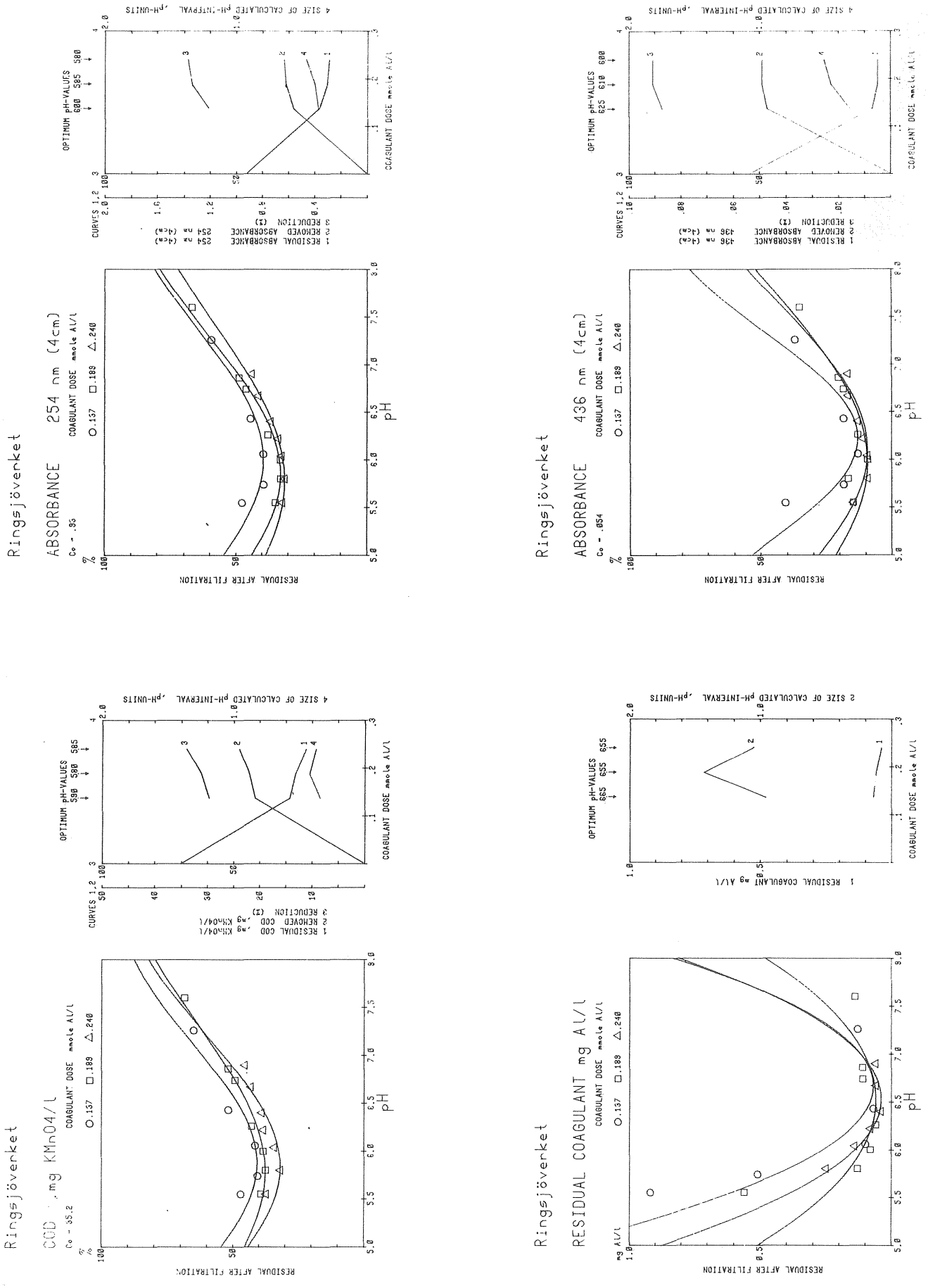

Fig 2-11. Results from coagulation tests at Helsingborg (Ringsjön) water treatment plant (contd)

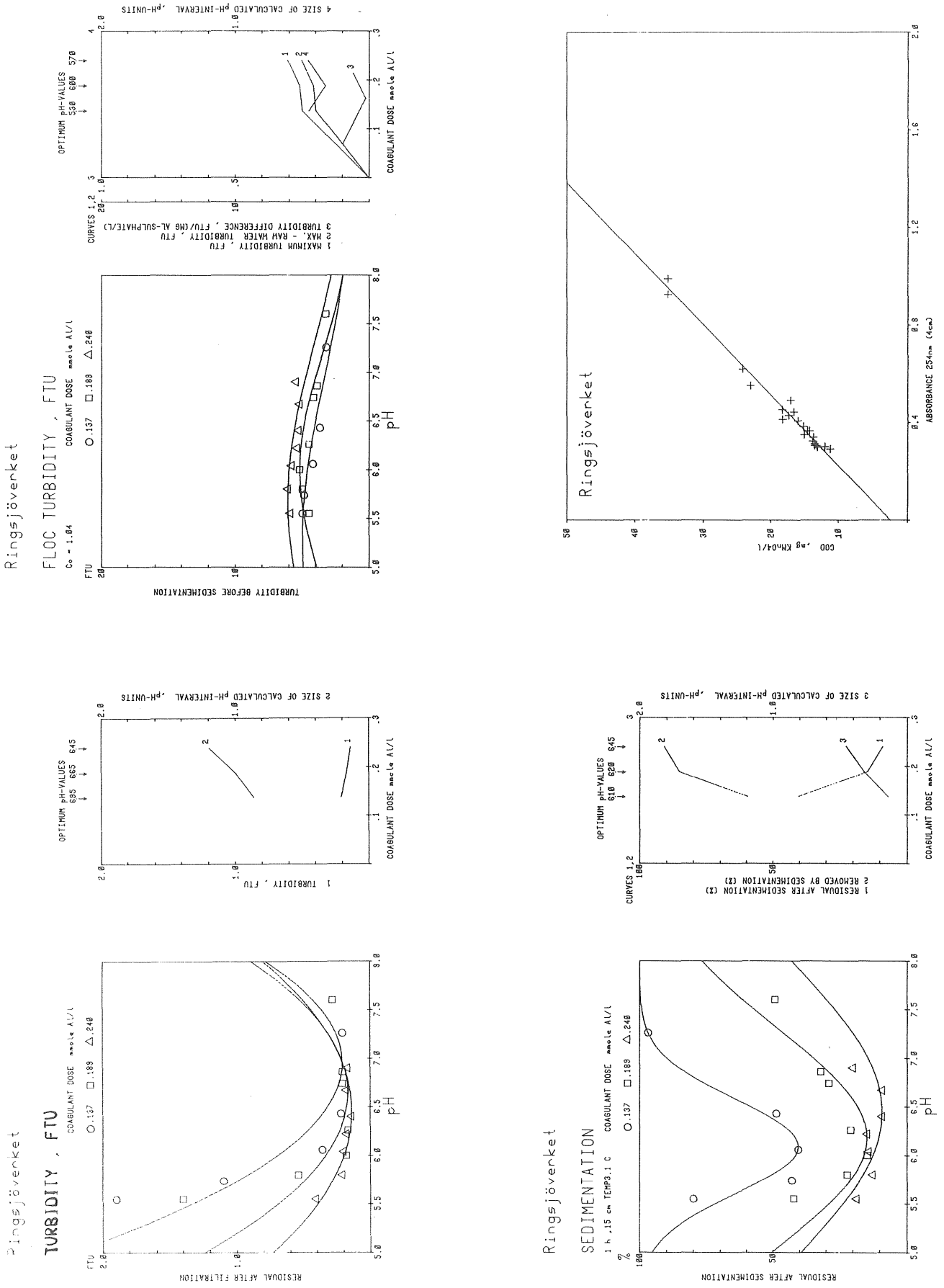

Fig 2-12. Results from coagulation tests at Härnösand water treatment plant

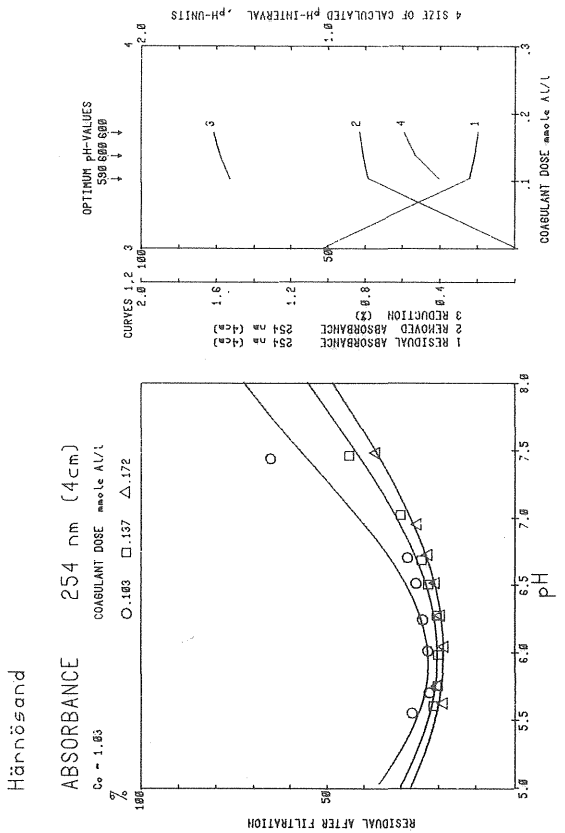

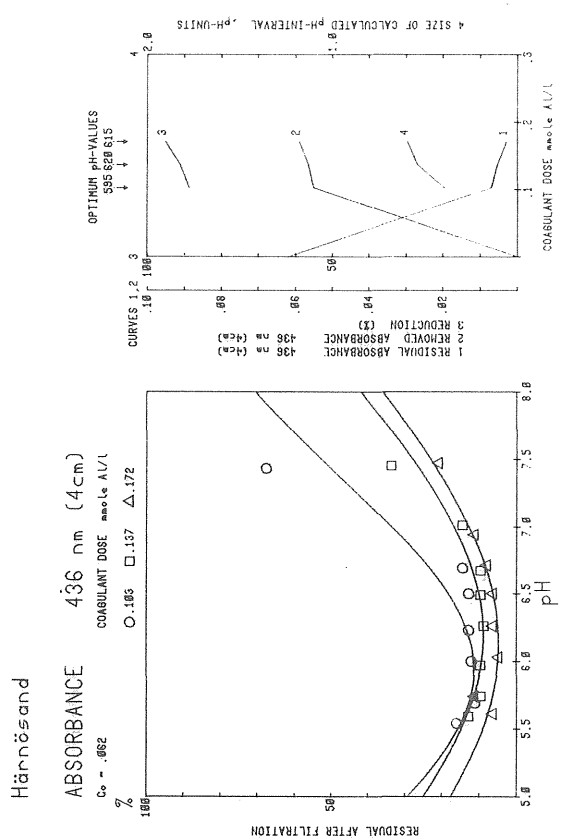

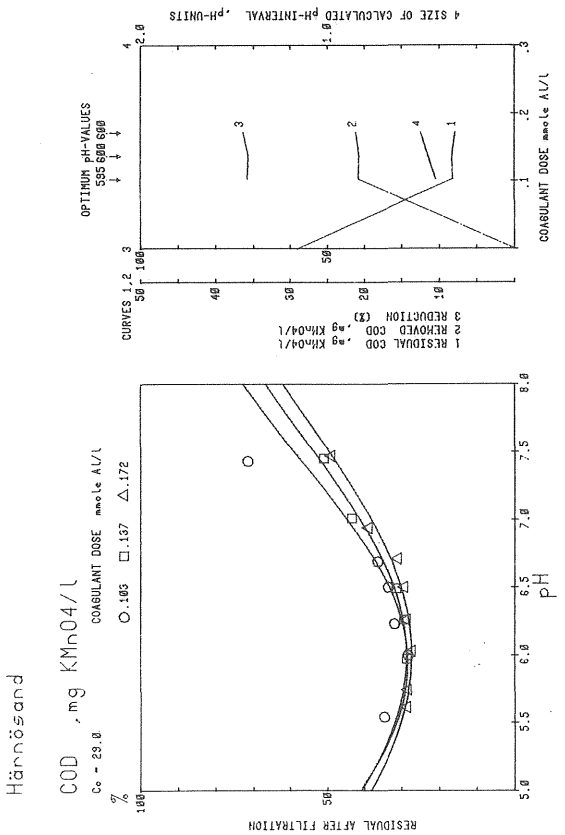

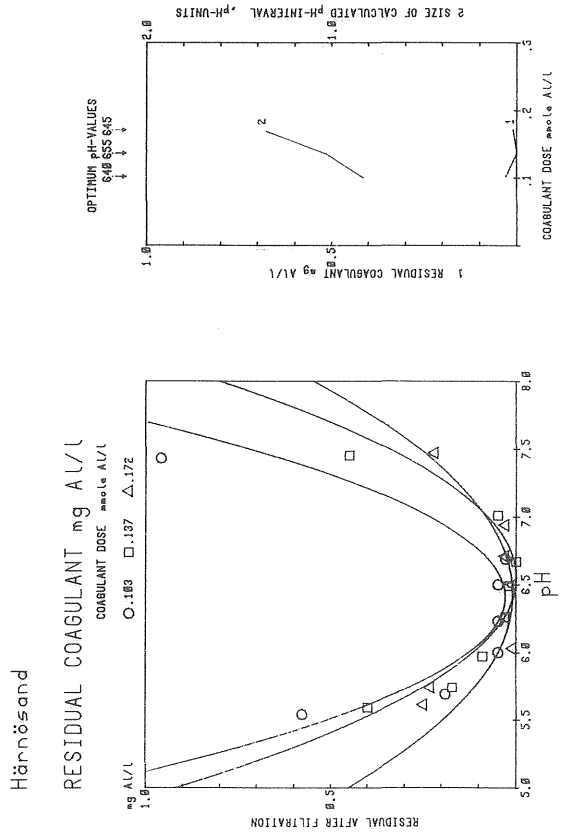

Fig 2-13. Results from coagulation tests at Härnösand water treatment plant (contd)

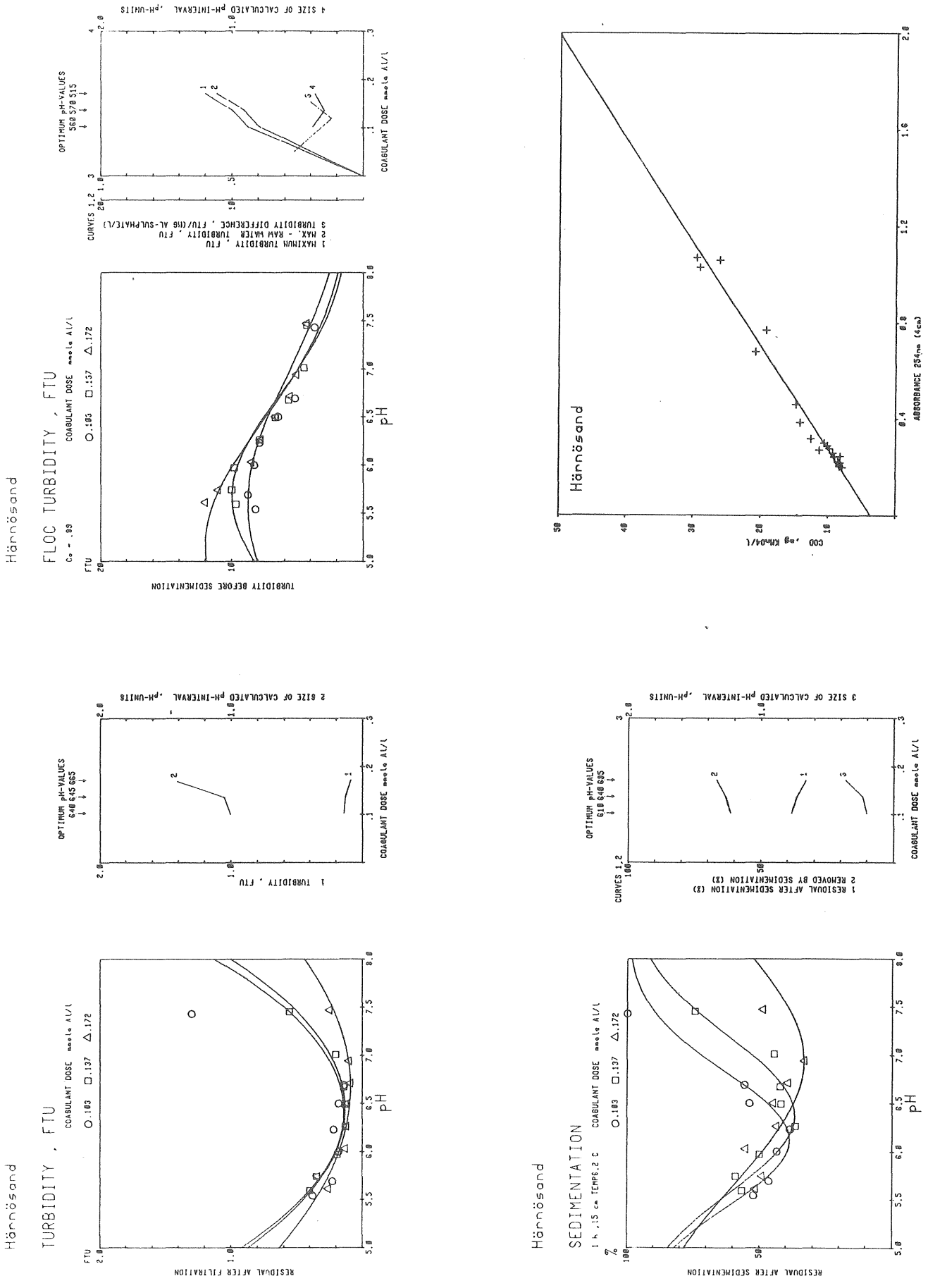

Fig 2-14. Results from coagulation tests at Karlshamn water treatment plant

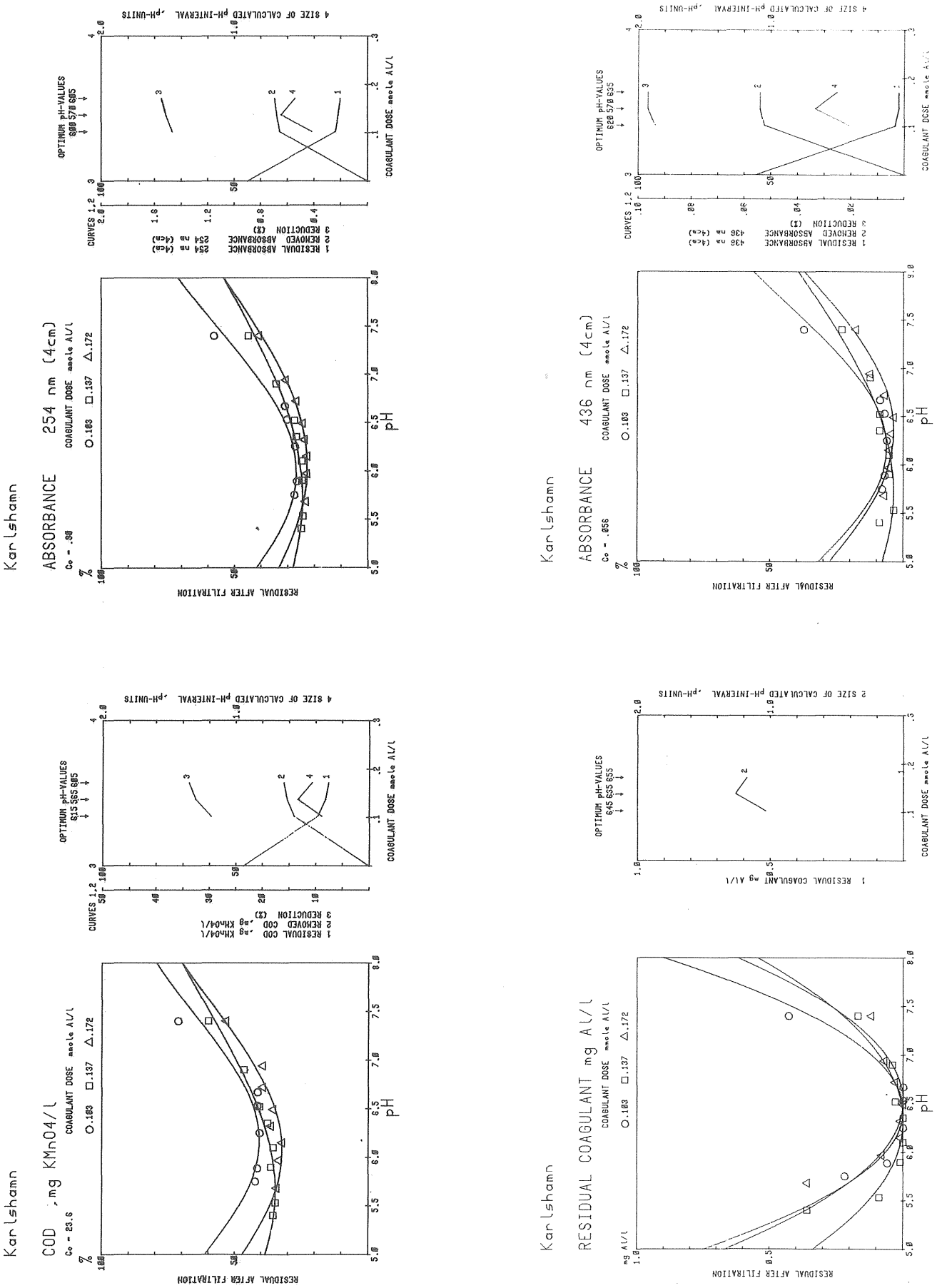

Fig 2-15. Results from coagulation tests at Karlshamn water treatment plant (contd)

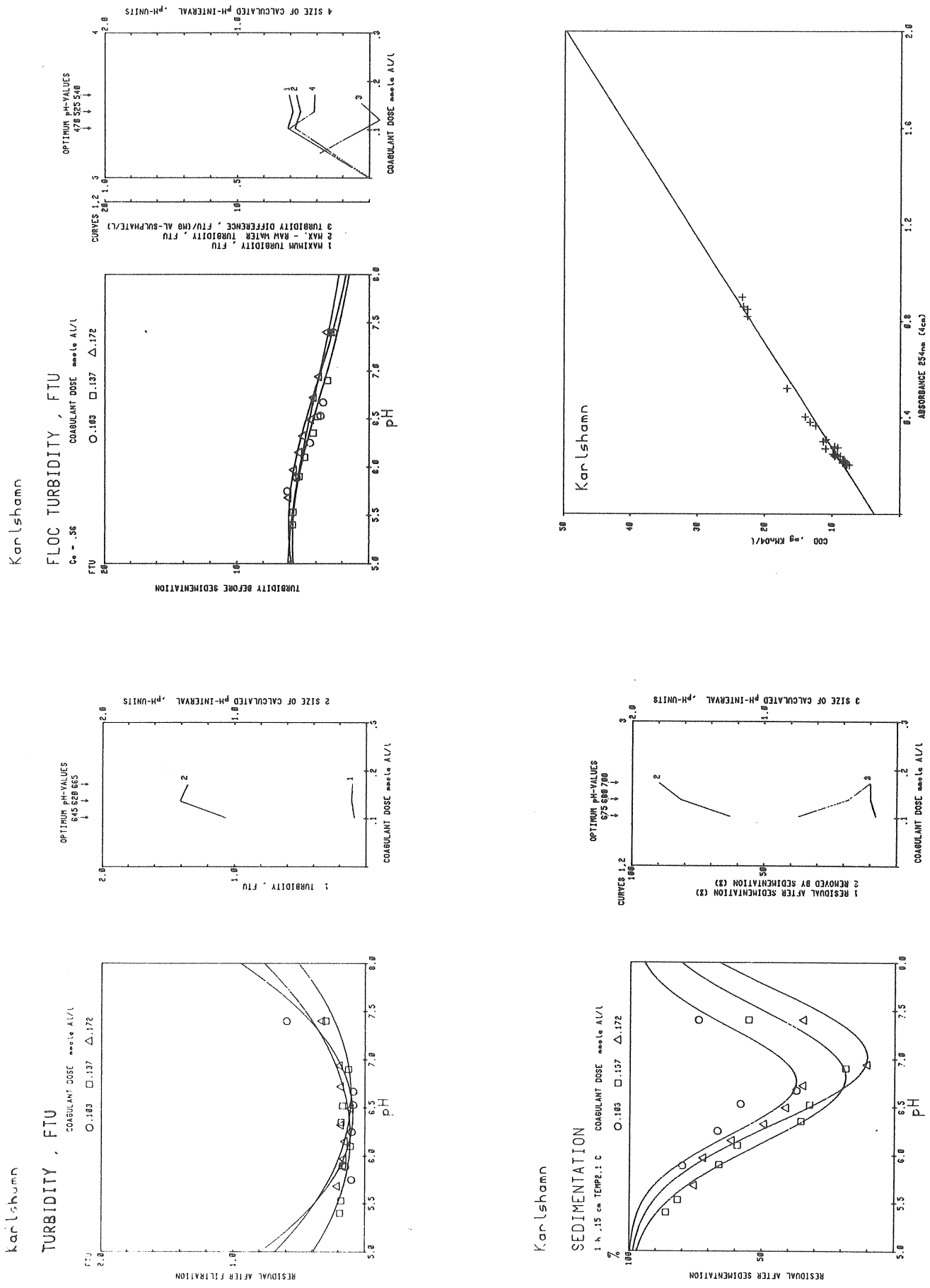

Fig 2-16. Results from coagulation tests at Kramfors water treatment plant

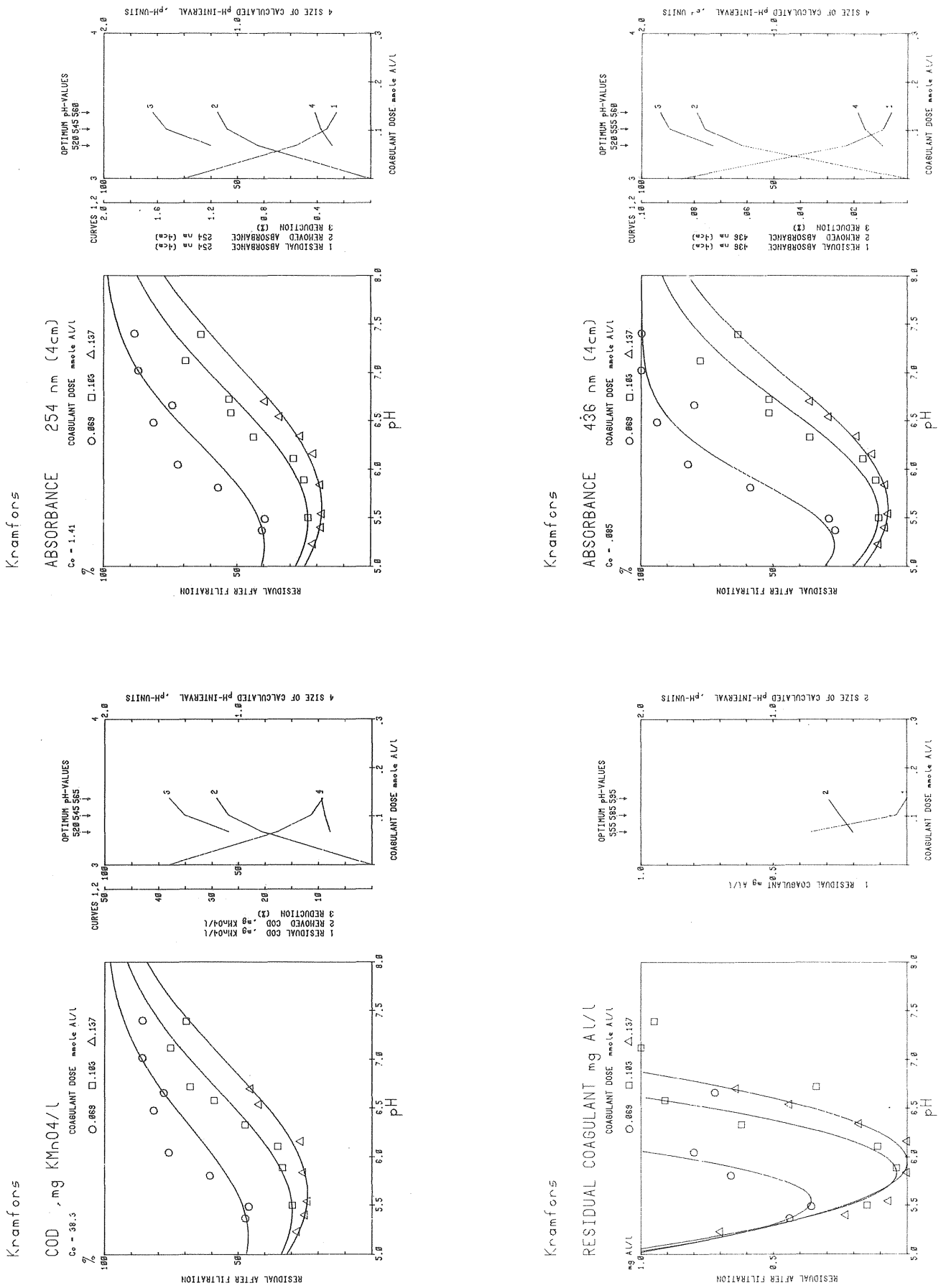

Fig 2-17. Results from coagulation tests at Kramfors water treatment plant (contd)

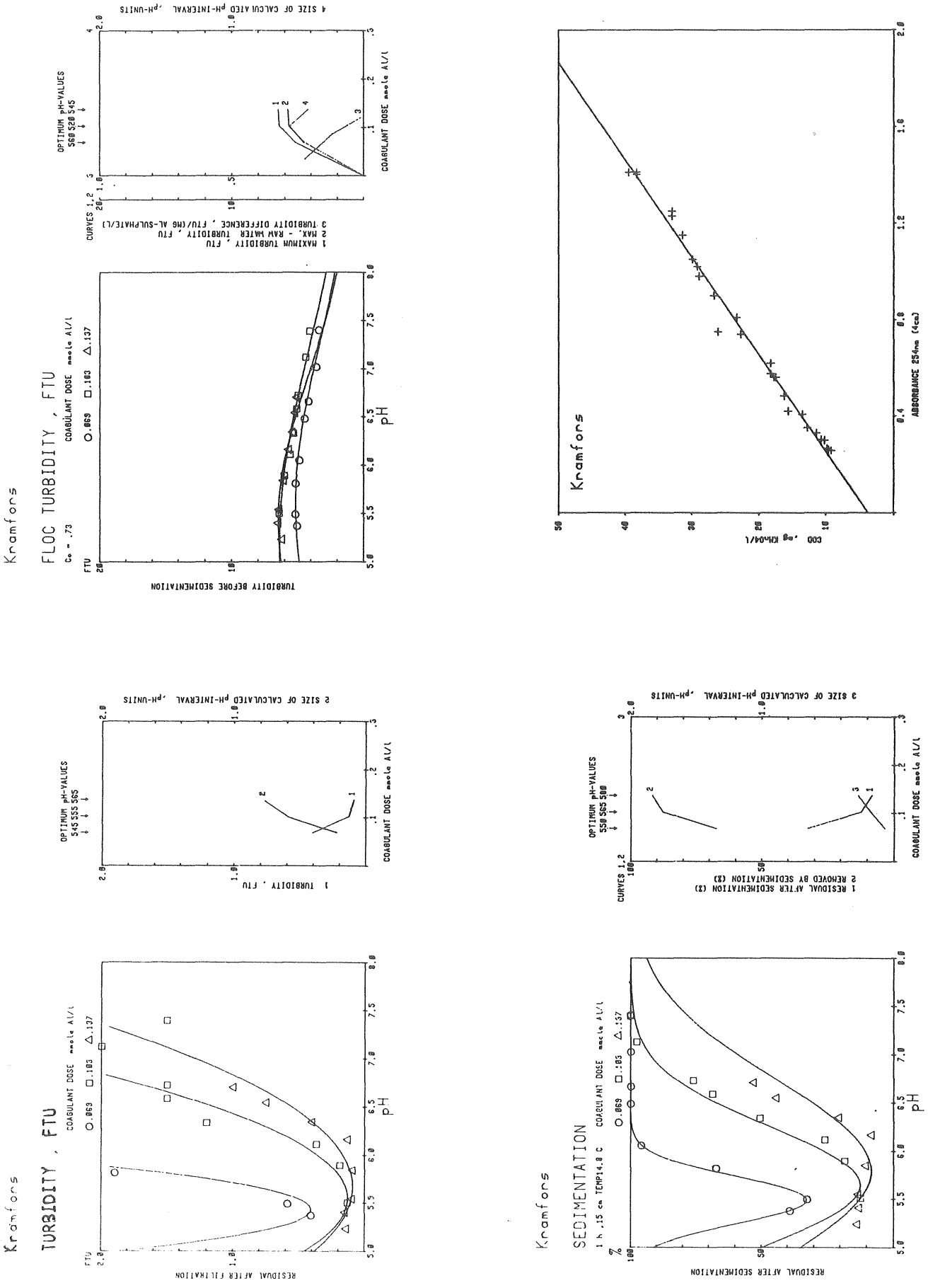

Fig 2-18. Results from coagulation tests at Lidköping water treatment plant

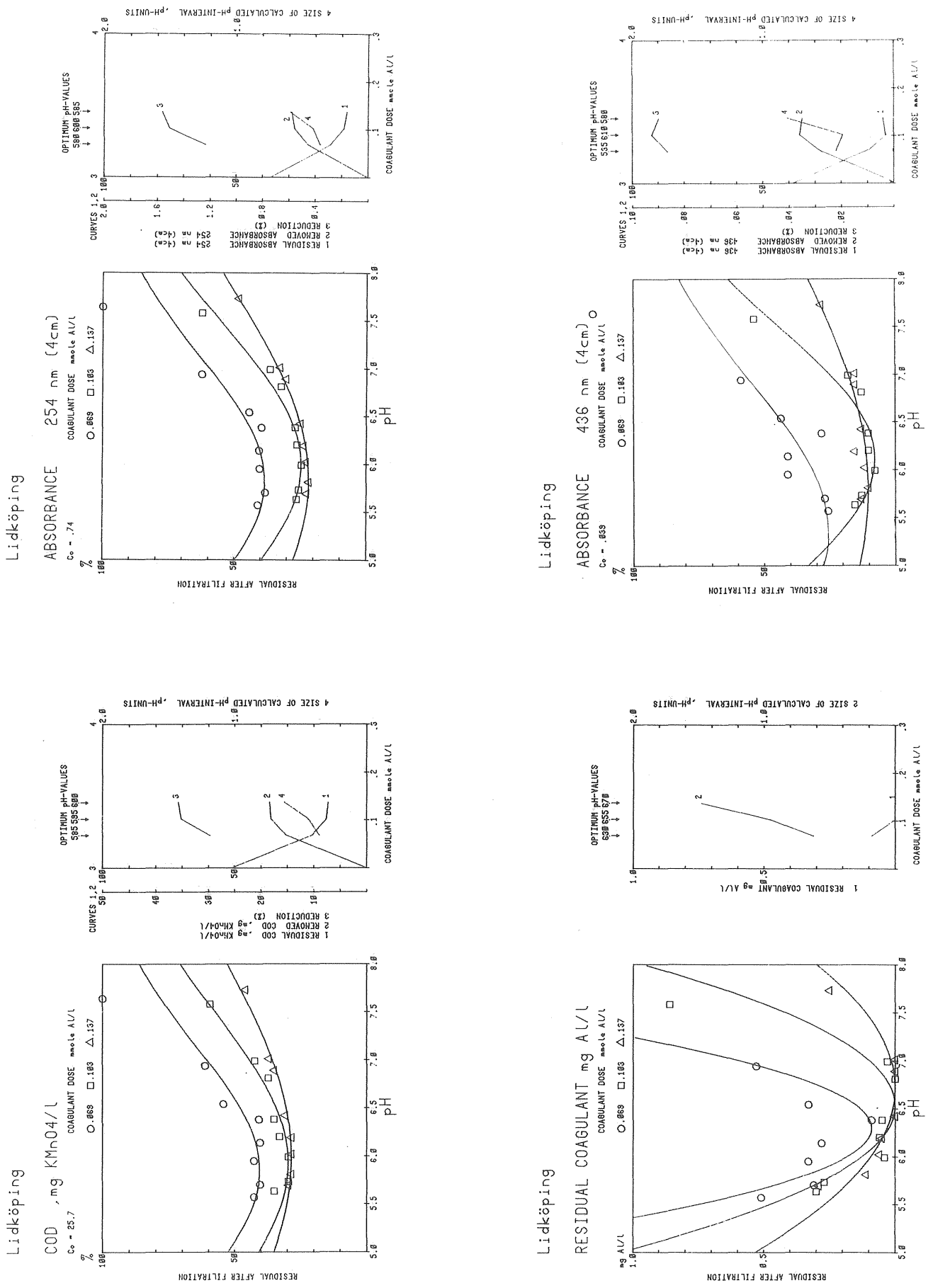

Fig 2-19. Results from coagulation tests at Lidköping water treatment plant (contd)

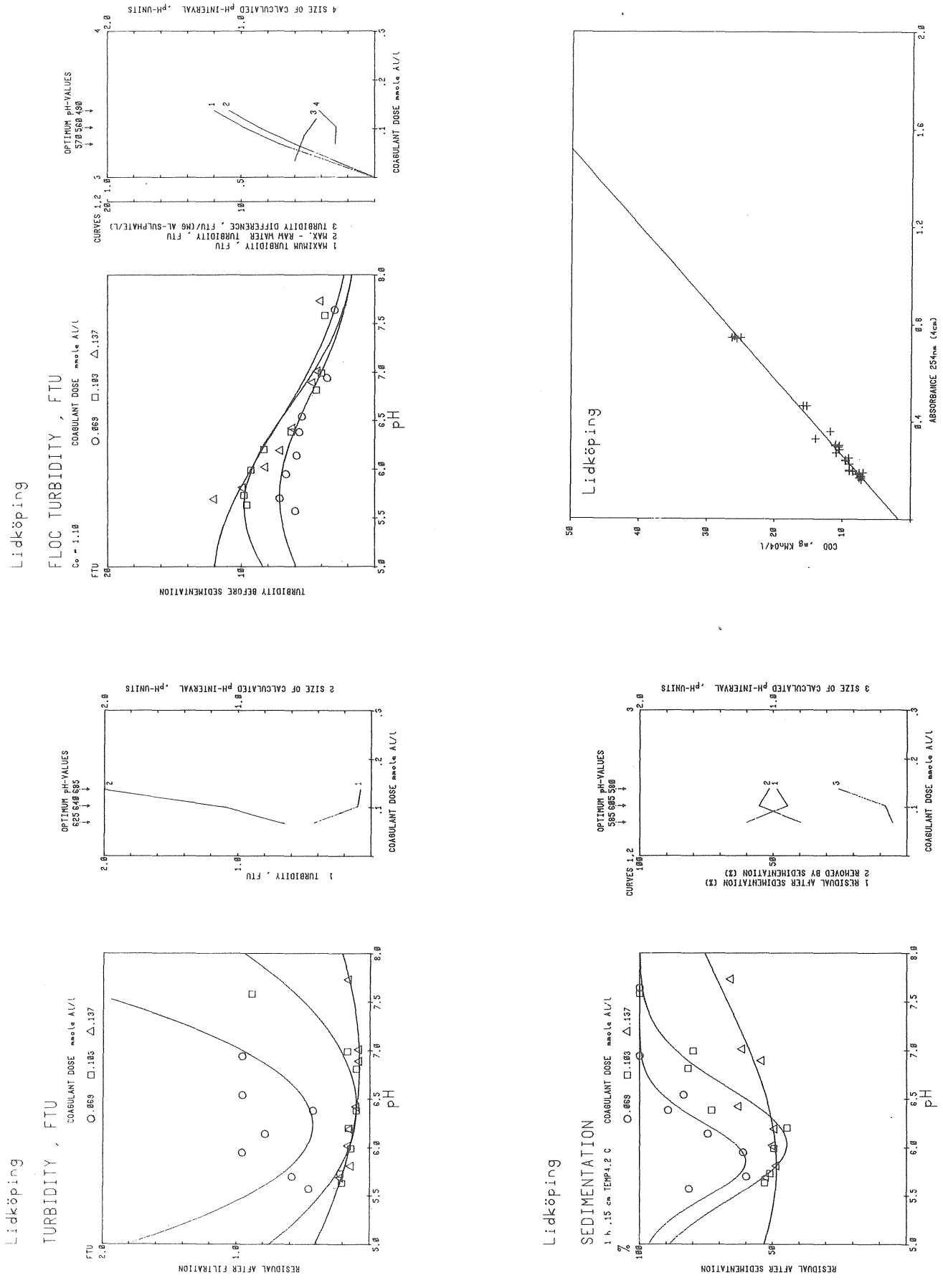

Fig 2-20. Results from coagulation tests at Lilla Edet water treatment plant

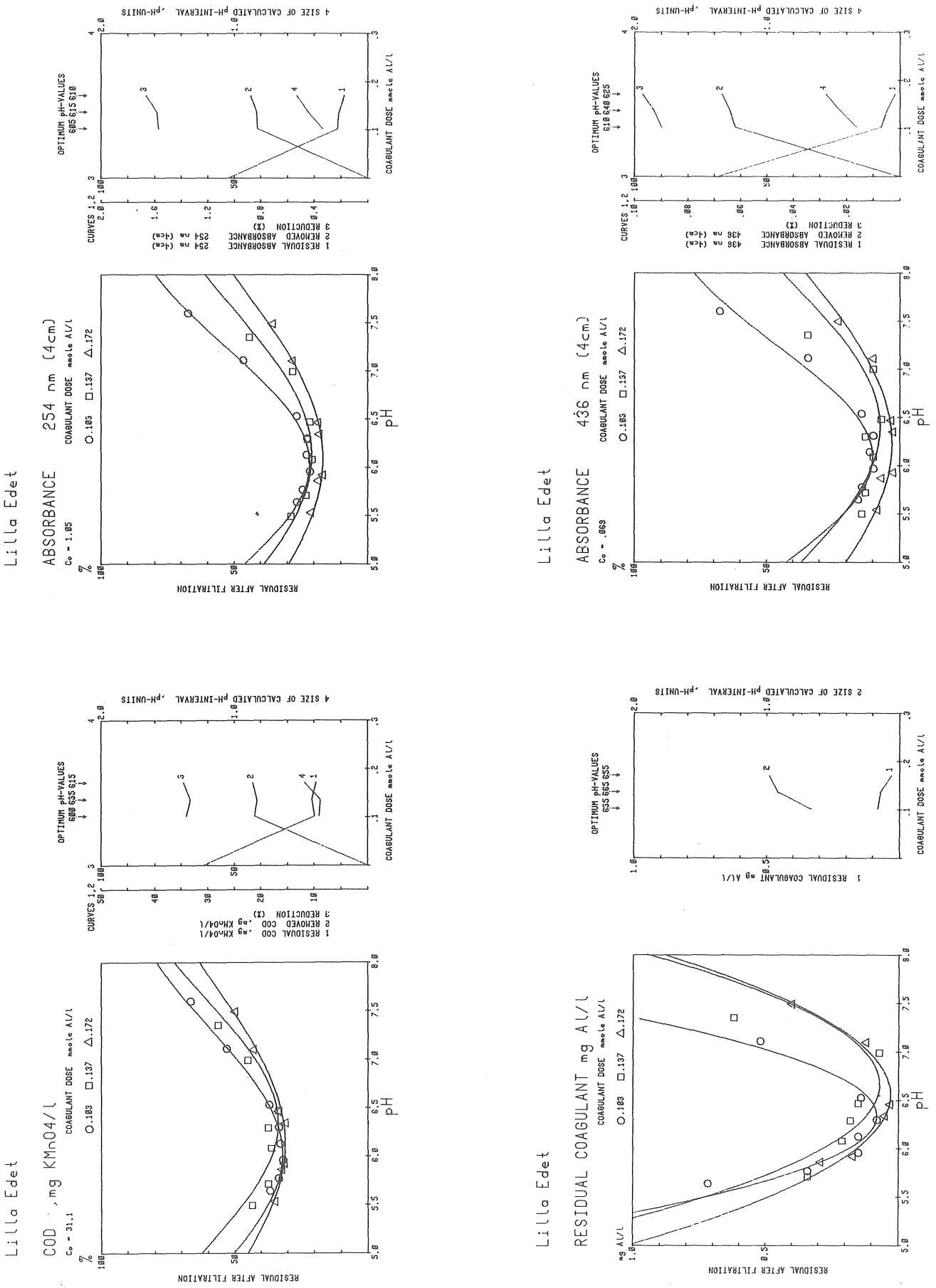

Fig 2-21. Results from coagulation tests at Lilla Edet water treatment plant (contd)

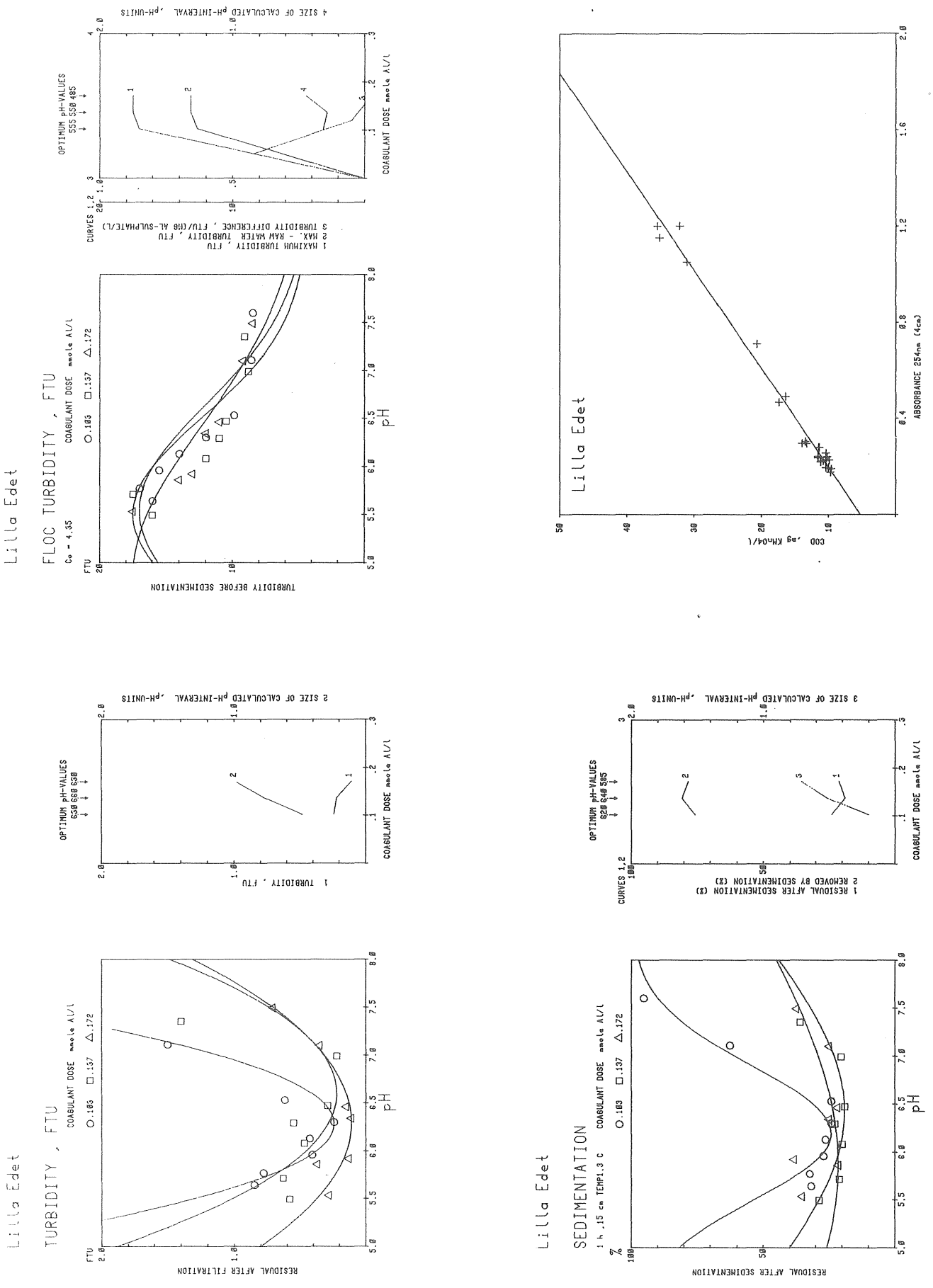

Fig 2-22. Results from coagulation tests at Mariestad water treatment plant

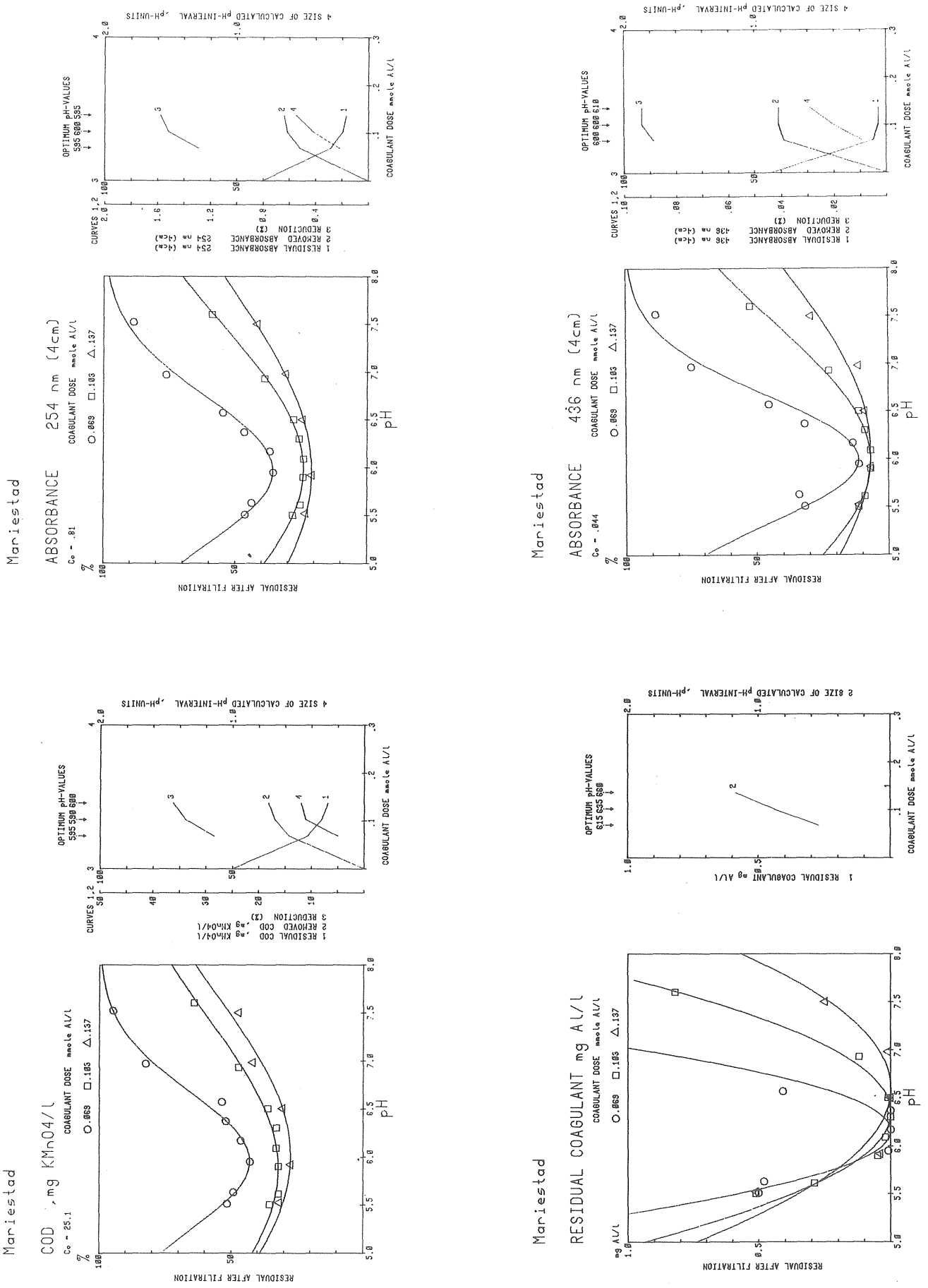

Fig 2-23. Results from coagulation tests at Mariestad water treatment plant (contd)

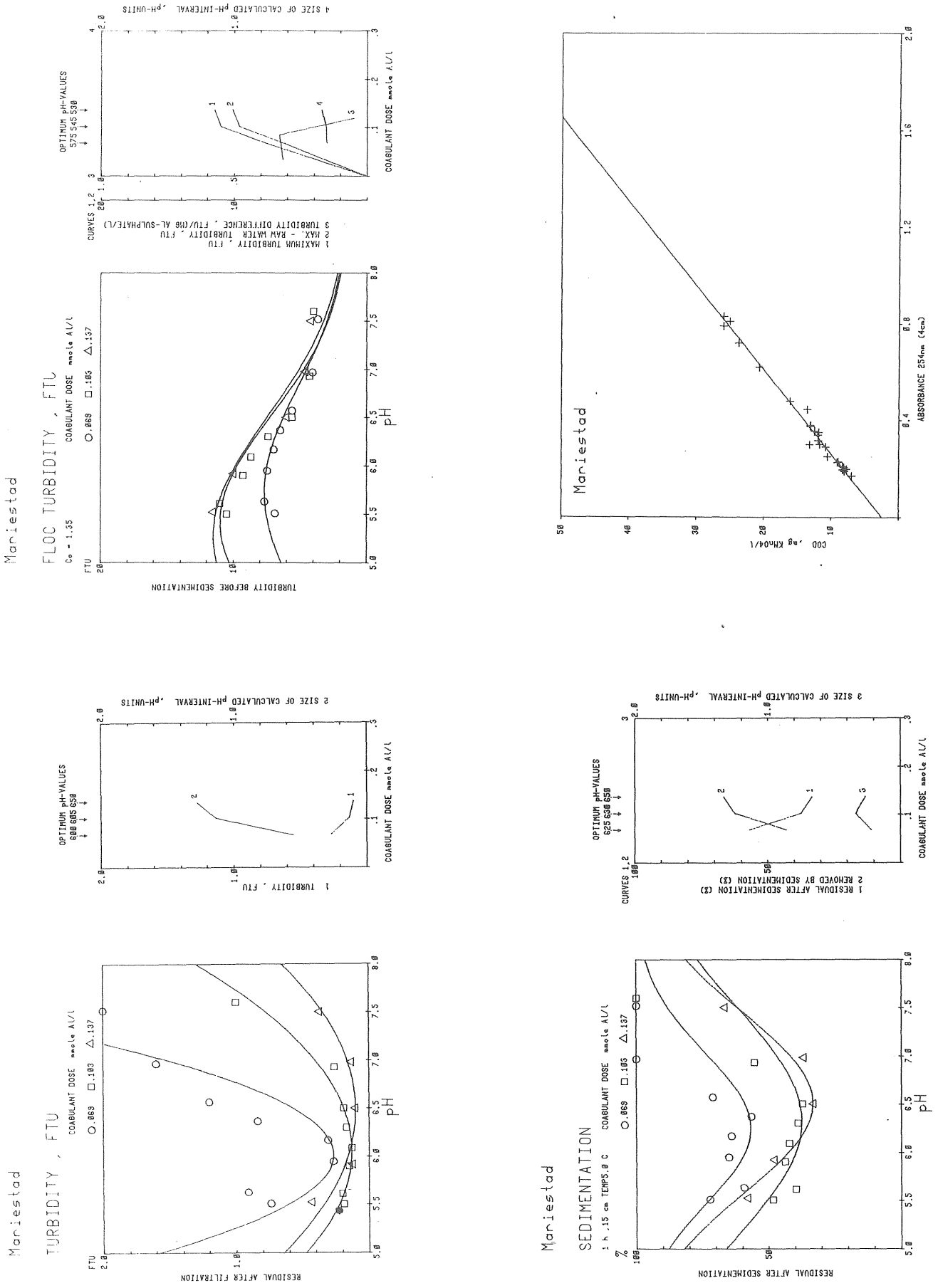

Fig 2-24. Results from coagulation tests at Mjölby water treatment plant

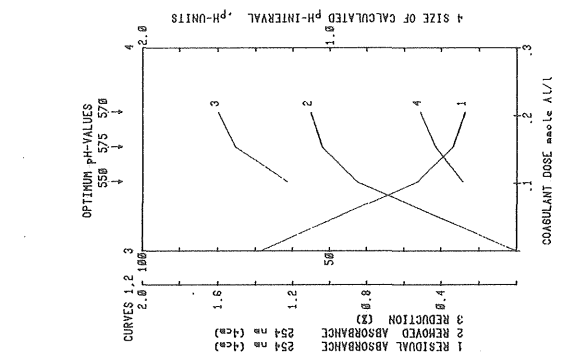

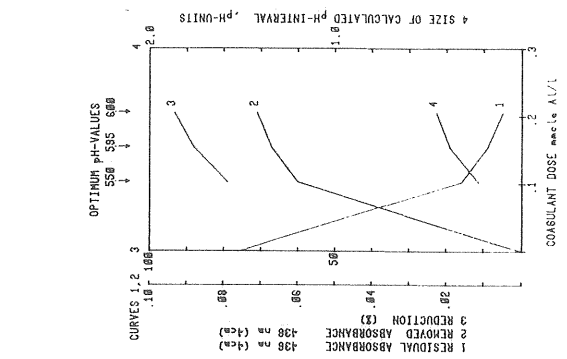

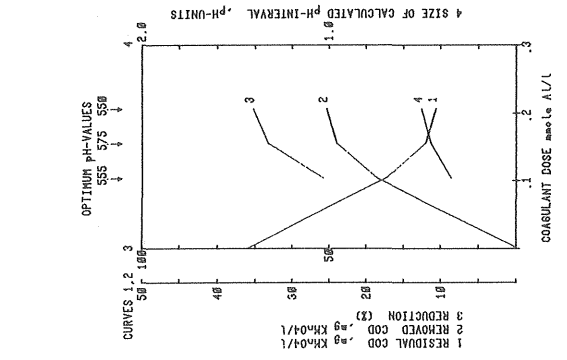

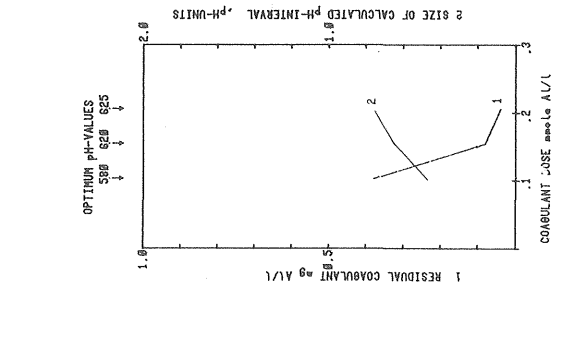

Fig 2-25. Results from coagulation tests at Mjölby water treatment plant (contd)

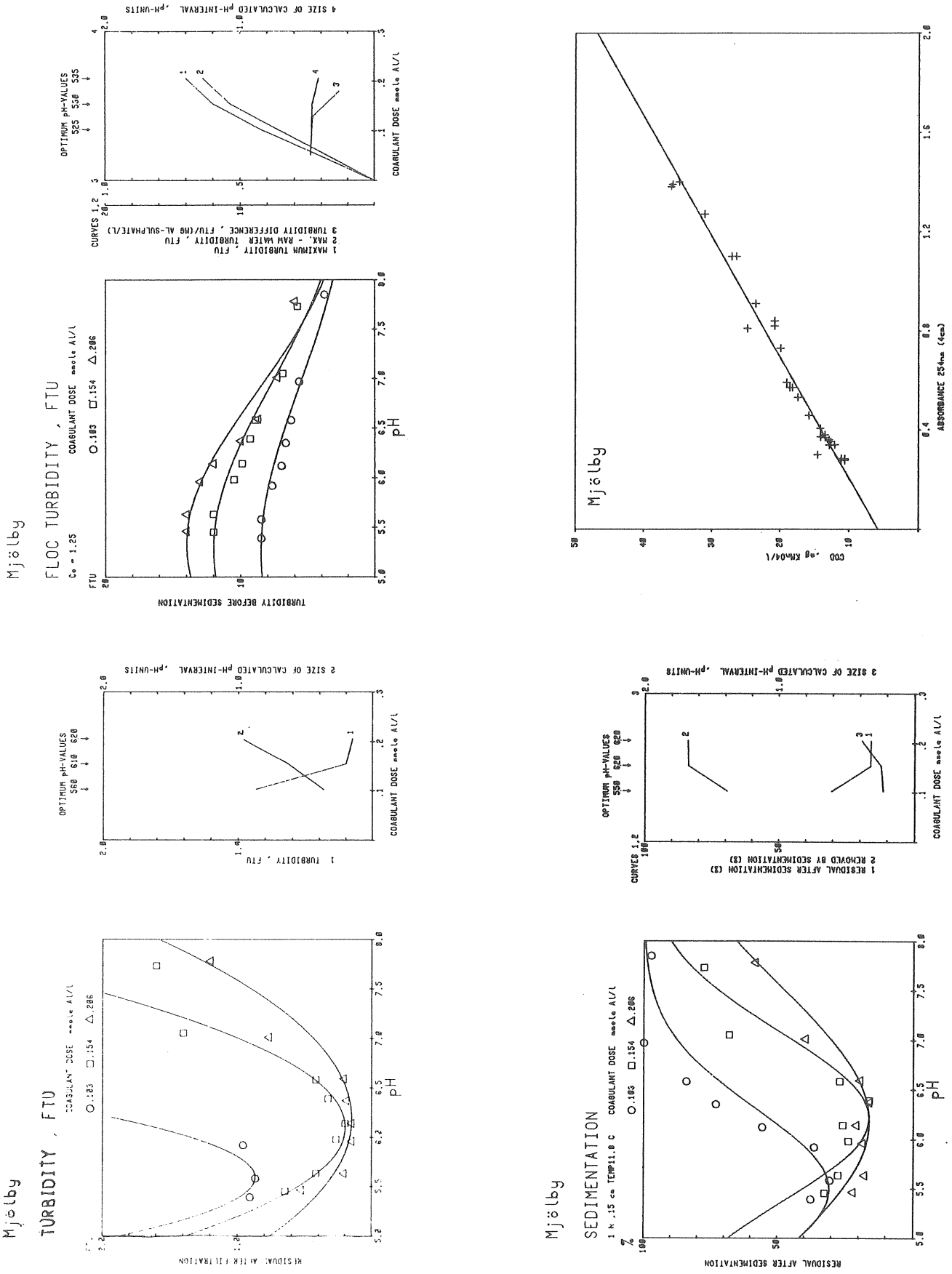

Fig 2-26. Results from coagulation tests at Mölndal water treatment plant

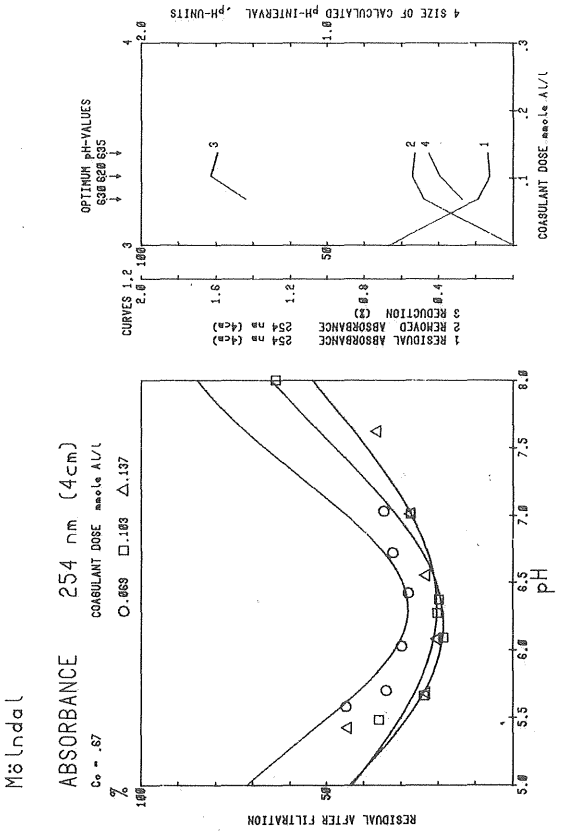

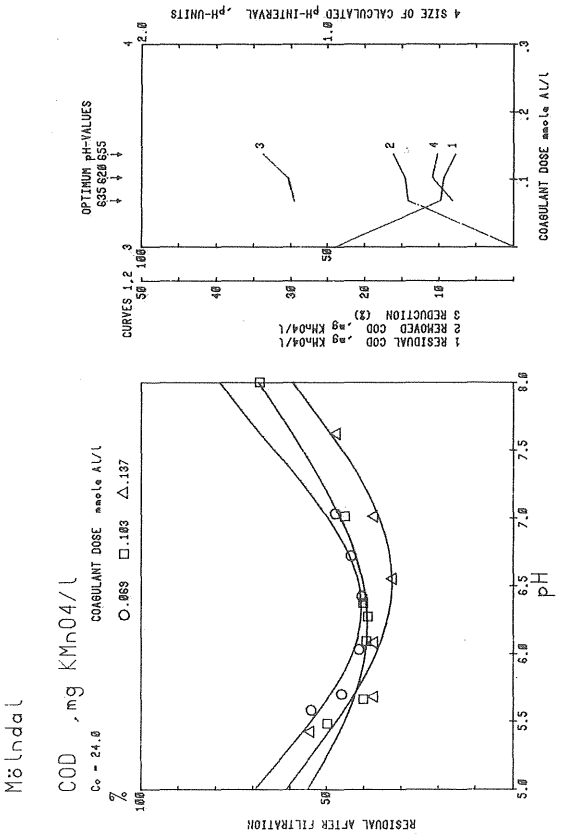

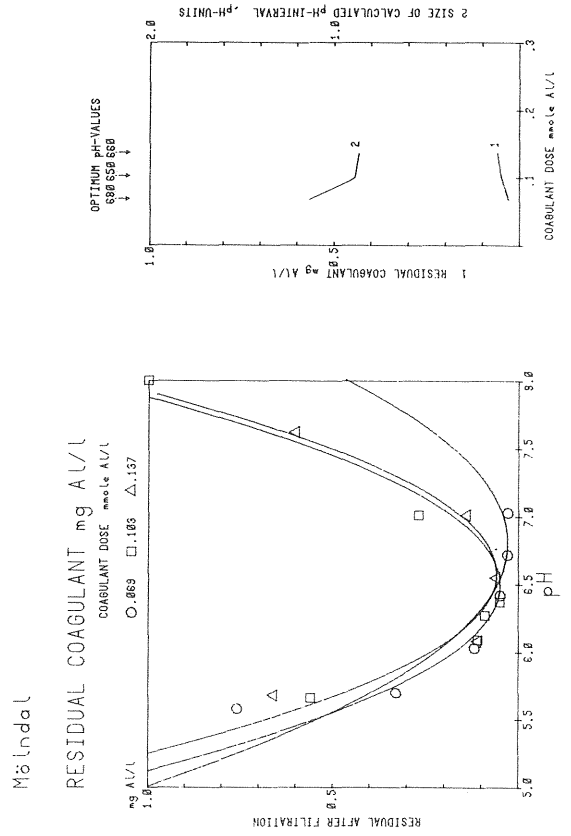

Fig 2-27. Results from coagulation tests at Mölndal water treatment plant (contd)

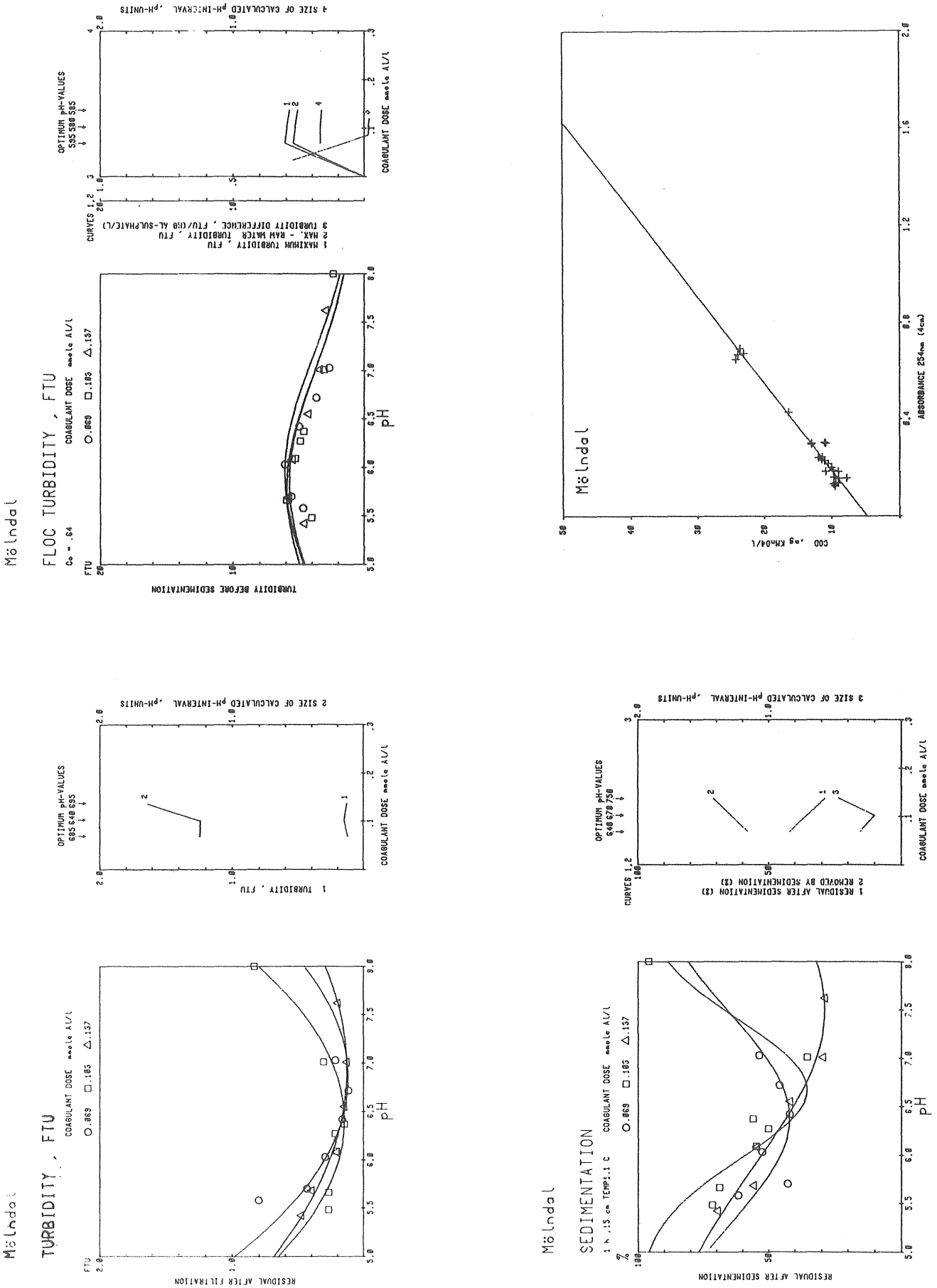

Fig 2-28. Results from coagulation tests at Mönsterås water treatment plant

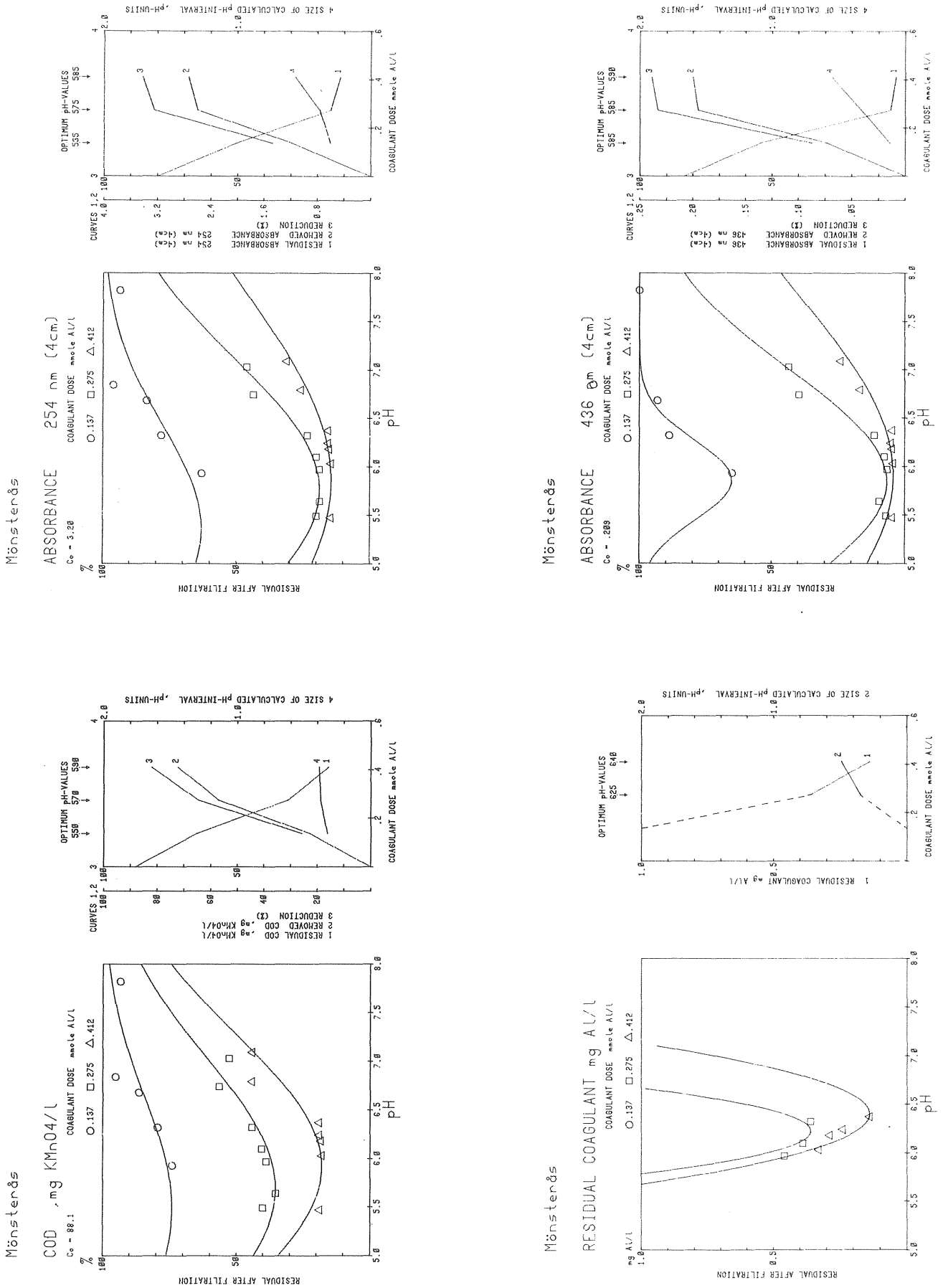

Fig 2-29. Results from coagulation tests at Mönsterås water treatment plant (contd)

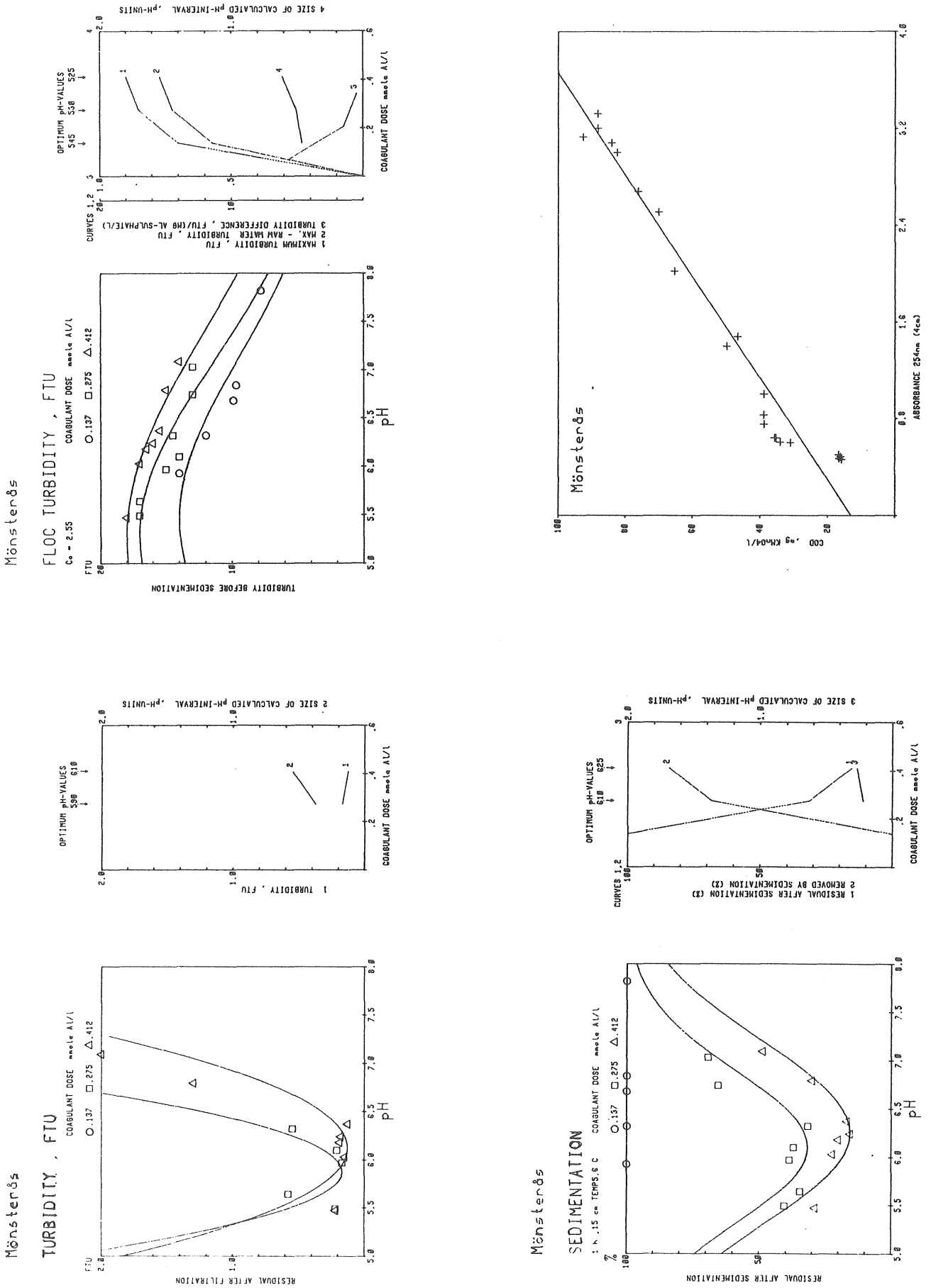

Fig 2-30. Results from coagulation tests at Norrköping water treatment plant

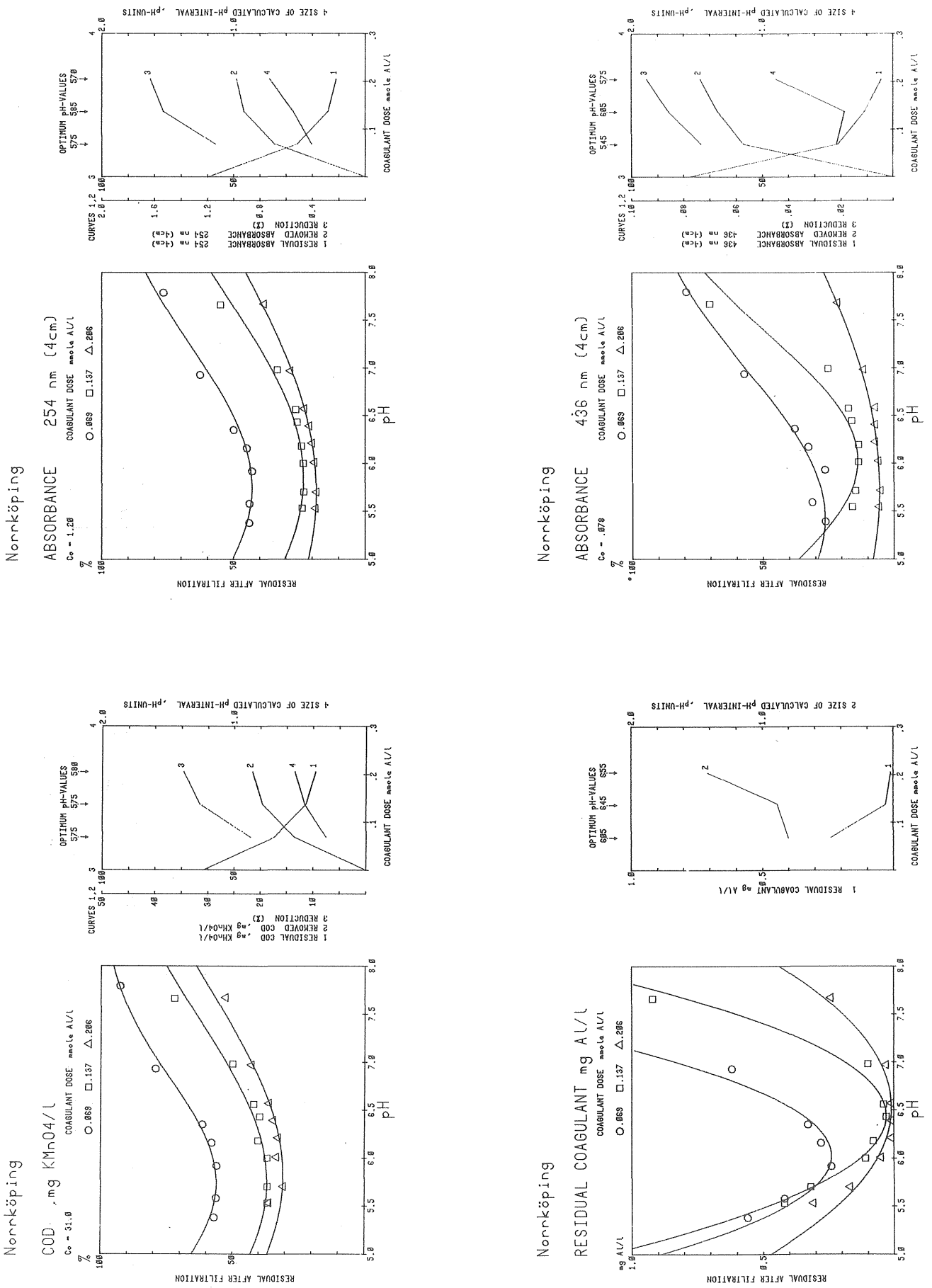

Fig 2-31. Results from coagulation tests at Norrköping water treatment plant (contd)

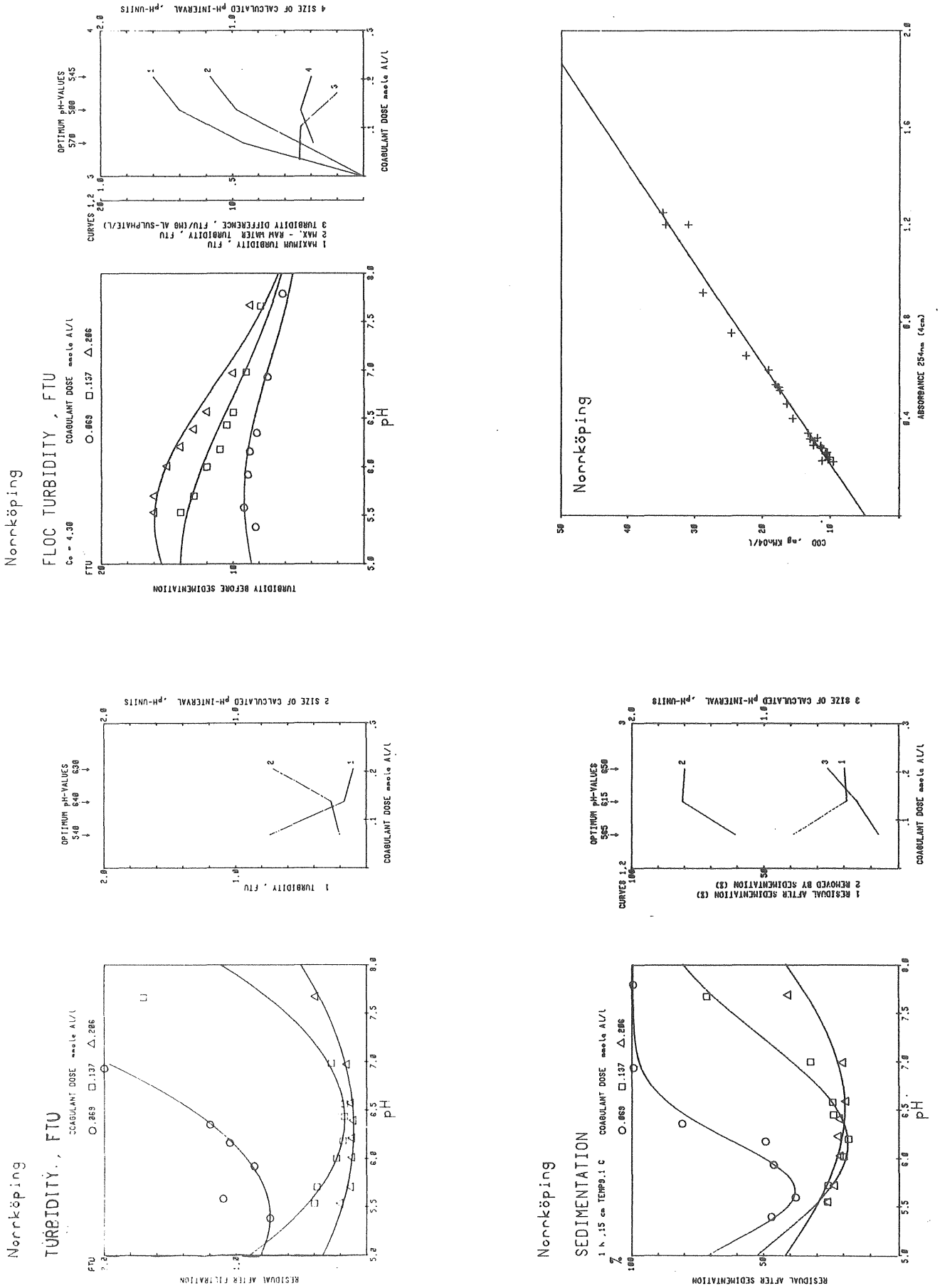

Fig 2-32. Results from coagulation tests at Nässjö water treatment plant

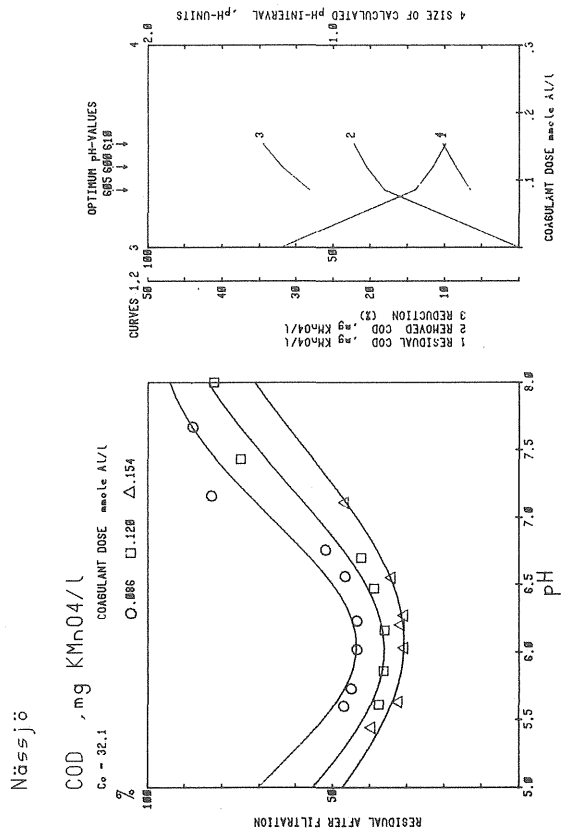

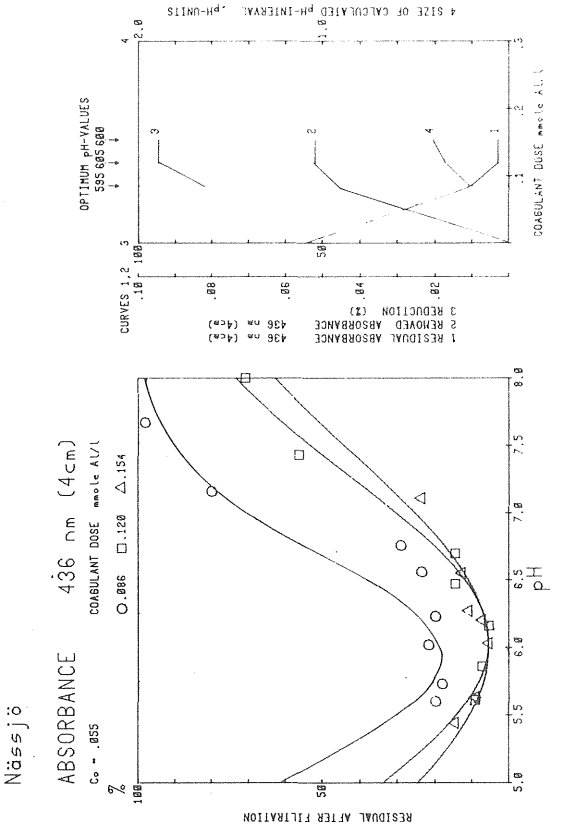

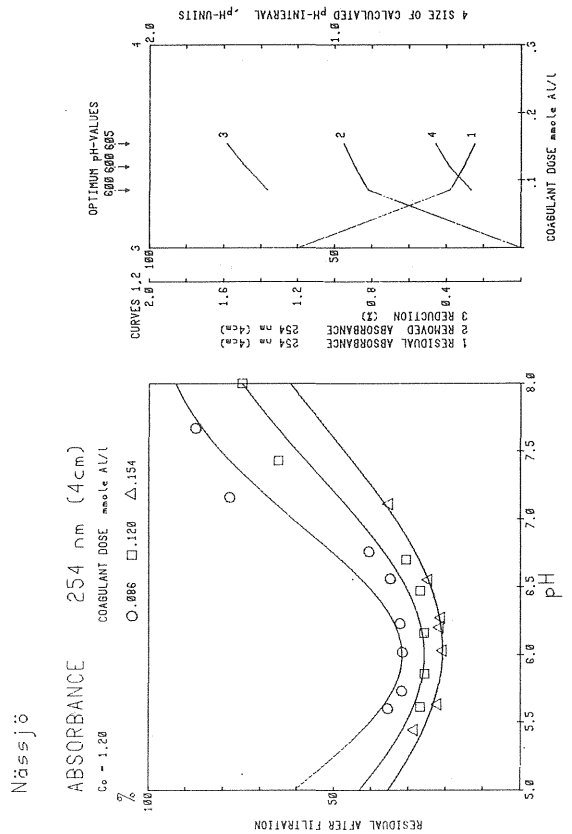

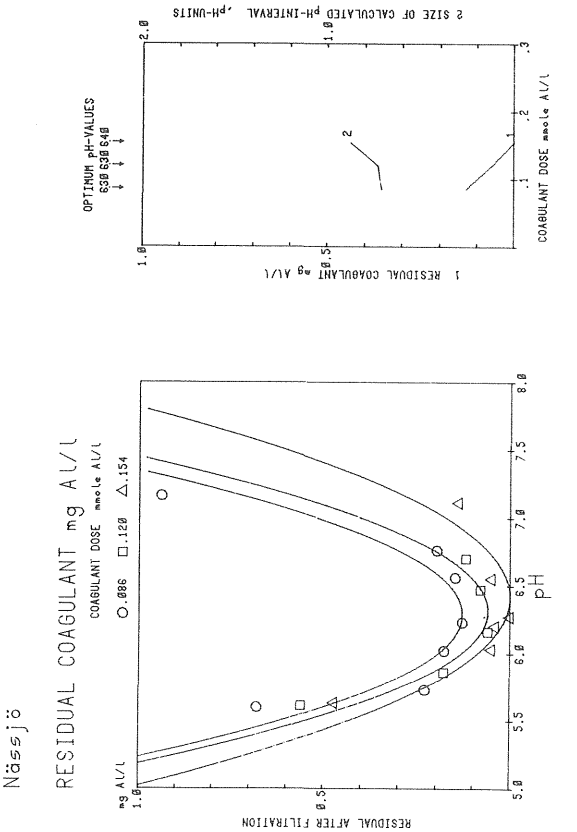

Fig 2-33. Results from coagulation tests at Nässjö water treatment plant (contd)

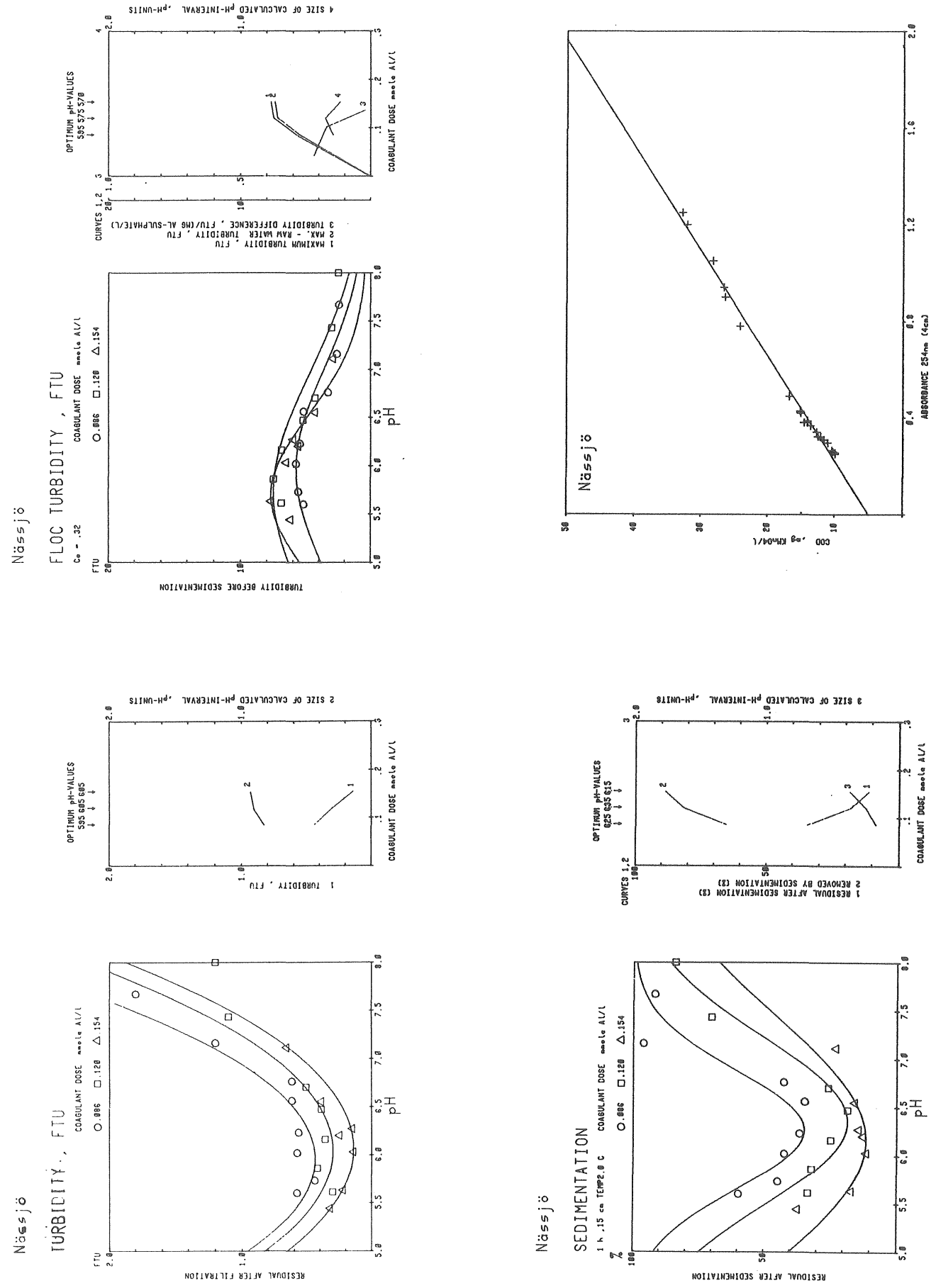

Fig 2-34. Results from coagulation tests at Säffle water treatment plant

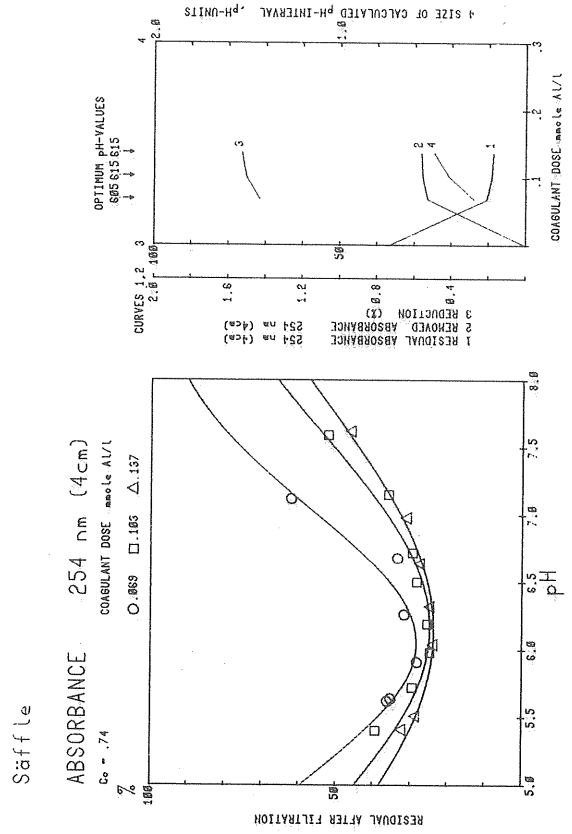

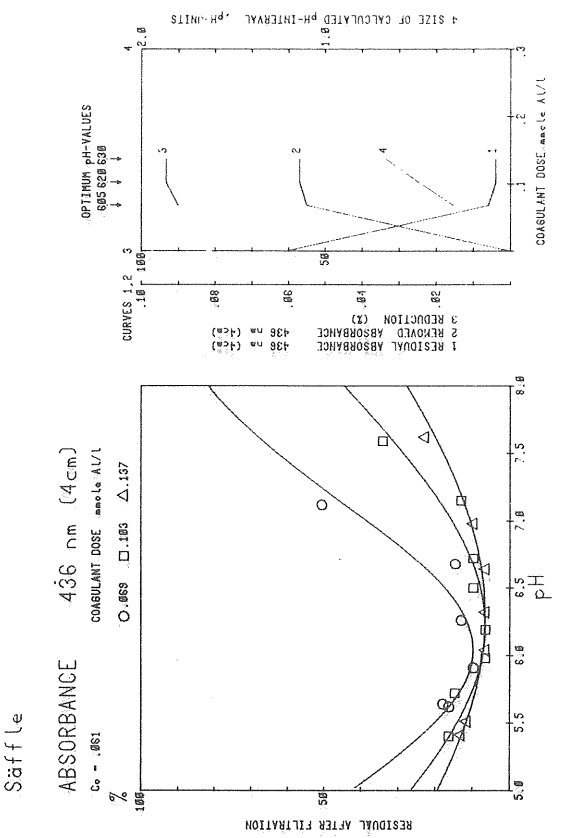

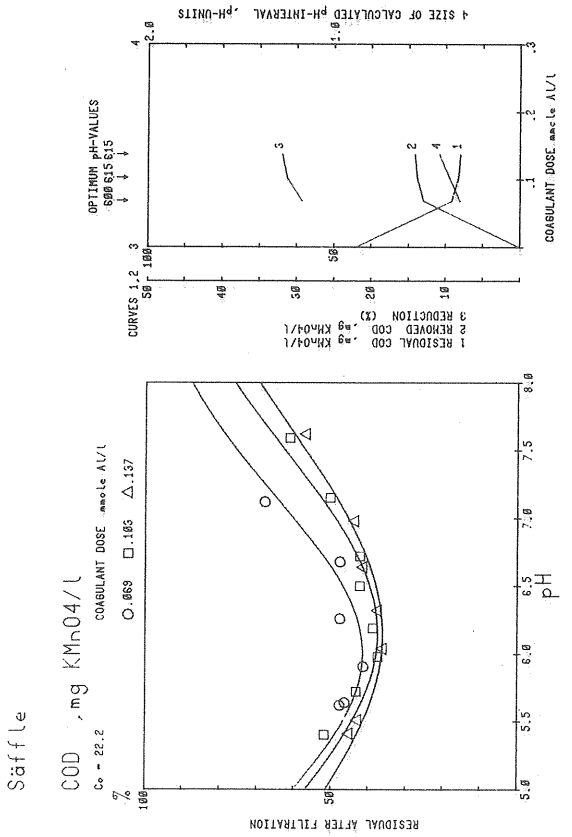

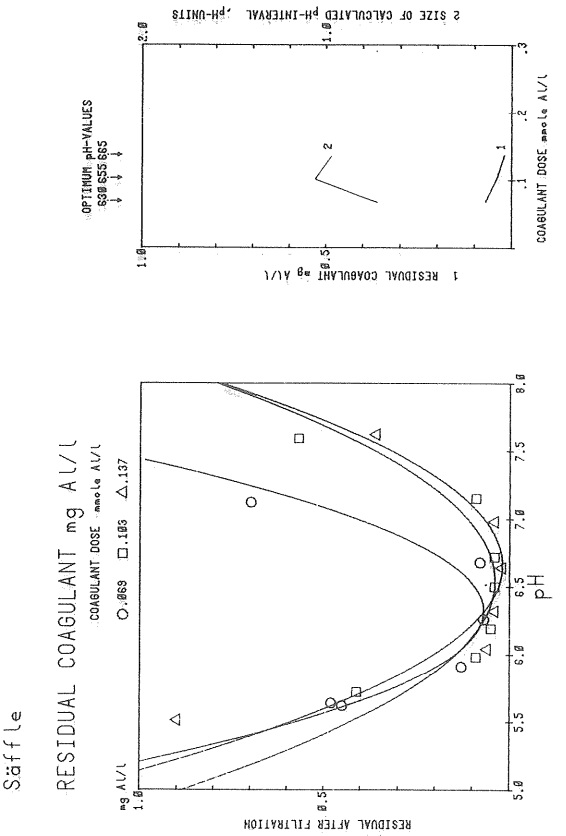

Fig 2-35. Results from coagulation tests at Säffle water treatment plant (contd)

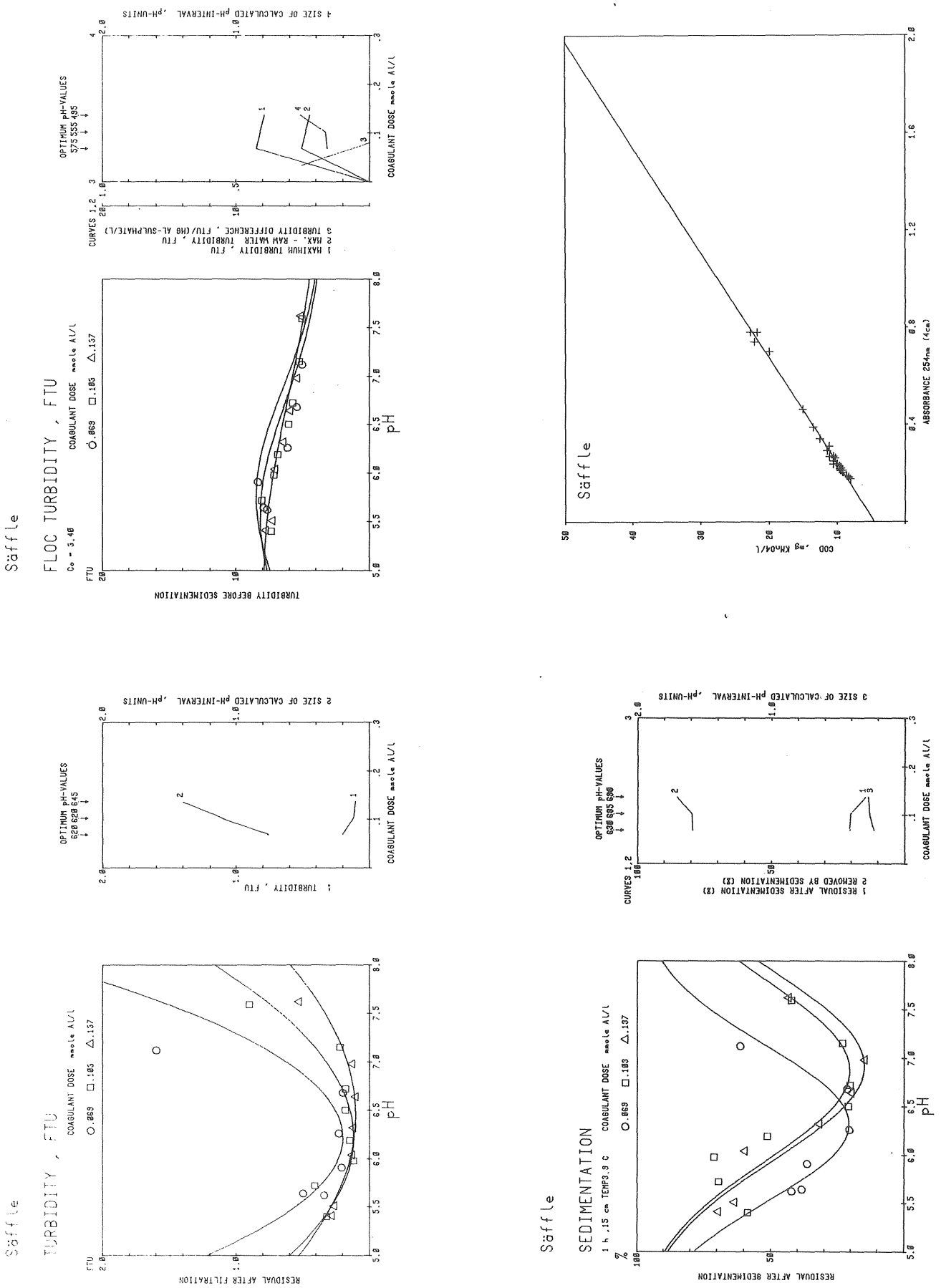

Fig 2-36. Results from coagulation tests at Västervik water treatment plant

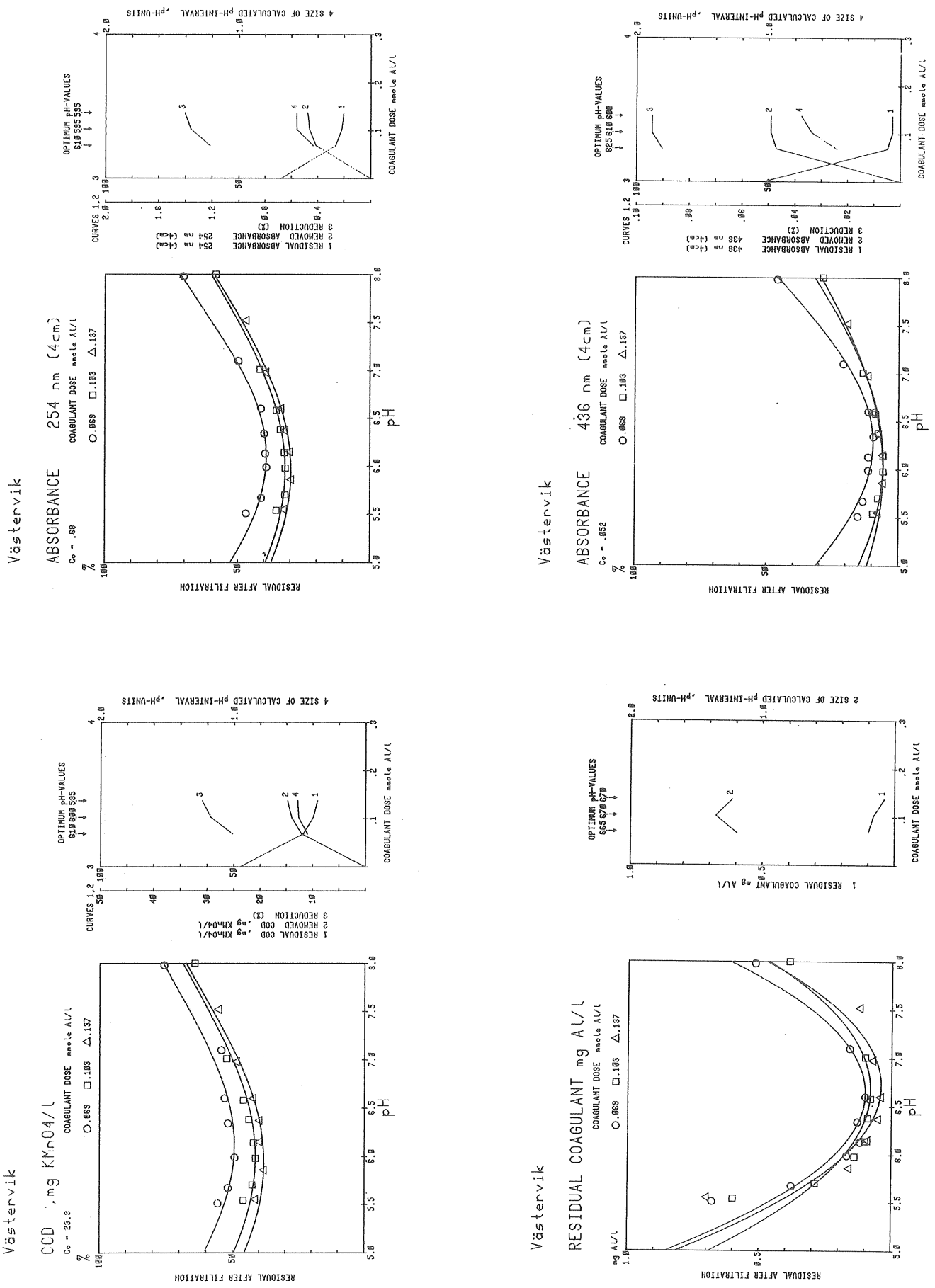

Fig 2-37. Results from coagulation tests at Västervik water treatment plant (contd)

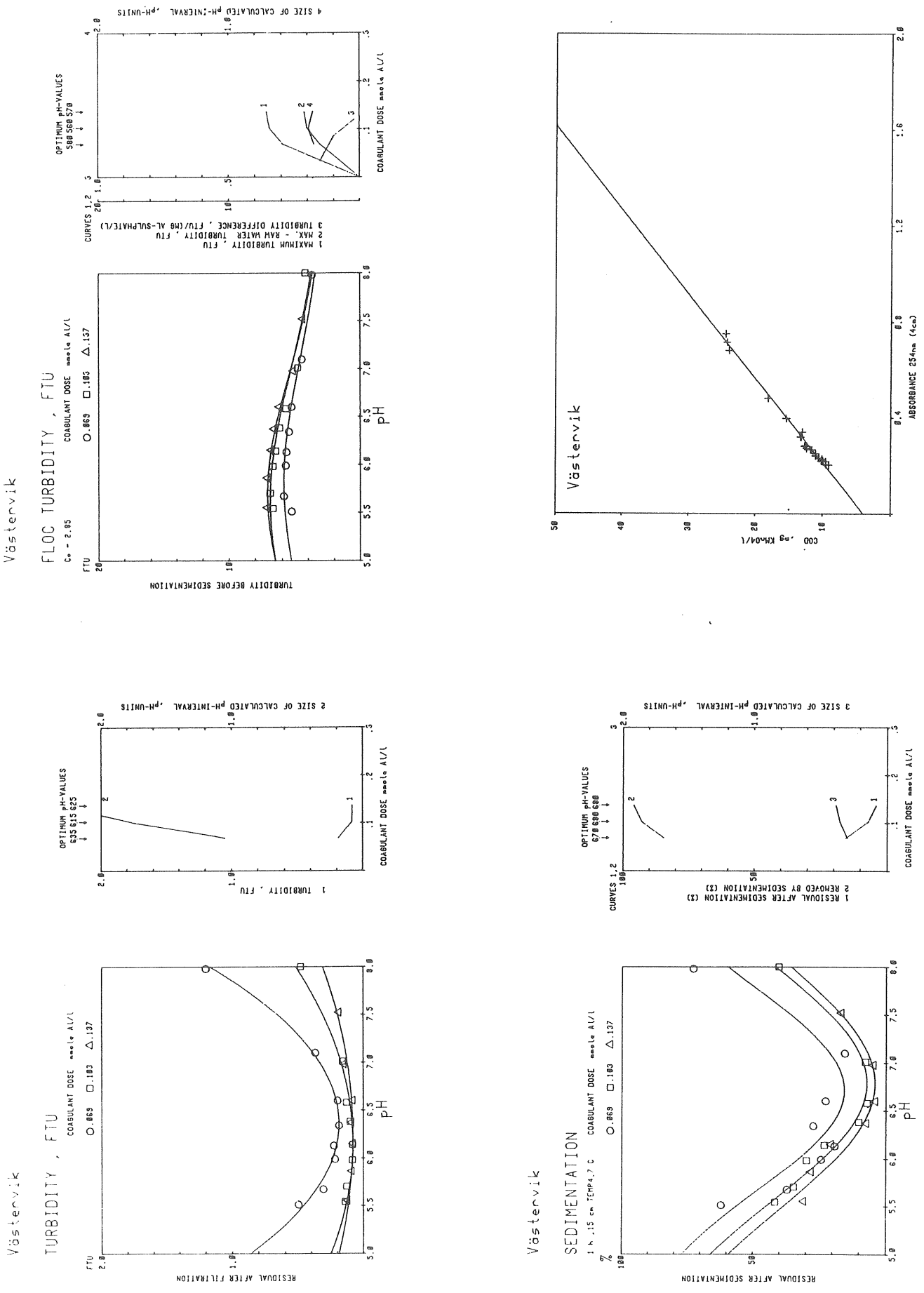

Fig 2-38. Results from coagulation tests at Uddevalla water treatment plant

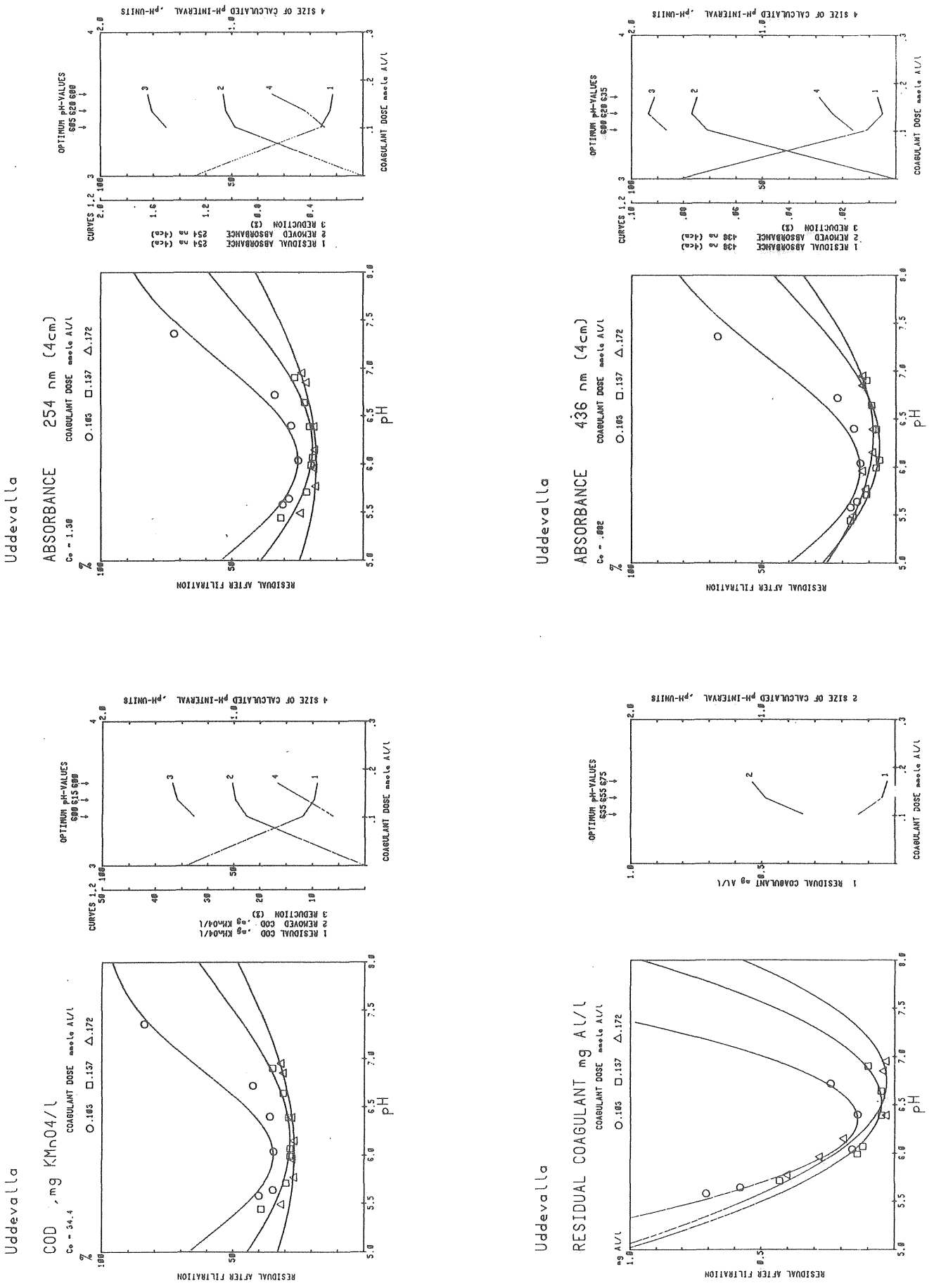

Fig 2-39. Results from coagulation tests at Udevalla water treatment plant (contd)

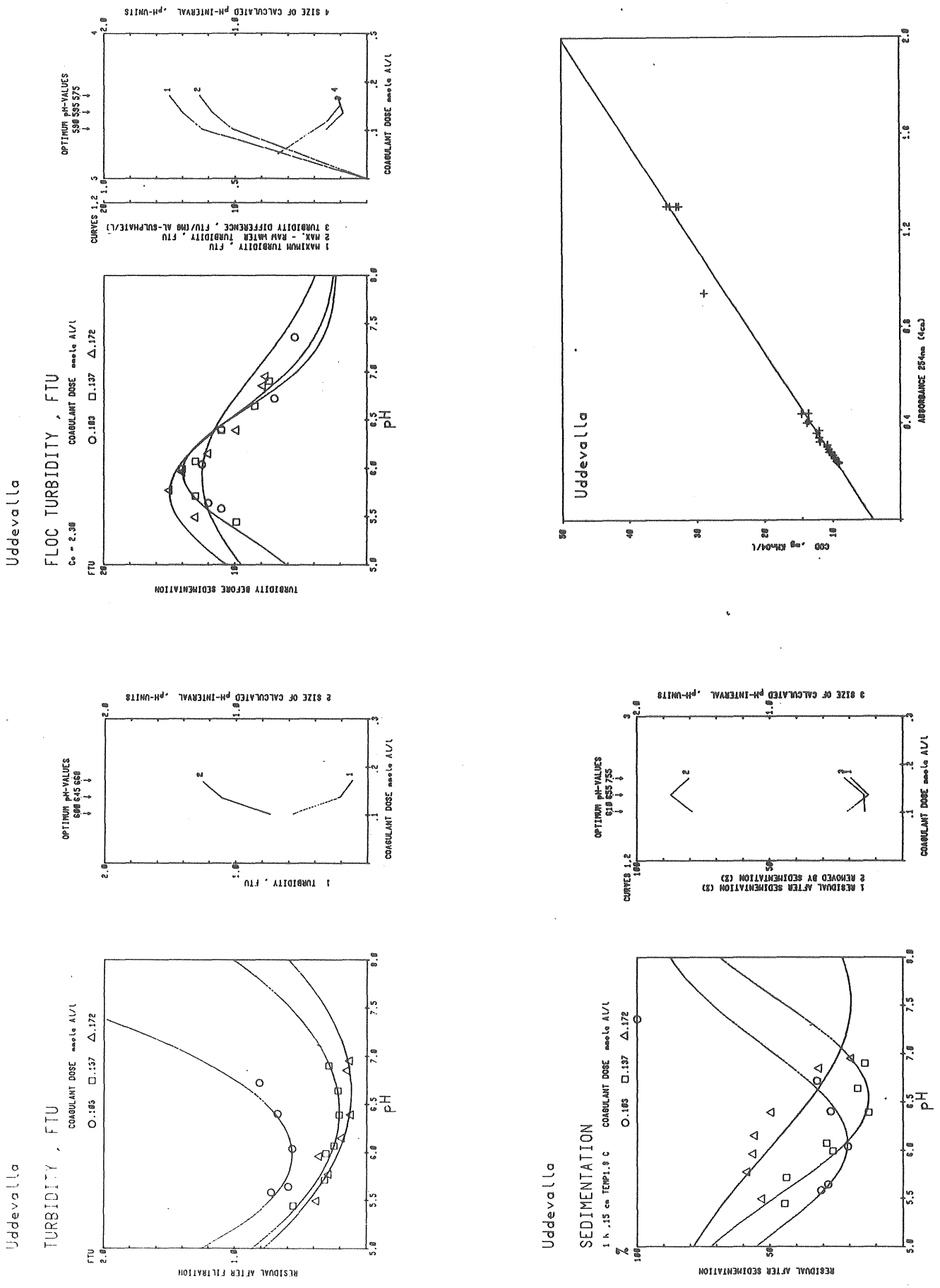

Fig 2-40. Results from coagulation tests at Åmål water treatment plant

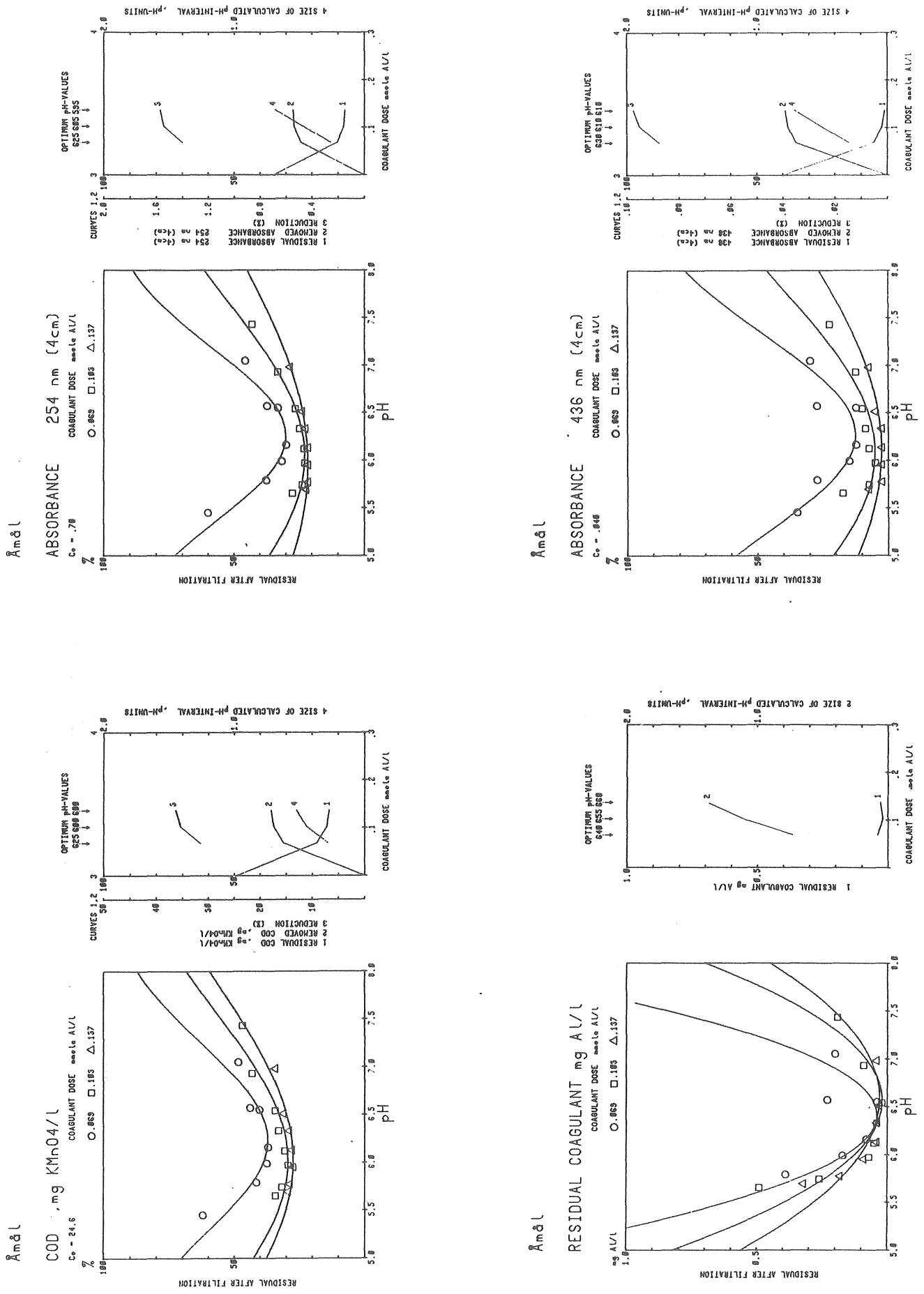

Fig 2-41. Results from coagulation tests at Åmål water treatment plant (contd)

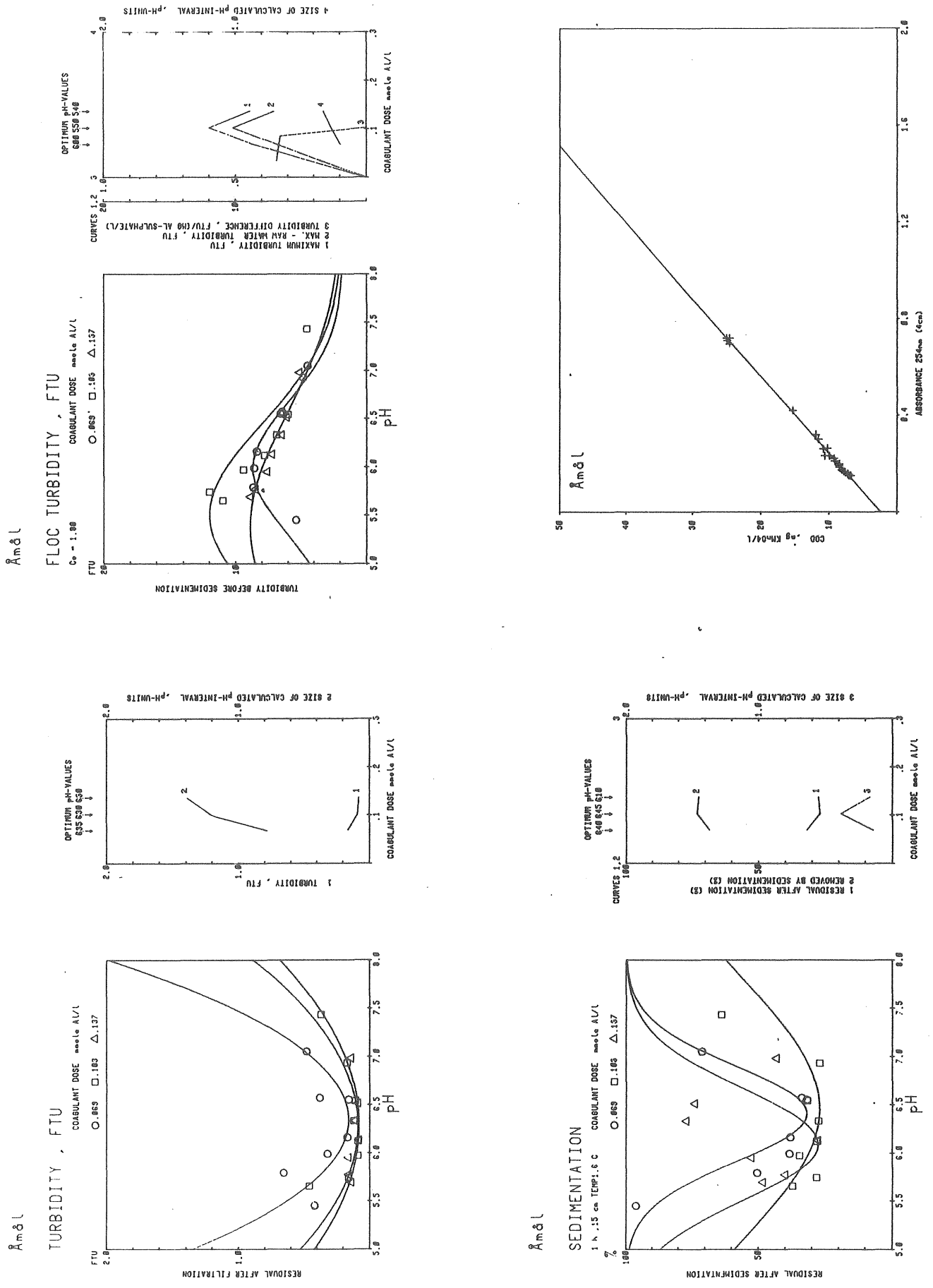

2.3.3 Summary of jar test results

2.3.3.1 General conclusions

The following general conclusion can be drawn from the figures 2.2 to 2.41:

Organic matter is removed to varying extent depending on the measure that is used. The removal efficiency, per unit of coagulant dose, decreases as the dose is increased; the total removal approaches a maximum value.

Typical values for the maximum removal of COD_{Mn}, E_{254} and E_{436} seem to be 70%, 80% and 95%. The latter value, because the absorbance at visible wavelengths is relatively low, includes an appreciable effect of the turbidity that is reduced at the same time.

A reasonably straight line is established when the two parameters COD_{Mn} and E_{254} are plotted against each other. In the permanganate analysis a constant amount, of maybe low molecular organic matter, is oxidized together with some of the total organic content. That part of the analysed value seems to be unaffected by the coagulant dose. As can be seen in the COD_{Mn}-E_{254} plots there is in all cases an intercept on the COD_{Mn}-axis.

With increased dosage, as removal increases, the characteristic pH-interval also increases. Optimum pH-values for removal of organics are virtually not effected by coagulant dose. Typical values are pH 5.7 - 5.8.

The minimum aluminium residual moves from pH-values around and below 6 up to ca. pH 6.5 as the dose is increased. The widening of the characteristic pH-interval is mainly due to increased removal efficiency (of Al) for higher pH-values. On the acid side the curve essentially remains the same. These effects are in accordance with the view presented by Packham, Section 2.3.1.

Hall and Packham (1965) proposed, as mentioned, a removal mechanism where humic substances are precipitated by the coagulant. In such a view, colloid destabilization mechanisms are not relevant and re-stabilization effects could not be expected. This is confirmed by the experiments. Not in any case, effects that could be interpreted as restabilization of humic colloids were observed.

Filtrate turbidity shows the same principal tendencies as the residual aluminium. However, the sensitivity to pH-changes is less, especially for low pH-values.

The pH for maximum floc turbidity, assumed to reflect optimum conditions for precipitation, essentially remains constant at the pH-values shown to be most effective for the removal of humic substances. This is not clearly understood. As shown to be the case for aluminium residual and turbidity in filtrate, and when sedimentation efficiency is measured, an increase of optimum pH-value can be observed as the aluminium sulphate dose increases. Thus the same behaviour for maximum floc turbidity was expected. Further it was expected that the floc turbidity should increase linearly with coagulant dose. This can be observed sometimes at moderate doses, but this effect does not always occur. The measured floc turbidity caused by the same coagulant dose varies considerably, if different raw waters are compared. Maybe these unexplained effects can be caused by errors inherent in the turbidity measurement. It is known that e.g. particle size distribution affects the light reflecting properties, but in the analysis efforts were made to minimize this influence.

2.3.3.2 Determination of required dose of coagulant

The determination of the required dose of aluminium sulphate is dependent on the acceptable residual of the parameter in consideration. Instead of a fixed residual, the dose to achieve a certain removal percentage can be determined. Packham (1963), studying turbidity removal, considered the dose that halved the initial turbidity.

The determination becomes more complicated when there are more than one parameter to take into account. Here it was decided to apply the following values as desirable limits for each analytical value:

Table 2-3. Analytical values for comparison with filtrate quality.

$E_{254}^{4\ cm} = 0.25$

$COD_{Mn} = 10$ mg $KMnO_4/l$

$E_{436}^{4\ cm} = 0.005$

Aluminium = 0.05 mg Al^{3+}/l

Turbidity = 0.15 FTU

These values were chosen to serve as a means to compare the different raw waters. They represent a reasonably good filtrate quality, that usually can be obtained without any great difficulty.

The required dose was calculated from the curves obtained according to Section 2.3.2.5, and was determined as the least amount of aluminium sulphate to be added for eq (2-17) to be valid at a certain pH-value:

$$\frac{\Sigma\left(\frac{Y_i}{Y_{k,i}} \cdot w_i\right)}{\Sigma w_i} < 1 \qquad (2\text{-}17)$$

where Y_i is filtrate residual, parameter i
w_i is weighing factors
$Y_{k,i}$ is values according to table 2-3.

The weighing factors were chosen to be 1.0 for turbidity, 2.0 for E_{254}, COD_{Mn} and E_{436} and 3.0 for aluminium residual.

In table 2-4 the obtained required coagulant doses and the optimum pH-values are shown.

Table 2-4. Required coagulant dose and optimum pH-value

	Dose mg aluminium sulphate/l	Optimum pH-value
Borås	40	6,4
Grängesberg	19	6,2
Göteborg (Lackarebäck)	28	6,5
Hofors	20	6,1
Helsingborg (Ringsjön)	87	6,5
Härnösand	29	6,5
Karlshamn	30	6,3
Kramfors	37	5,9
Lidköping	27	6,3
Lilla Edet	45	6,5
Mariestad	24	6,2
Mjölby	62	6,2
Mölndal	21	6,5
Mönsterås	145	6,5
Norrköping	53	6,3
Nässjö	40	6,3
Säffle	27	6,4
Västervik	35	6,6
Uddevalla	51	6,7
Åmål	25	6,3

Figures 2.42 to 2.44 shows how the required dose varies with COD_{Mn}, $E_{254}^{4\ cm}$ and $E_{436}^{4\ cm}$, respectively.

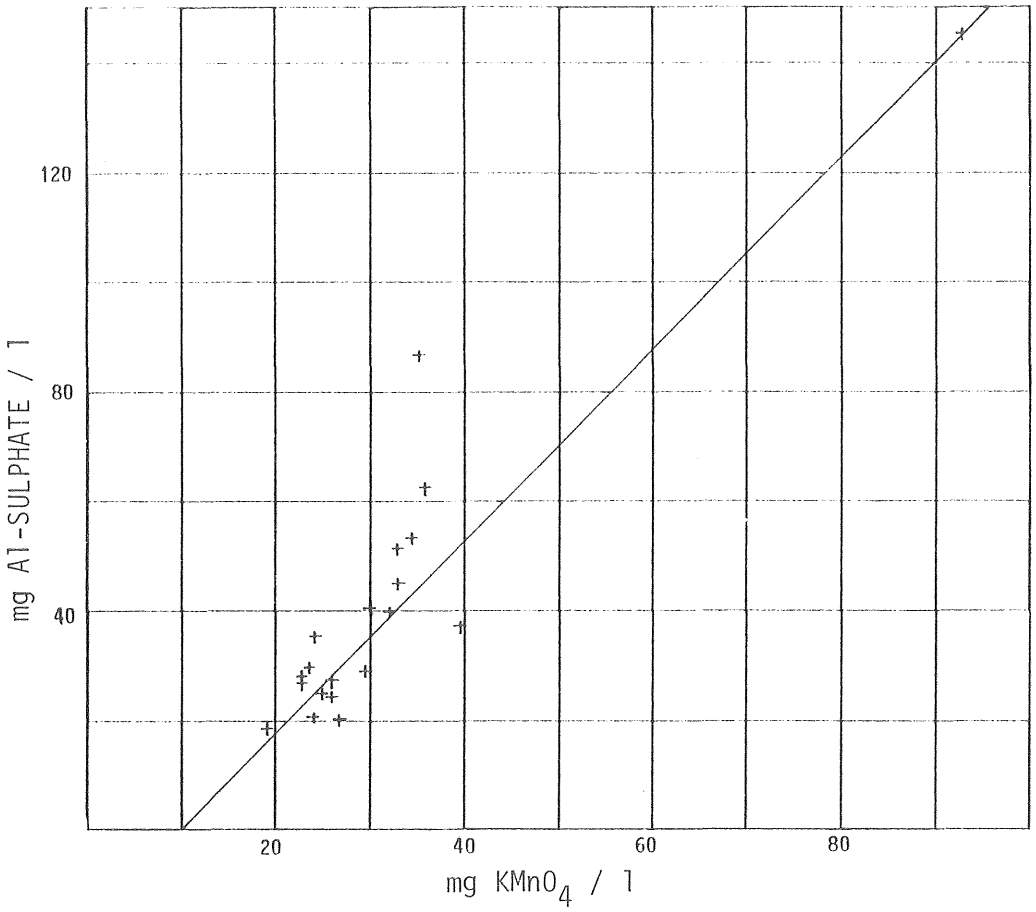

Fig 2.42. Required coagulant dose and organic content in the raw water (COD_{Mn}).

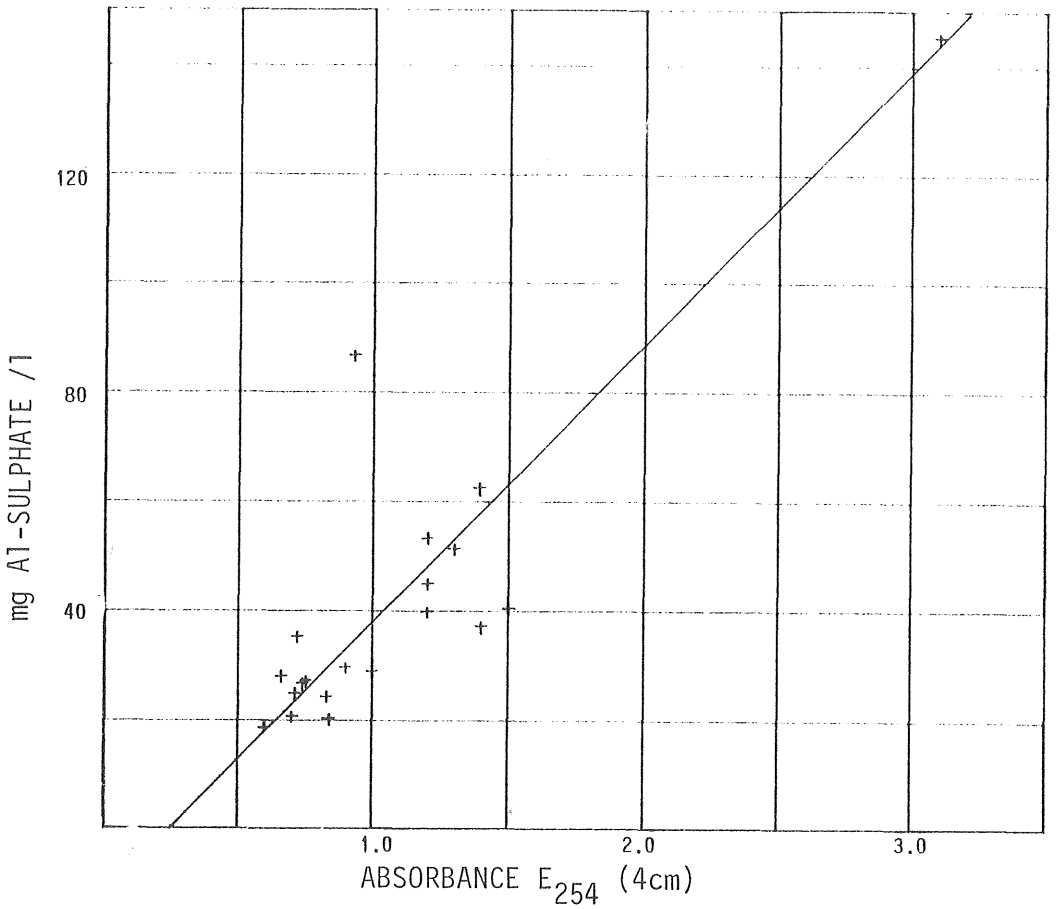

Fig 2.43. Required coagulant dose and organic content in the raw water $E_{254}^{4\ cm}$.

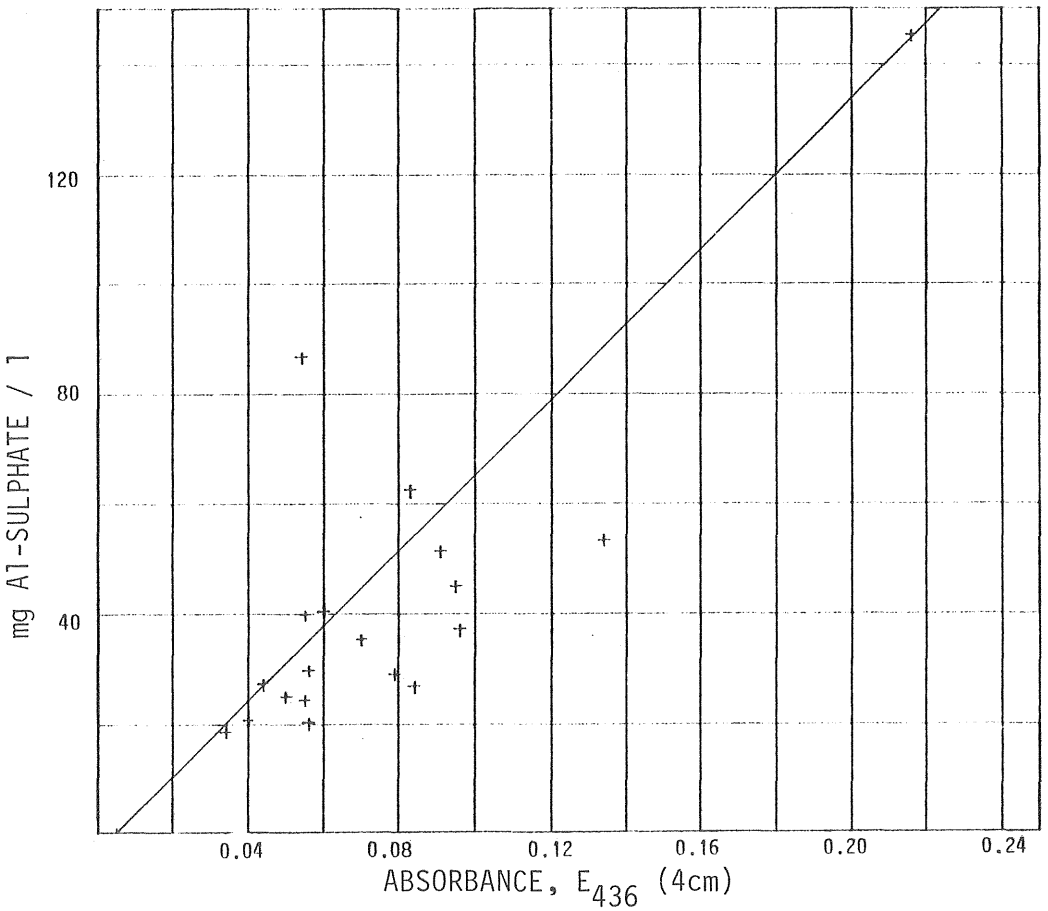

Fig 2.44. Required coagulant dose and organic content in the raw water $E_{436}^{4\ cm}$.

In figure 2.45 the absorbance values for visible light ($E_{436}^{4\ cm}$) are corrected for the influence of turbidity according to eq (2-5).

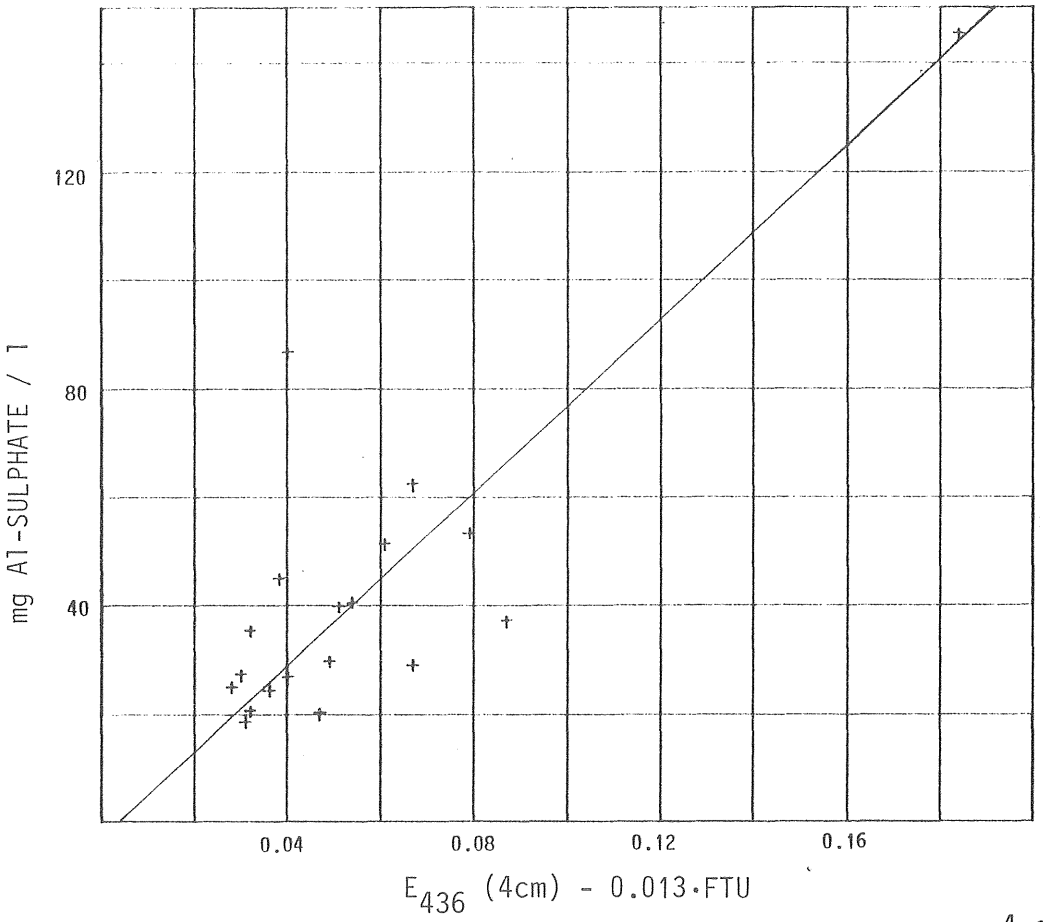

Fig 2.45. Required dose and organic content in the raw water, $E_{436}^{4\ cm}$ corrected for turbidity (eq (2-5)).

Obviously none of the single characteristics of the raw water measured here can be used to adequately predict the coagulant dose necessary for removal, neither can combinations of these rough measures of the humic content.

The lines indicated in the figures are originating from a point determined by table 2-3 at zero coagulant dose. That point is then simply connected with the point corresponding maximum values. A regression analysis was thought not to bring more information, because of the configuration of the data.

2.3.4 Comparison between jar test results and the results obtained on full scale

Samples were taken at the water treatment plants where the jar tests were carried out. Hereby, the ability of the jar test to predict a result at a certain coagulant dose and pH could be examined. The difficulty was of course, to obtain representative samples from the treatment plant. Sometimes the extraction of samples after a specific filter was impossible. Further the filtrate quality varies during a filter-cycle. It was decided that, when possible, a sample representing operation conditions a couple of hours after back washing should be used for comparison. When this was not possible the lowest value from a set of samples was chosen. The number of samples was limited; 2 to 5. When granulated activated carbon was used as filter-medium, the organic content measures are not included, as the filter operation involves an additional removal of humic substances.

In the figures 2.46 to 2.50 thus residuals after filtration calculated from jar test data are compared with the water treatment plant performances at corresponding coagulant doses and pH.

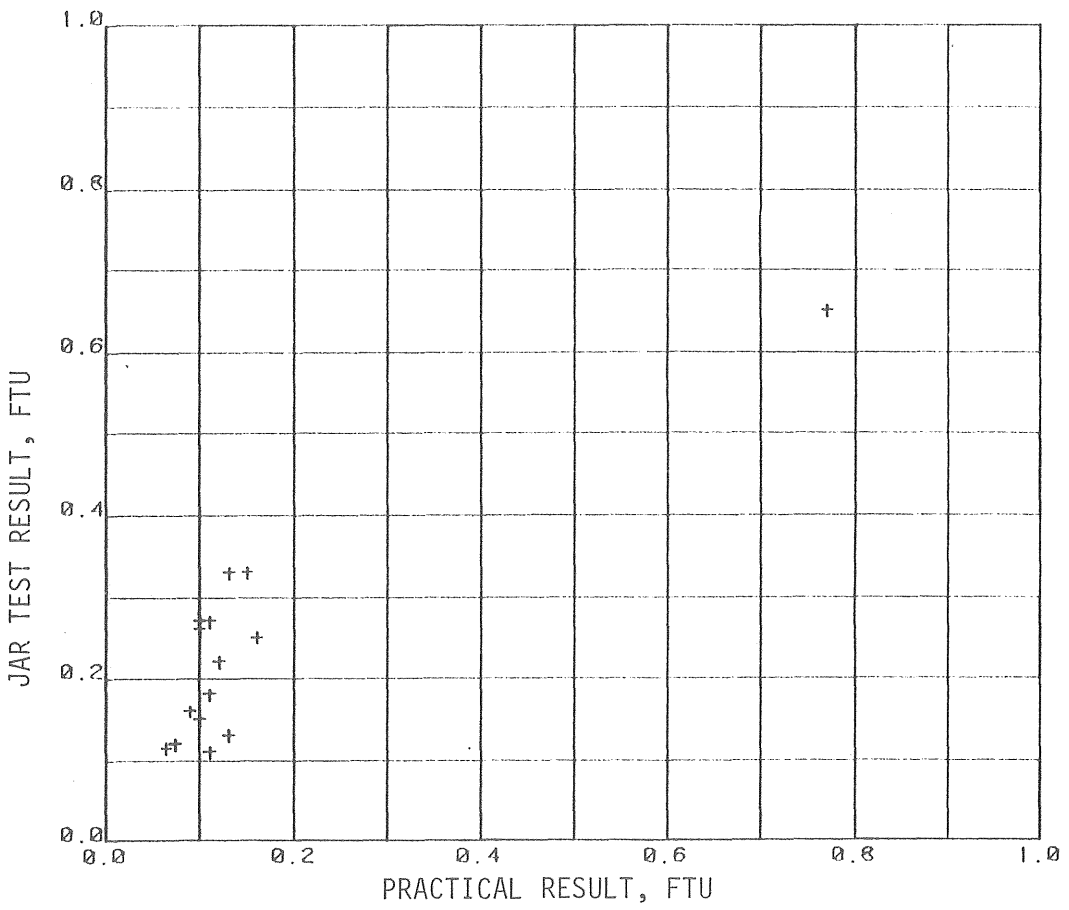

Fig 2.46. Filtrate turbidity. Jar test result and actual water treatment plant performance.

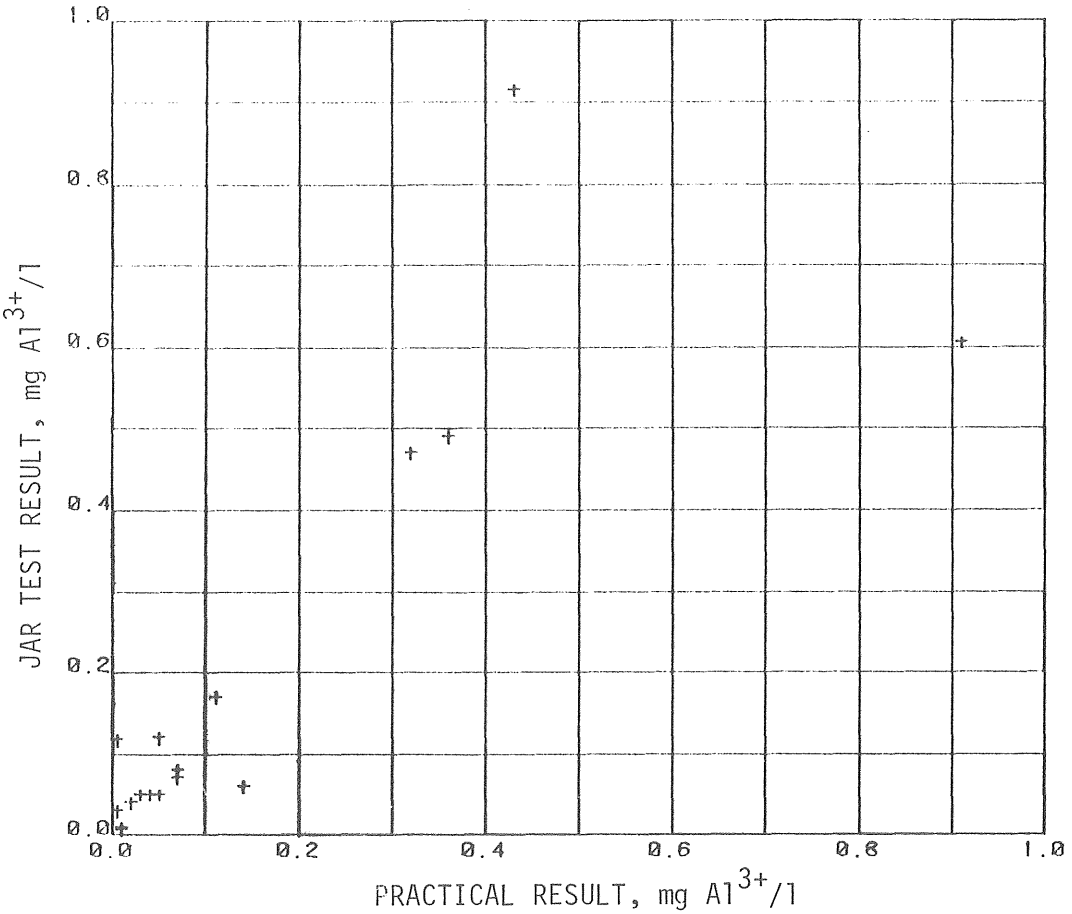

Fig 2.47. Filtrate aluminium residual. Jar test result and actual water treatment plant result.

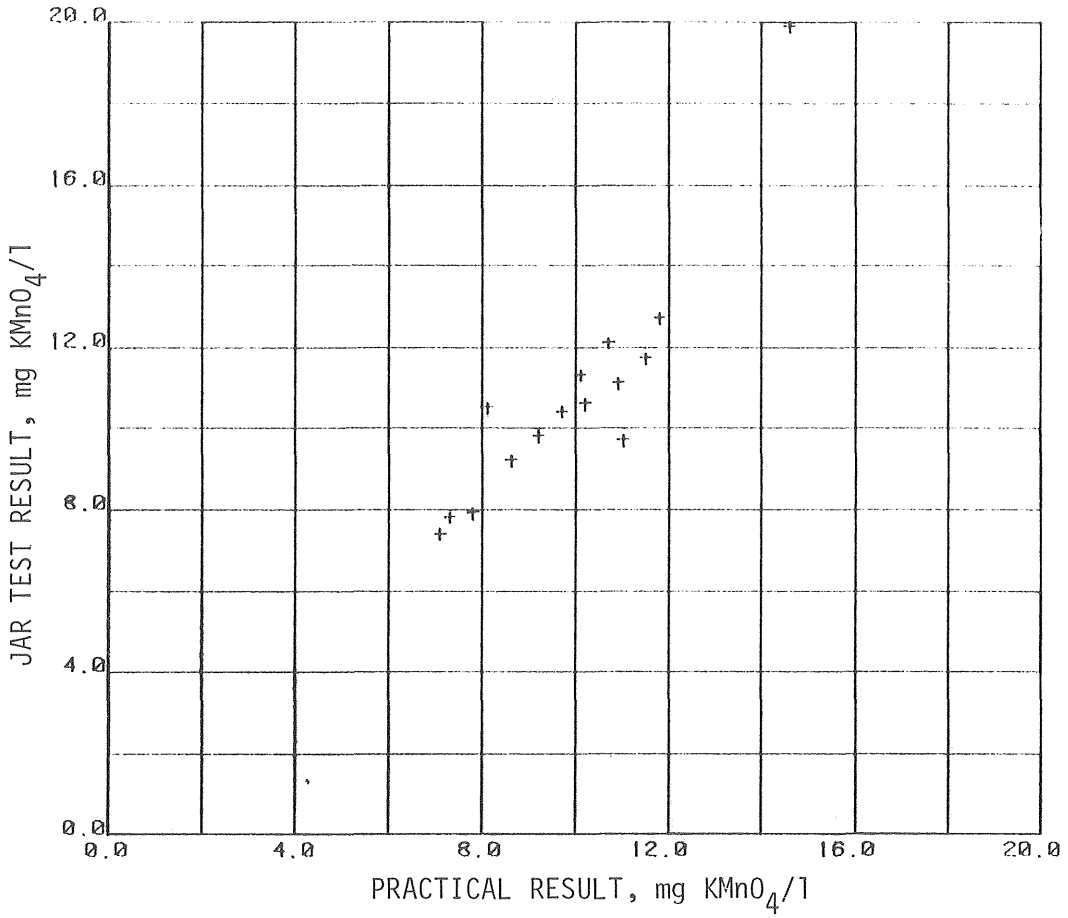

Fig 2.48. Filtrate COD_{Mn}. Jar test result and actual water treatment plant result.

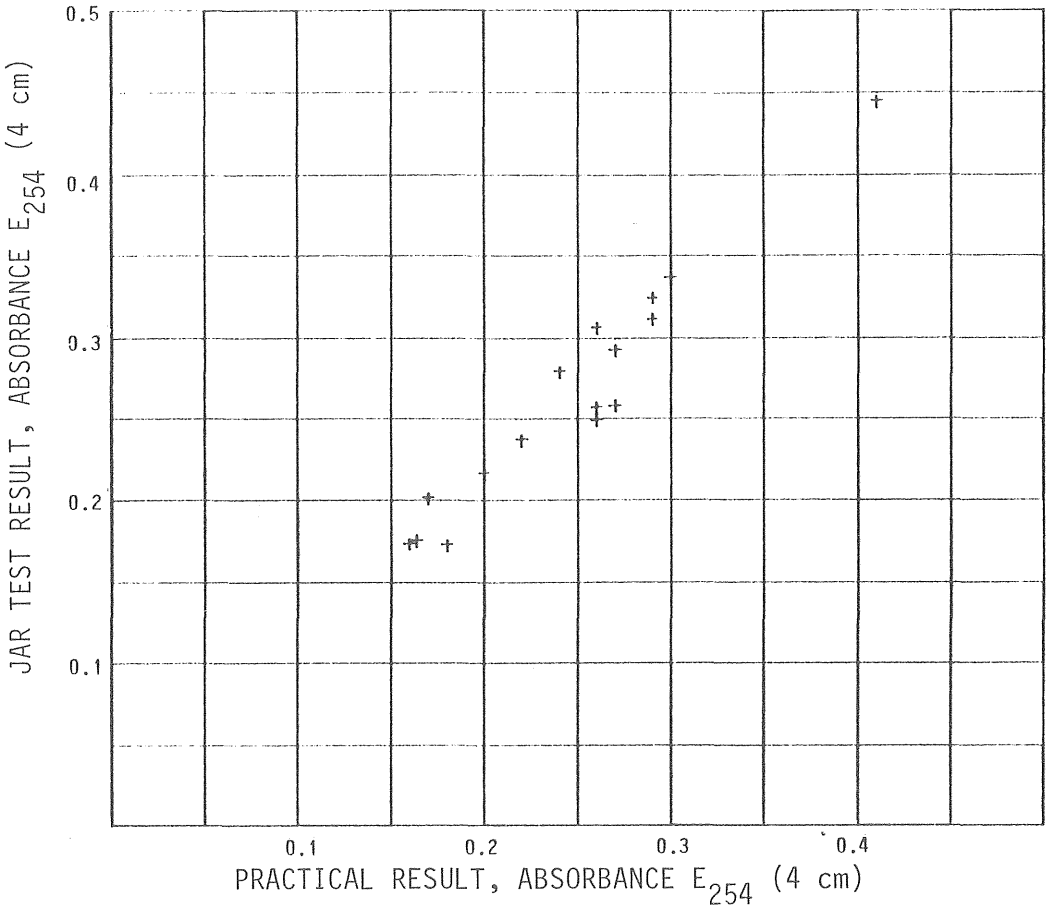

Fig 2.49. Filtrate $E_{254}^{4\ cm}$. Jar test result and actual water treatment plant result.

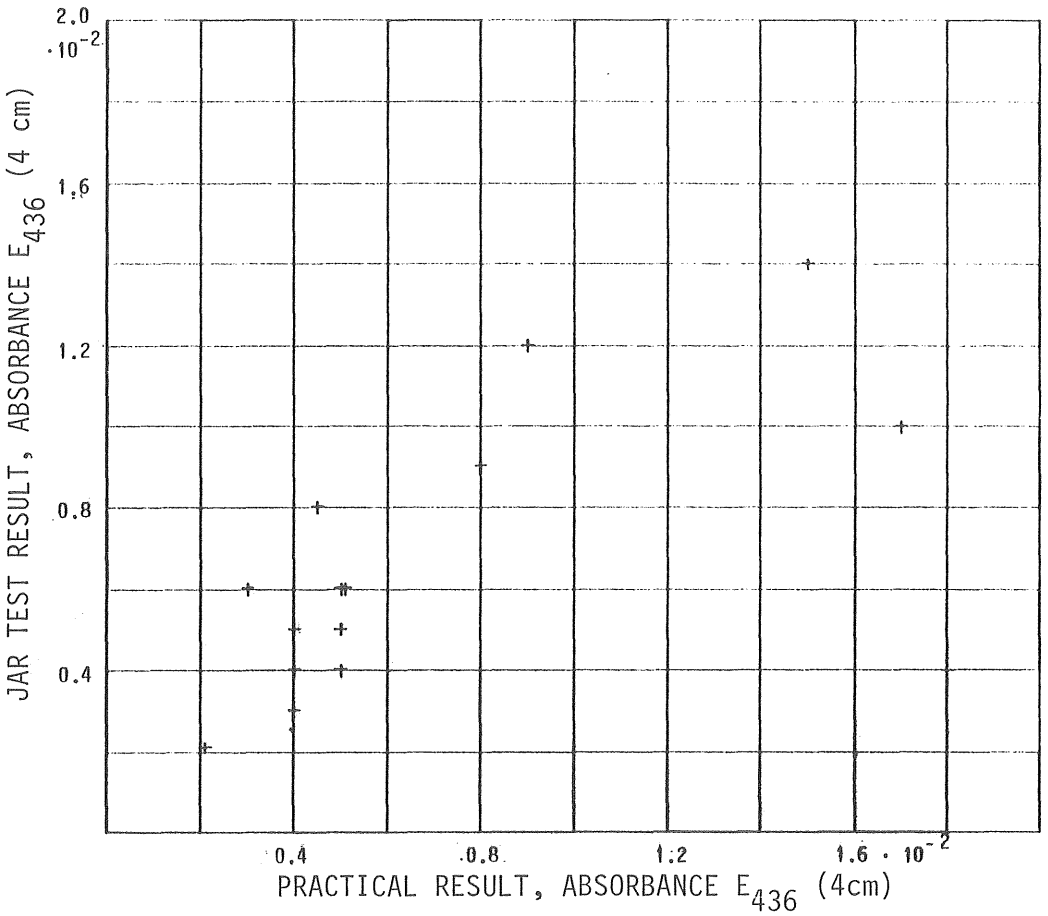

Fig 2.50. Filtrate $E_{436}^{4\ cm}$. Jar test result and actual water treatment plant result.

It can be seen that the filtrate turbidity has a tendency to be overestimated in the jar test. Partly due to that, the absorbance of visible light (E_{436}) shows poor agreement. The aluminium content corresponds relatively well at low values, but at high values the uncertainty is increasing due to the steep aluminium curve usually prevailing under such conditions.

The filtrate content of humic substances as measured by COD_{Mn} and E_{254} are rather well predicted.

3 FLOCCULATION

3.1 Flocculation theory

The aggregation of particles in a liquid is caused by their relative motion induced by Brownian motion or velocity gradients, the former usually called perikinetic, the latter orthokinetic flocculation. Some theories encountered in literature will be briefly summarized in this section. The main attention will be given to the orthokinetic flocculation. For more complete information, see the extensive literature surveys made by for example Ødegaard (1975) or Ives (1978 ed), Robinson (1964) Hudson (1965).

3.1.1 Perikinetic flocculation

When particle growth is governed by Brownian motion, aggregation proceeds spontaneously after the destabilization of the raw water colloids by means of an addition of a coagulant. If the colloid particles are completely destabilized, the collision efficiency is high, and most particle collisions lead to aggregation (rapid coagulation). This is assumed in the equations presented here; otherwise a collision efficiency factor(α) has to be introduced.

The reaction rate can be very high; Hahn and Stumm (1968) gave the value of about 10^{-3} s for the perikinetic coagulation half time. The halving time, however, is concentration dependent (Ives, 1978 b) but independent of particle size.

The equations describing the perikinetic coagulation of colloid particles was worked out by Smoluchowski (1917) and reviewed by, for example, Swift and Fiedlander (1964). The collision frequency between particles of radius r_i and r_j at numerical concentration n_i and n_j was shown to be given by the relation:

$$\frac{dn_{ij}}{dt} = \frac{2 \cdot k \cdot T}{3 \cdot \mu}(r_i + r_j)\left(\frac{1}{r_i} + \frac{1}{r_j}\right) \cdot n_i \cdot n_j \qquad (3\text{-}1)$$

where k is Boltzmann's constant, T the absolute temperature and μ the fluid viscosity. The diffusion coefficient for an individual particle with radius r is

$$D = \frac{k \cdot T}{6 \cdot \pi \cdot \mu \cdot r} \qquad (3\text{-}2)$$

If the total diffusion coefficient D_{ij} is the sum of D for i- and j-particles, respectively, eq (3-1) is obtained if D_{ij} is introduced in the general diffusion equation for a spherical collector (Ives, 1978 b).

$$\frac{dn_{ij}}{dt} = 4 \cdot \pi \cdot R_{ij} \cdot D_{ij} \cdot n_i \cdot n_j \qquad (3\text{-}3)$$

where R_{ij} is the collision radius (r_i+r_j).

With the assumption

$$(r_i+r_j)\left(\frac{1}{r_i} + \frac{1}{r_j}\right) = 4 \qquad (3\text{-}4)$$

which is exact for particles all of the same size, Swift and Freidlander (1964) simplified eq (3-1) for a monodisperse system to

$$\frac{dn_t}{dt} = -\frac{4}{3}\frac{k \cdot T}{\mu} \cdot n_t^2 \qquad (3\text{-}5)$$

where n_t is the total number of equally sized particles per unit of volume.

Ives (1978 b) derived an expression for the particle size when the rate of perikinetic and orthokinetic flocculation is equal. The order of magnitude was 0.2 - 1.0 μm, depending on the velocity gradient introduced to the water.

3.1.2 Orthokinetic flocculation

Camp (1943) showed that the rate of flocculation is directly proportional to the velocity gradient at a point, considering particles of two sizes, with diameter d_1 and d_2, respectively. If the centres of the particles are brought to the distance $1/2(d_1+d_2)$, the collision radius, they are assumed to join each other. Let the reference point be at the centre of a

particle with diameter d_1 and the fluid subjected to a velocity gradient G, or dv/dx, where v is the water velocity and the x-direction is normal to the flow. The collision rate for one d_1-particle (with d_2-particles) is then equal to the number of particles of size d_2 which by differential motion will be brought into a sphere with the radius equal to the collision radius. The flow, q_2, of d_2-particles into the volyme defined by the collision radius is, if streamlines are assumed not to be disturbed by the presence of particles:

$$q_2 = n_2 \cdot 4 \cdot \int_0^{(d_1+d_2)/2} \left(\left(\frac{d_1}{2} + \frac{d_2}{2}\right)^2 - x^2\right)^{1/2} \cdot x \cdot (dv/dx) \cdot dx \qquad (3\text{-}6)$$

n_2 is the number of particles with size 2 per unit of volume.

Integration yields:

$$q_2 = n_2 \cdot \frac{4}{3}\left(\frac{d_1}{2} + \frac{d_2}{2}\right)^3 \cdot \frac{dv}{dx} \qquad (3\text{-}7)$$

and with n_1 1-particles per unit of volume, the total collision rate will be

$$\frac{dn_{1,2}}{dt} = \frac{1}{6} \cdot n_1 \cdot n_2 \cdot G \cdot (d_1+d_2)^3 \qquad (3\text{-}8)$$

If not all collisions lead to attraction, a collision efficiency factor can be introduced.

$$\frac{dn_{1,2}}{dt} = \frac{G}{6} \cdot \alpha \cdot n_1 \cdot n_2 \cdot (d_1+d_2)^3 \qquad (3\text{-}9)$$

Hudson (1965) proposed that n_1 should represent the number of naturally occurring particles (with diameter d_1) and n_2 the number of flocs (with diameter d_2), thus postulating a flocculation mechanism where primary particles are captured by large floc particles. The number of primary particles is much greater, and the size is much smaller than the flocs; consequently, d_1 in eq (3-9) can be neglected in relation to d_2.

$$-\frac{dn_1}{dt} = \frac{G}{6} \cdot \alpha \cdot n_1 \cdot n_2 \cdot d_2^3 \qquad (3\text{-}10)$$

Since the total floc volume per unit volume of fluid can be calculated as

$$\Phi = n_2 \cdot \frac{\pi \cdot d_2^3}{6} \qquad (3\text{-}11)$$

the rate of primary particle capture can be written:

$$-\frac{dn_1}{dt} = \frac{G}{\pi} \cdot \alpha \cdot \Phi \cdot n_1 \qquad (3\text{-}12)$$

The assumption, however not likely to be fulfilled, that the particle size distribution is such that only one particle size is present, growing with time (O'Melia, 1972), introduced into eq (3-9) gives an expression for monodisperse growth. The particle volume fraction, $\Phi = n_i \cdot \pi \cdot d_i^3/6$, is assumed to be constant. The equation now expresses the decrease in the total number of particles, n_t. Since there is only one particle size ($d_1 = d_2$ in eq (3-9)), every particle collision is counted twice and:

$$-\frac{dn_t}{dt} = \frac{G}{6} \cdot \alpha \cdot n_t \cdot (2d)^3 \cdot \frac{1}{2} = \frac{4}{\pi} \cdot n_t \cdot \alpha \cdot G \cdot \Phi \qquad (3\text{-}13)$$

Though eq (3-12) and (3-13) are derived for different assumed flocculation patterns, the general conclusions are the same: The flocculation rate is proportional to the velocity gradient, floc volume fraction, collision efficiency and number of particles.

The equations related above give a qualitative description of the growth kinetics of flocs. One serious limitation of eq (3-9) is that it only takes into account two different sizes of particles. In an actual flow-through reactor, there is a heterodispersed system with a continous size distribution. One way to take the particle size distribution into account is to consider particles built up by primary particles. An i-particle contains of i primary particles. Thus discrete particle sizes are obtained with volumes being multiples of the primary particle. For natural waters

the difficulty consists of clearly defining the primary particle. If aggregation of artificial suspensions with added particles of known size is studied, the primary particle is well defined. However, in the case of simultaneous aggregation of colloid particles and the precipitate of a coagulant, this is not the case.

A continous particle size distribution has been used by Swift and Friedlander (1964). At this stage, however, the particle growth described by discrete particle sizes will be considered partly according to Ives (1978 b) and Harris *et al* (1966).

The appearance of aggregates of size k (k=i+j) is due to collision between i- and j-particles, and k-particles disappear due to collision with other particles. The rate of change of k-particles is

$$\frac{dn_k}{dt} = \frac{1}{2}\sum_{i=1}^{k-1} \frac{4}{3} \cdot n_i \cdot n_{k-i} \cdot R_{i,k-i}^3 \cdot G - n_k \sum_{i=1}^{\infty} \frac{4}{3} \cdot n_i \cdot R_{i,k}^3 \cdot G \quad (3\text{-}14)$$

The factor 1/2 in the first term is applied because each collision is counted twice. If coalescence is assumed, though strictly valid only for dispersed liquid drops, the volume of an i-particle can be expressed in terms of the primary particle radius r_1

$$V_i = i \cdot \frac{4}{3} \cdot \pi \cdot r_1^3 = \frac{4}{3} \cdot \pi \cdot r_i^3 \quad (3\text{-}15)$$

and thus

$$i \cdot r_1^3 = r_i^3 \quad (3\text{-}16)$$

and

$$R_{i,j} = r_i + r_j = r_1(i^{1/3} + j^{1/3}) \quad (3\text{-}17)$$

Then eq (3-14) can be written

$$\frac{dn_k}{dt} = \frac{2}{3} \cdot G \cdot r_1^3 \cdot \left(\sum_{i=1}^{k-1} n_i \cdot n_{k-i} (i^{1/3} + (k-i)^{1/3})^3 - \right.$$

$$\left. -2n_k \sum_{i=1}^{\infty} n_i (i^{1/3} + k^{1/3})^3\right) \quad (3\text{-}18)$$

The total floc volume fraction is

$$\Phi = \sum_{i=1}^{\infty} \frac{4}{3} \cdot \pi \cdot r_i^3 \cdot n_i = \frac{4}{3} \cdot \pi \cdot r_1^3 \sum_{i=1}^{\infty} i \cdot n_i \qquad (3\text{-}19)$$

and thus

$$\frac{dn_k}{dt} = G \cdot \Phi \cdot \frac{1}{2 \cdot \pi} \cdot \frac{1}{\sum_{i=1}^{\infty} i \cdot n_i} \cdot \left(\sum_{i=1}^{k-1} n_i \cdot n_{k-i} \left(i^{1/3} + (k-i)^{1/3} \right)^3 - \right.$$

$$\left. -2 n_k \sum_{i=1}^{\infty} n_i \cdot \left(i^{1/3} + k^{1/3} \right)^3 \right) \qquad (3\text{-}20)$$

For primary particles, the first term within the parenthesis disappears, and the rate of change of primary particles can be expressed as:

$$\frac{dn_1}{dt} = -G \cdot \Phi \cdot \frac{1}{\pi} \cdot n_1 \frac{\sum_{i=1}^{\infty} n_i (i^{1/3} + 1)^3}{\sum_{i=1}^{\infty} i \cdot n_i} \qquad (3\text{-}21)$$

The last part of the expression, with summation terms, is presented by Harris et al (1968) as a size distribution function, called δ if the summation goes to infinity (the floc size is unlimited). If the floc size for some reason is limited to a maximum floc size p, this is also the upper summation limit. The distribution function is then called ε. δ and ε have a maximum value of 8 (only primary particles present) and a minimum value of 1 (only particles with size p>>1). Eq (3-21) can be written:

$$\frac{dn_1}{dt} = -G \cdot \Phi \cdot \frac{1}{\pi} \cdot n_1 \cdot \delta \qquad (3\text{-}22)$$

The rate of change of the total number of particles can be achieved by a summation of eq (3-20) over all particle sizes. It is enough to consider the sum of the number of particles which disappear from each fraction; the first term within the parenthesis in eq (3-20) can be omitted. As each disappearance is assumed to be caused by the collision of two particles (forming an aggregate), the sum then must equal twice the total decline in number of particles. The rate of change of total number of particles, n_t, is:

$$\frac{dn_t}{dt} = G \cdot \Phi \cdot \frac{1}{2\pi} \frac{1}{\sum_{i=1}^{\infty} i \cdot n_i} \left(- \sum_{k=1}^{\infty} \sum_{i=1}^{\infty} n_k \cdot n_i (i^{1/3} + k^{1/3})^3\right) \qquad (3\text{-}23)$$

and as the total number of particles is

$$n_t = \sum_{j=1}^{\infty} n_j \qquad (3\text{-}24)$$

eq (3-23) can be written

$$\frac{dn_t}{dt} = -G \cdot \Phi \cdot \frac{1}{2\pi} \cdot n_t \frac{\sum_{j=1}^{\infty} \sum_{i=1}^{\infty} n_i \cdot n_j \cdot (i^{1/3} + j^{1/3})^3}{\sum_{j=1}^{\infty} \sum_{i=1}^{\infty} n_j \cdot n_i \cdot i} \qquad (3\text{-}25)$$

Harris et al (1968) derived the expression below, used by Ives and Bhole (1973):

$$\frac{dn_t}{dt} = -G \cdot \Phi \cdot \frac{1}{\pi} \cdot n_t \frac{\sum_{j=0}^{\infty} \sum_{i=0}^{\infty} n_i \cdot n_j (i^{1/3} + j^{1/3})^3}{\sum_{j=1}^{\infty} \sum_{i=1}^{\infty} n_j \cdot n_i \cdot (i+j)} \qquad (3\text{-}26)$$

which does not seem to be fully consistent with the derivation presented above.

If i~j, then eq (3-25) will be changed

$$- \frac{dn_t}{dt} = G \cdot \Phi \cdot \frac{1}{2\pi} \cdot n_t \frac{\sum_{k=1}^{\infty} n^2_k \cdot 8 \cdot k}{\sum_{k=1}^{\infty} n^2_k \cdot k} = G \cdot \Phi \cdot \frac{4}{\pi} \cdot n_t \qquad (3\text{-}27)$$

which in fact is eq (3-13).

Instead of particles built up by primary particles Spielman (1978) presented a continuous form for the floc growth equation in a system with a continuous size distribution function:

$$\frac{\partial n(v)}{\partial t} = \frac{1}{2} \int_0^v \beta(v, v-\tilde{v}) \cdot n(v) \cdot n(v-\tilde{v}) d\tilde{v} - \int_0^{\infty} \beta(v, \tilde{v}) \cdot n(v) \cdot n(\tilde{v}) d\tilde{v} \qquad (3\text{-}28)$$

Here n(v) is the number concentration function, the number of flocs per unit of volume with floc volumes in the size interval (v, v+dv). $\beta(v,\tilde{v})$ is the aggregation coefficient, which for laminar shear is defined as:

$$\beta(v,\tilde{v}) = \frac{G}{\pi}(v^{1/3}+\tilde{v}^{1/3})^3 \qquad (3\text{-}29)$$

The same form of equation had earlier been presented by Swift and Friedlander (1964):

$$\frac{\partial n(v,t)}{\partial t} = (\frac{3}{4\pi})^{1/3} \cdot \frac{2G}{3} \int_0^v n(v)\cdot n(v-\tilde{v})\cdot(\tilde{v}^{1/3}+(v-\tilde{v})^{1/3})^3 d\tilde{v} -$$

$$-(\frac{3}{4\pi})^{1/3} \cdot \frac{4\cdot G}{3} \cdot n(v) \int_0^\infty n(\tilde{v})\cdot(v^{1/3}+\tilde{v}^{1/3})^3 d\tilde{v} \qquad (3\text{-}30)$$

By substituting

$$n(v,t) = \frac{n_t^2}{\Phi}\cdot\Psi_1(\frac{v\cdot n_t}{\Phi}) \qquad (3\text{-}31)$$

(where n_t is the total number of particles, Φ the floc volume fraction and Ψ_1 a function that does not change with time) Swift and Friedlander showed that eq (3-31) is a self-preserving form for the size distribution function and a solution of equation (3-30) in a laminar shear field.

Tambo (1979 c) presented results that claim the existence of self-preserving normalized floc size distributions at the final stage of the flocculation process.

3.1.3 Turbulence and flocculation

In the equations hitherto describing flocculation kinetics, laminar conditions are presupposed.

Camp and Stein (1943) have reported the significance of a mean velocity gradient also under turbulent conditions, as will be discussed in Section 3.4.1.

Argaman and Kaufman (1970) argue that the principal objection in using an overall velocity gradient, G, in deriving the collision frequency, is that the length and time scales over which the turbulent fluctuations

occur are not taken into account. Particles suspended in a turbulent fluid move randomly, which can be characterized by a diffusion coefficient. After an analysis of the impact of the turbulence energy spectrum, an effective diffusivity is proposed, where the turbulence scale in relation to particle size is taken into account. The rate of collision between primary particles with the radius r_1 and flocs with the radius r_F ($r_F >> r_1$) obtained is:

$$\frac{dn_1}{dt} = 4 \cdot \pi \cdot K_s \cdot r_F^3 \cdot n_1 \cdot n_F \cdot \overline{u^2} \qquad (3\text{-}32)$$

where K_s is a proportionality coefficient expressing the effect of the turbulent energy spectrum. For a particular turbulence field and particle size, K_s is a constant.

The mean square velocity fluctuation ($\overline{u^2}$) and the G-value were shown experimentally by Argaman and Kaufman to be proportional to each other.

$$\overline{u^2} = K_p \cdot G \qquad (3\text{-}33)$$

where K_p is a constant characterizing the stirring equipment.

Tambo and Watanabe (1979 c) in their study of flocculation kinetics use an equation originally derived by Levich (1962) for turbulent conditions, based on the concept of locally isotropic turbulence with viscous subrange diffusion rate control. The number of collisions in a monodisperse suspension with particle diameter d and number n is

$$-\frac{dn}{dt} = 12 \cdot \pi \cdot \beta \cdot \sqrt{\frac{\varepsilon_o}{\mu}} \cdot d^3 \cdot n^2 \qquad (3\text{-}34)$$

Here ε_o is the mean rate of energy dissipation per unit volume effective for flocculation, β is a constant and μ the viscosity. The energy dissipation near walls and paddles is not considered effective in the aggregation process. ε_o is therefore only a part of the total power input (W). Tambo and Watanabe estimated the relation to $\varepsilon_o = 0.1\text{-}0.2 \cdot W$.

The turbulent approaches mentioned here thus confirm that the relation derived by Camp and Stein still can be used qualitatively in the description of flocculation kinetics. Both expressions related above, though derived in different ways, can be written:

$$-\frac{dn}{dt} = \text{const} \cdot G \cdot d^3 \cdot n^2 \qquad (3\text{-}35)$$

Also Spielman (1978), reviewing a turbulence theory developed by Saffman and Turner (1956), obtained a similar expression for the collision rate between two particle sizes as a result of an analysis where isotropic turbulence and particles, small compared to the turbulent microscale, were assumed:

$$\frac{dn_{1,2}}{dt} = n_1 \cdot n_2 \cdot (r_1+r_2)^3 \cdot \left(\frac{8\cdot\pi}{15}\right)^{1/2} \cdot G = 1.294 \cdot (r_1+r_2)^3 \cdot G \cdot n_1 \cdot n_2 \qquad (3\text{-}36)$$

The numerical constant 1.294 acheived is surprisingly close to 4/3 according to the fully analogous eq (3-8) derived by Camp and Stein for laminar conditions.

3.1.4 Floc breakup

As a floc is built up, it becomes more sensitive to disruption. The disintegrating force on aggregated particles in a shear field increases more than the attractive force (Hannah *et.al.*, 1967). The equilibrium between the aggregation and the breakup can be expressed as there is an inverse relationship between the maximum or stable particle size and the velocity gradient:

$$d_{max} = \frac{K_1}{G} \qquad (3\text{-}37)$$

This relation is given by numerous authors as a result of floc size measurements: Camp (1955), Richie (1956), Lagvankar and Gemmel (1968), Argaman and Kaufman (1968), Ives (1973).

Various floc breakup mechanisms have been proposed. Argaman and Kaufman (1970) postulate that primary particle erosion is the most credible mechanism. The expression for the rate of forming primary particles given is:

$$\left(\frac{dn_1}{dt}\right)_{breakup} = B \cdot r_F^2 \cdot \frac{n_F}{r_1^2} \cdot \overline{u^2} \qquad (3\text{-}38)$$

where B is a breakup constant.

After introduction of the floc volume fraction and the relation between floc size and G-value according to eq (3-37), eq (3-38) becomes:

$$\left(\frac{dn_1}{dt}\right)_{breakup} = B \cdot \frac{3 \cdot \Phi \cdot K_p}{r_1^2 \cdot 4 \cdot \pi \cdot K_1} \cdot G^2 = \text{const} \cdot G^2 \qquad (3\text{-}39)$$

Argaman and Kaufman presented the same expression, except for K_p, in that case raised to the exponent 2.

Parker et al (1972) consider two types of breakup mode: surface shearing and filament fracture. Depending on the floc size in relation to the turbulent microscale, different stable floc sizes and floc breakup rates are derived. The turbulent microscale (η) divides the region of eddy scale where dissipation takes place into two regions: the viscous dissipation range and a larger eddy size region, the inertial convection subrange. The Kolmogoroff microscale is determined by the power dissipated per unit mass (W_ρ), and thus the velocity gradient G, according to

$$\eta = \left(\frac{\nu^3 \cdot \rho}{W}\right)^{1/4} = \left(\frac{\nu}{G}\right)^{1/2} \qquad (3\text{-}40)$$

where ν is the kinematic viscosity.

The microscale for G-values usually encountered in flocculation practice ($10\text{-}100\ s^{-1}$) ranges from approximately 0.1 to 0.4 mm.

Parker et al presented a modification of eq (3-37), eq (3-41), where the G-value is raised to a stable floc size exponent n. The exponent for flocs greater and smaller than the microscale was derived to be 2 and 1, respectively, for surface shearing.

$$d_s = \frac{C}{G^n} \qquad (3\text{-}41)$$

In addition, the floc breakup rate is shown to vary according to scale. The general expression for the primary particle strip rate given by Parker et al is

$$\left(\frac{dn_1}{dt}\right)_{breakup} = K_B \cdot G^m \qquad (3\text{-}42)$$

The exponent m is shown to be 4 in the inertial convection subrange and 2 in the viscous dissipation subrange.

Tambo and Hozumi (1979 b) derived an expression for the maximum stable floc size considering the binding force in a plane of rupture through the floc (thus postulating a floc breakup into two equal parts) and the breakup force at the opposite sides of floc caused by microturbulent eddies.

The maximum stable floc size was found to be proportional to shaft rotational speed raised to the exponent 1.2-1.5 for particles greater than the turbulent microscale. The exponent was 1.0-1.1 for flocs smaller than the microscale.

3.1.5 Floc density

Theoretical studies and measurements have indicated that there is a size-density relationship for flocs: as the floc grows, the density is lowered.

Vold (1963) developed a computer simulation model for floc formation by random aggregation of primary particles. Flocs generated by the model were examined and the results generalized in terms of floc radius (r) and volume fraction of solids (Φ_f) for a floc containing n primary particles,

$$r = K_1 \cdot n^{0.429} \qquad (3\text{-}43)$$

$$\Phi_f = K_2 \cdot n^{-0.29} \qquad (3\text{-}44)$$

From these values, the bouyant density of flocs can be calculated to decrease with increasing size, proportionally to the projected area of the floc raised to the -0.338 power (Lagvankar and Gemmel, 1968). The latter authors carried out measurements of floc size with a microscope equipped with an optical micrometer. The density of flocs were determined by means of standard density solutions (sucrose and water), in which the flocs were pipetted. When no sedimentation occurred the density of the floc was considered to be the same as that of the fluid. Lagvankar and Gemmel obtained results quite comparable to the computer model for floc sizes of less than 1 mm^2 in projected area. The density of larger flocs were found to depend much less upon size. The flocs were generated with $Fe_2(SO_4)_3$ as coagulant. No artificial turbidity was added. The intensity of agitation was not found to affect the density of flocs of a given size, but, of course, the size distribution was affected.

Camp (1968) presented results from measurements of floc volume concentration by means of a microscope. The flocs were generated by a 15 mg/l dose of ferric sulphate to tap water. The flock volume concentration measured in that way was found to vary with the applied G-value and time. An increase in the G-value from 80 to 1000 S^{-1} made the floc volume concentration to decrease from 285 to 60 ppm.

Tambo and Watanabe (1979 a) measured floc size and settling velocity with probably a minimum of disturbance of floc structure. The buoyant (effective) density of the floc could be calculated from the settling velocity by applying Stokes' law in a modified form. The sphericity of the flocs was assumed to be around 0.8. The effective density was calculated from the equation:

$$v = \frac{g}{34\mu}(\rho_f - \rho_w)\cdot d_f^{\,2} = \frac{g}{34\mu}\,\rho_e \cdot d_f^{\,2} \qquad (3\text{-}45)$$

The relationship between floc effective density and floc diameter was expressed as:

$$\rho_e = \rho_f - \rho_w = \frac{a}{(d_f/1)^{K_\rho}} \qquad (3\text{-}46)$$

where ρ_e is the effective density, d_f the floc diameter (cm) and a and K_ρ constants. $d_f/1$ is a dimensionless floc diameter.

The values of the constants were for a, about 0.1 - 1.0 (kg/m^3) and K_ρ, 0.9-1.5.

The floc density function for clay-aluminium flocs was found not to be greatly affected by pH, agitation intensity, raw water alkalinity, and flocculant aid in small concentrations, but significantly dependent on the dosage of aluminium. The order of magnitude of K_ρ was confirmed by a two-dimensional computer simulation mode. The values found by Lagvankar and Gemmel correspond to a K_ρ-value of 0.68.

The floc density function obtained by Tambo and Watanabe cannot be applied to small floc sizes, too high a density will then be calculated for primary particles. They argue that there must exist a transition point below which the effective density is less influenced by the floc size.

The size-density relationship of flocs was shown to be of the same order of magnitude in terms of the exponent K_ρ for different conditions. However, the strength, or rupture resistance, is highly dependent on the constant a. Thus, the strength of flocs when coagulant aid (1 ppm activated silica) was added increased 4-fold. The floc strength was also shown to be dependent on pH and coagulant dosage.

Tambo and Watanabe have introduced the size-density relationship in equations describing the flocculation kinetics. The diameter of an i-fold particle can be expressed in terms of the primary particle diameter as:

$$d_i = i^{\frac{1}{(3-K_\rho)}} \cdot d_1 \qquad (3\text{-}47)$$

and the rate of change of k-fold particles

$$\frac{dn_k}{dt} = \frac{1}{2} \cdot A \cdot \sum_{i=1}^{k-1} \left[i^{\frac{1}{(3-K_\rho)}} + (k-i)^{\frac{1}{(3-K_\rho)}} \right]^3 \cdot n_i \cdot n_{k-i} -$$

$$- A \sum_{i=1}^{\infty} \left(i^{\frac{1}{(3-K_\rho)}} + k^{\frac{1}{(3-K_\rho)}} \right)^3 \cdot n_i \cdot n_k \qquad (3\text{-}48)$$

A is a constant, which includes the velocity gradient.

3.1.6 Theories for simultaneous growth and breakup of flocs

Parker et al (1972) presented an equation for the change in number of primary particles where simultaneously growth and floc breakup were taken into account (see eq (3-51) below). Argaman and Kaufman (1970) had earlier derived a similar expression.

The kinetics of the net disappeareance of primary particles can be expressed as:

$$-\frac{dn}{dt} = K_1 \cdot \Phi \cdot G \cdot n - K_2 \cdot \Phi \cdot G^m \qquad (3\text{-}49)$$

where n is the number concentration of primary particles

K_1 and K_2 constants

m floc breakup exponent

G velocity gradient, and

Φ floc volume fraction.

For a completely mixed flocculation reactor with the volume V, a mass balance relationship of the number of primary particles yields:

$$Q \cdot n_{i-1} - (K_1 \cdot \Phi \cdot G \cdot n_i - K_2 \cdot \Phi \cdot G^m) \cdot V = Q \cdot n_i \qquad (3\text{-}50)$$

where Q is the flow, n_{i-1} and n_i are the number of primary particles in the inlet and outlet respectively.

Rearrangement of eq (3-50) gives the expression:

$$n_i = n_{i-1} \frac{1+\frac{K_2}{n_{i-1}} \cdot \Phi \cdot G^m \cdot T}{1+K_1 \cdot \Phi \cdot G \cdot T} \qquad (3\text{-}51)$$

where T is the mean residence time (V/Q).

For N flocculation compartments in series, with the total residence time T, Ødegaard (1975) has shown that the relation between the number of primary particles in the inlet (n_o) and the outlet (n_N) could be written:

$$\frac{n_o}{n_N} = \frac{(1+K_1 \cdot \Phi \cdot G \cdot \frac{T}{N})^N}{1+\frac{K_2}{K_1}\frac{G^{m-1}}{\Phi}\{(1+K_1 \cdot \Phi \cdot G \cdot \frac{T}{N})^N - 1\}} \qquad (3\text{-}52)$$

A constant G-value throughout the process and an equal compartmentalization of the total flocculation volume are presupposed.

With varying G-value and unequal compartmentalization, Hedberg and Hernebring (1975) presented an expression of the form:

$$\frac{n_o}{n_N} = \prod_{i=1}^{N} \left(\frac{1+K_1 \cdot \Phi \cdot G_i \cdot r_i \cdot T}{1+\frac{K_2}{n_{i-1}} \cdot G_i^{\,m} \cdot \Phi \cdot r_i \cdot T}\right) \qquad (3\text{-}53)$$

where r_i accounts for the part of the total residence time in the i-th compartment.

Besides the surface erosion breakup, Ødegaard derives an expression for what is called 'collision breakup'. The breakup is assumed to be caused by unsuccessful collisions, which come about as an increase in the number of primary particles. If the rate of forming primary particles this way is considered proportional to the number of primary particles, floc volume fraction, G-value, and fraction of collisions that leads to breakup, the latter in turn proportional to the G-value, the floc breakup rate can be written:

$$\frac{dn}{dt} = K_2 \cdot n \cdot \Phi \cdot G^2 \qquad (3\text{-}54)$$

For N identical completely mixed compartments in series, with an overall residence time T and constant G-value, the flocculation performance can be derived:

$$\frac{n_o}{n_N} = (1+K_1 \cdot \Phi \cdot G \cdot \frac{T}{N} - K_2 \cdot \Phi \cdot G^2 \cdot \frac{T}{N})^N \qquad (3\text{-}55)$$

It is not obvious why the rate of forming primary particles should be proportional to the number already present. Omitting n in eq (3-54), however, would convert eq 3-55 to an expression similar to eq (3-51).

The equations presented above in this section have been concerned with the removal of primary particles. The size distribution of the total number of flocs is not considered. To account for the breakup of flocs for a descrete particle size distribution, the upper summation limit in for example eq (3-18) is changed from infinity to a maximum floc size, determined by, e.g., eq (3-37) (Harris et al (1966) and others).

Tambo and Watanabe (1979) compared numerical solutions of eq (3-48) with experimental results. Hereby an empirical collision-agglomeration factor α_K depending on the considered particle size k and the maximum floc size s, had to be introduced:

$$\alpha_K = \alpha_o(1-\frac{k}{s+1})^n \qquad (3\text{-}56)$$

where the value of the exponent n was empirically found to be 6.

The rate equation could then be written:

$$\frac{dn_k}{dm} = \frac{1}{2}\sum_{i=1}^{k-1} \alpha_o(1-\frac{k}{s+1})^6\left[i^{(\frac{1}{3-K_\rho})}+(k-i)^{(\frac{1}{3-K_\rho})}\right]^3 N_i \cdot N_{k-i} -$$

$$- N_k \sum_{i=1}^{s-k} \alpha_o(1-\frac{k+i}{s+1})^6\left[i^{(\frac{1}{3-K_\rho})}+k^{(\frac{1}{3-K_\rho})}\right]^3 \cdot N_i \qquad (3\text{-}57)$$

where m is a dimensionless time variable, N_i a dimensionless number of particles of size i - number of i-particles divided by the total number of particles.

Fair and Gemmel (1964), Ives (1973), Bhole (1973 b) in their computer simulations of flocculation allowed the primary particles to aggregate up to a maximum size determined by the G-value. The breakup was accounted for by one of the following procedures:

1. No aggregation of particles of greater size than the limit was allowed.

2. Aggregation was allowed but immediately followed by split-up into two, three or four equal parts.

Spielman (1978) defined a statistical breakup function $B(v,\tilde{v})$, as a means to accomplish the equations governing the continuous floc size distribution earlier given as eq (3-28). $B(v,\tilde{v})$ is defined in such a way that the product $B(v,\tilde{v})\cdot n(\tilde{v})\cdot d\tilde{v}\cdot dv$ is the rate of production of flocs in the interval $(v,v+dv)$ formed by breakup of greater flocs in the interval $(\tilde{v},\tilde{v}+d\tilde{v})$. If $v > \tilde{v}$, the value of the breakup function is zero, because no floc can be formed by breakup from sizes less than its own size.

The concept of a stable floc size below which no breakup occurs, implies a step change when this size is reached. Flocs then suddenty disrupt. Spielman argues that it is more credible that B is a continuous function. On a statistical basis, there should be at least some possibility that even a comparably small floc is disrupted by locally large fluid forces and/or occasional weakness of the floc.

The incorporation of the breakup function into the size distribution according to eq (3-28) gives:

$$\frac{\partial n(v)}{\partial t} = \frac{1}{2}\int_0^v \beta(v,v-\tilde{v})\cdot n(v)\cdot n(v-\tilde{v})d\tilde{v} -$$

$$- \int_0^\infty \beta(v,\tilde{v})\cdot n(v)\cdot n(\tilde{v})d\tilde{v} +$$

$$+ \int_v^\infty B(v,\tilde{v})\cdot n(\tilde{v})d\tilde{v} -$$

$$-n(v)\int_0^v \frac{\tilde{v}}{v} B(\tilde{v},v)d\tilde{v} \qquad (3\text{-}58)$$

The first two terms, presented earlier in eq (3-28), describe the change in number of particles of size v, due to aggregation (the first: binary aggregation of smaller particles to size v, the second: combination to larger particles). The last two terms account for the breakup, the first of which describes the forming of flocs from greater sizes, the latter denotes the breakup of flocs with size v to smaller sizes. A $\tilde{v}$-particle that breaks up into v-particles causes an increase in the number of v-particles in relation to the ratio between their volumes ($\tilde{v}/v$).

Unfortunately, Spielman does not give any information concerning a reasonable form of the breakup function B.

3.2 Flocculation efficiency

The objective of flocculation is the agglomeration of particles in order to make them separable by means of sedimentation or flotation and/or filtration. Seen in that context, an efficient flocculation is the same as successfully combined aggregation-separation operation. Provided the conditions causing optimal colloid destabilization described in Chapter 2 are fulfilled, the problem now is making separable aggregates in an efficient way.

The conditions of the particle growth up to a size of about 1 μm, are given by, e.g., the dosage and kind of coagulant, initial mixing and the composition of raw water impurities. In subsequent chapters, the starting point for the possibilities of manipulating the process will in many ways be considered as the stage of the particle growth where velocity gradients govern the growth pattern, i.e., orthokinetic flocculation.

The perikinetic flocculation is by rate theories shown to be dependent on, e.g., temperature. Orthokinetic flocculation equations show no temperature effect. As these two rates are assumed to be additive, Ives (1978 a) argues that the perikinetic flocculation first has to be observed so that a baseline for the orthokinetic flocculation can be established. The practical difficulties in that procedure are, however, great as the borderline between the two stages is not easily distinguished. It is questionable if efforts to isolate "true" orthokinetic flocculation would increase the possibilities of understanding the overall process.

On the other hand, if flocculation efficiency is measured as separation properties of the formed particle aggregates, the procedure that will be used by the present author, new difficulties will arise in characterizating the "true" flocculation mechanisms independent of the separation stage. The separation may be affected by conditions probably not affecting the flocculation. Here again, temperature is a good example. The conclusion is that often a joint effect on perikinetic flocculation, orthokinetic flocculation, and the separation step will be observed, with small possibilities to isolate the impact on either of the stages.

The advantage of such an approach is that the results can more easily be applied to practical operating conditions. The procedure will make it possible, within some limits, to quantitatively predict the treatment result after a manipulation in a treatment plant, which often is not the case for many laboratory studies encountered in litterature.

The numerical concentration of dispersed particles is the only parameter of flocculation effect encountered in elementary flocculation theories. Of course, a decrease in the particle number is related to an increase in particle size and thus an increase in settling velocity, but only in a qualitative way because, e.g., density may vary according to size; what a specific decrease in number means in terms of resulting absolute size distribution is often not quite clear.

The use of the flocculation performance parameter defined as the ratio between the number of primary particles before and after flocculation (n_0/n_N) presupposes first of all that there are identifiable particles of equal size building up the floc structure. The flocculation performance parameter would be fully useful if the assumptions underlying the evaluation of flocculation test data presented by Harris et al (1966) were valid:

There are principally two particle sizes present after the flocculation. On one hand flocs, which will settle in a reasonable short time and on the other hand primary particles with no measurable settling velocity.

The residual turbidity after a certain (long) time of settling then will be a measure of the number of primary particles still present.

In practice, for a continuous sedimentation process, that would mean a sedimentation result independent of small to medium overflow rates with a sudden breakup, when the flow is increased above a certain limit. Measurements presented later will, however, not justify such simplifications because there naturally is a continuous size distribution.

Hedberg (1976) in his extensive study and mathematical modelling of flocculation-sedimentation-filtration processes in water treatment, postulated that there are unambiguous relationships between residual turbidity on one hand and mean settling velocity and its standard deviation on the other. This will later be shown not to be universally true.

In some cases, fundamental flocculation equations can lead to false conclusions concerning the treatment result if not, e.g., the separation step is considered. Take as an example the equation below, used by O'Melia (1978 b) in discussing flocculation efficiency.

$$\frac{n_0}{n_1} = \alpha \cdot \Phi \cdot G \cdot T \qquad (3\text{-}59)$$

where α is the collision efficiency
Φ the floc volume fraction
G the velocity gradient
T the flocculation time

Here, of course, a higher collision efficiency (more effective destabilization) with hardly no reservation would increase the flocculation efficiency independent of what method is used in measuring the efficiency.

For the equation to remain valid the velocity gradient has to be varied in such a way that no extensive breakup of flocs will occur.

The floc volume fraction will according to the equation proportionally increase the efficiency, which may be true if this fraction is due to an increased dosage of hydrolysing metal as coagulant (and thus causing an increasing destabilization efficiency). However, the absolute treatment result may not be better or even deteriorate because of an increase in the raw water impurities or sludge returning to the flocculation reactors, despite the fact that the relative flocculation efficiency is increased. In fact, the simplified eq (3-59) indicates the same absolute numerical concentration in the outlet independent of floc volume fraction. n_1 is a constant if Φ/n_0 is a constant, as approximately is the case if, for example, sludge recirculation is assumed to increase the number of primary particles.

If Φ denotes 'the flocs', the volume of primary particles is assumed to be neglible. It can be seen as a stationary phase, most evident in sludge blanket treatment, which in fact is a kind of filtration (beyond the scope of this dissertation). Thus, an increase in flocculation efficiency could be expected with increasing floc volume fraction in this case. If that view is correct also for suspended flocculation in stirred tanks, one has to bear in mind the possible increased difficulties in the sedimentation operation caused by higher particle concentration.

A strict fulfillment of the equations presented in Section 3.1 implies flocculation performance measurement by particle counting, which practically is a difficult task for floc sizes with a sedimentation velocity of the order of magnitude required in practical operation. The measurement by particle counting instruments introduces high shear forces on the flocs, which will deteriorate. As a matter of fact, particle counting has been used to measure the strength of flocs (Hannah et al, 1967).

In summary it is the opinion of the present author that the flocculation efficiency measured as the settling properties of flocs is the most relevant parameter in this context. In Section 3.3, the measurements will be discussed. In Chapter 5 efforts are made to incorporate settling properties into flocculation rate theories described in Section 3.1.

3.3 Floc settling properties

3.3.1 Quiescent column settling

Evaluation of the flocculation efficiency in terms of the settling characteristics can be carried out in a column where the flocs are allowed to settle under quiescent conditions. Conventional quiescent column techniques are described by, for example, McLaughlin (1959) and Villemonte *et.al.* (1966). The procedure consists of the extraction of samples at a certain depth, or at different depths, for varying time intervals. The particle content in the samples is usually analyzed by means of a turbidity measurement or suspended solids determination.

The settling properties measured are highly dependent on how the measurement is carried out, and as no standard procedure exists, some measurement and evaluation techniques presented by other authors will be breifly outlined. The basis of the procedure used by the present author is presented together with its consequences for the interpretation of floc settling properties.

McLaughlin (1959) defined the local instantaneous mean settling velocity ($\bar{w}$) as a property characterizing the settling of suspended particles. $\bar{w}$ varies with time and depth depending on the concentration of particles, mean settling velocity, the standard deviation of settling velocity, and on flocculation during settling. Even in the absence of flocculation and hindered settling, $\bar{w}$ and the cange of $\bar{w}$ will depend on $\bar{w}$ itself and the standard deviation of settling velocity.

Tryland (1977 and 1978) has developed computer models for calculating $\bar{w}$ from tube settling test data.

However theoretically informative, $\bar{w}$ will include consequences of the settling dynamics itself. For practical purposes, it is enough to calculate the settling velocity distribution at different depths. Such a set of data contains information to fully characterize the settling properties of the suspension, from which $\bar{w}$ as defined by McLaughlin can be calculated if necessary.

Villemonte *et.al.* (1966) extracted samples at depth intervals that divided the total column depth into 10 equal parts. The time-concentration curves achieved were used for the evaluation of the sedimentation tank performance.

Ødegaard (1975) calculated parameters in an equation of the form

$$\frac{C}{C_o} = A \cdot e^{-B \cdot t} + D$$

to fit the time-concentration curves. The exponent B was used as a measure of the floc settling properties.

Rosén (1967) measured how the turbidity changed with time at a 1-m sampling depth and thus obtained a time-turbidity curve (fig 3.1). The settling velocity distribution was obtained by transforming the time scale to a settling velocity scale(sampling depth divided by time). If the tails of the curves are omitted and the turbidity is recorded as a percentage of gs'-gr', where gs' and gr' are "practical" start and residual turbidity respectively, an approximately normal settling velocity distribution will be achieved.

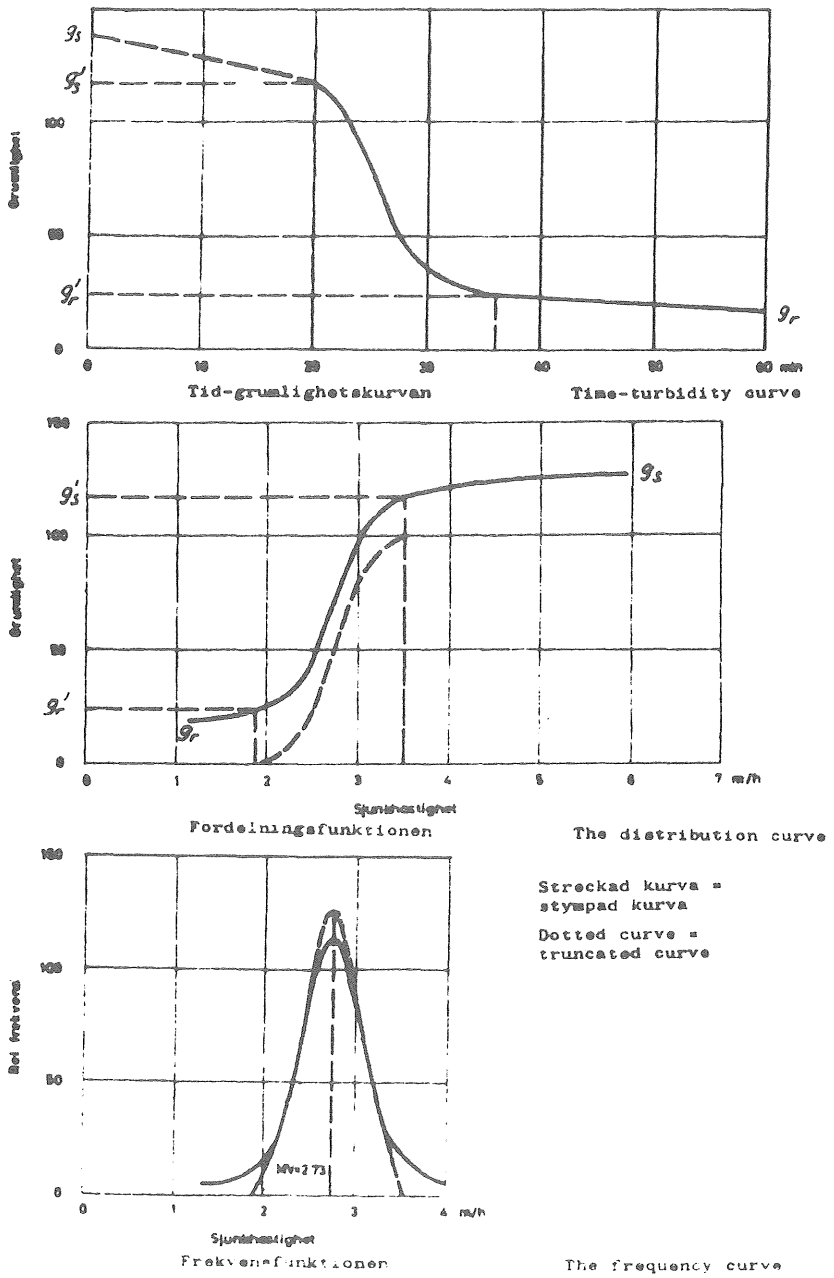

Fig 3.1. Analysis of floc settling data, Rosén (1967).

The floc dispersion in this case will be characterized by three parameters: mean settling velocity, settling velocity standard deviation and residual turbidity.

The samples were drawn from an opening in the wall of a flocculation tank where the paddles and the water flow were stopped during

sedimentation. Rosén also designed a column which could be lowered into a flocculation chamber. While being lowered, it was open at top and bottom and was then closed with two lids to accomplish undisturbed sedimentation. The floc concentration at a level of 30 cm below the top was registered by means of a photoelectric cell. Because of different techniques for measuring floc content, comparable results were not achieved by the two methods.

3.3.2 The present quiescent column settling test procedure

A routine procedure for performing settling analysis was developed, which is suitable for tests of both pilot-plant-scale and full-scale water-treatment plants.

A 1.25-m column with the diameter 150 mm is carefully lowered into the flocculation tank (fig 3.2 and 3.3). The upper part of the column is fixed ca 5 cm over the water surface. From the enclosed water volume, samples are withdrawn, normally after 10, 20, 40, 60 and 120 minutes at a depth of 30 cm. The original particle content is measured in a sample taken directly in the flocculation tank. The bottom of the column is open and in connection with the surrounding water. Thus, a constant water level is maintained despite the extraction of samples. The samples were withdrawn by means of a vacuum pump or, when possible, by a siphon tubing.

Generally the depth under the sample point was enough to prevent turbulence in the flocculation volume from affecting the settling of the flocs in the upper part of the column. The continuous flocculation process did not have to be stopped in order to ascertain quiescent settling conditions.

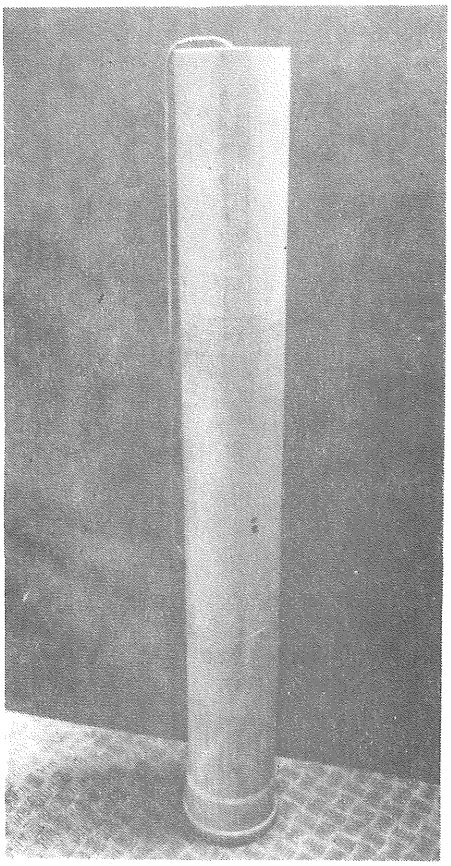

Fig 3.2. Column for settling analysis.

Only at very high mixing intensities in the flocculation tank it was impossible to carry out the settling analysis in the described manner because turbulence was induced also in the upper part of the column. Particulars concerning this problem are given in Section 3.3.5.

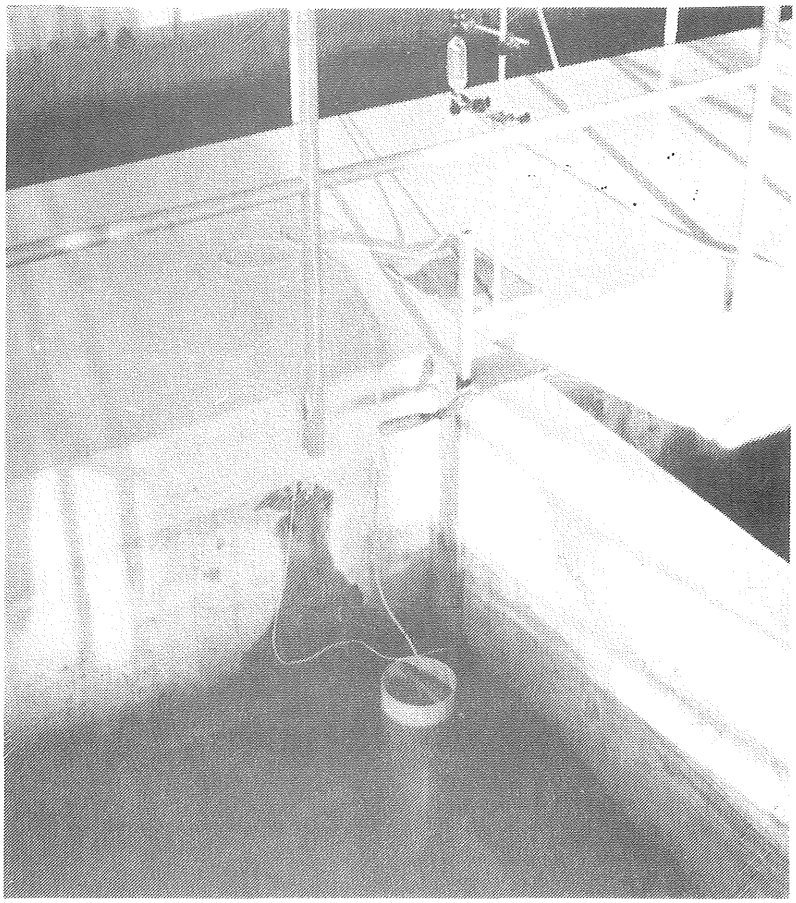

Fig 3.3. Settling column applied in a flocculation tank.

The flocs to be measured usually have a mean settling velocity of about 1 m/h. Thus it is desirable to take samples in such a way that a certain range above and below this value is covered. The sampling procedure takes some time. Then, in practice, the uncertainty of the sample time (ca. 15-30 seconds) may affect the accuracy of the obtained results. On the other hand a reasonable short duration of the whole procedure is desired. These two factors led to the following settling test sampling procedure:

Sample depth: 0,3 m

Sample times: 0, 10, 20, 40, 60 and 120 minutes

The samples were vigorously shaken in order to get as uniform particle size distribution as possible before the turbidity measurement took place.

In figure 3.4 the result of settling tests carried out in three consecutive flocculation tanks in series is exemplified.

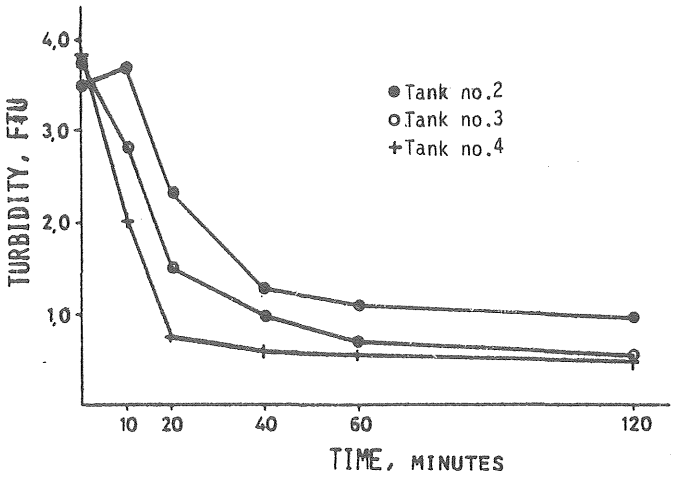

Fig 3.4. Example of time-turbidity curves from settling tests in three consecutive flocculation tanks.

If settling properties are good as for example in the lower curve in figure 3.4, an approximation with exponential curve would be possible. When the settling properties are poor, curves of another type are obtained, with an initial almost constant particle content.
The applied sample depth consequently leads to a type of time-turbidity curves often not suitable for a direct fitting of an equation as proposed by Ødegaard. A method similar to that used by Rosén (1967) will be applied, which is suitable for a great variety of settling properties.

The relative turbidity is calculated, turbidity divided by the initial turbidity value. When settling tests are performed simultaneously in successive flocculation chambers in series, the mean initial value is taken as a reference. In that way concentrations are achieved which are assumed to express the portion of the original particle content still present in the sample.

3.3.3 Settling velocity distribution

If no flocculation during settling is presupposed together with the absence of turbulence and hindered settling, the relative turbidity value of a sample (T_{rel}) taken at a depth h at the time t represents the value of the cumulative frequency distribution of the settling velocities F(v) at the settling velocity v=h/t

$$T_{rel}(h,t) = F(h/t) \qquad (3\text{-}60)$$

This can be shown by considering a settling column according to figure 3.5.

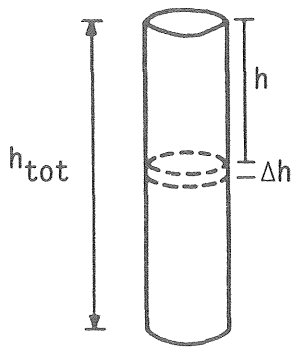

Fig 3.5. Settling column.

Suppose that the settling velocity of the flocs can be described by a settling velocity frequency function f(v) such that:

$$\int_{-\infty}^{\infty} f(v)dv = 1 \qquad (3\text{-}61)$$

For analytical purposes the frequency function can be assumed to exist also for negative settling velocities. In practice, the part of the frequency function where $v < 0$ can be interpreted as the portion of particles with a settling velocity equal to 0, i.e. the residual turbidity.

The total flux of particles (N_i) through a section at the depth h during the time t is:

$$N_i = \frac{V \cdot h}{h_{tot}} \left(\int_{h/t}^{\infty} f(v)dv + \int_{o}^{h/t} \frac{v}{h/t} f(v)dv \right) \qquad (3\text{-}62)$$

where V is the volume of the column.

The corresponding particle flux (N_o) at the depth h + Δh is:

$$N_o = \frac{(h+\Delta h) \cdot V}{h_{tot}} \left(\int_{\frac{h+\Delta h}{t}}^{\infty} f(v)dv + \int_{o}^{\frac{h+\Delta h}{t}} \frac{v}{(h+\Delta h)/t} \cdot f(v)dv \right) \qquad (3\text{-}63)$$

The increase in particle content per unit of volume within the volume with height Δh in fig 3.5 after a sedimentation time t then can be derived as:

$$\Delta T_{rel} = \frac{V}{\Delta h \cdot A} \left(-\frac{\Delta h}{h_{tot}} \int_{h/t}^{\infty} f(v)dv \right) \qquad (3\text{-}64)$$

where A is the section area of the column and thus $A \cdot h_{tot} = V$.

The actual particle concentration is:

$$T_{rel}(t) = T_{rel}(t=0) + \Delta T_{rel} = \int_{-\infty}^{\infty} f(v)dv - \int_{h/t}^{\infty} f(v)dv =$$

$$= \int_{-\infty}^{h/t} f(v).dv = F(h/t) \qquad (3\text{-}65)$$

where F(h/t) by definition is the cumulative distribution function of the frequency function f(v).

If this distribution of settling velocities could be represented by a function easy to handle it would be of great advantage. Therefore the obtained values of the cumulative distribution function have been compared with a Gaussian distribution. This has been carried out the following way:

The value of the normalized variable x was determined for which $\Phi(x)$, normally distributed (0,1), was equal to the relative turbidity. If these x-values plotted against the corresponding h/t values are forming a straight line, the settling velocity distribution can be considered normal. This procedure corresponds to a normal distribution plot with a linearized equidistant vertical axis, and a regression calculation can be performed.

The settling data from figure (3.4) are plotted in figure 3.6.

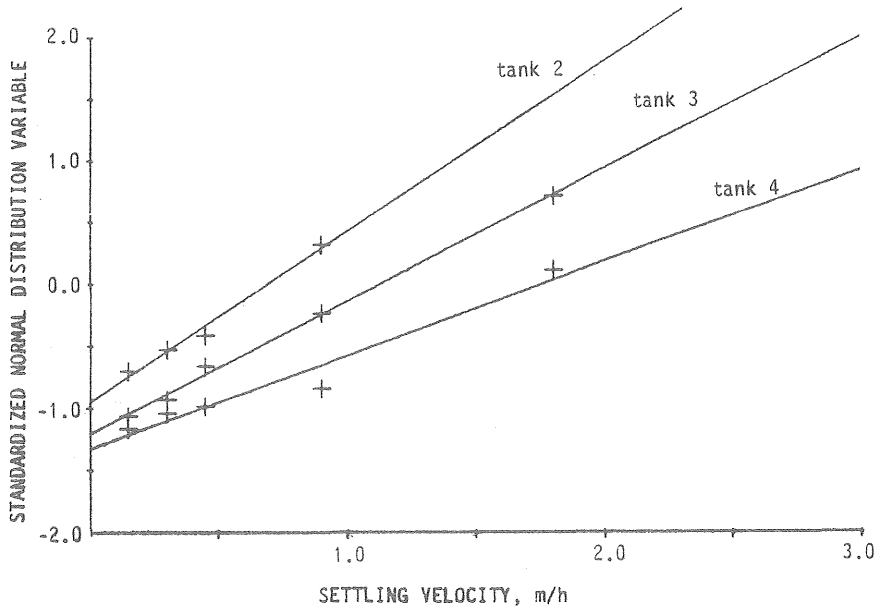

Fig 3.6. Normal distribution plot of settling analysis data according to figure 3.4.

The regression line can be determined by the least squares method. The equation obtained is of the form:

$$x = A \cdot v + B \qquad (3\text{-}66)$$

where x is the normalized variable $(v-v_m)/\sigma$
v_m mean settling velocity (m/h)
σ settling velocity standard deviation (m/h)

and consequently:

$$\sigma = 1/A \qquad (3\text{-}67)$$

$$v_m = -B/A \qquad (3\text{-}68)$$

As a rough measure of the appropriateness of the normal distribution assumption, the square of the correlation coefficient (R^2) can be given. It will give the part of the original variance "explained" by normal distribution (Hald, 1952). Table 3-1 summarizes the results of 265 settling analyses on a pilot-plant-scale, with mean settling velocities ranging from 0.1 to 4 m/h.

Table 3-1. Distribution of R^2-values for 265 settling analyses.

R2	Relative number of analyses (%)
0.99 - 1.00	40.4
0.98 - 0.99	17.4
0.97 - 0.98	15.5
0.96 - 0.97	7.9
0.95 - 0.96	5.3
0.93 - 0.95	6.0
0.90 - 0.93	4.5
< 0.90	3.0

From the table it can be seen that in more than 80% of the cases, at least 96% of the original variance is explained by the normal distribution assumption. It should be mentioned, however, that the conditions for regression calculations are not strictly fulfilled, e.g., for each calculation only a few values (4-5) are used.

The main point is not whether the settling velocity distribution is really normal or not. The question is whether the procedure described is appropriate in summarizing the settling test data into two parameters, the mean settling velocity (v_m) and the standard deviation (σ). Numerous tests have shown that the method proposed is applicable to a great variety of settling properties.

A visual impression for a judgement of the ability of the method to approximate settling velocity data is obtained if using the achieved mean settling velocity and standard deviation, a time-turbidity curve is plotted and compared with measured values. In figure 3.7 this is done for data according to figure 3.4. The values of R^2 are, as an example, 0.98, 0.99 and 0.95 for tank 2, 3 and 4, respectively.

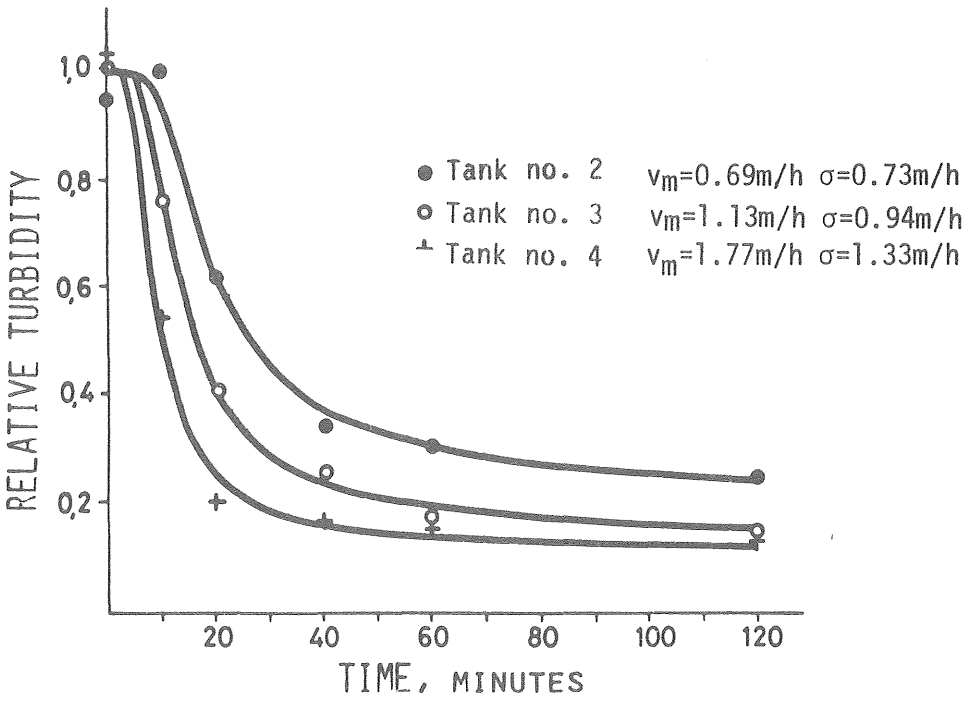

Fig 3.7. Comparison between calculated curves and obtained settling test data.

In figure 3.8 a similar plot is done for extremely poor settling properties.

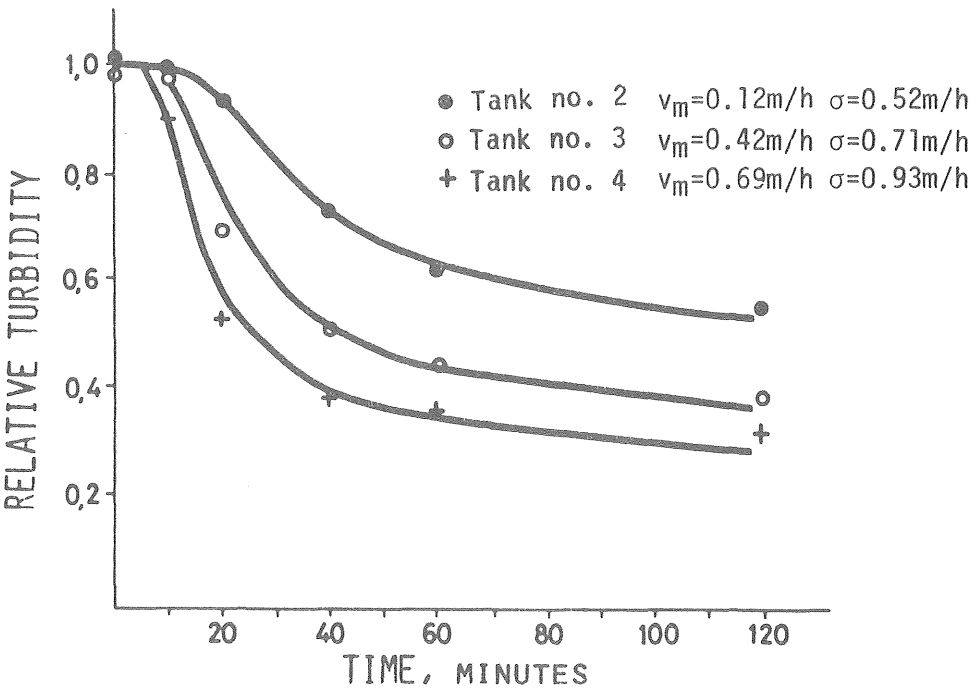

Fig 3.8. Comparison between calculated curves and obtained settling test data. Poor settling properties.

3.3.4 Interpretation of settling test data

The analysis gives as a result two parameters, mean settling velocity (v_m) and standard deviation (σ). It is not necessary, however, according to Rosén (see figure 3.1) to define any "practical" residual turbidity, which by necessity to some extent will be arbitrary. Further, it is preferable to keep the number of estimated parameters as low as possible.

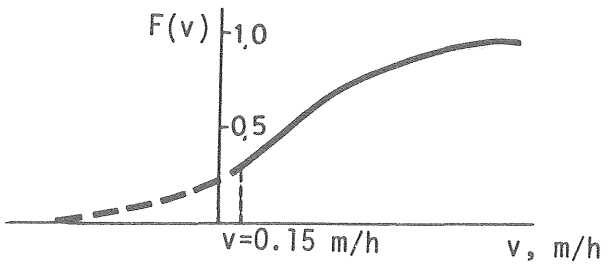

Fig 3.9. Cumulative settling velocity distribution.

A normally distributed cumulative function can be represented by means of the parameters vm and σ. The continuous line in fig 3.9 denotes the area where measurements are carried out. If the curve is extrapolated to zero settling velocity, a theoretical residual turbidity value (T_o) is obtained, which is determined by the mean settling velocity and standard deviation.

$$T_o = \int_{-\infty}^{0} f(v)dv = \Phi\left(-\frac{v_m}{\sigma}\right) \qquad (3\text{-}69)$$

$\Phi \in N(0, 1)$

A negative mean settling velocity is, though physically impossible in this context, a conceivable result of a calculation according to this method, because the mean settling velocity is calculated on the basis of the total particulate content in the water (measured as turbidity). The implication is only that the residual turbidity is greater than 50%, which, of course, means a floc with extremely poor settling properties, but nevertheless fully possible to obtain.

The difference compared with the method related by Rosén is that his calculations of v_m and σ are based on that part of the particulate matter that settles (within the duration of the measurement). The limit between settling and nonsettling matter is defined by the "practical residual turbidity", i.e., the turbidity after a (long) period of settling.

By these differences in calculation procedure it is obvious that the mean settling velocities and standard deviations obtained are not comparable, even if identical time-turbidity curves are analyzed. The difference is increased with increasing residual turbidity. Generally, higher mean settling velocities are obtained by the method according to Rosén.

To what extent the theoretically extrapolated residual turbidity (F(v=0)) will deviate from the value after a long time of settling (e.g., 2 h, 0.3m $\rightarrow$ v = 0.15 m/h) depends on v_m and σ. The difference can be estimated as:

$$\Delta\Phi = \Phi\left(\frac{0.15 - v_m}{\sigma}\right) - \Phi\left(-\frac{v_m}{\sigma}\right) \sim$$

$$\sim \Delta x \frac{d\Phi(x)}{dx} = \frac{0.15}{\sigma} \cdot \varphi(x) = \frac{0.15}{\sigma} \frac{1}{\sqrt{2\cdot\pi}} \cdot e^{-\left(\frac{v_m^2}{2\sigma^2}\right)} \qquad (3\text{-}70)$$

where $\varphi(x)$ is the standardized normal distribution function.

If v_m is assumed to be equal to σ, which sometimes can be a fair approximation, the expression can be simplified to:

$$\Delta\Phi = 0.036 \cdot \frac{1}{v_m} \qquad (3\text{-}71)$$

With the standard deviation as ordinate and the mean settling velocity as abscissa, corresponding values for constant residual turbidity can be aligned according to eq (3-72).

$$T_o = \Phi\left(-\frac{v_m}{\sigma}\right) = 1 - \Phi\left(\frac{v_m}{\sigma}\right) \qquad (3\text{-}72)$$

$$\Phi^{-1}(1-T_o) = \frac{v_m}{\sigma} \qquad (3\text{-}73)$$

where Φ^{-1} is the inverse function of Φ

For a certain value of T_o, the ratio v_m/σ is a constant and the related values of v_m and σ can be written:

$$\sigma = K_r \cdot v_m \qquad (3\text{-}74)$$

where K_r is a constant

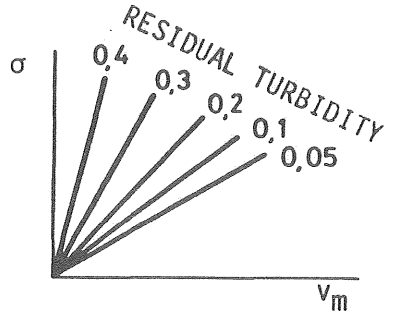

Fig 3.10. v_m and σ for constant residual turbidity.

In figure 3.10 the relation between the mean settling velocity and the standard deviation is shown. Table 3-2 gives the value of the constant K_r, calculated from normal distribution and depending on the residual relative turbidity.

Table 3-2. Calculated values of K_r.

T_o	$1-T_o$	$\Phi^{-1}(1-T_o)$	K_r
0.00	1.00	+ ∞	0
0.05	0.95	1.645	0.608
0.10	0.90	1.282	0.780
0.15	0.85	1.036	0.965
0.20	0.80	0.842	1.188
0.25	0.75	0.675	1.481
0.30	0.70	0.524	1.908
0.35	0.65	0.385	2.597
0.40	0.60	0.253	3.953
0.45	0.55	0.125	7.955
0.50	0.50	0	+ ∞

Instead of the residual turbidity after an infinite sedimentation time, the turbidity after a finite time corresponding a certain settling velocity, e.g. 0.15 m/h, can be chosen. That will change eqs (3-72), (3-73), and (3-74) to

$$T_o' = \Phi\left(\frac{0.15-v_m}{\sigma}\right) = 1 - \Phi\left(\frac{v_m-0.15}{\sigma}\right) \qquad (3\text{-}75)$$

$$\Phi^{-1}(1-T_o') = \frac{v_m-0.15}{\sigma} \qquad (3\text{-}76)$$

$$\sigma = K_r \cdot (v_m-0.15) \qquad (3\text{-}77)$$

After a settling time corresponding to a settling velocity of 0.15 m/h figure 3.11 shows the relative turbidity to be expected for any combination of mean settling velocity and standard deviation.

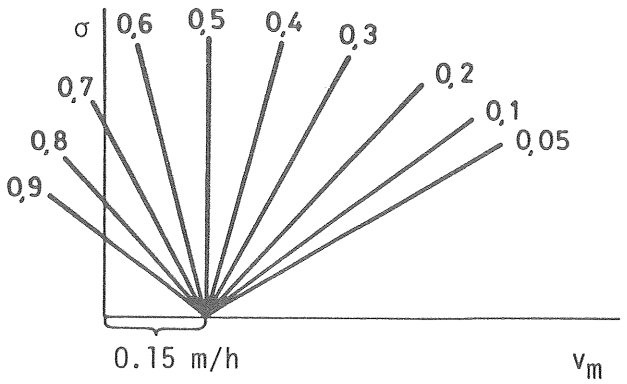

Fig 3.11. The relation between v_m and σ for a settling time corresponding to v = 0.15 m/h.

Generally the relative turbidity at any moment can be estimated by translating the lines defining the turbidity level to a distance corresponding the settling depth divided by the time (h/t). The turbidity can be read on the translated sloping lines where the present combination (v_m,σ) of the fixed coordinate system coincides (see figure 3.12).

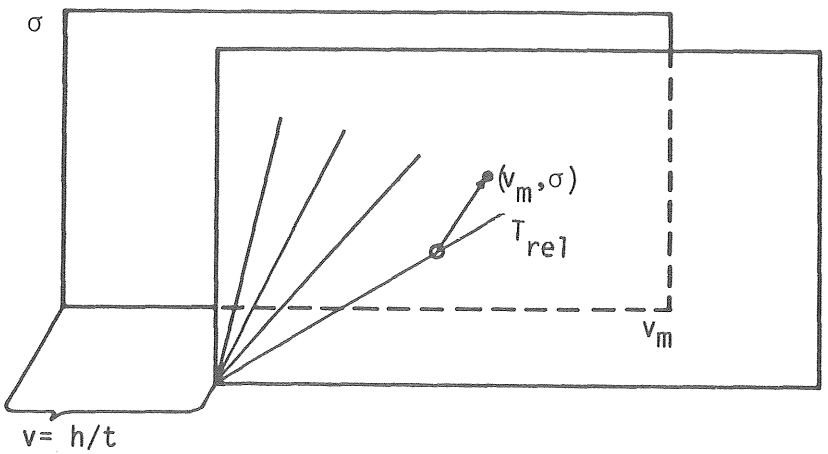

Fig 3.12. Graphical calculation of relative turbidities at different times when v_m and σ are known.

3.3.5 The effect of depth and column design on the settling test result

As mentioned earlier the settling test was standardized to be carried out at a depth of 0.3 m in a column with a diameter of 150 mm with a total length of 1.25 m. A number of experiments were performed in order to determine the impact of some different test designs.

Aluminium hydroxide flocs are by their nature highly flocculent. A change in settling properties according to flocculation caused by differential settling is therefore to be expected. The result will be that different settling properties are measured, depending on the sampling depth. This can be shown by a multiple-depth settling analysis as reported by Villemonte *et.al.* (1966).

Hedberg (1976) showed the influence of sedimentation depth and compared his findings with data according to Villemonte.

Figure 3.13 (from Hedberg, 1976) shows how the mean settling velocity (v_{fm}) and the settling velocity representing a removal of 95% (v_{f5}) of "practically settlable flocs", change with sedimentation depth. The settling velocities are defined according to Rosén, as described in Section 3.3.1.

An increase in the sedimentation depth from 0.1 to 1.0 m can rougly be said to double the settling velocity.

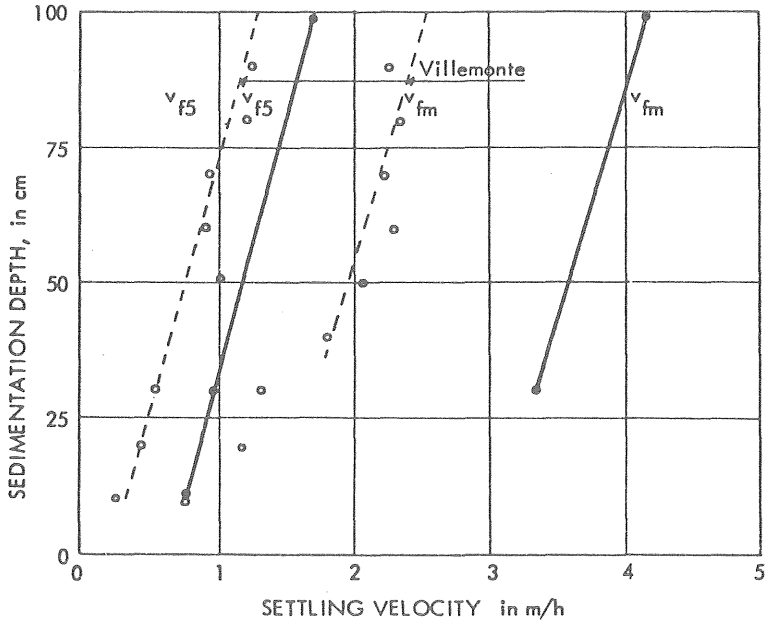

Fig 3.13. Settling velocity and depth. Hedberg (1976) v_{fm} is the mean settling velocity, v_{f5} is the settling velocity corresponding to the removal of 95% of the flocs that will settle.

Multiple depth analyses carried out by McLaughlin (1959) showed that the effect of flocculation increased with the depth from the surface.

Examples of two multiple-depth settling analyses are given in fig 3.14 and 3.15. They were both performed in the final flocculation tank of the pilot plant.

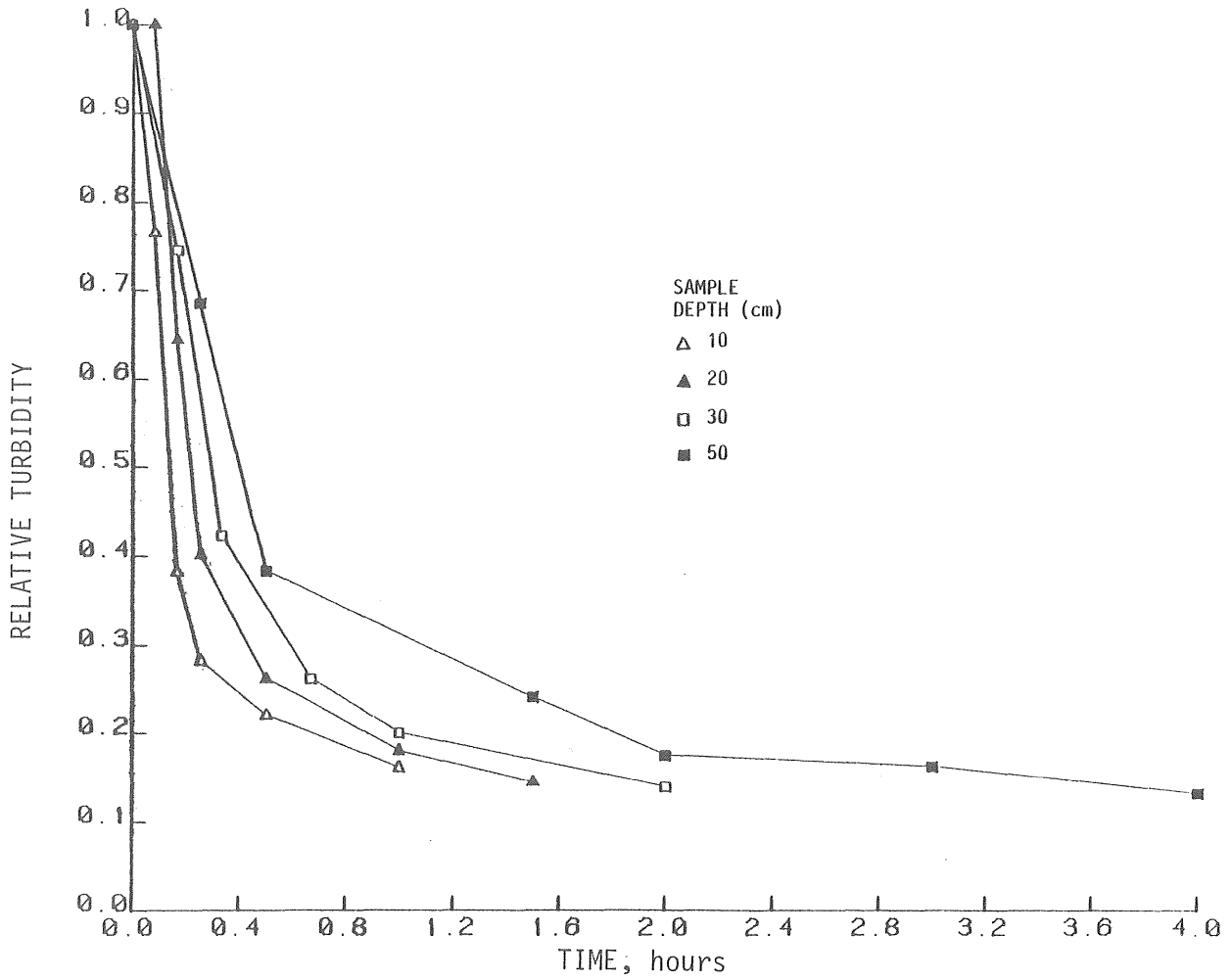

Fig 3.14. Multiple depth settling test. Final flocculation tank of the 7 m^3 pilot plant. Alum 40 ppm, temp 18°C. No activated silica.

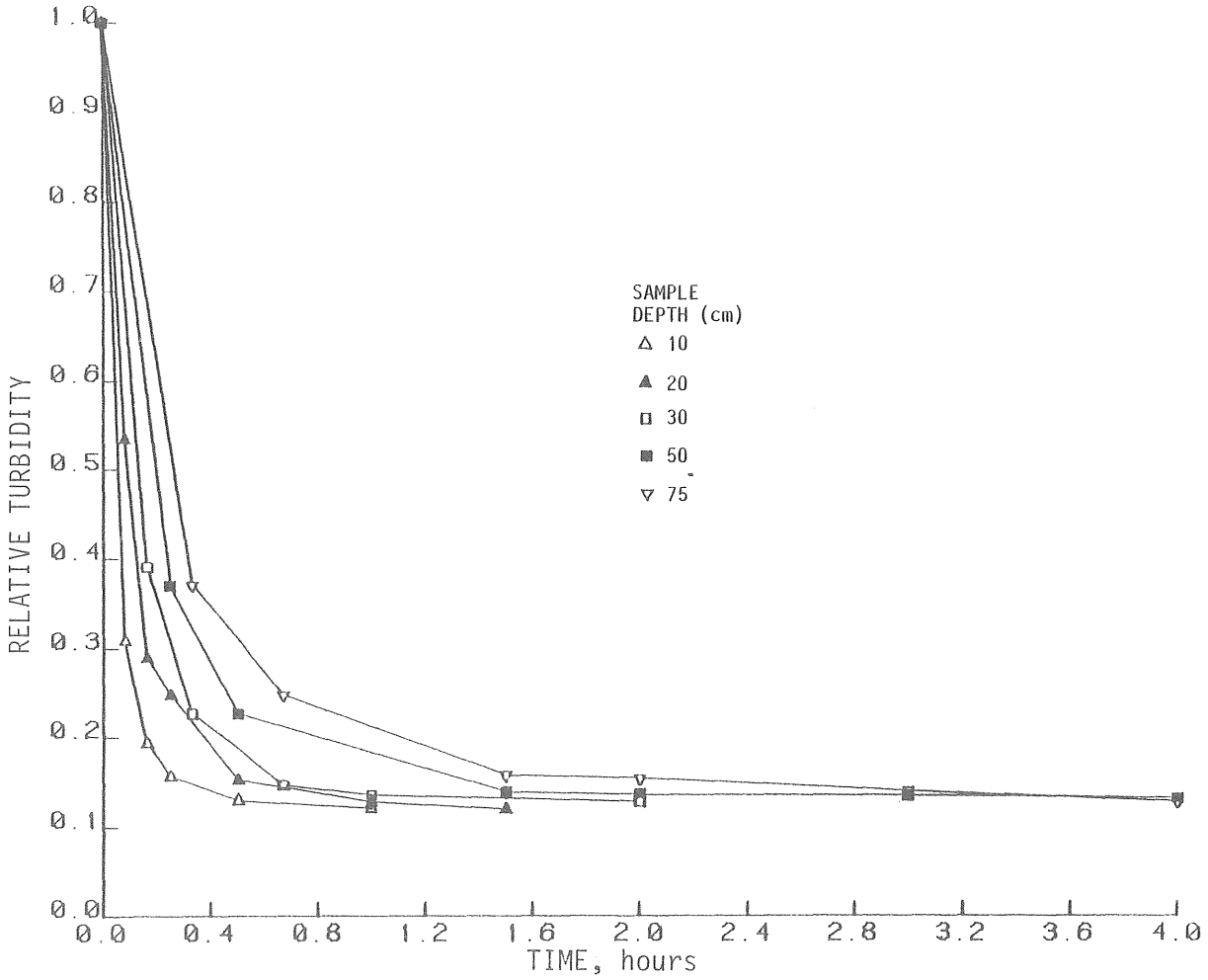

Fig 3.15. The same conditions as in figure 3.14 except for an activated silica dosage of 2 ppm.

From the settling test data according to figs 3.14 and 3.15, the settling properties can be calculated (table 3-3).

Table 3-3. Mean settling velocity (v_m) and standard deviation. Data from figs 3.14 and 3.15.

	Depth (m)	v_m (m/h)	σ (m/h)	v_m/σ
No activated silica	0.1	0.75	0.66	1.14
	0.2	0.94	0.78	1.21
	0.3	1.13	0.98	1.15
	0.5	1.38	1.24	1.11

	Depth (m)	v_m (m/h)	σ (m/h)	v_m/σ
2 ppm activated silica	0.1	2.01	1.62	1.24
	0.2	2.20	1.79	1.23
	0.3	2.32	1.85	1.25
	0.5	2.77	2.31	1.20
	0.75	3.04	2.58	1.18

It can be seen from table 3-3 that v_m and σ increase with depth, however, in a proportional way so that the ratio v_m/σ essentially is a constant characteristic for each experimental condition. This is another way of expressing the fact that the residual turbidity is a constant, unaffected by the depth. The flocculation that obviously occurs, does not seem to incorporate small particles that represent the residual turbidity.

The settling tests shown in figures 3.16 and 3.17 were performed at the same depth (0.3 m) but with different kinds of columns.

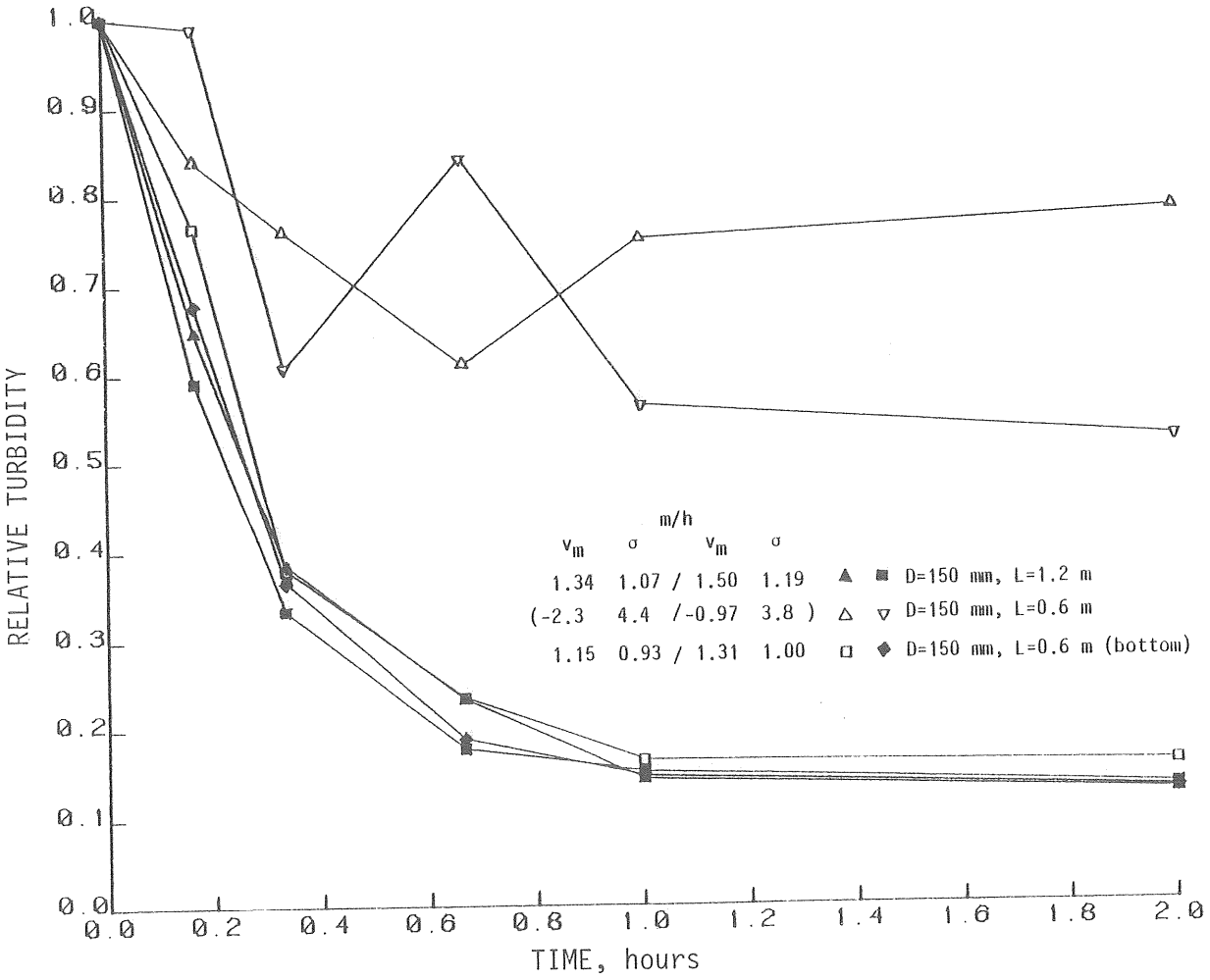

Fig 3.16. Settling tests with a sampling depth of 30 cm. Column diameter 150 mm. Column length 1200 and 600 mm, the latter with closed and open bottom.

In figure 3.16 the column diameter is 150 mm. As can be seen, if the column length under the sample point (with open bottom) is reduced too much, the test is impossible to carry out, because the turbulence in the flocculation volume will impose unfavorable conditions for sedimentation at the sample point.

One way of dealing with that problem is to close the bottom after lowering the column into the basin, as can also be seen in fig 3.16. Two successive sets of settling tests were carried out in order to estimate the reliability of the measurements. The flocculation conditions were kept constant throughout the test; thus the curves represent the same floc quality. The lower curves are almost identical, with the exception of some differences in the first sample, which result in some deviations in the calculated parameter of the normal distribution.

Figure 3.17 shows that with constant column length (L=600 mm) and open bottom, the effect of turbulence can be reduced if the column diameter is decreased.

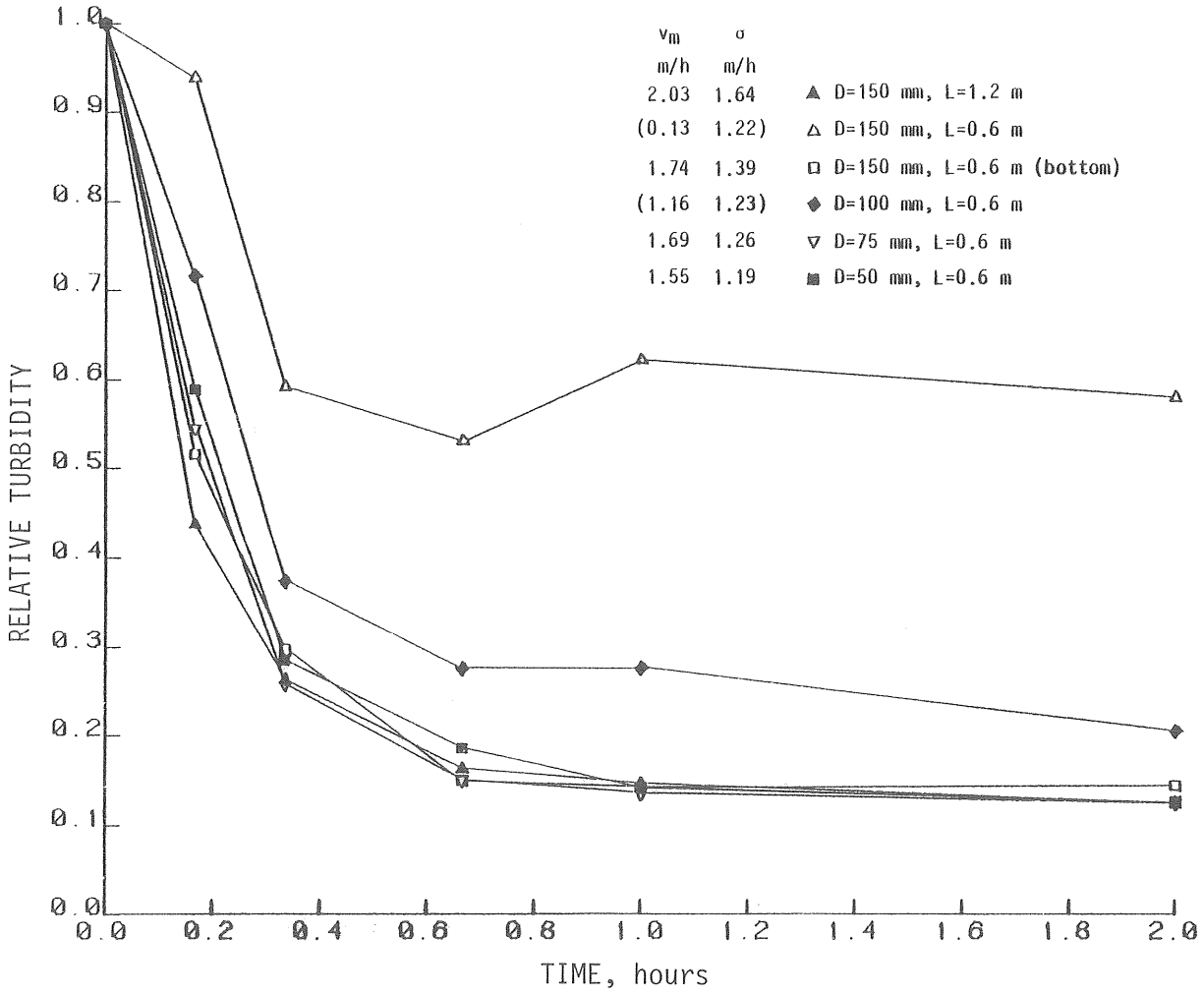

Fig 3.17. Settling test with a sampling depth of 30 cm. Varying column length and diameter. 2 ppm activated silica.

With column diameters of 75 and 50 mm, practically the same result was obtained as with the standard test design. The result gradually deteriorates when the column diameter is increased to 100 and 150 mm.

A multiple-depth settling test with a considerably longer settling column (L = 3.5 m, diameter 200 mm) was carreid out in the last flocculation tank of the Lackarebäck water treatment plant, Gothenburg. The settling properties found are shown in figure 3.18. The attempt to measure settling properties at a depth of 3.0 m failed because the sample point was too close to the opening in the bottom. The settling velocity and standard deviation at 0.3 and 0.5 m show the same values. probably because the samples from the 0.3 m depth were drawn from a separate column of ordinary dimensions beside the large one, with the possibility that the samples represent slightly different suspension properties.

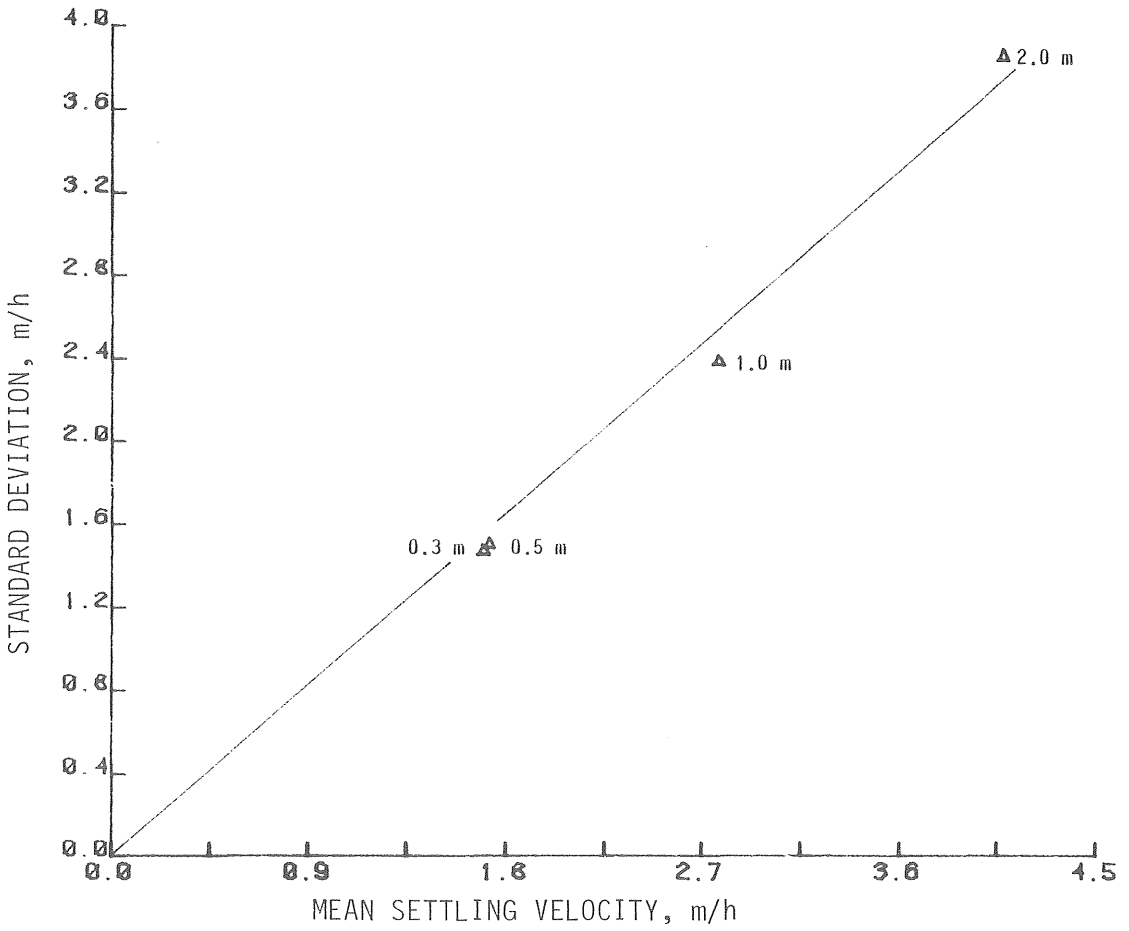

Fig 3.18. Settling properties at different depths. Lackarebäck treatment plant. Temp 4°C. 38 ppm alum. 2 ppm activated silica.

Despite the relatively limited number of settling tests carried out at different depths and with varying column design, however, some general conclusions can be made.

It is possible to carry out settling of aluminium hydroxide floc in a tube open in the bottom and lowered in a flocculation tank in operation, if $H_B/D > 4$, where H_B is the distance from the sample point to the opening in the bottom and D is the column diameter. It should be mentioned that the turbulence level in the flocculation tanks was moderate. The results in fig 3.14 and 3.15 were achieved in a flocculation tank with a G-value of about 5 s^{-1}. Naturally, intense mixing will make the kind of procedure suggested here impossible. The limit where some influence could be seen, which disappeared when the stirrer in the flocculation volume was stopped, was about $H_B/D = 3$.

In figure 3.19 the influence of settling depth for varying conditions is roughly summarized. As a comparison, the mean settling velocity at 30 cm depth is given the relative value 1.0.

The number of settling analyses (21) on which the figure is based is limited, so the generality can be questioned. Each point at the depth of 0.75 m and more only represents one value.

According to the data, there seems to be a linear growth of mean settling velocity with depth. The same relationship is valid for the settling velocity standard deviation (σ) as it earlier has been shown that the ratio v_m/σ is a constant unaffected by sedimentation depth.

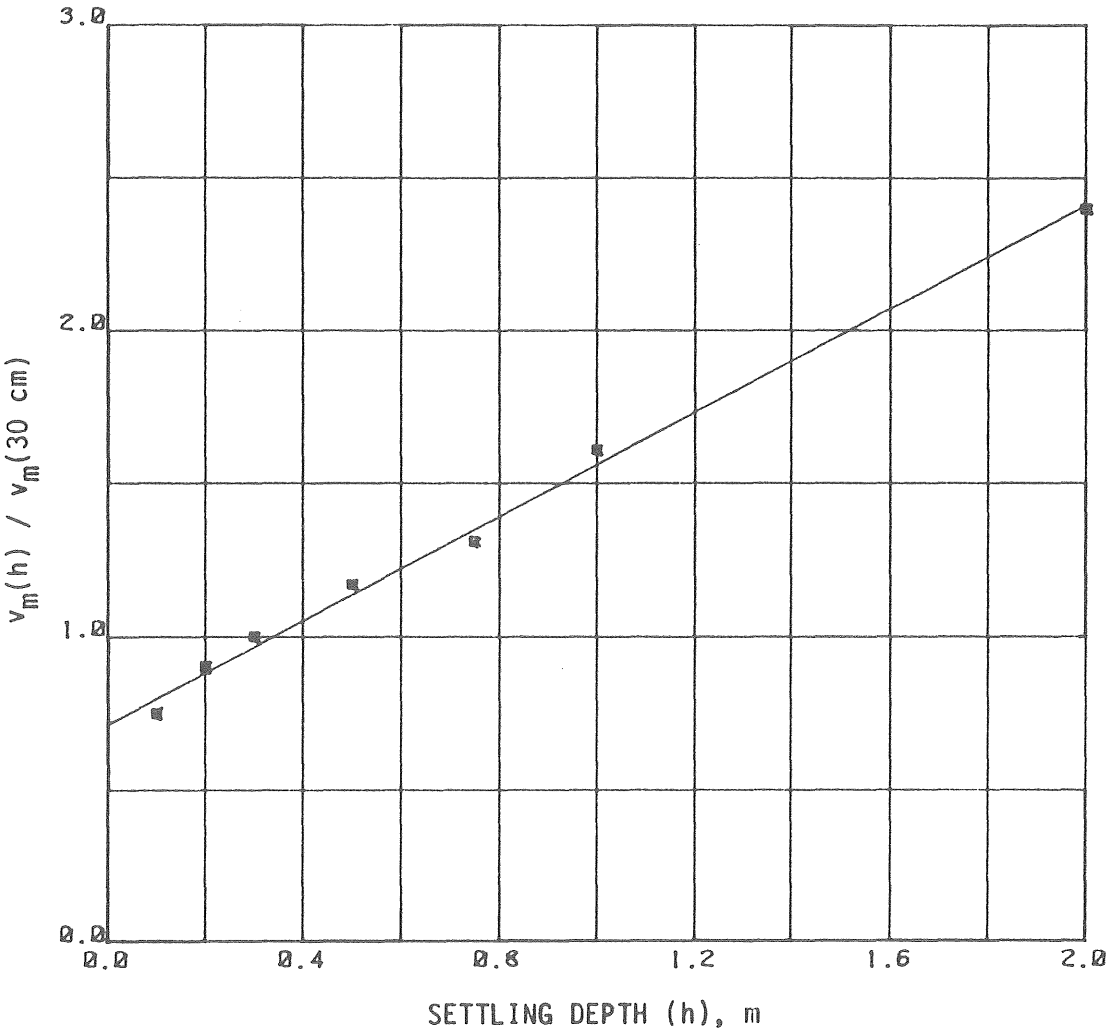

Fig 3.19. Mean settling at different depths compared with the standarized depth of 30 cm.

3.3.6 Settling in a continuously operating sedimentation basin

When data obtained from a quiescent column settling test are used to predict the result of a continuous sedimentation process, the hydraulic characteristics of the sedimentation basin will add complexity to the problem. At this stage some assumptions will be made to facilitate the calculations.

The hydraulic conditions in the sedimentation unit are assumed to appropriately be described as plug-flow, that is, no longitudinal mixing, no short circuiting. In- and outflow are evenly distributed in a section perpendicular to the flow.

No hindered settling; the effect of the settled sludge layer is neglected.

The settling velocity distribution is assumed not to change with depth.

If these assumptions are fulfilled, the sedimentation result can be obtained by considering a fictive settling column moved from the inlet to the outlet at a velocity determined by the flow. Figure 3.20 shows a fictive settling column in a lamella sedimentation unit used in pilot-plant studies.

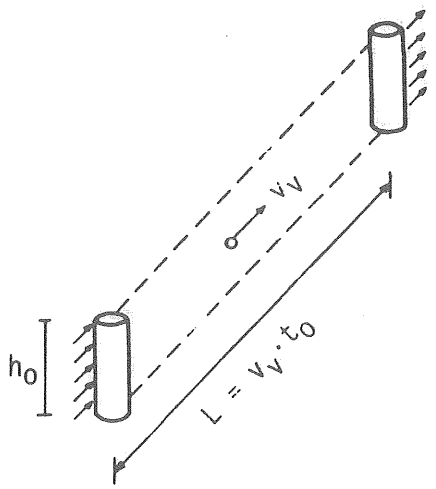

Fig 3.20. A fictive settling column in a lamella sedimentation unit.

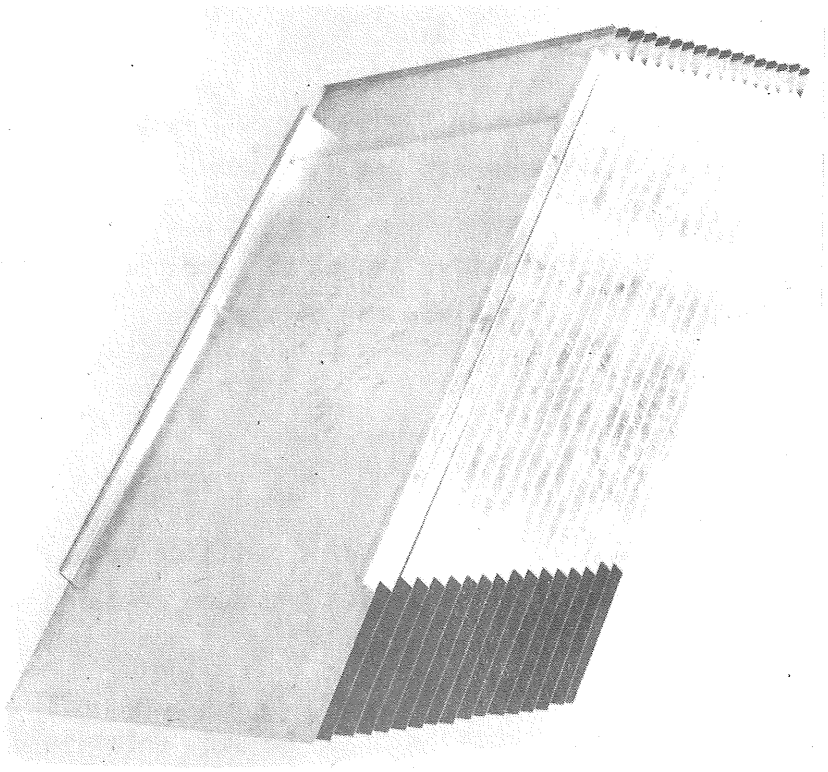

Fig 3.21. Lamellae photographed outside the sedimentation basin.

The removal of particles in the sedimentation unit then can be considered as the same as within the settling column after the time $t_o = L/v_v$, the detention time in the sedimentation basin.

All particles with a settling velocity greater than the column height (h_o) divided by the residence time (t_o) will be removed. This settling velocity equals the overflow rate, the flow divided by the projected horizontal area (A), and will be denoted v_F. The equation (3-78) is well known as Hazen's ideal sedimentation theory:

$$v_F = Q/A = h_o/t_o \qquad (3\text{-}78)$$

For lamella sedimentation Weijman-Hane (1963) developed equation (3-79) (upflow lamella sedimentation). For further details, see Hedberg (1976). Within parentheses the actual values for the pilot plant sedimentation unit are given.

$$v_F = \frac{Y_a}{\frac{L}{s} \cdot \cos\alpha + 1} \qquad (3\text{-}79)$$

where Y_a is flow divided by water surface area
L is lamella length (1.9 m)
s is horizontal lamella distance (0.1 m)
α is lamella inclination angle (55^o)

The value of the denominator in eq (3-79) for the lamella sedimentation unit used in pilot-plant experiments was 11.9.

According to eq (3-60), the relative amount of flocs not removed at varying depth h in the fictive column can be written:

$$F(h/t_o) = F(v) = \Phi\left(\frac{v-v_m}{\sigma}\right) \qquad (3\text{-}80)$$

F is the cumulative distribution function of settling velocities, which is assumed to be normally distributed with the mean settling velocity v_m and standard deviation σ.

The mean floc residual in the outflow from the sedimentation unit can be obtained as the mean value in the column considered from h = 0 to $h = h_o$ or:

$$T_{rel}^{sed} = \frac{1}{v_F} \int_o^{v_F} F(v)dv \qquad (3\text{-}81)$$

An identical expression is obtained if the settling velocity frequency distribution f(v), is considered (fig 3.22).

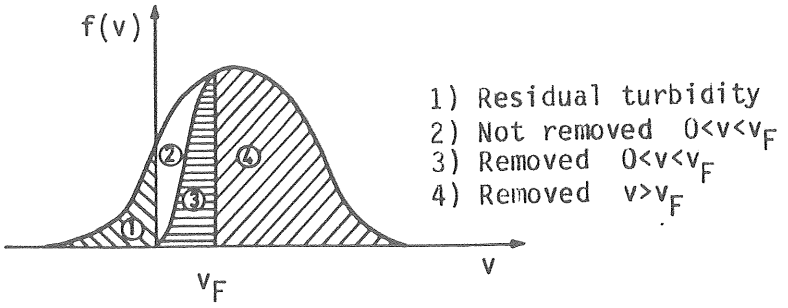

Fig 3.22. Settling velocity distribution function and removal in a sedimentation unit.

The residual after sedimentation can be written:

$$T_{rel}^{sed} = F(v_F) - \int_0^{v_F} \frac{v}{v_F} \cdot f(v)\, dv \qquad (3\text{-}82)$$

The identity of eqs (3-81) and (3-82) is revealed if eq (3-82) is developed according to

$$T_{rel}^{sed} = F(v_F) - \int_0^{v_F} \frac{v}{v_F} f(v)\cdot dv = F(v_F) - \left(\left[\frac{v}{v_F} \cdot F(v) \right]_0^{v_F} - \right.$$

$$\left. - \frac{1}{v_F} \int_0^{v_F} F(v)\cdot dv \right) = F(v_F) - \left[F(v_F) - \frac{1}{v_F} \int_0^{v_F} F(v)dv \right] =$$

$$= \frac{1}{v_F} \int_0^{v_F} F(v)dv \qquad (3\text{-}83)$$

If the settling velocity is normally distributed, eq (3-84) is valid.

$$T_{rel}^{sed} = \frac{\sigma}{v_F \cdot \sqrt{2\pi}} \left(e^{-\frac{(v_F - v_m)^2}{2\cdot\sigma^2}} - e^{-\frac{v_m^2}{2\cdot\sigma^2}} \right) +$$

$$+ \frac{v_m}{v_F} \cdot \Phi\left(-\frac{v_m}{\sigma}\right) + \frac{v_F - v_m}{v_F} \cdot \Phi\left(\frac{v_F - v_m}{\sigma}\right) \qquad (3\text{-}84)$$

The removal efficiency of a sedimentation basin according to equations (3-81) and (3-82) can be approximated if some simplifications are introduced. As is most evident in eq (3-81), the sedimentation result is obtained as a mean value of residual particle content over all depths. One possible approximation of that value, used by, for example, Ødegaard (1975) is:

$$T_{rel}^{sed} \simeq \frac{1}{2}(F(v_F) + F(o)) \qquad (3\text{-}85)$$

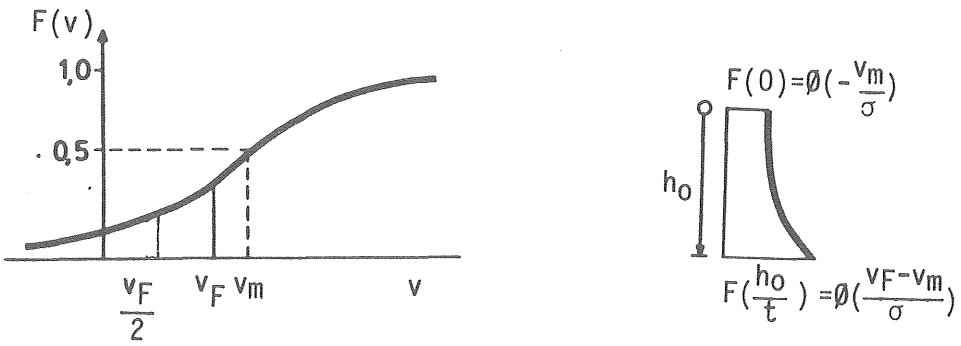

Fig 3.23. Simplified calculation of sedimentation result.

Another way is to use the residual at the mean depth as illustrated in figure 3.23, equation (3-86).

$$T_{rel}^{sed} \simeq F(v_F/2) \qquad (3\text{-}86)$$

An approximation according to eq (3-85) will usually result in a slightly higher value than the "exact" residual. The opposite is the case with eq (3-86).

If the settling velocity distribution is symmetrical around the mean settling velocity v_m (as the normal distribution is), both expressions will give the exact value when $v_F = 2 \cdot v_m$. It will be shown that an

approximation according to eq (3-86) is a convenient means of illustrating and interpreting flocculations results in terms of the distribution of settling velocities, in spite of some underestimation of the theoretically correct sedimentation result. The error introduced depends on the settling properties and the sedimentation load and has been calculated for varying conditions in figure 3.24. The dotted curves are approximated residual values and the continuous curves are calculated according to eq (3-82).

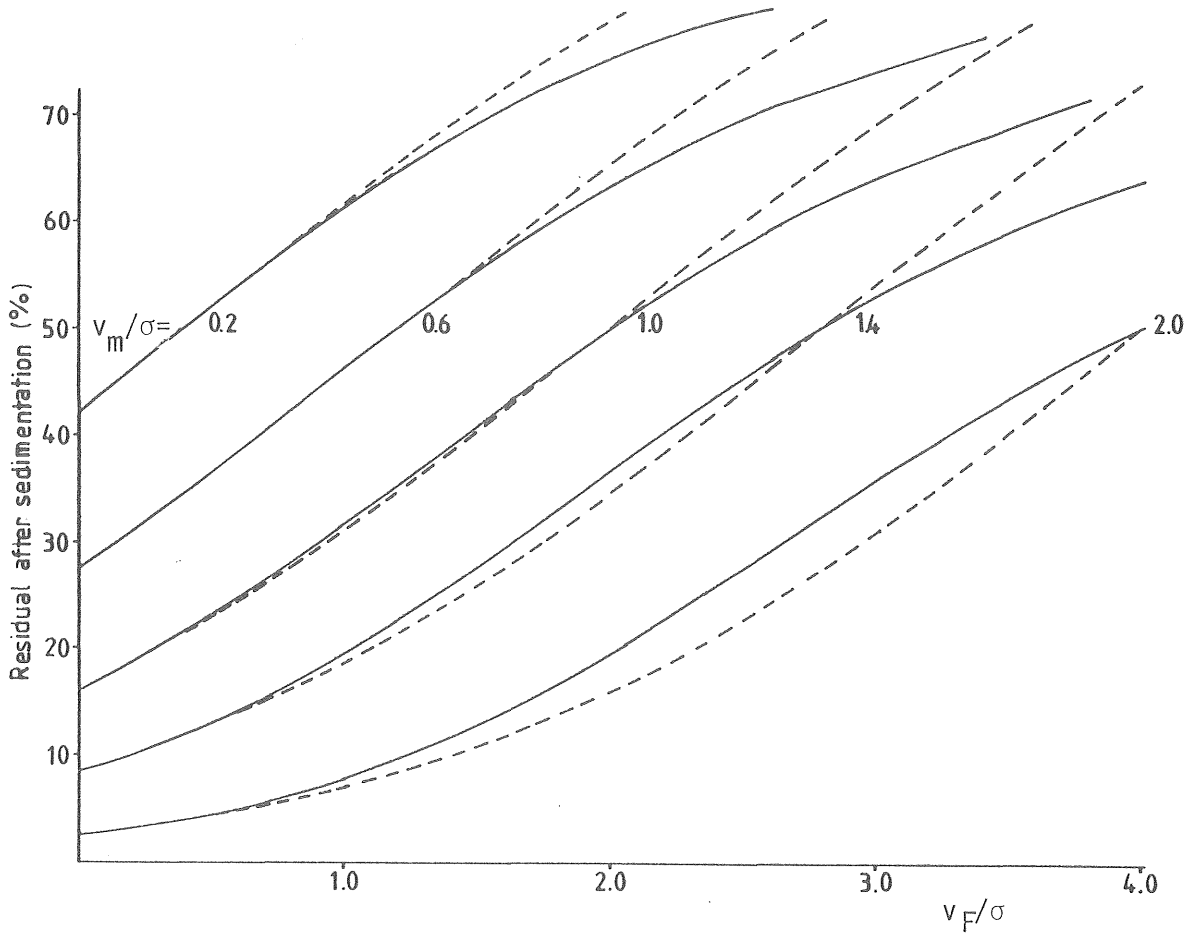

Fig 3.24. Residual after sedimentation depending on settling characteristics (v_m, σ) and overflow rate (v_F). Calculated values (eq 3-82 - continuous line). Approximated values (eq 3-86 - dotted line).

To account for the influence of sedimentation depth on the sedimentation result, figure 3.24 can also be used. As shown, the ratio v_m/σ is a constant independent of depth. It determines the appropriate curve in figure 3.24. An increase in depth will result in a decrease in the ratio v_F/σ (see figure 3.19), and the calculated sedimentation result will be altered according to the curve under consideration.

A graphical method to determine the sedimentation result according to eq (3-86) can be given as a consequence of the procedure already described in figure 3.12. Eq (3-86) can be written:

$$T_{rel}^{sed} \simeq \Phi\left(\frac{v_F/2-v_m}{\sigma}\right) \qquad (3\text{-}87)$$

The relation between v_m and σ for a constant sedimentation result is given by

$$\sigma = \frac{1}{\Phi^{-1}(1-T_{rel}^{sed})} \cdot (v_m-v_F/2) = K_r\cdot(v_m-v_F/2) \qquad (3\text{-}88)$$

The value of K_r calculated from the normal distribution is given in table 3-2 and in figure 3.25.

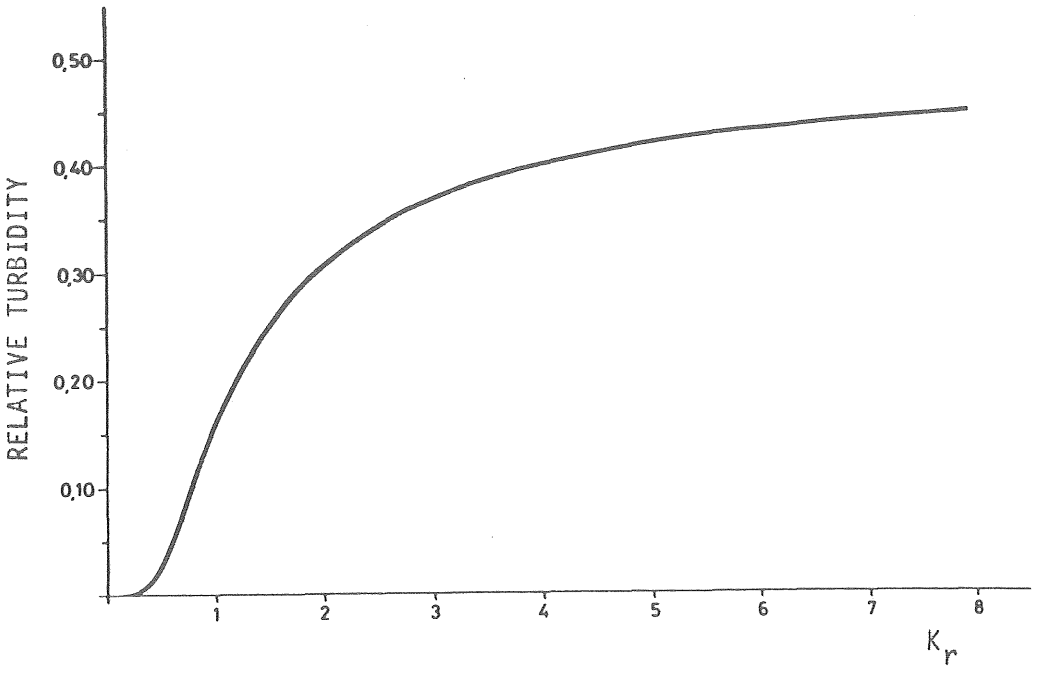

Fig 3.25. K_r and residual after sedimentation.

Corresponding values of v_m and σ for a constant relative turbidity after sedimentation are thus described by straight lines starting at the point $(v_F/2,0)$ on the v_m-axis in a v_m-σ diagram. The slope of the line can be determined by means of figure 3.24 or table 3-2.

Figure 3.26 shows how changes in settling properties at a given overflow rate will change the sedimentation result.

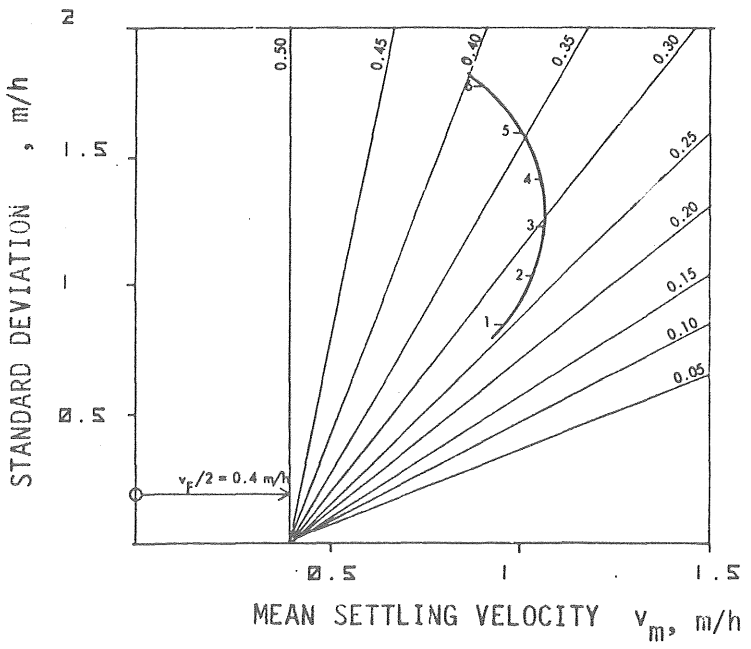

Fig 3.26. Illustration of graphical calculation of sedimentation result at a given overflow rate for different settling properties.

3.3.7 Comparison with actual sedimentation result obtained

Villemonte *et.al.* (1966) developed a technique where dispersion curves for the flow through the settling basin together with settling curves were used to predict removal efficiency. A multiple-depth column settling was carried out. The depth that gave a removal closest to observed data was selected as the "critical settling depth", which was used as a criterion for basin performance.

By means of eqs. (3-81), (3-82) or (3-84), the theoretical sedimentation result can be calculated if the floc settling properties are known. Flocculation during sedimentation is neglected.

The actual sedimentation result obtained will differ from the calculated one, because of the design and hydraulic characteristics of the sedimentation unit. These discrepancies are not considered here to be of primary concern. They will be taken into account in a general way.

Results obtained for a pilot-scale operation, in a shallow depth sedimentation unit, included generally higher residuals than theoretically could be expected. Besides flocculation - settling depth was about 14 cm compared to the column settling depth 30 cm - the results can be interpreted as the effect of an unfavorable flow pattern. The lamella areas was only partly used for sedimentation. Mathematically, it can be expressed in a coefficient K_{lam}, by which the overflow rate is to be multiplied to give a removal equal to observed data. Eq (3-79) then can be written

$$v_F = \frac{K_{lam} \cdot Y_a}{\frac{L}{s} \cdot \cos\alpha + 1} \qquad (3\text{-}89)$$

where v_F is the theoretical overflow rate.

If K_{lam} is calculated from a number of experiments in pilot-scale (fig 3.27), a decrease in the effective sedimentation area (increase of K_{lam}) with increasing hydraulic load can be detected. The following relationship was chosen to express this effect:

$$K_{lam} = 1 + 0.083 \cdot Y_a \qquad (3\text{-}90)$$

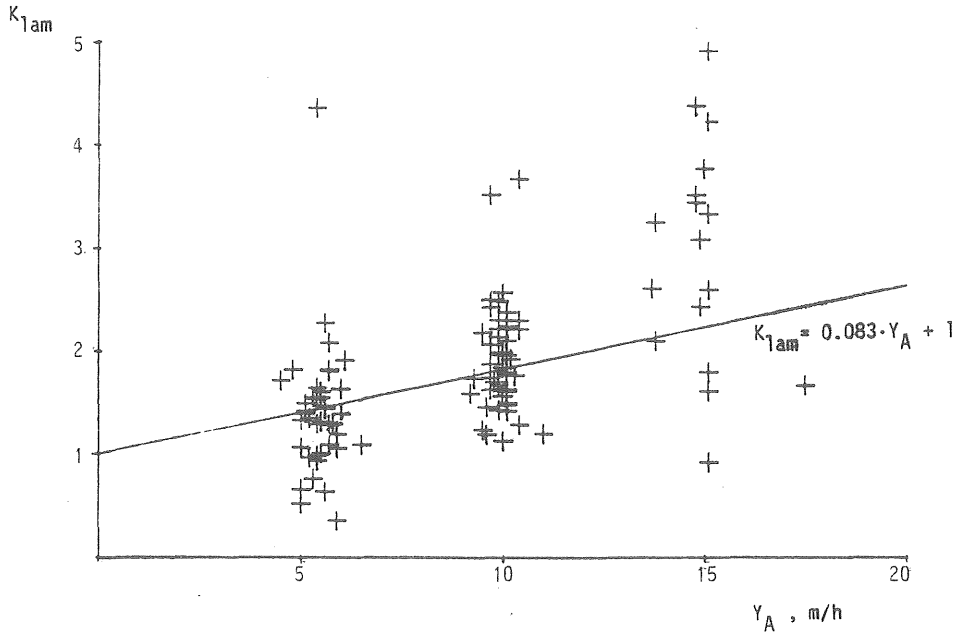

Fig 3.27. Relationship obtained between K_{lam} and Y_a.

The figure does not give a correct impression of how accurate the removal is predicted. At low surface loads a small error in the measured residual causes a large uncertainty in the determination of K_{lam}, because the slope of the settling curve is low. At high loads, flocculation effects become more accentuated, to a varying extent depending on settling characteristics. It can consequently be seen that deviations from the line are smaller at medium overflow rates.

In figure 3.28 the line represents the calculated residual after sedimentation. According to eq (3-90), a correction of the overflow rate has been introduced. Data have been taken from the settling test in figure 3.4. Observed data are indicated.

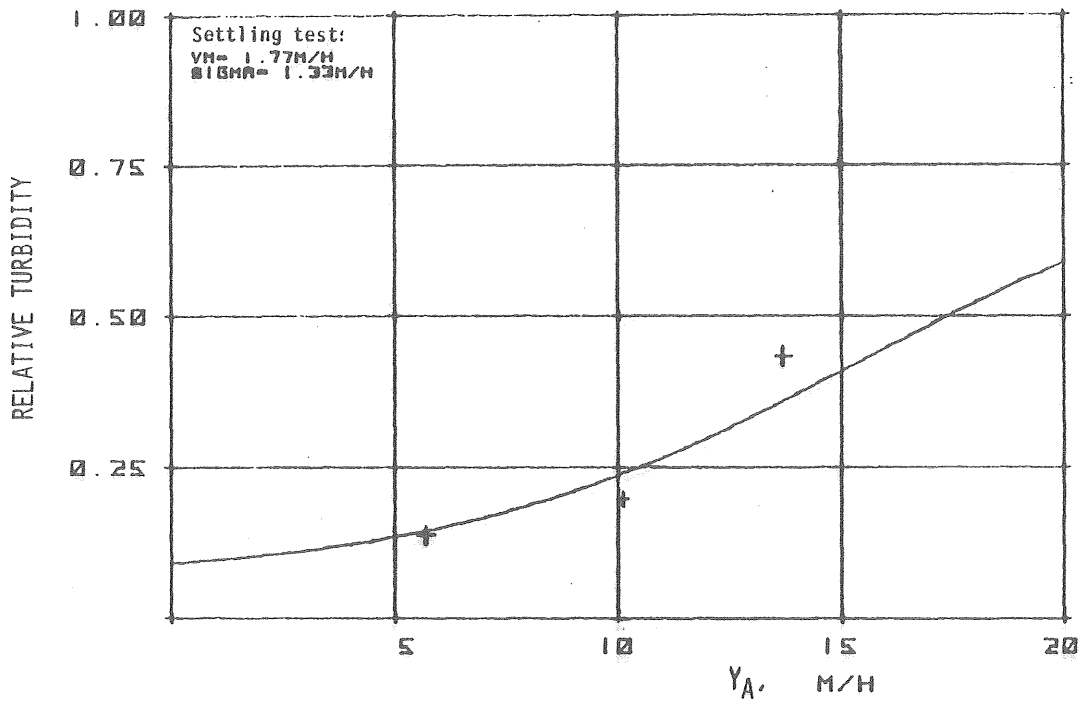

Fig 3.28. Actual sedimentation results (points) and sedimentation result calculated from settling test (continuous curve).

The situation is somewhat different in deeper conventional horizontal sedimentation basins. Measurements carried out at 19 Swedish water treatment plants generally showed a higher removal than was predicted from a settling test performed in the final flocculation tank. Fig 3.29 shows the agreement between actual removal and removal calculated from the settling test. The calculations were simplified: The relative turbidity value on the time-turbidity curve was chosen at the time corresponding to $h/0.5v_F$, where h (the sampling depth) was 0.3 m and v_F the overflow rate.

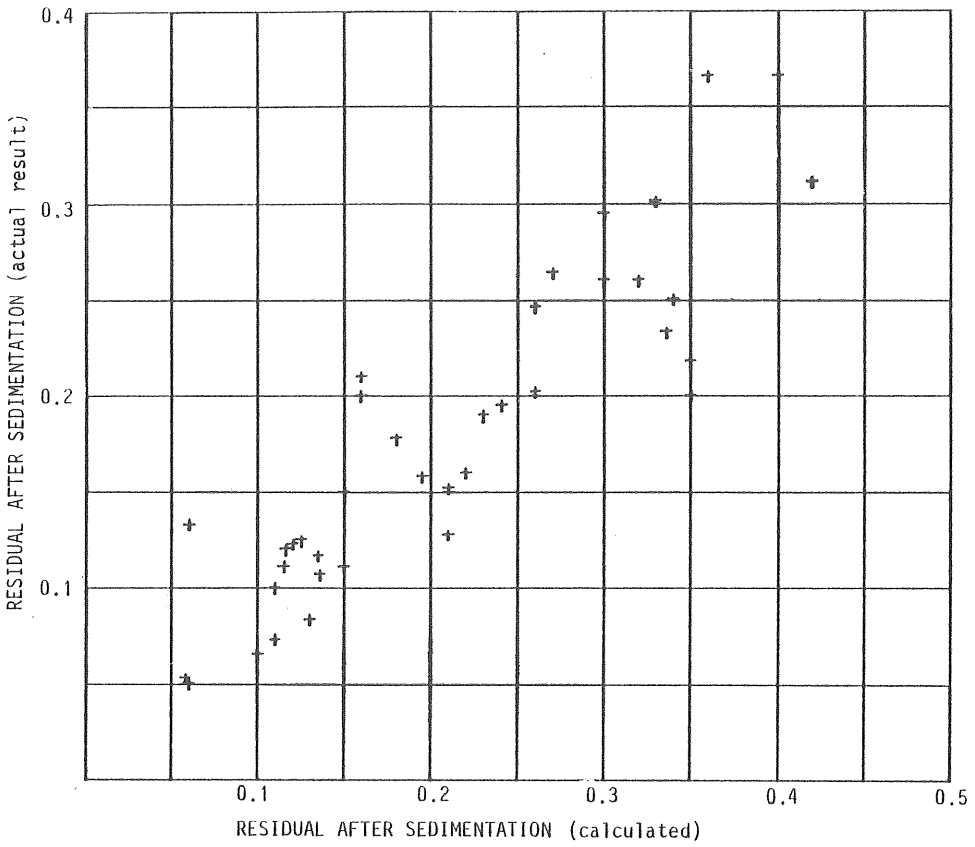

Fig 3.29. Residual after sedimentation. Calculated and actual results. Data from 19 water treatment plants.

3.4 Power input determination

3.4.1 Calculations

In a stirred tank a uniform velocity gradient does not exist. Camp and Stein (1943) showed that a mean velocity gradient could be defined as:

$$G = \sqrt{\frac{W}{\mu}} \qquad (s^{-1}) \qquad (3\text{-}91)$$

where W is the overall work input per unit of time and unit of volume (watt/m^3) and μ the viscosity (Ns/m^2).

The equation is based on the fact that work is only done by shearing stresses dissipated as heat. Camp and Stein showed that for a small element an orientation is always possible to find, which reduces the deformation to a two-dimensional angular distortion. The work done in that plane (per unit of volume and unit of time) equals:

$$w = \tau \cdot \gamma = \mu \cdot \gamma^2 \qquad (3\text{-}92)$$

where τ is the shear stress (N/m^2)
γ is the rate of angular distortion = velocity gradient (s^{-1})

When the work input is performed by rotation paddles, the drag on each paddle can be calculated as:

$$F_D = C_D \cdot A_p \cdot \frac{\rho \cdot v_{rel}^2}{2} \qquad (3\text{-}93)$$

where C_D is the doefficient of drag
A_P the cross section area of the paddles normal to the direction of motion (m^2)
v_{rel} the velocity of the paddles with respect to the liquid (m/s)

Camp (1973) derived the following expression for applied work per unit volume and unit of time:

$$W = \frac{F_D \cdot v_{rel}}{V} = \frac{C_D \cdot A_p \cdot \rho \cdot (1-k)^3 \cdot n^3 \cdot r^3 \cdot (2\pi)^3}{2 \cdot V} \qquad (3\text{-}94)$$

where r is the distance from the paddle blade to the shaft (m)
n is the speed of the shaft (rev/s)
V is the volume of the tank (m^3)
and $k \cdot n$ the revolution speed of the water.

Several authors have referred to this equation, for example, Bolasek (1979), Bhole, (1980), Ives (1978 b) and Ødegaard (1975), when stating that "G-values are calculated according to Camp". Unfortunately this equation cannot be quite correct for the following reasons:

The only way work is introduced to the water is by paddle shaft. If the torque on the shaft is measured, the power input can be calculated as:

$$W = \frac{T \cdot \omega}{V} \qquad (3\text{-}95)$$

where T is the torque (Nm)
ω is the rate of angular displacement, $2 \cdot \pi \cdot n$ (s^{-1})

The torque imposed on the shaft is at every moment counterbalanced by an action of the water towards the paddles. Thus:

$$F_D \cdot r = T \qquad (3\text{-}96)$$

Eq (3-96) and (3-93) inserted into (3-95) give

$$W = \frac{C_D \cdot A_p \cdot \rho \cdot v_{rel}^2 \cdot r \cdot \omega}{2 \cdot V} = \frac{C_D \cdot A_p \cdot \rho (1-k)^2 \cdot n^3 \cdot r^3 \cdot (2\pi)^3}{2 \cdot V} \qquad (3\text{-}97)$$

which differs from eq (3-94) in the exponent for the factor (1-k). Obviously, eqs (3-95) and (3-94) cannot be valid at the same time; some authors refer to both of them.

Eq (3-97) is always valid for the calculation of the power input, regardless of how the energy is dissipated, whether part of the energy is dissipated in friction losses near the walls or by built-in stators. The problem is that the water rotation is seldom known, unless it is

measured. Neither is the coefficient C_D known exactly. Values of 1.2-2.0 are usually given depending on paddle shape for the magnitude of the Reynolds number usually present in this case (see below).

When rotation of the water is reported, it is usually calculated from eq (3-94) after measurement of the torque and with assumed values of the coefficient C_D. For example, Harris, Kaufman and Krone (1968) reported k = 0.355 and Ødegaard (1975) k = 0.42.

It is significant that the values of the water-to-paddle-rotation-ratio often are higher when the water velocity is measured, as a consequence of the error introduced in the equation. Hudson (1965) reports 53% and Eikebrokk and Liengen (1977) state 50-85%.

Bhole (1980) has measured the water velocity in a stirred tank. The ratio between the tangential velocity of the water and the velocity of the paddle blade (k) was almost constant at the paddle blade tip: 0.52 for G-values of 10-50 s^{-1} under his experimental conditions. With all variables known but C_D, the latter is possible to calculate. The values thus obtained by Bhole is decreased from 1.8 at G = 10 s^{-1} to 0.94 at G = 50 s^{-1}.

If k is constant with paddle speed, the use of eq (3-94) instead of (3-97) would mean no difference in the variation of C_D other than that too high a C_D is calculated, with a constant ratio to the "real" C_D. But if k varies, this variation to some extent will be incorporated in C_D. It is not possible by the information given by Bhole to find out how the calculations are made. If, however, data given in diagrams are used to calculate mean k values along the paddle radius, a slight decrease with increasing G is obtained, but this variation only explains a part of the total variation of C_D obtained by Bhole.

As will be seen in Section 3.4.4 it is probable that the measurements presented by Bhole has been carried out in the transition region below fully developed turbulence. Using eq (3-94) in calculating C_D instead of the correct expression in eq (3-97) would underestimate the real value by a factor of (1-k). If the lowest C_D-value reported by Bhole (0.94) is considered to represent fully turbulent conditions,

the real C_D would be obtained by division by (1-k). As Bhole measured K = 0.52, the correct C_D-value would be 0.94/0.48 = 1.96, a value fully in accordance with the coefficient of drag for a flat plate usually tabulated in hydraulic literature (e.g. Daily and Harleman, 1966).

If the torque on a paddle shaft is measured and according to eqs (3-93) and (3-96) a relationship close to a quadratic function of the rotation speed of the shaft is obtained, the concept of a variable coefficient of drag must mean an exact balancing variation of the water co-rotation, which seems most unlikely. Results of this kind will be presented later in this chapter, and though neither k nor C_D is measured, there is strong evidence they are constants within the measured power input interval. The influence of the tank scale is estimated in section 3.4.4.

3.4.2 Measurements

The power introduced into a stirred tank is easily calculated from measurements of the torque on the paddle shaft. The torque can be measured by means of a strain gauge on the shaft if the torque strain is calibrated against an applied torque of known value. Ødegaard (1975) carried out such measurements on a laboratory scale and calculated G-values according to eq (3-98), which follows from eqs (3-95) and (3-91).

$$G^2 = \frac{2 \cdot \pi \cdot n \cdot T}{V \cdot \mu} \qquad (3\text{-}98)$$

G was found to be proportional to $n^{1.49}$, which is very close to the expected value of $n^{1.5}$. An interesting observation made with the aid of an oscilloscope was that the strain during one revolution varied considerably depending on the position of the paddle in the square flocculation chamber. The variation in the strain and thus in the torque, was in the order of 30-50% of mean strain.

An alternative way in measuring the torque is presented by, for example, Lentvaar and Ywema (1979), who supported the mixing vessel on a free-hanging frame, movable around a vertical axis. The torque measured was the reaction of the vessel to the rotating agitator with the liquid as a transmitting medium. With varying types of vessels (cylindrical, cylindrical with baffles, and square) and different impeller types, the

exponent q for the rotational speed in (3-99) was close to 1.5.

$$G = p \cdot n^q \qquad (3\text{-}99)$$

Hemenway and Keshawan (1968) constructed a torquemeter for determinations of the power input. The device used the angular displacement, indicated on a rotating disc, of a spring-loaded shaft to measure the moment applied to the shaft.

Indirect measurements of the power input by measuring the difference in power input to an electric motor with load (in water) and without load (in air) are difficult to carry out. The losses of energy in the drive motor usually depend on the applied load to an undesirable extent. In addition, there may be uncontrolled friction losses in bearings and gears. Bhole, Dhabadgaonkar and Tarnekar (1975) tried to overcome these difficulties by means of a special type of speed control. The resulting relationship between G and the paddle rotational speed, however, differs from the one related above. Eikebrokk and Liengen (1977) used a similar approach without success.

Rosén (1967) presented another method in which the power input to the electric drive motor is used to measure the power input to the water.

Here the power consumption of the motor with water in the flocculation chamber is compared with the power consumption without water but with an applied torque caused by an artificial brake attached to the shaft. The brake torque can easily be measured. When the power consumption of the motor, with constant shaft speed, is the same as with water in the tank, the measured brake torque is assumed to be of the same magnitude as that caused by the water.

Rosén succeeded in establishing a relationship between the power input and the rotational speed with an exponent of n near 3, which indicates good reliability.

3.4.3 Results of torque measurements

Torque measurements were carried out on three different scales, the same ones from which flocculation results are presented later. Firstly, the power input was measured in 2-l beakers, where jar-tests were performed; secondly on a pilot-plant scale (tank volume 0.2-1.7 m^3) and finally on a full scale in a water treatment plant (volume 31 m^3).

3.4.3.1 Laboratory scale

The measurement was performed with a square beaker equipped with the type of stirrer seen in fig. 3.30

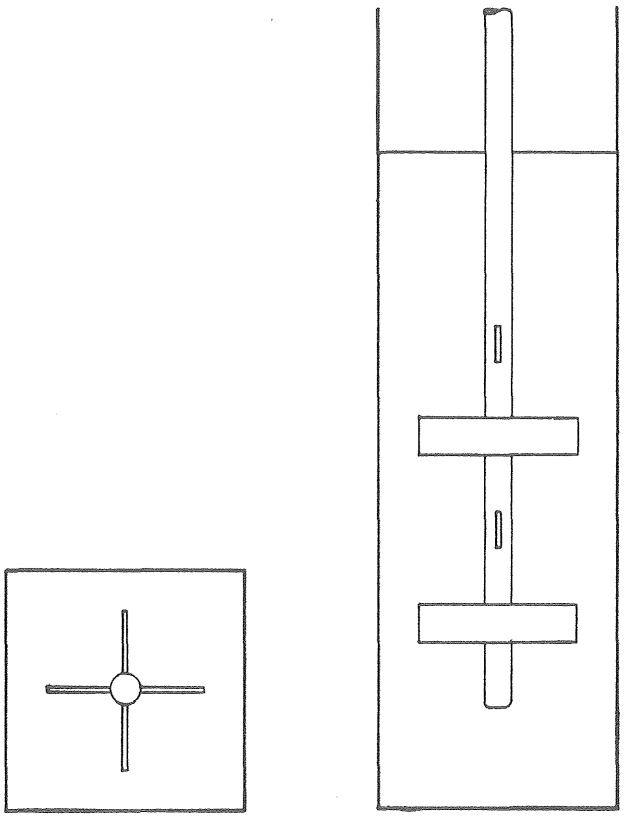

Fig 3.30. Jar-test apparatus used in the measurements.

The beaker was supported at a point in the middle of the bottom and at the top by a low friction plastic ring, penetrated by the paddle shaft and connected with he beaker walls. Thus, the vessel could freely rotate around a vertical axis. At the beaker an arm was attached where the torque transmitted through the water was measured by a spring balance.

A plot of the torque versus rotational speed is shown in fig. 3.31.

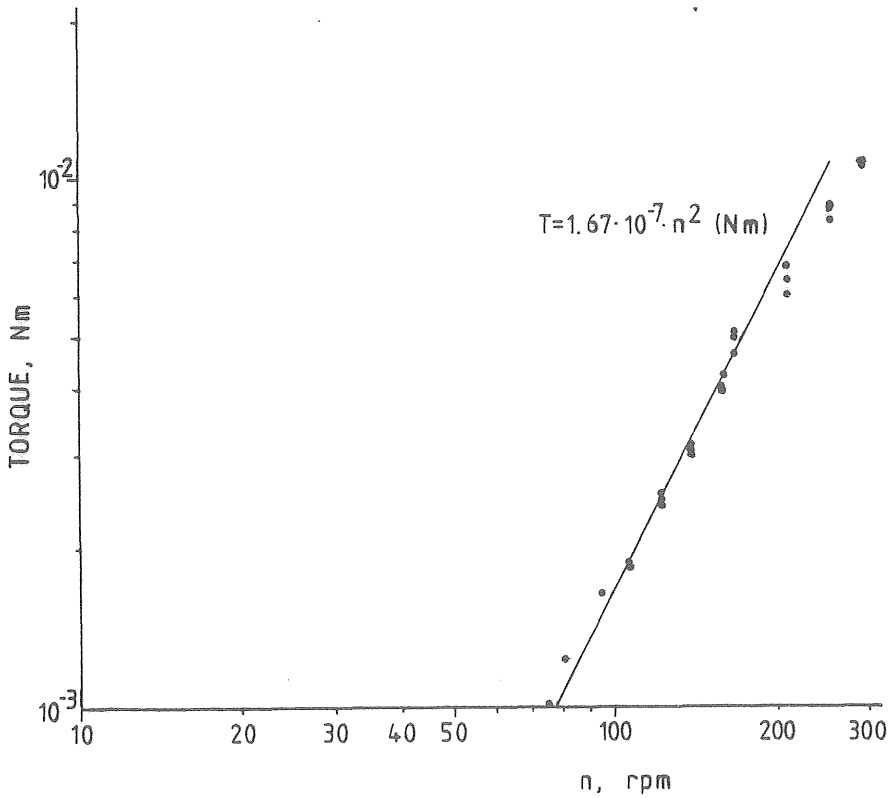

Fig. 3.31. Torque as a function of rotational speed.

The exponent for n was in the log-log-plot 1.86, not far from the expected value 2.0. If the latter is assumed to be correct (regression line in the figure), the expression for the power input per unit of volume is:

$$W = 8.7 \cdot 10^{-6} \cdot n^3 \quad (watt/m^3) \qquad (3\text{-}100)$$

where n is the rotational speed (rev/min).

If C_D is assumed to be 2.0 the value of k is 0.25, calculated according to eq (3-97). The paddle area percentage of the least total area of the vessel in a vertical section is 15%. The G-values in the measured interval range from 50 to 410 s^{-1}.

3.4.3.2 Pilot-plant scale

Seven different kinds of paddles in flocculation tanks of four sizes (0.19, 0.25, 0.43, and 1.7 m^3) were measured. The drive motor was equipped with a ball bearing so it could rotate freely in relation to the flocculation tank. The torque to keep the motor in a fixed position was measured by a spring balance. Fig. 3.32 shows the design of the paddles in the pilot plant. The figure depicts only one fourth of the

paddle mechanism. Two sets of paddle arms were located at right angles to each other.

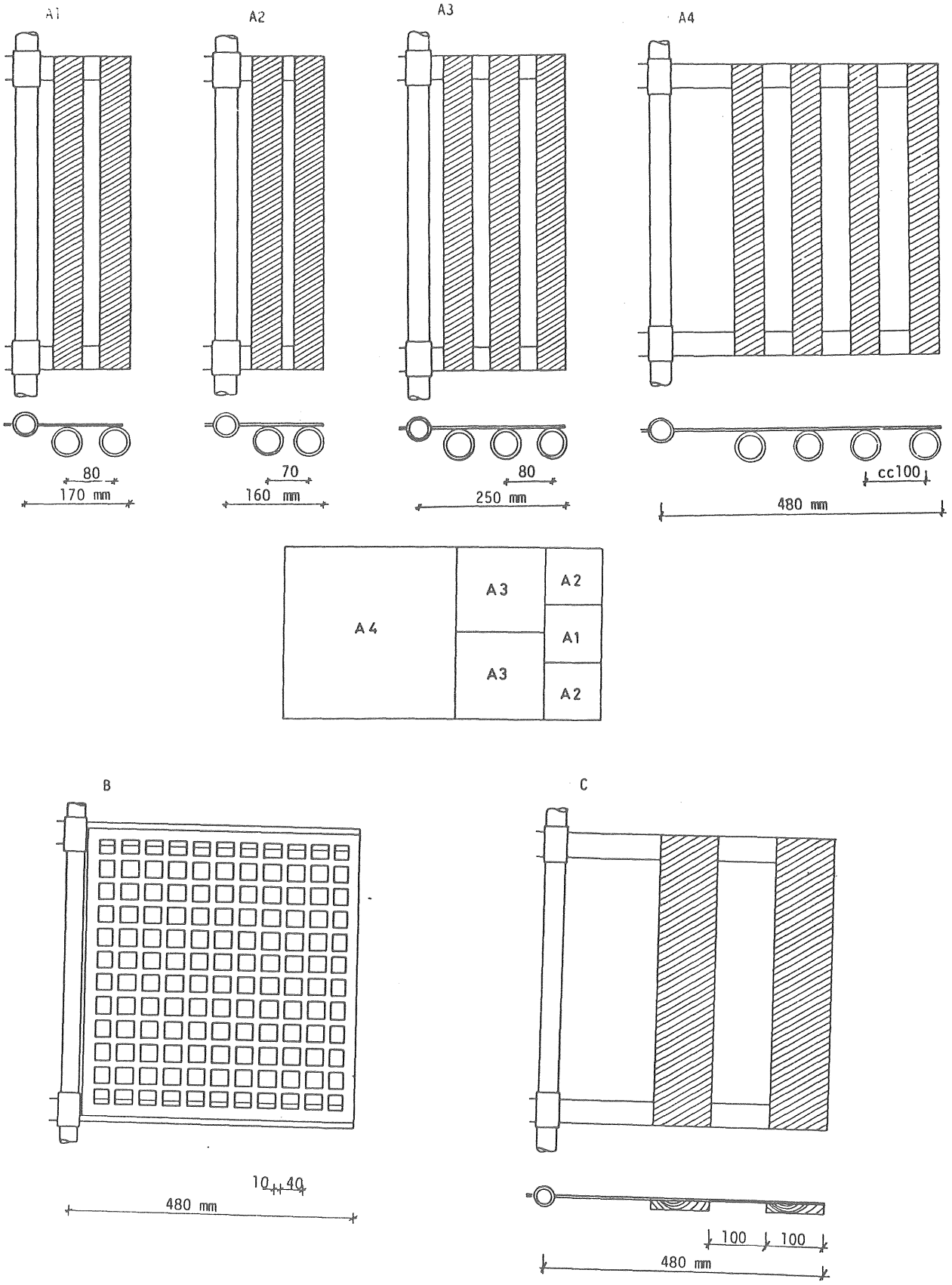

Fig 3.32. Paddle types used in pilot plant experiments.

Another pilot plant where the power input was measured was designed as pictured in fig. 3.33. The paddle construction can be seen in fig. 3.34. In the following these will be referred to as type R.

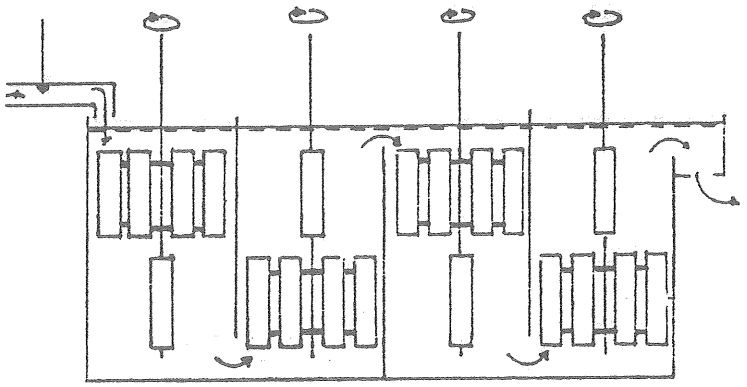

Fig 3.33. Pilot plant with paddles of type R.

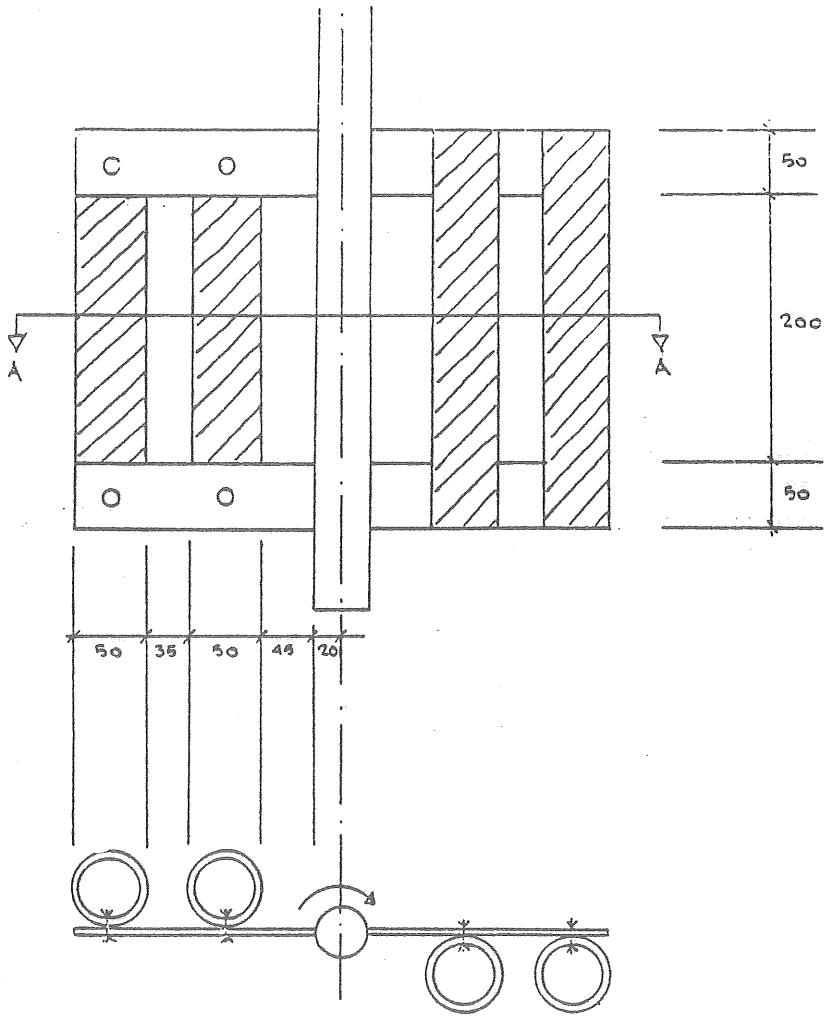

Fig 3.34. Paddle construction type R.

In figures 3.35 to 3.40 the results of torque measurements are plotted.

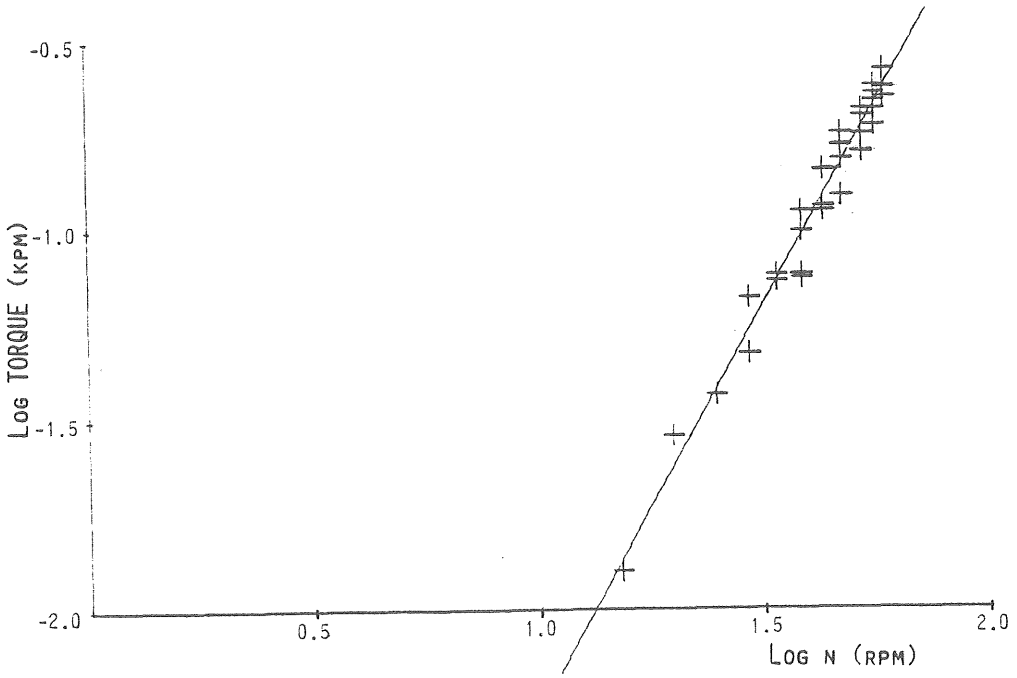

Fig 3.35. Torque measurements. Paddle type A1.

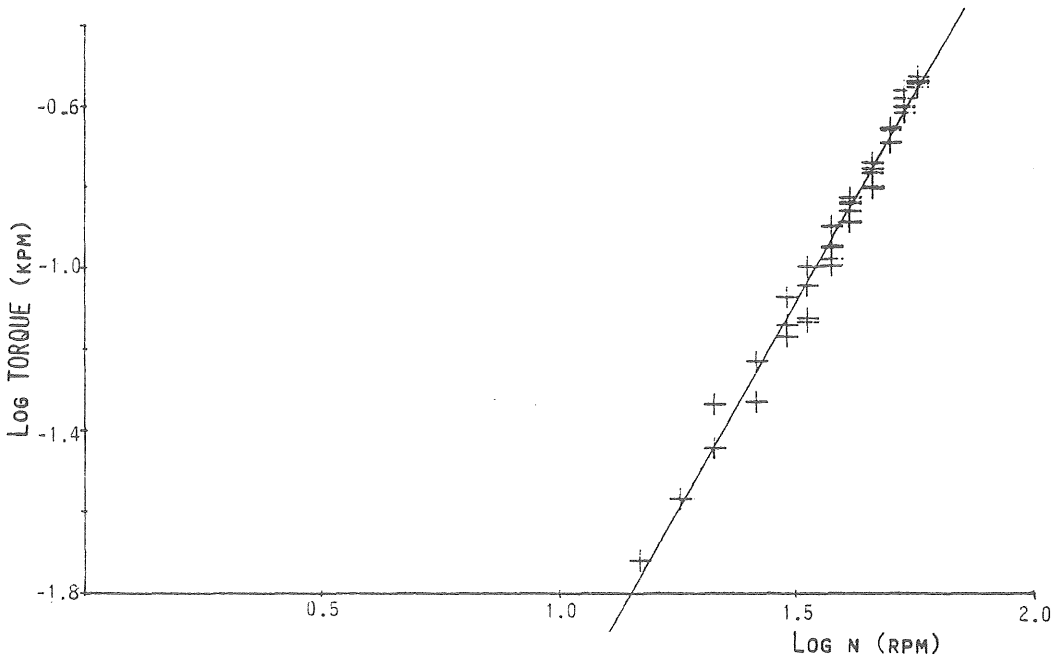

Fig 3.36. Torque measurements. Paddle type A2.

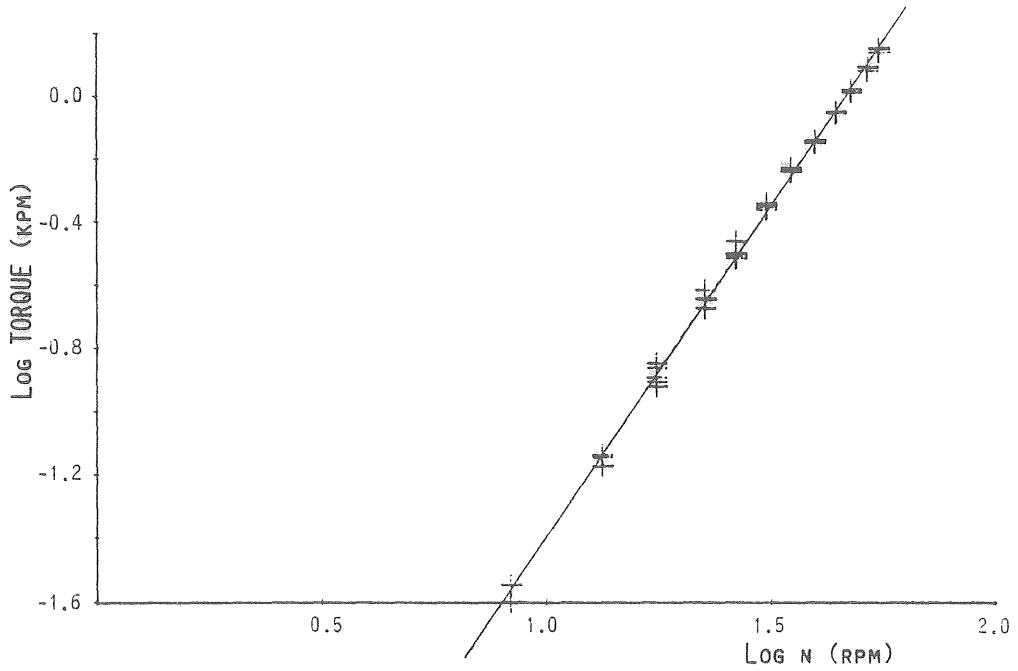

Fig 3.37. Torque measurements. Paddle type A3.

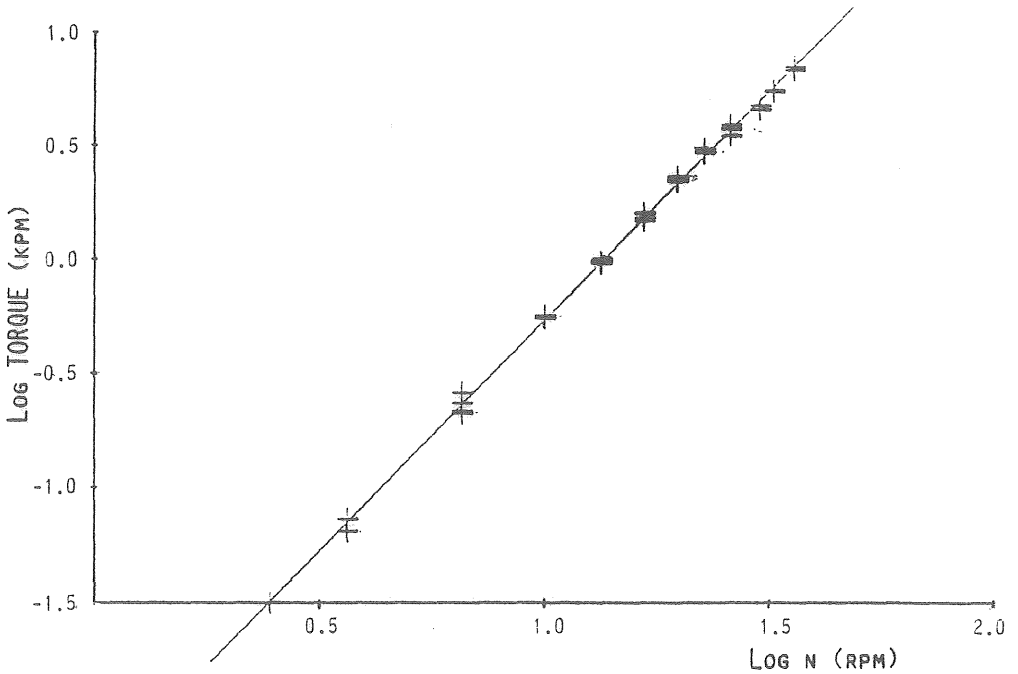

Fig 3.38. Torque measurements. Paddle type A4.

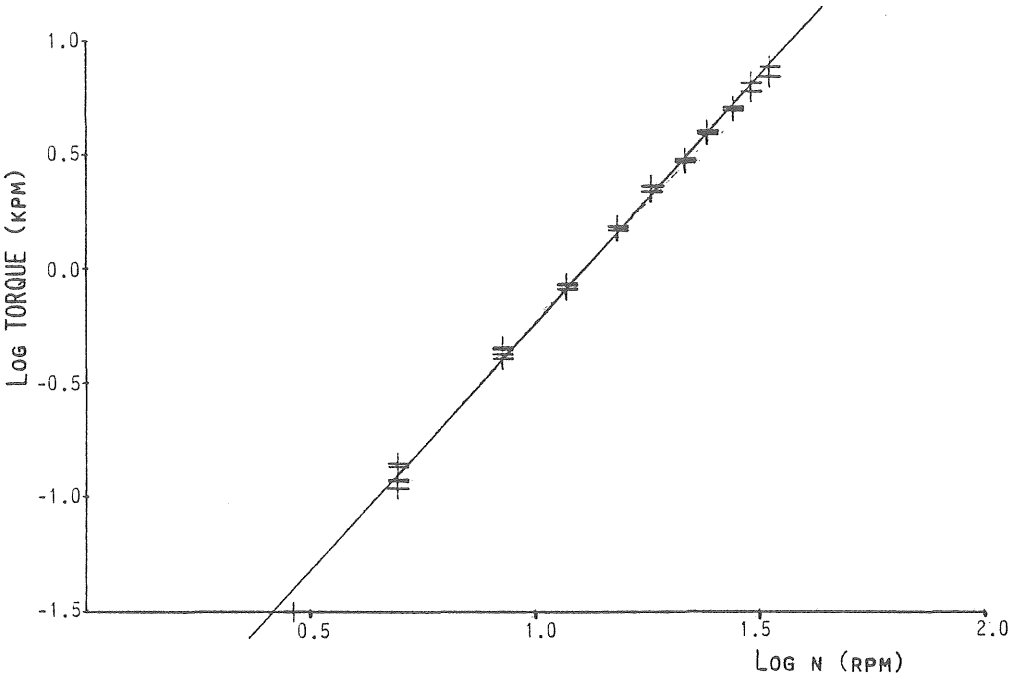

Fig 3.39. Torque measurements. Paddle type C.

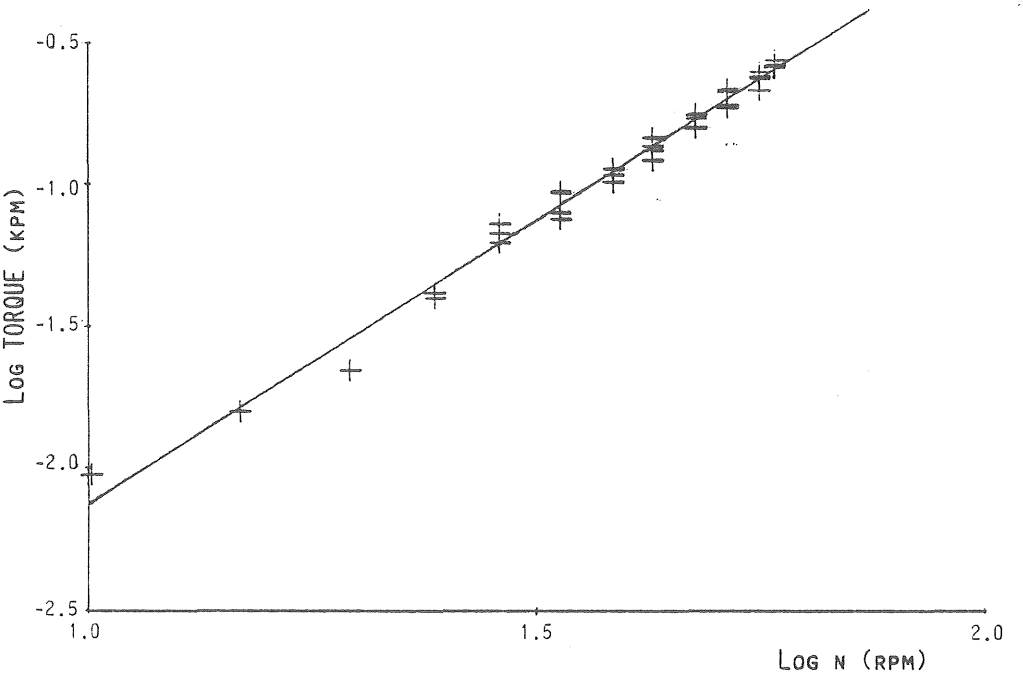

Fig 3.40. Torque measurements. Paddle type R.

In table 3-4 the results of the measurements are summarized. It can be seen that the exponent for n obtained is very close to 2.0.

Table 3-4. Results of regression analysis. Log torque as a function of log n.

Stirrer type	Number of values	Exponent for n	Correlation coefficient
A1	36	2.080	0.983
A2	43	2.037	0.991
A3	51	2.088	0.999
A4	43	2.010	0.999
B	35	2.152	0.999
R	42	1.989	0.994

If the constant K in the expression $W = K \cdot n^3$ is calculated, the values in table 3-5 are obtained (n is shaft revolutions per minute).

Table 3-5. Values of K in the expression $W = K \cdot n^3$ (watt/m^3) for different stirrers.

Stirrer type	Obtained constant (watt·min^3/m^3)
A1	$3.4 \cdot 10^{-4}$
A2	$4.4 \cdot 10^{-4}$
A3	$1.1 \cdot 10^{-3}$
A4	$3.2 \cdot 10^{-3}$
B	$3.6 \cdot 10^{-3}$
C	$5.4 \cdot 10^{-3}$
R	$3.0 \cdot 10^{-3}$

With a known power input and assuming that the drag coefficient $C_D = 1.2$ for cylindrical paddles and 2.0 for flat paddle shapes (Cederwall and Larsen, 1977) the water co-rotation can be calculated from eq (3-97). The values of k thus obtained are listed in table 3-6 together with the relative paddle area and tank proportions. All tanks used in the experiments have square horisontal sections.

Table 3-6. The water co-rotation related to paddle speed (k) in different stirring systems.

Stirrer type	Calculated water rotation to paddle speed ratio (k)	Ratio of paddle area to least vertical tank section area	Tank height-to-width ratio
A1	0.53	0.52	3
A2	0.49	0.52	3
A3	0.46	0.52	2
A4	0.41	0.38	1
B	0.42	0.38	1
C	0.41	0.38	1
R	0.53	0.40	2

3.4.3.3 Full scale

Power input into the flocculation tanks in the water works at Åmål was measured according to the method described by Rosén (1967). This treatment plant was chosen because it is one of the few in Sweden with stirrer speed control. The electric drive motors could operate at three rotational speeds controlled by a switch.

The electric power consumption was first measured with a watt-meter. Then two drawbacks of the method where energy input into the water is measured indirectly by motor energy consumption became apparent. Firstly the power consumption during one revolution varied to such an extent that a reliable measure of the mean power energy consumption was almost impossible to achieve. Secondly, the energy consumption was in this case not related to the speed control adjustment. A higher rotational speed sometimes resulted in lower power consumption, depending on the activation of windings with varying efficiency.

The power consumption of the motor had to be measured with a sensitive energy meter, registering Wh, over a period of time, allowing a mean power value to be calculated.

The energy consumption with water in the flocculation tank was compared with the values obtained without water but with a brake applied to the axis. Varying brake torques were measured with a spring balance and the motor energy consumption was registered simultaneously.

Thus, the power input to the water could be obtained indirectly as the value of the braking torque power when the motor energy consumption was the same as with water in the tank.

It could be seen from the measurements that the power requirement of the motor increased more than the applied braking power. An erroneous calculated power input would be the result if a simple subtraction was made of energy consumption without water in the tank from the value under working conditions.

In figure 3.41 the relationship obtained between power input and shaft rotational speed is reproduced.

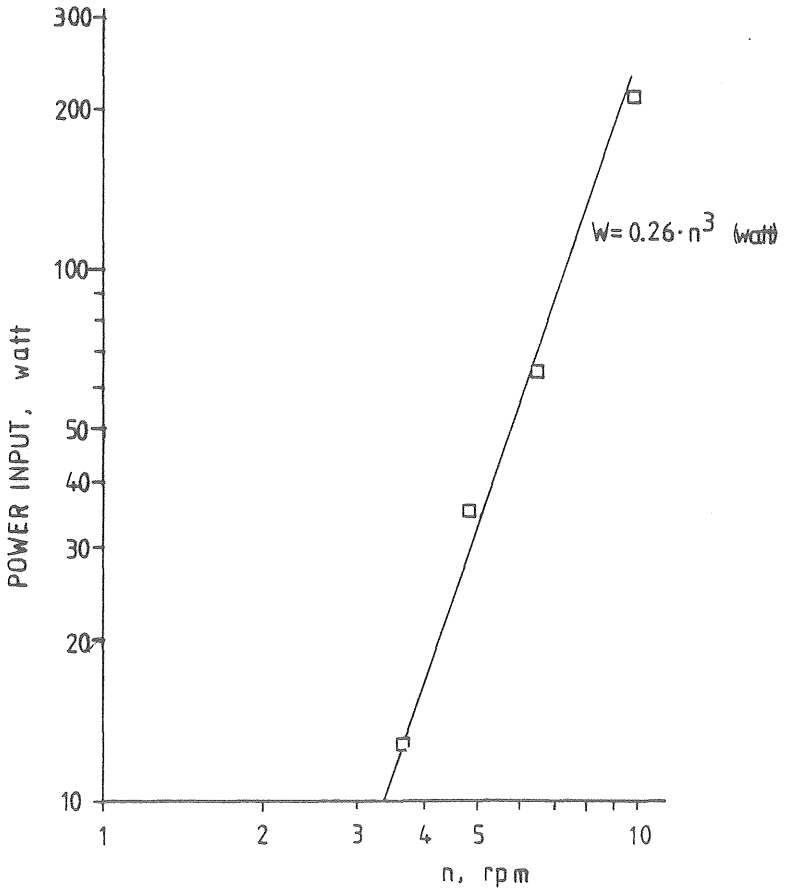

Fig 3.41. Power input (watt) versus shaft speed (rpm) Water work at Åmål.

The calculated k-value according to eq (3-97), with C_D=2.0 is 0.29. Paddle area to tank section area is 11%. The measured power input interval corresponds to G-values of 17-80 s^{-1}.

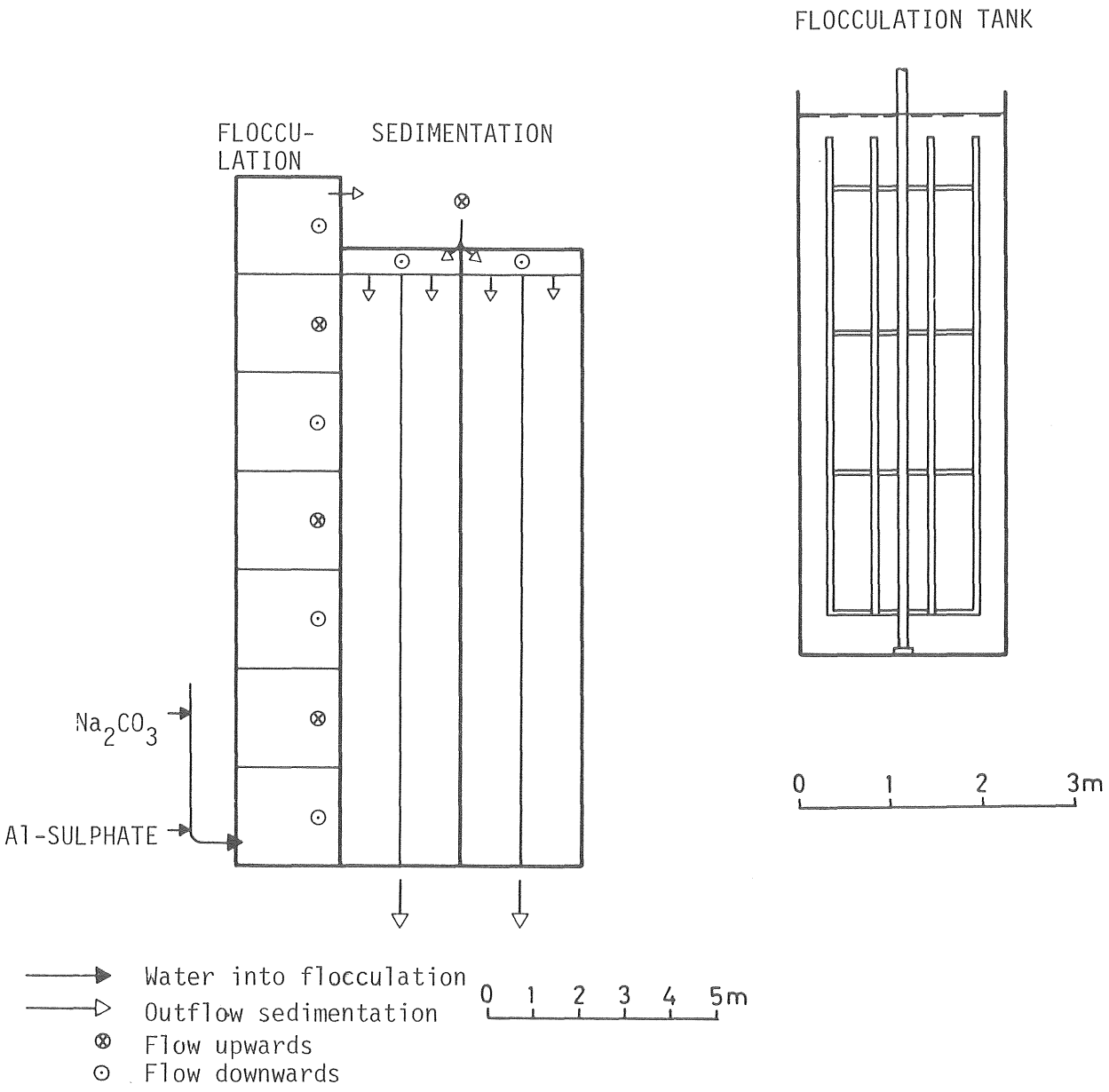

Fig 3.42. Water work at Amål.

3.4.4 Power input determination and tank scale

A general flocculation tank has been considered, with characteristics usually regarded as beneficial to flocculation: cubic with a volume of L^3 m^3, equipped with paddles ranging from the radius $0.05 \cdot L$ to $0.4 \cdot L$ and with a total paddle area of $0.2 \cdot L^2$ m^2. If C_D is assumed to be 2.0 and k=0.5, the power input can be calculated as:

$$W = \frac{C_D \cdot \rho}{2 \cdot L^3} \left(\frac{2 \cdot \pi}{60}\right)^3 \cdot (1-k)^2 \cdot n^3 \cdot 0.2 \cdot L^2 \cdot \frac{(0.4^4 - 0.05^4) \cdot L^4}{4(0.2-0.05) \cdot L} \qquad (3\text{-}101)$$

n is revolutions per minute.
Which can be reduced to:

$$W = 2.45 \cdot 10^{-3} \cdot L^2 \cdot n^3 \qquad (3\text{-}102)$$

From the equation it can be seen that the rotational speed producing a certain power input W is related to the length scale according to:

$$n = \sqrt[3]{\frac{W}{L^2 \cdot 2.45 \cdot 10^{-3}}} \qquad (3\text{-}103)$$

The velocity at the paddle tip is:

$$v = n \cdot 0.4 \cdot L \cdot \frac{2\pi}{60} \qquad (3\text{-}104)$$

If the size of the paddle is assumed to be related to the length scale a characteristic length, i.e. paddle width d, could be:

$$d = 0.05 \cdot L \qquad (3\text{-}105)$$

The Reynolds number, characterizating the flow conditions at the paddle tip can now be calculated:

$$R_e = \frac{v \cdot d}{\nu} = \sqrt[3]{\frac{W}{L^2 \cdot 2.45 \cdot 10^{-3}}} \cdot 0.4 \cdot L \cdot \frac{2\pi}{60} \cdot 0.05 \cdot L \cdot \frac{1}{\nu} = 1.55 \cdot 10^{-2} \sqrt[3]{\frac{W \cdot L^4}{\nu}} \qquad (3.106)$$

Since:

$$G = \sqrt{\frac{W}{\mu}} \rightarrow W = G^2 \cdot \nu \cdot \rho \rightarrow R_e = 0.155 \cdot G^{2/3} \cdot \nu^{-2/3} \cdot L^{4/3} \qquad (3\text{-}107)$$

and $\nu \sim 1.3 \cdot 10^{-6}$

$$R_e = 1.3 \cdot 10^3 \cdot G^{2/3} \cdot L^{4/3} \qquad (3\text{-}108)$$

If $G = 10\ s^{-1}$, a velocity gradient usually recommended at the end of the flocculation process, is assumed, Reynolds number for the Laboratory scale (L = 0.1 m) up to the full scale (L = 5 m) will vary from 280 to $5 \cdot 10^4$, which certainly means turbulent conditions for the large scale (see e.g. Bates, Fondy and Fenic (1966)). The turbulence field should by necessity be of different length scale characteristics but a viscous drag should never be present under the specified conditions. Drag in the transitional range is possible on a small scale as proposed by Saatci and Cleasby (1980), which could explain the results obtained by Bhole (1980), referred to in Section 3.4.1. His experiments were carried out in 1-l beakers.

The G-value above which turbulent conditions are prevalent, a Reynolds number greater than 10^3 (Cederwall and Larsen (1976)), can be calculated from the relationship:

$$G = \left(\frac{1}{1.3 \cdot L^{4/3}}\right)^{3/2} \qquad (3\text{-}109)$$

For laboratory, pilot plant and full scale (L = 0.1, 0.5 and 5 m) the corresponding G-values are 67,2 and 0.02 s^{-1}.

That means, that above these values, when the power input is measured, a rotational speed exponent of 3.0 should be expected; otherwise there is an indication that the measurement of the torque has failed.

In the measurements referred to above, in square vessels without stators, there is some evidence, independent of scale, that the paddle area percentage, naturally, is an important factor in causing water rotation. If the total paddle area is approximatively 50% of the smallest vertical tank section, the water co-rotation was found to be around 50% of the paddle shaft rotational speed. This figure is lowered to about 30% if the paddle area percentage is 15%.

If G-values are to be calculated without any power input measurements a value of k has to be assumed. An uncertainty in k means an uncertainty in calculated G-values of the same relative magnitude for:

$$G \propto \sqrt{(1-k)^2} = (1-k) \qquad (3\text{-}110)$$

Stators and friction against the wall will determine the value of k. The fundamental equations to calculate G do not change with varying wall friction and stator design, but k does. Some authors have proposed the introduction of a gross turbulent drag coefficient, C_t (e.g. Camp (1969), Bhole (1980)). It is doubtful whether this concept would facilitate power calculations. Furthermore, the theory behind it does not seem to be accurate.

C_t is defined by Camp (1969) according to:

$$W = \frac{(2\pi)^3}{2} \cdot \rho \cdot A_p \cdot C_t \cdot n^3 \qquad (3\text{-}111)$$

where ρ is the mass density of the liquid

A_p the projected area of the paddle blades

C_t a dimensionless turbulence gross drag coefficient determined by the geometry of the system

n is the rotor speed in revolutions per second

Camp expressed C_t in terms of the drag on the rotors, stators and walls as:

$$C_t = \frac{C_D}{V \cdot Ap} \left[(1 - k)^3 \cdot A + k^3 \left(B + \frac{f}{C_D} \cdot C \right) \right] \qquad (3\text{-}112)$$

where A, B and C are dimensionless work parameters for the rotors, stator and walls, respectively. f is the Weisbach-Darcy wall friction factor. For narrow paddle blades the parameter A was stated to be $Ap \cdot r_p^3$. Thus C_t only can consist of the first term within the parenthesis (with the exponent 2 instead of 3 as mentioned earlier) in eq 3-112 according to eqs 3-111 and eq 3-97

As a matter of fact C_t can, if eqs 3-111 and 3-97 are combined, be calculated as:

$$C_t = C_D (1 - k)^2 \frac{r^3}{V} \qquad (3\text{-}113)$$

Then in eq 3-112, the first term expresses the power input and the second the power lost within the water volyme by dissipation at stators and walls. The summation of these two terms cannot be correct. As a conclusion the C_t-parameter can be considered unnecessary, not adding any further information to the problem of calculating the power input.

4 THE EFFECT OF SOME IMPORTANT FACTORS ON FLOCCULATION EFFICIENCY

4.1 Literature

Many factors have been reported to have an impact on flocculation efficiency. In Section 4.2 results from experiments with varying power input and flocculation time and with varying paddle and reactor design are reported. In addition the effects of temperature and addition of activated silica are outlined.

Some results found in literature concerning effects of the power input, paddle form and reactor design are reported below.

The literature study has mainly been concentrated on reported effects of factors considered later in the present treatise.

For example, effects of the initial mixing stage have not been investigated and will not be discussed here. (See e.g. Vråle, 1971).

4.1.1 The impact of the power input

Rosén (1967) studied the impact of the power input on flocculation efficiency. The result was evaluated in terms of average settling velocity and standard deviation, calculated on the settling part of the settling flocs. In addition the residual turbidity was used as an additive independent variable to characterize the floc settling properties.

The raw water was extracted from the River Göta Älv. As a coagulant 50 mg alum/l was added. 8 mg activated silica/l served as flocculation aid. The experiments were carried ot in a pilot plant with four flocculation basins, each of a volume of 3.6 m^3. The total flocculation time was kept constant at 60 minutes.

The investigation was concerned mainly with the effect of variations of the power input during the first 10-15 minutes of the flocculation process. The power input in the last two flocculation tanks was throughout the experiments kept low: 0.002 watt/m^3. The power input in the first and second flocculation tanks could be varied from 0-10 and 0-1 watt/m^3 respectively.

After the first flocculation tank the mean settling velocity and standard deviation was found to decrease when the power input was increased. The residual turbidity, however, showed a minimum value at the power input 1-1.5 watt/m^3. Similar residual turbidity minima were detected in the second and third flocculation tanks for the power input (in the first tank) of 1.4 and 1.0 watt/m^3, respectively. A comparison between the third and fourth flocculation tank showed little improvements between 45 and 60 minutes flocculation time.

The conclusion was drawn that the power input should be high during the first 10-15 minutes, 1.0-1.5 watt/m^3, whereupon it should be decreased rather instantly to a low value.

Ødegaard (1975), in his study on flocculation of phosphate precipitates in waste water treatment, investigated how the power input in the flocculation stage affected on the one hand flocculation performance and on the other hand settling performance parameters.

The flocculation performance parameter is defined as the particulate phosphate into the flocculator divided by the amount found in a sample at 5 cm depth after 30 minutes of settling (quiescent conditions). A high correlation was found between particular phosphate, which was the subject of the study, and turbidity, however different for different precipitants. This parameter therefore is proportional to the inverted value of the residual turbidity.

As mentioned in Section 3.3.1 the settling (at 5 cm depth) was characterized by calculation of parameters in an expression of the form $C/Co=A.\exp(-B.t)+D$. The parameter B, describing the form of the settling curve, was used as a relative measure of the settling properties.

The experiments carried out by Ødegaard comprised, as mentioned, phosphorous removal in waste water treatment. This implies different precipitate properties compared to those encountered in coagulation of surface waters, even if aluminium sulphate is used in both cases. The high phosphate content in the precipitate causes relatively compact flocs with good settling properties compared to "pure" hydroxide flocs. This is confirmed by the observation made by Ødegaard that sedimentation properties were deteriorating above a certain Al/P mole ratio.

It is believed, however, that some of his findings also can be applicable in this context.

The flocculation experiments were carried out in a pilot plant consisting of six compartments with a through-flow of 1-5 l/min. A dosage of 180 mg alum/l (Al/P mole ratio 1.8) was used. Most of the experiments were performed with constant power input throughout the flocculation process.

The flocculation performance was found to increase with increasing velocity gradient up to a certain value, and then to decrease at higher velocity gradients.

With aluminium sulphate as a precipitant the G-value for optimum flocculation was 20-50 s^{-1}. The higher value was obtained when only one compartment was considered, the lower value is related to 3-6 compartments in series.

The settling performance as expressed by the parameter B, was found to be considerably influenced by the velocity gradient. Settling performance decreased with increasing G when $G > 10\ s^{-1}$. However, the settling performance did not vary much neither with residence time nor compartmentalization of the flocculation volume.

Generally lower flocculation performance was detected for the various tapered flocculation paths examined, compared to untapered flocculation. The settling performance, however, was essentially the same for tapered and untapered flocculation when flocculation compartments with the same G-value was considered.

Ødegaard concluded that his results indicated that the most favourable tapered flocculation path (to improve floc settleability) would be to apply a relatively high velocity gradient in the first compartment, and then a lower G-value for a longer flocculation time, and at last the lowest possible velocity gradient for a shorter time immediately before settling.

TeKippe and Ham (1971) studied the effect of various velocity gradient paths on alum coagulation of a silica suspension. The residual turbidity after sedimentation (30 minutes) and the time required for visible floc formation were studied in jar-test experiments. In continuous-flow pilot-plant studies the effluent turbidity from the settling tank was used for evaluation of the results.

The dimensionless product G.t, where G is the velocity gradient (s^{-1}) and t the flocculation time (s), was kept constant at the value 72000. The total flocculation time was 21 minutes, terminated by 1 min mixing at G=50 s^{-1}, thus simulating possible high velocity gradients encountered during the transport to a settling tank.

The 20 minutes, within which the velocity-gradient path was to be varied, was divided into four 5-min periods, each with a constant velocity gradient.

The best results generally were obtained from the experiments with the highest velocity gradient in the first quadrant. Such paths led to rapid formation of visible floc.

The G.t parameter alone was found to be inadequate for flocculation basin design.

The initial portion of the velocity-gradient path was found to have a pronounced effect on settling properties of the flocs. A suspension which had been subjected to high G-values (up to 200 s^{-1} was applied) until visible flocs were formed and then flocculated at G=50 s^{-1} formed a relatively uniform, well settling floc. If the period of high G-value was followed by a period of very low velocity gradient, the suspension was found to form a nonuniform floc with large particles that settle rapidly as well as small particles suspended in the supernatant.

Bhole and Krishna (1978) reported results from coagulation with alum of clay suspensions on a laboratory scale. During 15 minutes flocculation time the G-value was varied so that the average value always was 60 s^{-1}. Thus the product G.t was 54000. The results led to the following conclusions:

Tapered flocculation was more efficient compared to uniform velocity gradient.

Tapered flocculation with a broad spectrum of velocity gradients was more efficient compared to a narrow spectrum.

Efficiency was found to increase with more gradual tapering of the velocity gradient. Sudden reductions of the velocity gradient were less effective.

Efficiency of the tapered flocculation increased with more uniform distribution of time among the various velocity gradients in the spectrum.

Andreu-Villegas and Letterman (1976) presented results from jar-tests with untapered flocculation. To 1-l kaolin clay suspension various amounts of alum was added. The residual turbidity following initial mixing, slow mixing and sedimentation was measured.

An optimum G-value (causing minimum residual turbidity) for each coagulant dose and flocculation time was determined. The optimum G-value was found to decrease with increasing flocculation time. A relationship was presented, where this G-value raised to the power 2.8 was stated to be proportional to the inverse value of the flocculation time. The proportionality factor was depending on the coagulant dose.

The residual turbidity, resulting from the optimum G-value at a time T, decreases as T increases. The rate of decrease diminishes after a flocculation period of approx 20 min.

Ives and Bhole (1973) made computer simulations of the flocculation equations described in Section 3.1.2, assuming various breakup patterns. The computed results were then qualitatively confirmed by laboratory experiments. The most interesting conclusions were:

The tapered flocculator achieved more coarse size distribution of particles compared to the uniform velocity gradient flocculator.

Tapered flocculation attains better clarification compared to uniform flocculation watever the mode of breakup of flocs.

The efficiency of the tapered flocculator compared to the untapered increased with an increase of the velocity gradient.

4.1.2 Reactor and paddle design

A main problem in a stirred flocculation tank reactor is often considered to be the inevitable uneven distribution of the energy dissipation within the tank volume. The uneven power input can according to Robinson (1964) be attributed to three factors:

Zones with small velocity gradients appear between paddles.

The paddle velocity increases with paddle arm radius.

Between the paddle and the tank wall high velocity gradients can occur if the distance is small.

Fisherström and Larsen (1968) conclude from considerations founded on turbulence theory, that the possibility for locally high shear rates and subsequent floc breakup is limited. In that case paddle design would be of less importance compared to the general power input.

Hyde and Ludwig (1944), on the other hand, attached great importance to the paddle design. The attention to the design was motivated by the consideration that paddles and other devices in the flocculation tank should ensure that an adequate portion of the applied power input was transfered to a reasonable turbulence level, beneficial for the floc formation.

Tolman (1942) looked upon the small eddies at the paddle blade tips as the essential flocculation mechanism. Mainly for that reason paddle design was considered important for the flocculation result.

Flat paddle blades give intense eddying, and streamline blades give intense local shear (Robinson, 1964). Hyde and Ludwig (1944) found that half-hexagon, semi-circular, or V-shaped blades (compared to flat and S-shaped) created turbulence conditions most favourable for flocculation.

Drobny (1963) investigated by means of jar-tests the importance of the paddle design in the following respects: Surface roughness, perforation in the paddles, paddle curvature, paddle area, and height to width ratio. From the experimental results he concluded that an optimal combination of these parameters would result in a good floc formation at a relatively low power input.

Tolman (1942) recommended many small paddle blades, to increase the effect of eddies at the paddle tips. Riddik (1961) as a consequence of the same considerations, suggested a coarse mesh instead of paddle blades. Thereby he claimed to have increased the possibility for particle aggregation compared to conventional design.

The inevitable uneven velocity distribution along the paddle arm in a stirred tank has motivated different designs. For example can the distance between the paddle blades be increased as the radius increase. If tapered flocculation is desired and the paddle axes in different compartments are operated at the same rotational speed (for example through a common horisontal axis) one way to lower the power input is to increase the distance between paddles (and decrease the paddle area). The drawback with increased paddle distance is that the non-uniformity of the power input is increased. In the latter case true tapered flocculation is not achieved (Robinson, 1964).

4.2 Experiments on pilot plant scale

4.2.1 The effects of power input and activated silica

According to the literature quoted earlier in this chapter the power input during flocculation ought to be carried out in such way that an initial high power input is successively decreased to a low value at the end of the flocculation process, tapered flocculation.

Compared to flocculation with constant power input, a type of tapered flocculation can always be found, that leads more rapidly to the desired efficiency.

The impact of a constant power input, however, is more easy to study. Results presented on tapered flocculation are difficult to interpret. In the practice, the important question is how the tapered flocculation is to be carried out. Usually specific answers are difficult to find.

Here, the hypothesis has been that an exponentially tapered power input would give a reasonable scheme of variation. Within this variation pattern the magnitude of the power input has been varied. The numerical expression for the variation chosen here can be expressed as in eq (4-1).

$$W_i(\frac{t}{T}) = \frac{90}{4^{i-1}} \cdot (\frac{4^{i-1}}{6000})^{t/T} \quad \text{watt/m}^3 \qquad (4\text{-}1)$$

where t/T is relative flocculation time

T is the total flocculation time

i is an integer, defining the order of magnitude of the power input

For every step "i" the power input at the time t/T=0 is divided by 4 (the G-value is halved). The ultimate power input (t/T=1) is the same $1.5 \cdot 10^{-2}$ watt/m^3. The upper limit (i=1) was determined by available equipment. Further on it will be referred to this number "i", which according to eq (4-1) determines the power input into each flocculation tank. A maximum of six different variation patterns have been examined.

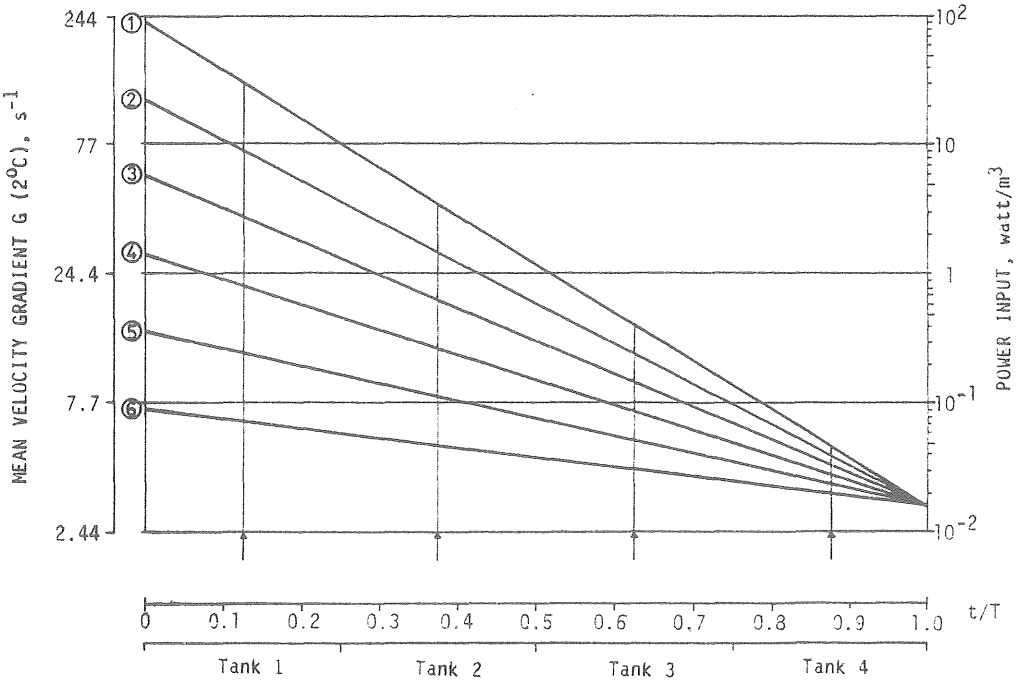

Fig 4.1. Variation of power input.

Figure 4.1 shows how the power input is chosen for four equally sized flocculation tanks in a series. In this case a variation is achieved from maximally 30 watt/m^3 in the first flocculation tank down to $1.8.10^{-2}$ watt/m^3 as the lowest value in the fourth. In the figure corresponding G-values are indicated, calculated for the temperature $2^{o}C$. The magnitude of the power input at different shaft rotational speeds for each type of stirrer is determined according to results presented in Section 3.4.3.

At a constant total flocculation time (20 min) a number of experiments were carried out, where the power input was varied according to the scheme in figure 4.1. Settling analyses in the flocculation tanks number 2, 3 and 4 gave as a result a number of corresponding values of the mean settling velocity (v_m) and the standard deviation (σ). It was found that settling analyses in the first flocculation tank was difficult to carry out; the mixing intensity was usually rather high and the floc settling velocity so small that reliable results could not be obtained.

The corresponding values of v_m and σ were found to vary in general terms according to figure 4.2. The numbers in the figure corresponds the integer "i" in eq (4-1).

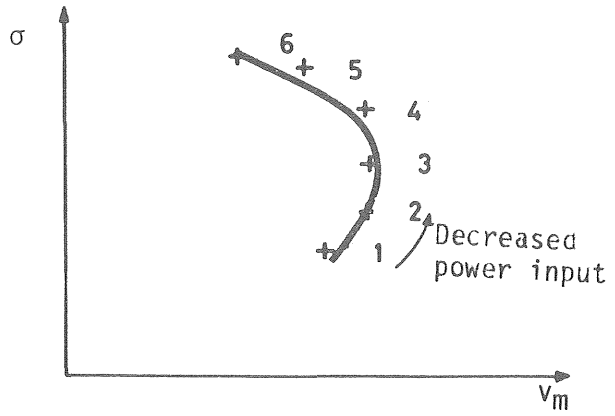

Fig 4.2. The principal effects on settling properties caused by changed power input.

With lowered power input the standard deviation (σ) of the settling velocity is increased. Hereby the mean settling velocity (v_m) increases up to a certain value. A further decrease in power input will then cause v_m to decrease.

To be able to describe the changes mathematically, these were assumed to follow a parabolic curve with its symmetry axis parallel to the v_m-axis. Together with the condition that the curves should originate from the point (0.0) the maximum point (v_m^{max}, σ_o) determined the location of the parabola.

The equation for the parabola can be calculated by the method of least squares. Corresponding values of v_m and σ are then described with eq (4-2).

$$v_m = \frac{v_m^{max}}{\sigma_o^2} (2\sigma_o - \sigma) \cdot \sigma \qquad (4\text{-}2)$$

Besides the values v_m^{max} and σ_o the corresponding power input is of interest. Because "i" in eq (4,1) not necessarily has to be an integer, a real number corresponding "i" in the following will be called "x".

The value x_o denominates the power input pattern, which causes the settling properties (v_m^{max}, σ_o), and can be calculated by an interpolation. The real number x thus, analogically to eq (4-1), is defining the power input according to eq (4-3).

$$W_x(t/T) = \frac{90}{4^{x-1}} \left(\frac{4^{x-1}}{6000}\right)^{t/T} \qquad watt/m^3,\ x < 7.3 \qquad (4\text{-}3)$$

The value x=7.3 implies a constant power input throughout the flocculation process.

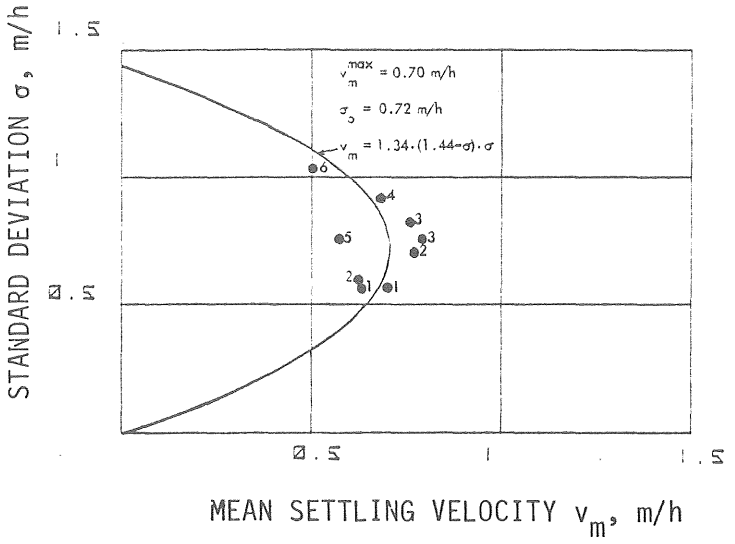

Fig 4.3. Example of the influence of the power input on settling properties. 20 min flocculation time. Temperature 20C.

In figure 4.3 is shown an example of how v_m and σ are affected by the power input at constant flocculation time (20 min) without any flocculation aid. The settling analyses are carried out in the fourth flocculation tank. The points numbered 1, 2 and 3 are results from settling tests carried out twice, on two different occasions supposed to represent the same flocculation conditions. The parabola which best fits the points is indicated in the figue, with the maximum point (v_m^{max}, σ_o equal to (0.70, 0.72). The x-value according to eq (4-3) that corresponds that maximum value (x_o), becomes 2.7. The value of x_o is calculated in a regression analysis, where σ/σ_o has been plotted against the present x-value (1, ...,6). x_o is achieved as the x-value that according to the regression line gives σ/σ_o=1.

In figure 4.4 is shown the resulting theoretical picture after treatment of data according to figure 4.3 . With only three values the impact of the power input can be described: (v_m^{max}, σ_o, x_o).

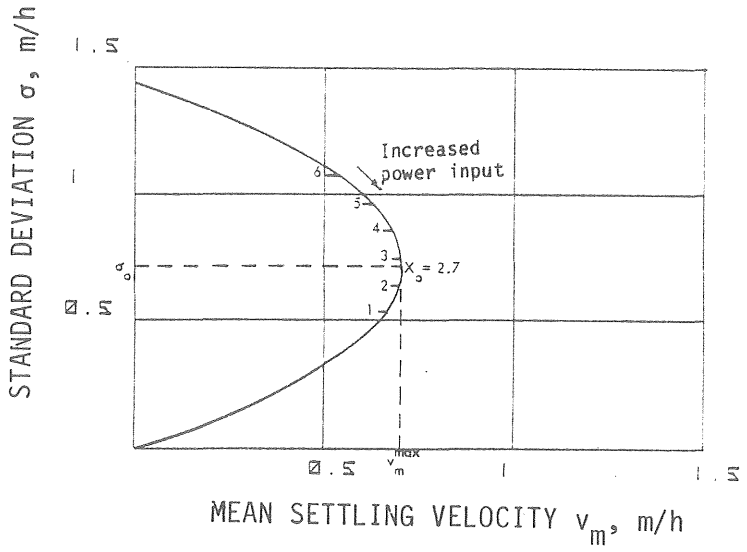

Fig 4.4. Simplified theoretical picture developed from data in fig 4.3.

This model presupposes that the change of σ is equal at every step of change of the power input.

$$\frac{d(\sigma/\sigma_o)}{dx} = \text{constant} = m \qquad (4\text{-}4)$$

This hypothesis seems to be reasonable in comparison with experimental data (compare, for example figure 4.3 and 4.4). An analysis was made of 28 sets of data, each set (of the type seen in fig 4.3) containing 3-6 different power input levels, with varying flocculation conditions, such as flocculation time, number of flocculation tanks, stirrer type and temperature.

It gave the mean value of m=0.15. The standard error of this estimate was 0.067. For simplicity this value will be used in the following. The value of m, in summary, expresses how much the standard deviation, related to the maximum standard deviation (σ/σ_o), will increase if the power input is decreased one step. The magnitude of these "steps" are defined by eq (4-1) and fig 4.1.

In table 4-1 values of σ_o, v_m^{max} and x_o are shown as results of experiments at the flocculation time 20 min, low water temperature (ca 2^oC) and with paddles type A4 (figure 3.32). The original data on which the calculations of these values are based, can be found in the Appendices 2 and 6.

Table 4-1. Values of v_m^{max}, σ_Θ and x_o. Total flocculation time 20 min. Temperature 1.5-1.9°C. Paddle type A4.

	No activated silica			Activated silica, 2 mg/l		
	Tank 2	Tank 3	Tank 4	Tank 2	Tank 3	Tank 4
σ_o, m/h	0.36	0.55	0.72	0.64	0.81	1.27
v_m^{max}, m/h	0.22	0.46	0.70	0.36	0.66	1.07
x_o	1.7	2.9	2.7	1.6	2.1	3.2

Table 4-1 shows the mean settling velocity that maximally can be obtained under the present conditions. As the total flocculation time is 20 minutes, the time for flocculation tank 2 and 3 becomes 10 and 15 minutes, respectively.

v_m^{max} is roughly doubled for each step in the flocculation tank series, while the corresponding standard deviation increases to a lower extent. The power input level at the maximum point is decreasing as a rule (x_o is increased) from one flocculation tank to another.

The addition of activated silica made v_m^{max} increase about 50%, while the increase in σ_o is more accentuated. As the flocculant aid may increase flocculation rate and floc strength (two effects that affect x_o, but in opposite directions) the tendencies according the power input are not quite clear.

In fig 4.5 the results from tank 4 with and without activated silica are compared.

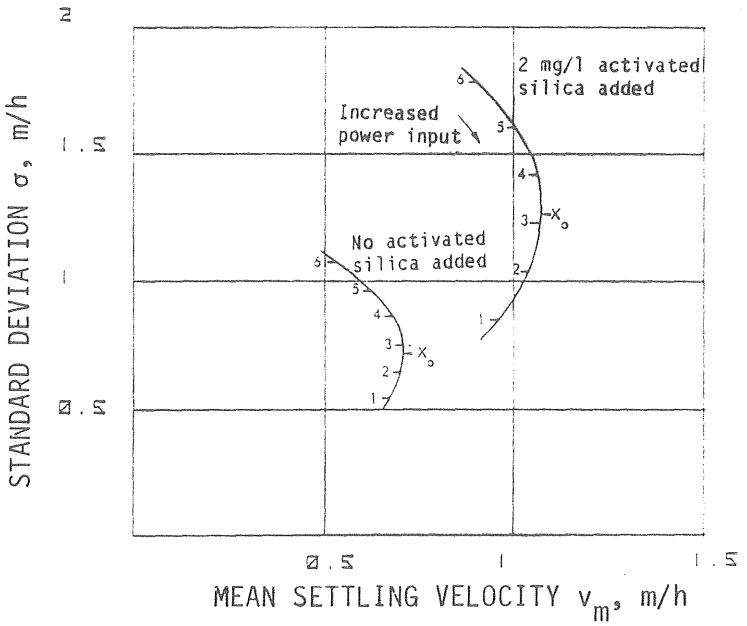

Fig 4.5. Comparison betwen the impact of power input on settling properties, with and without activated silica dose.

The values in table 4-1 will be used as a reference when the effect of, e.g., temperature, paddle design and flocculation time is described later.

If the equations (4-2) and (4-4) are valid there is a possibility to calculate the optimum power input for a certain overflow rate. Considerations made in Section 3.3.6 will then be used. There it was shown that in a v_m-σ diagram the slope (K_r) of a line from the point ($v_F/2$, 0), where v_F is the sedimentation overflow rate, to the point describing the actual floc settling properties (v_m, σ), determined the performance (see figures 3.25 and 3.26).

Eq (4-4) can be written:

$$\frac{\sigma}{\sigma_o} = 0.15(x-x_o) + 1 \qquad (4\text{-}5)$$

or

$$\sigma = (0.15(x-x_o)+1) \cdot \sigma_o \qquad (4\text{-}6)$$

Eq (4-6) inserted in eq (4-2) gives:

$$v_m = (1-\{0.15\cdot(x-x_o)\}^2) \cdot v_m^{max} \qquad (4\text{-}7)$$

K_r can now be calculated as the slope of the line from$(v_F/2, 0)$ to the point (v_m, σ).

$$K_r = \frac{\sigma}{v_m - v_F/2} = \frac{(0.15(x-x_o)+1)\cdot\sigma_o}{(1-\{0.15\cdot(x-x_o)\}^2)\cdot v_m^{max} - v_F/2} \qquad (4\text{-}8)$$

For $x = x_o$ is

$$K_r = \frac{\sigma_o}{v_m^{max} - v_F/2} \qquad (4\text{-}9)$$

For each overflow rate v_F, a tangent to a v_m-σ curve (for example in figure 4.5) can be found, representing minimum residual turbidity after sedimentation. The slope for this tangent (K_r) can be derived to:

$$K_r = \frac{\sigma_o}{2\cdot v_m^{max} - \sqrt{2\cdot v_m^{max}\cdot v_F}} \qquad (4\text{-}10)$$

The coordinates for the tangent point becomes:

$$\sigma = \sigma_o \cdot \sqrt{\frac{v_F}{2\cdot v_m^{max}}} \qquad (4\text{-}11)$$

$$v_m = \sqrt{2\cdot v_F \cdot v_m^{max}} - \frac{v_F}{2} \qquad (4\text{-}12)$$

If eq (4-5) is combined with eq (4-11) the optimum power input as a function of the sedimentation load v_F can be calculated:

$$x_{opt} = \left(\sqrt{\frac{v_F}{2\cdot v_m^{max}}} - 1\right) \cdot \frac{1}{0.15} + x_o \qquad (4\text{-}13)$$

As an example the values in table 4-1 for tank 4 with activated silica dose is chosen: σ_o = 1.27 m/h, v_m^{max} = 1.07 m/h and x_o = 3.2.

For four different overflow rates the optimum power input is calculated according to eq (4-13).Then K_r can be determined by means of eq (4-10), and the sedimentation result can be found in figure 3.25.

$$x_{opt} = \left(\frac{\sqrt{v_F}}{\sqrt{2.14}} - 1\right) \cdot \frac{1}{0.15} + 3.2$$

$$K_r = \frac{1.27}{2.14 - \sqrt{2.14 \cdot v_F}}$$

v_F, m/h	0.5	1.0	1.5	2.0
x_{opt}	-0.2	1.1	2.2	3.0
K_r	1.15	1.88	3.65	17.8
T^{sed}_{rel}	0.19	0.30	0.39	0.48

A value of $x_{opt}<1$ means that the theoretically needed power input is higher than has been applied at the present experiments. It is possible by means of eq (4-3) to calculate the corresponding power input for this case, but this implies an extrapolation beyond available experimental results.

If a fixed power input is applied, e.g. x = 3, calculations can be carried out according to eq (4-8):

v_F, m/h	0.5	1.0	1.5	2.0
K_r	1.50	2.17	3.86	17.9
T^{sed}_{rel}	0.25	0.32	0.40	0.48

The sedimentation results here lies more or less above the "optimum" according to the previous table.

4.2.2 Temperature

Experiments were carried out for the same flocculation conditions as in Section 4.2.1 but at a considerably higher water temperature, around 20^{o}C. In table 4-2 values, which can be compared with those in table 4-1, are listed.

Table 4-2. Values of v_m^{max}, σ_o and x_o. Total flocculation time 20 min. Temperature 18.6-20.0°C. Paddle type A4.

	No activated silica			Activated silica, 2 mg/l		
	Tank 2	Tank 3	Tank 4	Tank 2	Tank 3	Tank 4
σ_o, m/h	0.63	1.3	2.3	2.0	2.8	4.9
v_m^{max}, m/h	0.41	0.84	1.6	1.1	1.8	3.5
x_o	1.8	5.3	7.2	3.9	4.7	6.8

Compared to the lower temperature the mean settling velocity and standard deviation are roughly doubled when no activated silica is used. An addition of activated silica increases these values with a factor 3. The standard deviation can be seen to have increased somewhat more than the mean settling velocity.

Considering the level of the power input needed to achieve the maximum point, the same tendencies, but more accentuated as at the lower temperature can be observed: A decrease of required power input after each flocculation tank.

Throughout, considerably lower power input levels (higher x_o) are required to obtain maximum settling velcoity.

In the figures 4.6 and 4.7 the results can be found on which the values in table 4-2 are based (see Appendix 5).

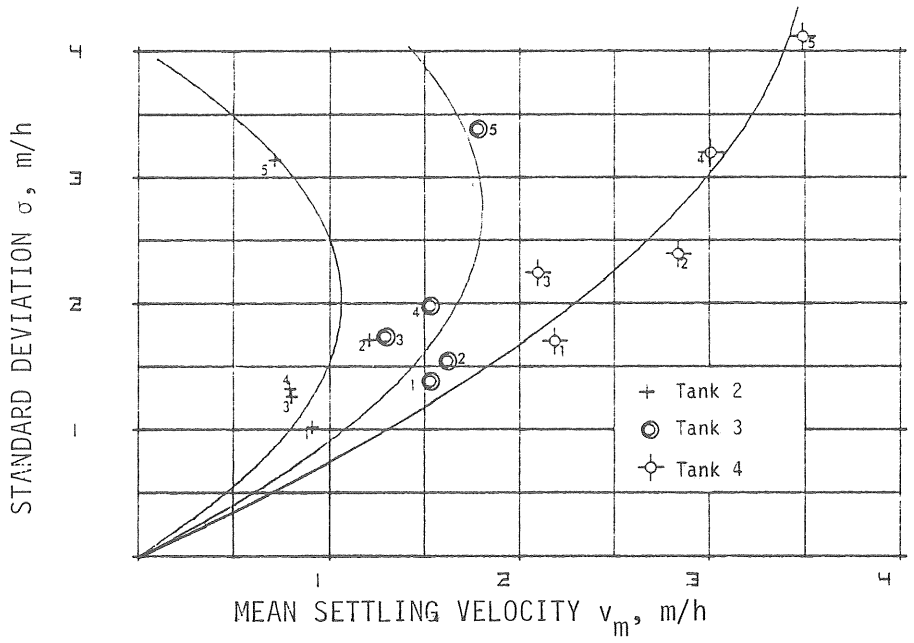

Fig 4.6. Corresponding values of mean settling velocity and standard deviation. Flocculation tanks 2, 3 and 4. Temperature 20°C. Activated silica 2 mg/l. Paddle type A4. Total flocculation time (tank 4): 20 min. The number beside each point defines the power input level. (Low number = high level).

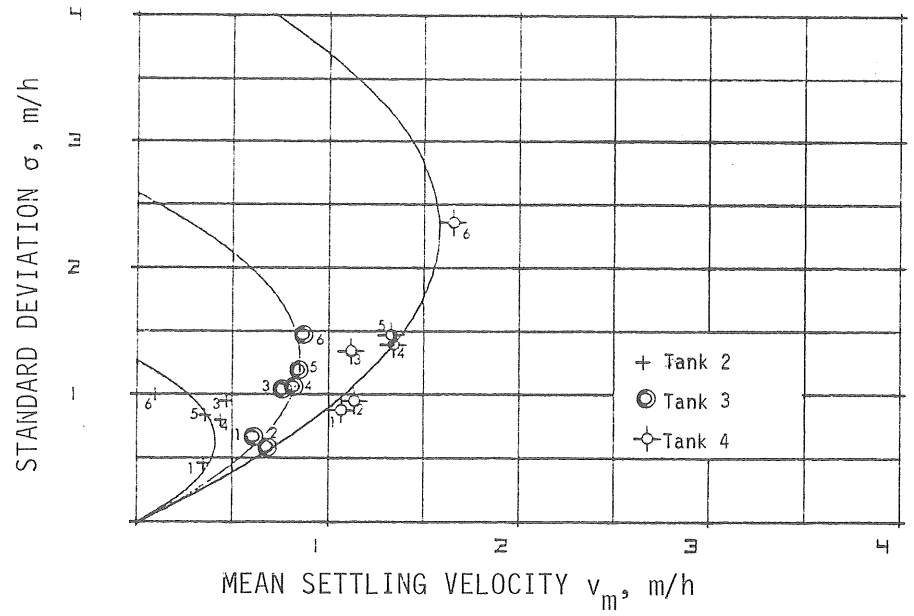

Fig 4.7. The same conditions as in fig 4.6, but without activated silica dose.

4.2.3 Paddle design

The influence on floc settling characteristics of three paddle designs, named A4, B and C, presented in Section 3.4.3.2, was tested. These three paddle designs differ from each other though their paddle area is the same.

In figures 4.8, 4.9 and 4.10 the paddle shapes can be seen (see also fig 3.32).

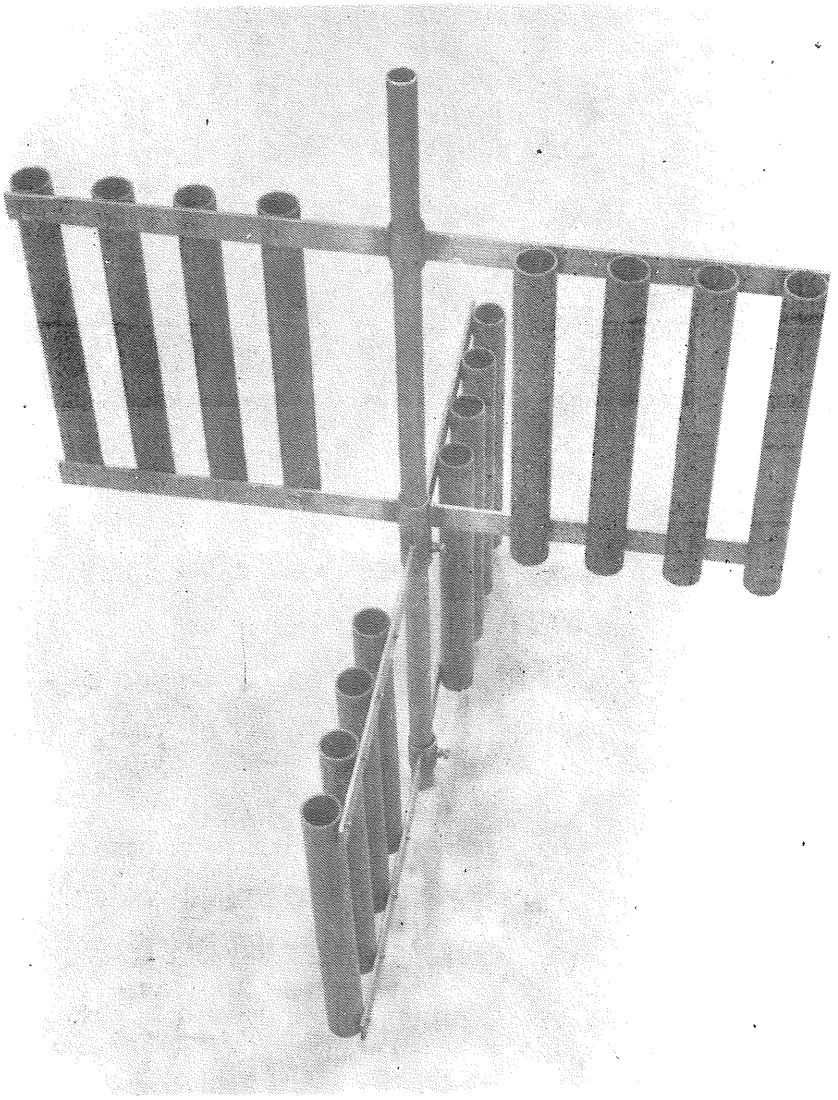

Fig 4.8. Paddles type A4.

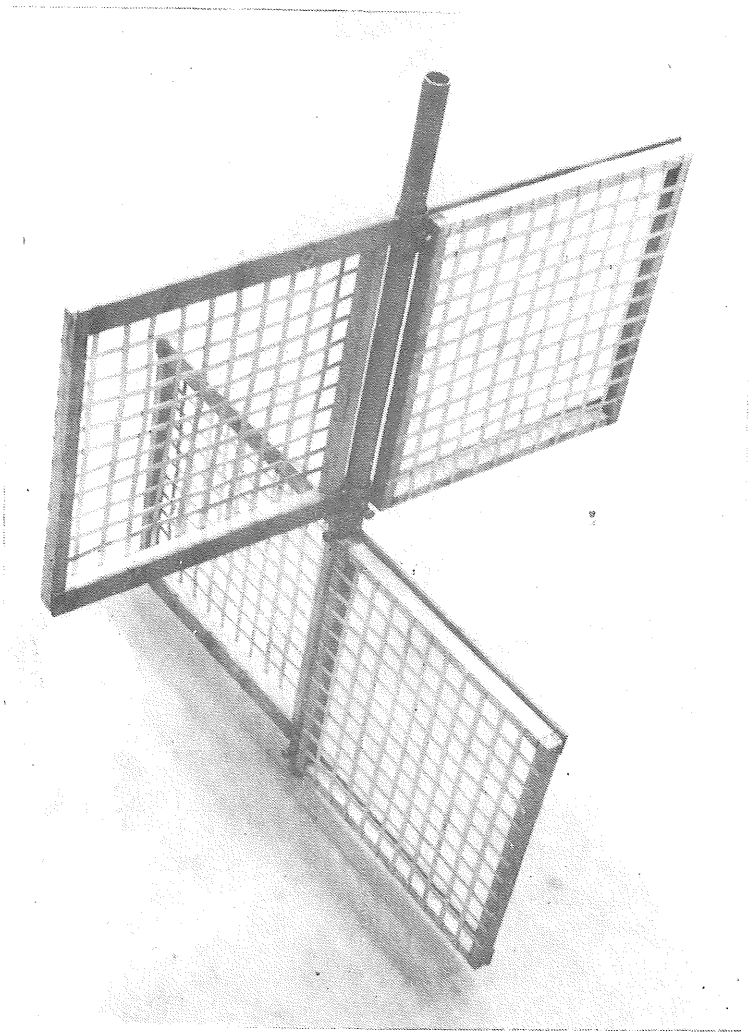

Fig 4.9. Paddles type B.

The paddle of shape B consists of a net of aluminium bands, 10 mm wide at a centre distance of 40 mm. The most concentrated paddle area is in paddle type C, where two 100 mm wide boards are forming vertical paddles on each pair of paddle arms. The total relative paddle edge length is about 1:2:20 for the paddle types C, A4 and B, respectively.

According to measured power input, Section 3.4.3.2, the appropriate rotational speed could be determined for each type. Because of some differences in paddle form and the location of the paddle area along the paddle arm, it was shown that the relative rotational speeds for identical power input, (see table 3-5) was

$$\sqrt[3]{5.4} : \sqrt[3]{3.6} : \sqrt[3]{3.2}$$

or

1.19 : 1.04 : 1.00

for paddle type C, A4 and B respectively.

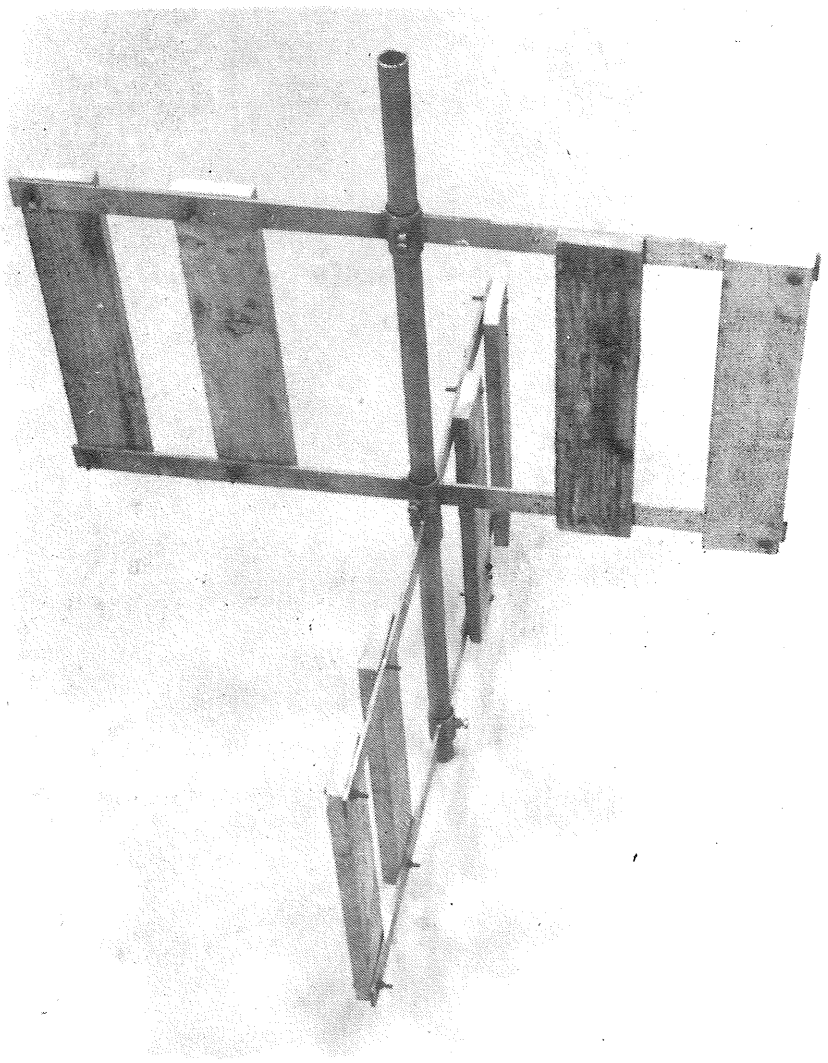

Fig 4.10. Paddles type C.

In table 4-3 and 4-4 the results obtained with paddle type B and C are summarized (see original data in Appendices 7 and 8). They can be compared with the results of paddle type A4, for the same flocculation conditions, in table 4-1.

Table 4-3. Values of v_m^{max}, σ_o and x_o. Total flocculation time 20 min. Temperature 1.5-1.6°C. Paddles type B and C. No activated silica.

	Paddle type C			Paddle type B		
	Tank 2	Tank 3	Tank 4	Tank 2	Tank 3	Tank 4
σ_o, m/h	0.37	0.66	1.03	0.31	0.45	0.70
v_m^{max}, m/h	0.19	0.45	0.74	0.26	0.42	0.64
x_o	~1.0	3.7	4.3	0.5	1.5	3.1

Table 4-4. Values of v_m^{max}, σ_o and x_o. Total flocculation time 20 min. Temperature 1.5-1.6°C. Paddle type B and C. Activated silica 2 mg/l.

	Paddle type C			Paddle type B		
	Tank 2	Tank 3	Tank 4	Tank 2	Tank 3	Tank 4
σ_o, m/h	0.53	0.72	1.0	0.37	0.64	1.1
v_m^{max}, m/h	0.36	0.66	1.1	0.27	0.55	0.96
x_o	~1.8	2.0	1.9	0.8	1.5	3.4

In the figures 4.11 and 4.12 the effect of the power input on mean settling velocity and standard deviation for the fourth flocculation tank are shown, for the three types, with and without activated silica dose.

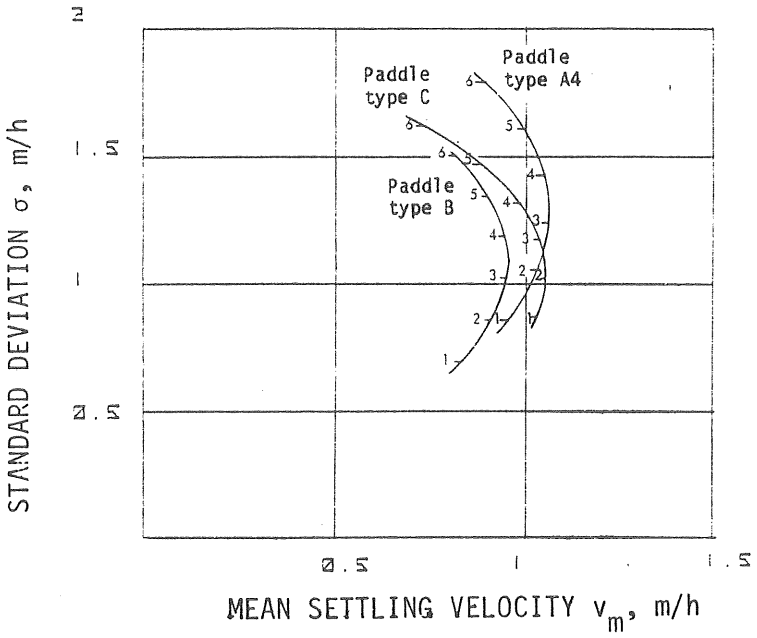

Fig 4.11. The effect of power input on mean settling velocity and standard deviation. Comparison between paddle types A4, B and C. Activated silica 2 mg/l. Tank 4. Flocculation time 20 min. Temperature ca 2°C.

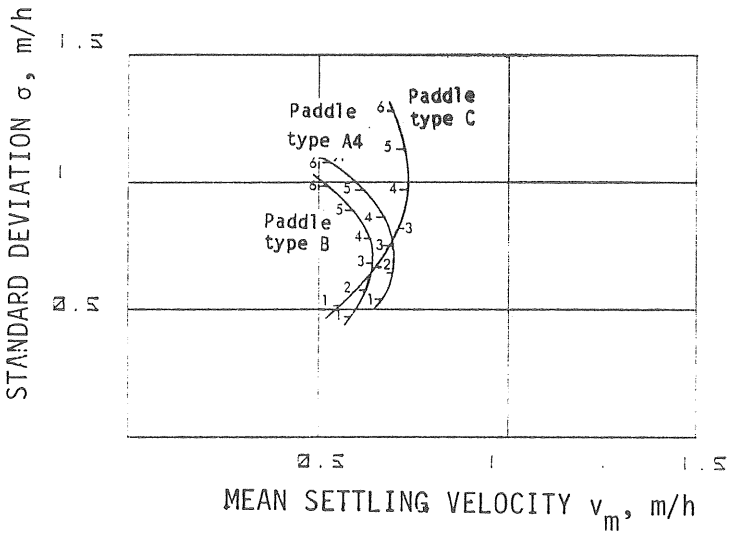

Fig 4.12. The same conditions as in figure 4.11, but without activated silica.

The difference between the results obtained by the different paddle types are small, which indicates that the magnitude of the power inputs is of much greater importance than the paddle shape. It should be mentioned that the related experiments were carried out with a constant total paddle area. If this varies the conclusion may not longer be valid.

Flocs formed by the net-formed paddles, type B, has throughout a somewhat smaller mean settling velocity than the other paddle types.

When no activated silica is added the paddle type C causes noticably higher σ-values and somewhat higher v_m-values, at a low power input, than the other types. In the power input area of interest (the three highest levels, x = 1, 2, 3) however, the differences are small, and may be attributed to experimental errors.

Additional experiments carried out at ca. 15^{o}C water temperature (see Appendix 4) confirmed that the three different paddle types caused essentially the same floc settling properties, at a constant power input (X = 2).

4.2.4 Flocculation time

Hitherto only experiments carried out at a total flocculation time 20 minutes has been described. On the basis of experiments carried out at 10 and 30 minutes it is possible to outline the effect of flocculation time varies. The experiments carried out at 10 and 30 minutes flocculation time have not been as extensive as those at 20 min. Only the highest power input levels, numbered 1, 2 and 3, were applied.

With the assumption that the same pattern of influence of the power input on mean settling velocity and standard deviation is valid, as been applied in Section 4.2.1, the values of v_m^{max}, σ_o and x_o can be estimated. The uncertainty of course, becomes greater as only three values are used for their determination. The results from such calculations can be seen in table 4-5, where values from table 4-1 also are inserted as a comparison. The values that are considered too uncertain are omitted. Original data can be found in Appendix 2.

Table 4-5. Values of v_m^{max}, σ_o and x_o. Total flocculation time 10, 20 and 30 minutes. Temperature ca 2°C. Paddle type A4.

	Total flocculation time	Activated silica 2 mg/l			No activated silica		
		10 min	20 min	30 min	10 min	20 min	30 min
Tank 2	σ_o	0.39	0.64	1.15	-	0.36	0.85
	v_m^{max}	0.29	0.36	0.80	-	0.22	0.69
	x_o	-	1.6	3.0	-	1.7	3.3
Tank 3	σ_o	-	0.81	1.34	0.51	0.55	1.41
	v_m^{max}	-	0.66	1.25	0.36	0.46	1.16
	x_o	-	2.1	3.8	2.5	2.9	4.7
Tank 4	σ_o	-	1.27	2.49	0.57	0.72	1.30
	v_m^{max}	-	1.07	2.37	0.54	0.70	1.40
	x_o	-	3.2	4.1	1.8	2.7	4.4

Based on table 4-5, now a simple model for the simultaneous effect of flocculation time and power input can be outlined.

The objective was to obtain a mathematical description of how v_m and σ, for each flocculation tank and dose of activated silica, changed with flocculation time (T) and power input variant (x). For that purpose three additional relationships, besides the equations (4-2)and (4-5) already given, was introduced:

$$\sigma_o = m_1 \cdot v_m^{max} + b_1 \qquad (4\text{-}14)$$

$$v_m^{max} = m_2 \cdot T \qquad (4\text{-}15)$$

$$x_o = m_3 \cdot \sigma_o \qquad (4\text{-}16)$$

The limited amount of data, does not permit any evaluation of the accuracy of these equations. They were considered, however, to give a sufficiently appropriate estimate of the floc settling properties under varying conditions, to illustrate the general effect.

In table 4-6 calculated values of the parameters according to eqs. (4-14) to (4-16) is shown.

Table 4-6. Calculated values of m_1, m_2, m_3 and b_1 in eqs (4-14) to (4-16). The values are calculated from data in table 4-5. Paddle type A4. Temperature ca 2^oC.

Equation	Parameter	No activated silica			2 ppm activated silica		
		Tank 2	Tank 3	Tank 4	Tank 2	Tank 3	Tank 4
$\sigma_o = m_1 \cdot v_m^{max} + b_1$	m_1	1.05	1.17	0.85	1.39	0.91	0.93
	b_1 (m/h)	0.13	0.06	0.12	0.05	0.20	0.28
$v_m^{max} = m_2 \cdot T$	$m_2(\frac{m}{h} \cdot \frac{1}{min})$	0.034	0.044	0.044	0.048	0.080	0.068
$x_o = m_3 \cdot \sigma_o$	$m_3(\frac{h}{m})$	4.09	3.42	3.42	2.58	2.77	1.96

If the equations (4-14), (4-15) and (4-16) are inserted into eqs (4-2) and (4-5) the mean settling velocity and the standard deviation of the settling velocity are obtained as functions of flocculation time T (minutes) and power input level (x):

$$\sigma = \{(x - m_1 \cdot m_2 \cdot m_3 \cdot T - m_3 \cdot b_1) \cdot 0.150 + 1\} \cdot (m_1 \cdot m_2 \cdot T + b_1) \qquad (4\text{-}17)$$

$$v_m = (1 - \{0.150 \cdot (x - m_3 \cdot (m_1 \cdot m_2 \cdot T + b_1)\}^2) \cdot m_2 \cdot T \qquad (4\text{-}18)$$

The ability of the equations (4-17) and (4-18) to approximate the given data has been estimated by dividing the value obtained by the model with the result obtained in practice. In table 4-7 the result of such a comparison for flocculation tank 4 is shown.

Table 4-7. Comparison between values of the model according to eqs (4.17) and (4.18) (v_m^{est}, σ^{est}) and obtained results (v_m^{obt}, σ^{obt}).

		v_m^{est}/v_m^{obt}		$\sigma^{est}/\sigma^{obt}$	
	Number of values	Mean value	Standard deviation	Mean value	Standard deviation
Activated silica, 2 ppm	14	1.17	0.23	1.16	0.25
No activated silica	15	1.14	0.18	1.10	0.20

In table 4-7 can be seen that v_m and σ will be somewhat overestimated. The standard deviation of the ratio is decreased to some extent when no activated silica is added.

The figures 4.13 and 4.18 demonstrate in graphical form the information given in eqs (4-17) and (4-18) together with table 4-6. The mean settling velocity and the standard deviation of the settling velocity are shown, depending on flocculation time and power input for flocculation tanks 2, 3 and 4. The flocculation time given in the figures (unlike in table 4-5) is the residence time after each flocculation tank. Thus if the floc growth pattern is to be followed e.g. at the total flocculation time 20 minutes, the results from tank 2 and 3 should be read as values at 10 and 15 minutes, respectively, for the power input level in question.

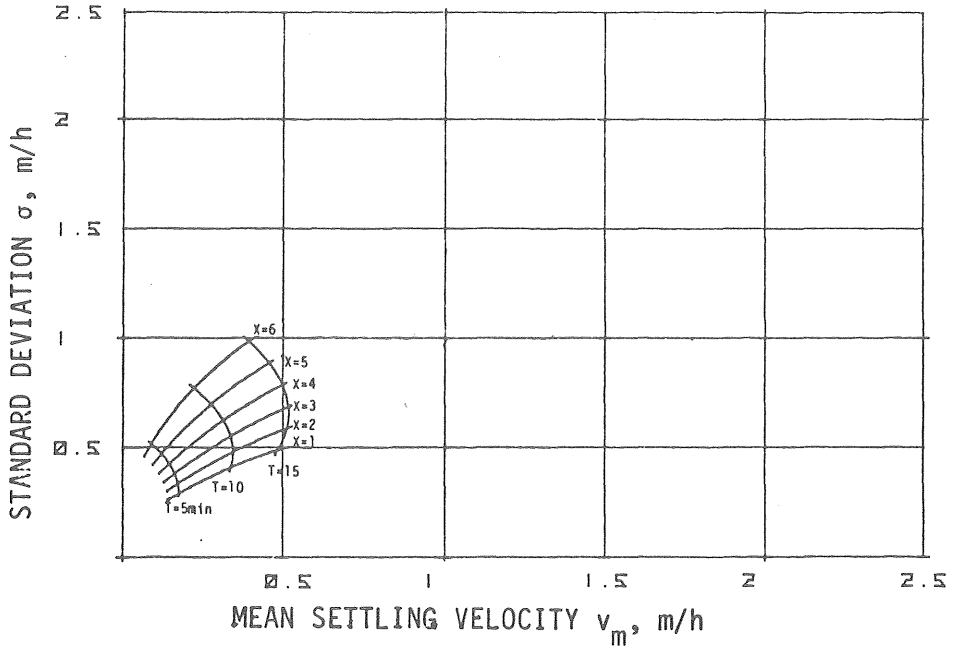

Fig 4.13. Mean settling velocity (v_m) and settling velocity standard deviation (σ) depending on power input (x) and flocculation time (T). No activated silica. Flocculation tank nr 2. Paddle type A4. Temperature 2°C.

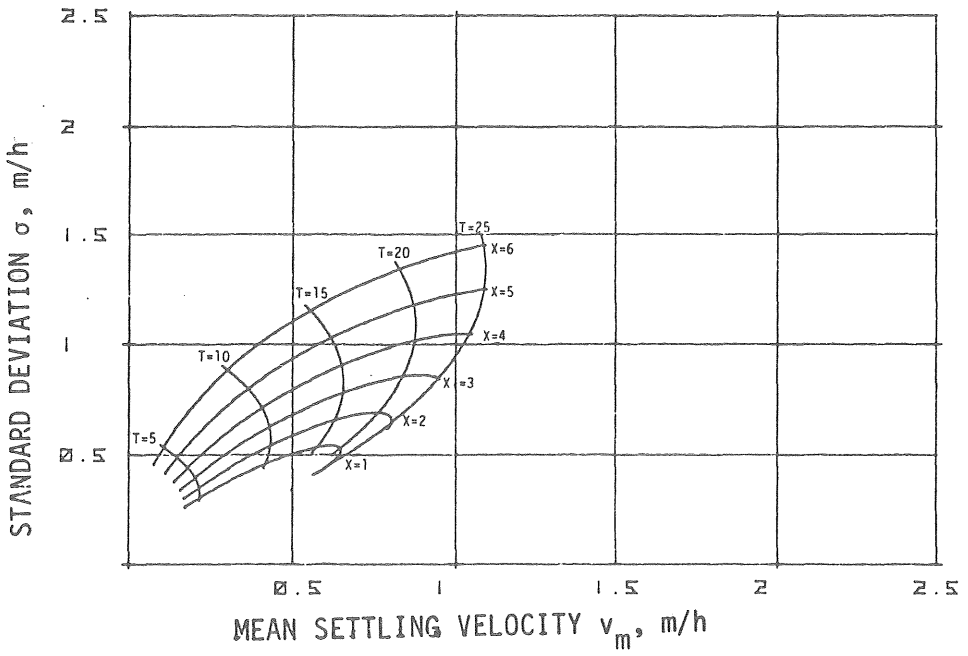

Fig 4.14. The same conditions as in fig 4.13. Flocculation tank nr 3.

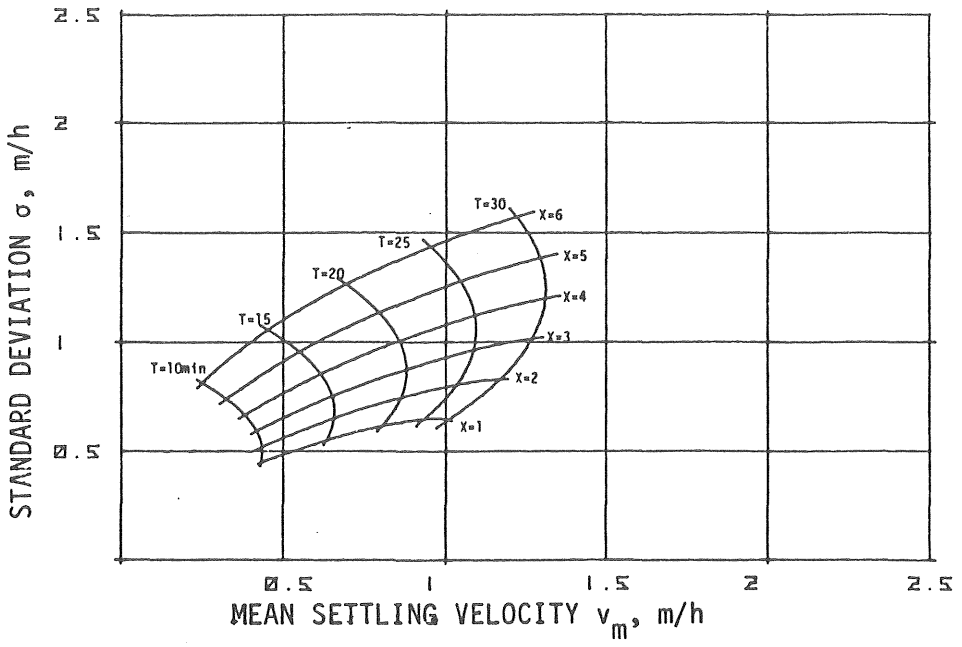

Fig 4.15. The same conditions as in fig 4.13. Flocculation tank nr 4.

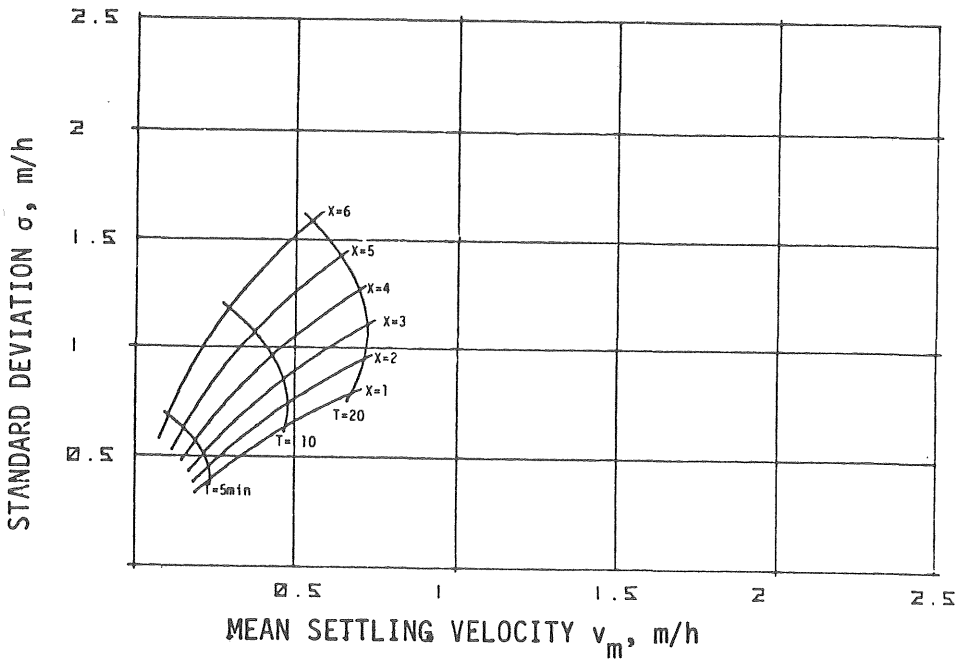

Fig 4.16. Flocculation tank nr 2. 2 ppm activated silica. Otherwise, the same conditions as in fig 4.13.

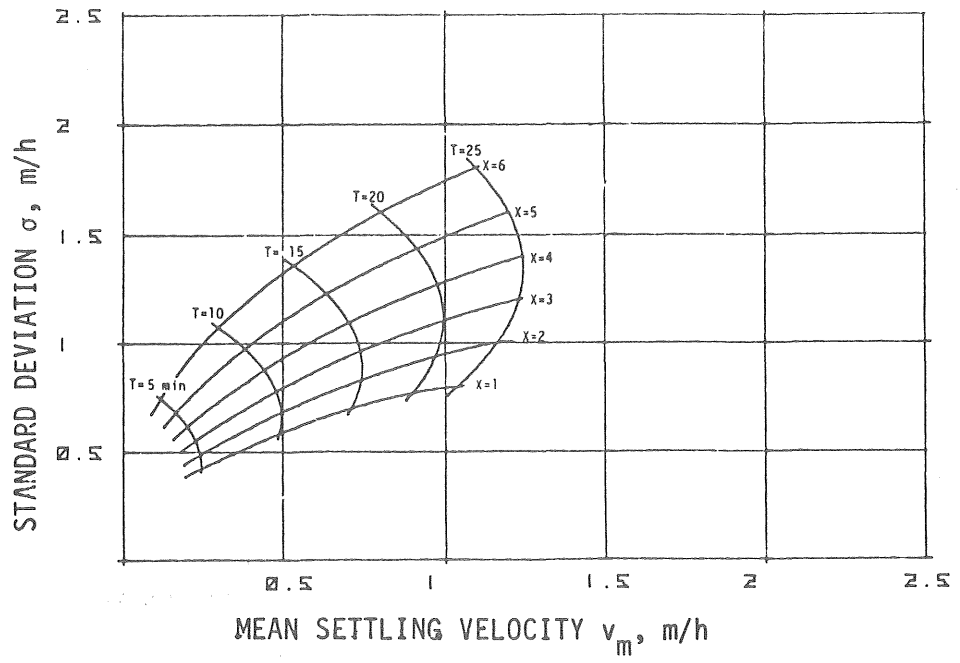

Fig 4.17. Flocculation tank nr 3. 2 ppm activated silica. Otherwise, the same conditions as in fig 4.13.

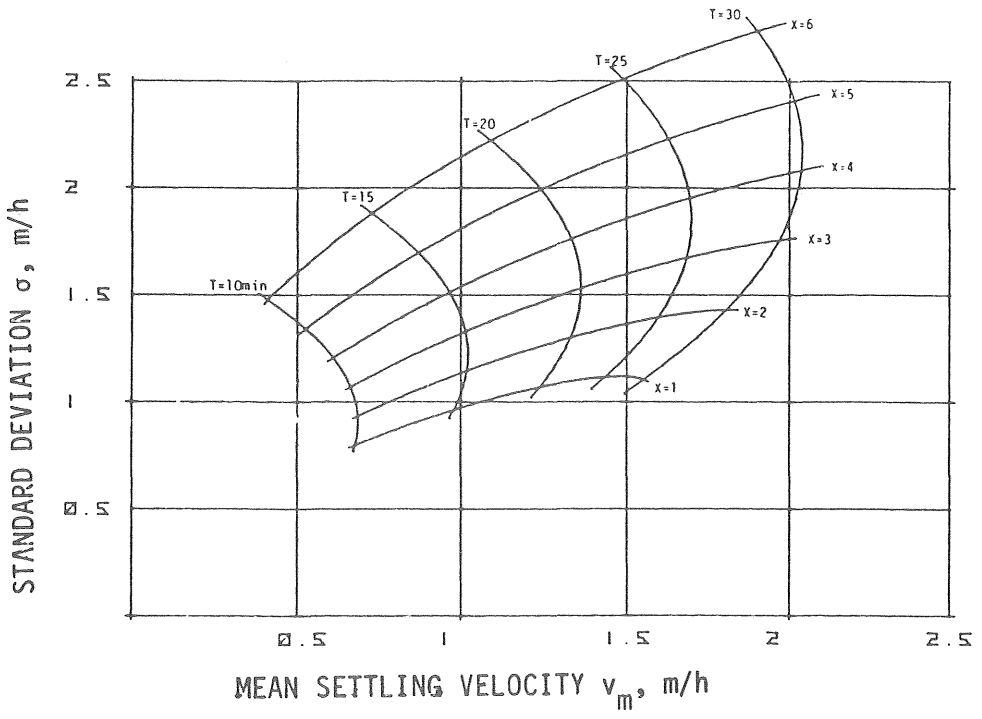

Fig 4.18. Flocculation tank nr 4. 2 ppm activated silica. Otherwise, the same conditions as in fig 4.13.

As an illustrative example of the use of the figures 4.13 to 4.18, when the sedimentation load and the required sedimentation result are fixed, the possible combination of power input and flocculation time can be obtained according to fig 4.19. The curves in fig 4.18 has been used for the example. The sedimentation load (v_F) is 0.6 m/h and the relative turbidity after sedimentation (T_{rel}^{sed}) is fixed to the value 0.2. As can be seen in the figure the following combinations of power input and flocculation time would give the prescribed sedimentation result:

Flocculation time T (min)	Power input x
20	1.5
22	2
25	3
30	4

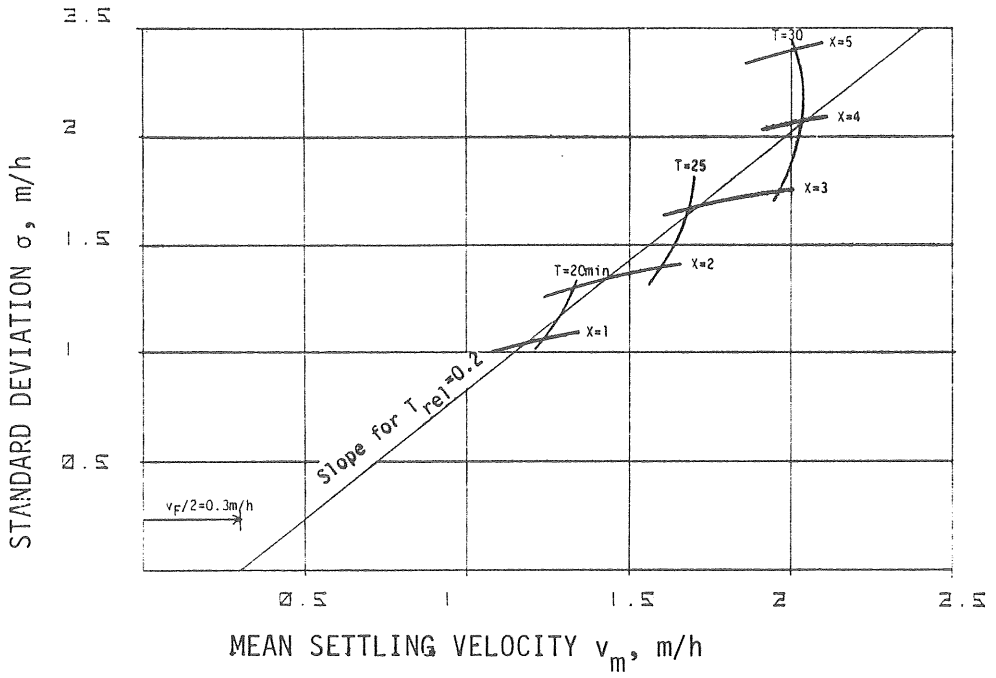

Fig 4.19. Determination of the combinations of flocculation time (T) and power input (x), that will give the relative turbidity 0.2 after sedimentation at the sedimentation load v_F=0.6 m/h.

How the power input is to be changed at an increase of the flow through the treatment plant is shown in figure 4.20. Here, curves according to figure 4.15 has been used. It is assumed that the flocculation time and overflow rate originally are 30 minutes and 0.8 m/h, respectively. Then the power input corresponding to x=1 gives the lowest residual after sedimentation. At an increase of the flow with 50%, i.e. the flocculation time becomes 20 minutes and the overflow rate 1.2 m/h the power input should be decreased to x=2 to minimize the increase of the turbidity in the outlet of the sedimentation basin.

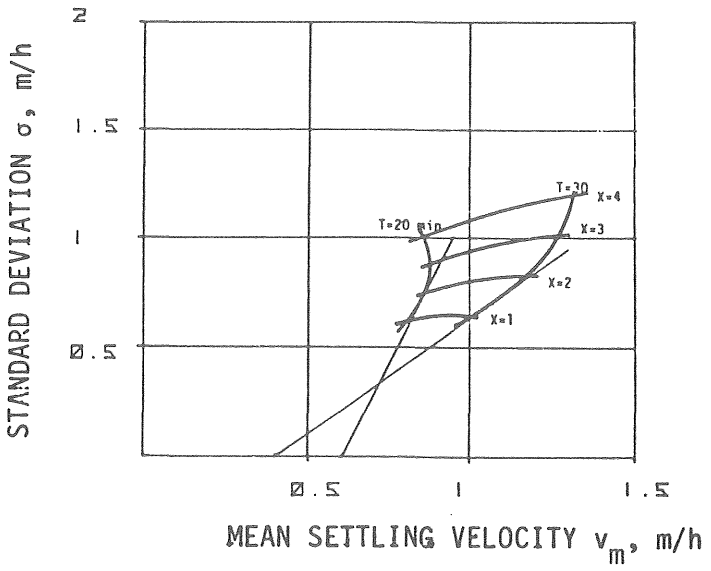

Fig 4.20. The effect of an increased flow. Data from figure 4.15.

4.2.5 Reactor design

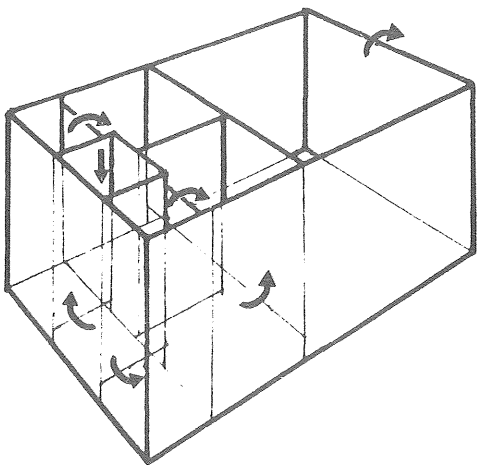

Fig 4.21. Reactor design with gradually increased tank size.

With a reactor design according to fig 4.21 the size of consecutive tanks are roughly doubled. The number of flocculation tanks in series is four, also for this design. After a common first tank, the flow is divided into two parts and then again united in the last flocculation tank. The part of the total flocculation time in each tank becomes 6%, 12%, 27% and 54% respectively. The paddle designs and results from power input measurements are shown in Section 3.4.3.2 and fig 3.32 (paddle type A1, A2, A3 and A4).

The principle of variation of the power input as described in eq (4-1) and fig 4.1 was chosen. Only the three highest levels (x=1,2,3) were applied. In fig 4.22 can be seen how the power input for each flocculations tank was determined.

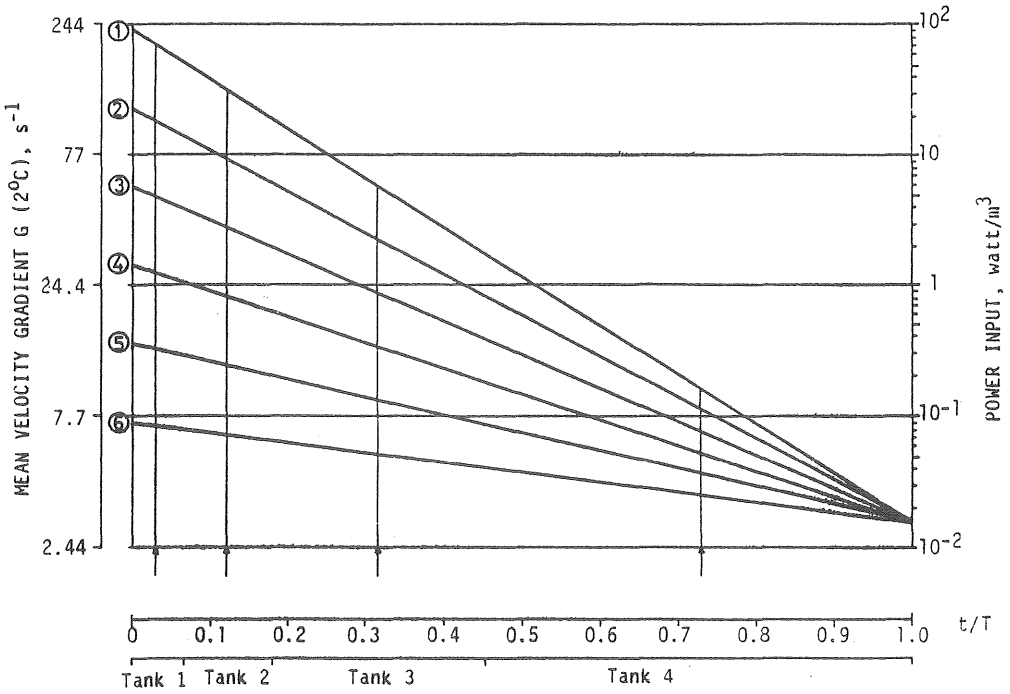

Fig 4.22. Variation of power input.

With the reactor design under consideration the power input varied from maximally 70 watt/m^3 (corresponding G(2°C)=200 s^{-1}) in the first flocculation tank down to the minimal value 0.08 watt/m^3 in the last. In the last flocculation tank the variation is from 0.08 to 0.16 watt/m^3 (corresponding G(2°C) 7 to 10 s^{-1}).

By this procedure the mean power input will be comparable to that obtained at a corresponding power input scheme, when the flocculation volume is equally compartmentalized. A side-effect is that the power input in the last flocculation tank will vary at the different power input levels to a higher extent than in the conventional design. This has to be taken into account when the flocculation result is to be interpreted.

At the total flocculation times 10, 20 and 30 minutes respectively, the three power input levels were studied. Experiments were carried out with and without activated silica dose.

For practical reasons settling tests were only carried out in the final flocculation tank.

As there is not enough data to develop a model similar to that presented in the previous section, it is chosen here to present the results as a direct comparison of the two designs. This shows for which conditions an unequal compartmentalization is favourable compared to the conventional design, which is more simple to construct. In table 4-8 and 4-9 the v_m- and σ-values obtained (see Appendix 3) are compared to the corresponding values according to Section 4.2.4 (calculated from eq (4-17) and (4-18) with values from table 4-6).

Table 4-8. Comparison between the floc settling characteristics achieved at successively increasing tank size design (v_m^{ol}, σ^{ol}) and the corresponding values for conventional compartmentalization (v_m^t, σ^t) according to Section 4.2.4. Flocculation tank nr 4, no activated silica.

Power input	Flocculation time (min)	v_m^t m/h	σ^t m/h	v_m^{ol} m/h	σ^{ol} m/h
x = 1	10	0.435	0.440	0.69	0.62
x = 2	10	0.438	0.514	0.79	0.68
x = 3	10	0.422	0.587	0.83	0.79
x = 1	20	0.803	0.611	0.58	0.37
x = 2	20	0.860	0.740	0.82	0.56
x = 3	20	0.878	0.869	1.1	0.78
x = 1	30	1.01	0.639	0.66	0.44
x = 2	30	1.17	0.824	0.54	0.35
x = 3	30	1.27	1.01	0.79	0.56

Table 4-9. 2 ppm activated silica. Otherwise, the same conditions as in table 4.8.

Power input	Flocculation time (min)	v_m^t m/h	σ^t m/h	v_m^{ol} m/h	σ^{ol} m/h
x = 1	10	0.670	0.802	1.3	0.95
x = 2	10	0.678	0.938	1.7	1.4
x = 3	10	0.656	1.08	1.3	1.4
x = 1	20	1.23	1.07	1.1	0.86
x = 2	20	1.33	1.30	1.6	1.1
x = 3	20	1.36	1.54	2.2	1.7
x = 1	30	1.55	1.11	1.2	0.8
x = 2	30	1.80	1.44	1.2	0.8
x = 3	30	1.96	1.76	1.7	1.2

From the tables it can be concluded that a striking improvement compared to the conventional design is achieved at short flocculation times, while the results at 30 minutes flocculation time rather can be characterized as a deterioration (at least concerning no activated silica dose). The comparison at the activated silica dose 2 ppm and 30 minutes flocculation time is complicated by the fact that simultaneously, lower mean settling velocities and considerably lower standard deviation values occur, compared to the conventional system.

An explanation to these effects, which are difficult to interprete, can be that, together with the better adaption to floc growth kinetics (high power input - short reaction time - consequently a small reactor volume and vice versa)an unfavourable residence time distribution occurs. The flow conditions cannot any longer be characterized as four completely mixed tank reactors in a series (equal in size).

Measurements of residence time distributions confirm these considerations. Response curves for tracer concentration in the outlet from the fourth flocculation tank, caused by an instant dose to the inlet to the flocculation unit, was recorded. For the conventional system the time to reach maximum concentration in the outlet was appr 80% of the mean residence time. This value was ca 70% for the flocculation volume with unequal compartmentalization. It is possible that the more unfavourable flow pattern is of less importance at short flocculation times (the positive effects of the design are dominating), while they become more important as the flocculation time is increased.

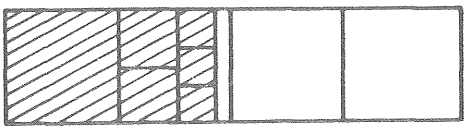

The flocculation tanks with varying size were built inside the ordinary flocculation system according to fig 4.23. Somewhat less than half of the ordinary flocculation volume was occupied by this construction. The results in table 4-8 and 4-9 indicate that with only 10 min flocculation time results can be obtained comparable with 20 min flocculation time in the conventional system. Fig 4.23, therefore also shows the increased flocculation efficiency at that flocculation time.

4.3 Full scale experiments

The pilot plant experiments were carried out in a pilot plant situated in the water treatment plant Lackarebäck, Göteborg. The water used for flocculation tests was the raw water of the water treatment plant, from the Lake Delsjön (originally the River Göta Älv). Consistently only one dose of coagulant, 40 ppm aluminium sulphate, was used. The object of the full scale experiments was to investigate if the pilot plant results could be generally applied to water treatment practice. Factors as e.g. varying raw water quality, coagulant dose and different operating conditions are of importance for the flocculation efficiency. In order to get at least a qualitative picture of how such variations influence flocculation efficiency, 20 Swedish water treatment plants were visited and settling tests in the flocculation tanks were carried out. In Section 4.3.2 results from these tests are reported together with some operation conditions on the treatment plant that affect the flocculation and floc settling properties.

This section can be seen as a survey of the floc qualities that can be encountered in practice. Here no attempts are made to draw more general inferences from these results.

In the water treatment plant at Åmål some experiments were performed. These are reported in Section 4.3.2.

It is inevitable when full scale experiments are carried out, that all factors affecting the experimental result cannot be controlled. That may cause the result to be ambiguous and difficult to interpret. For practical reasons the experiments reported in Section 4.3.1 was only carried out once, with the possibility that uncontrolled factors introduced accidental errors in the measurements. Results which obviously cannot be correct, however, are not reported, whether the cause is known or not.

4.3.1 The impact of power input and avtivated silica. Experiments in the water treatment plant at Åmål.

The water treatment plant at Åmål consists of one flocculation system followed by four sedimentation basins in parallel. The flocculation unit has 7 flocculation tanks in series with a total volume of 216 m^3. The design of the flocculation tanks can be seen in figure 3.42. The power input into the flocculation tanks was measured. The result are presented in Section 3.4.3.3. When the flocculation experiments were carried out, the coagulant dose was 35 mg aluminium sulphate/l and the raw water temperature 4,5^{o}C. The flow was 300 m^3/h and thus the nominal total flocculation time 43 minutes was obtained.

The plant was chosen for experiments because, first of all, the stirrer speeds could easily be changed; each stirrer could operate at three different rotational speeds. In addition, the unusual large number of flocculation tanks in series provided seven sample points for settling analyses throughout the flocculation time.

Some problems were encountered during the practical experiments. The settling tests carried out in the first flocculation tank showed generally no measurable settling, probably because of the high mixing intensity which disturbed the settling. The same conditions usually occured in the second flocculation tank. Further, the flocculation tanks are relatively deep (6 m) in comparison with the section area (2,3 x 2,3 m^2). It is therefore questionable if a settling test carried out on a sample at the top of the tank can be considered as representative for the whole tank, i.e. if the tank is completely mixed. If not, settling test carried out in two consecutive tanks, connected with an opening near the top, could be expected to produce results close to each other. This is also sometimes the case. Thus it should be remembered when in the evaluation of the results presented here, that the odd-numbered flocculation tanks are connected with the succeeding tank at the surface.

Another factor that makes the interpretation of the results more difficult is that the pH-regulating equipment, though satisfactory for practical operation, induced a pH-value with unsatisfactory stability for experimental purpose. The pH-intervals measured are

indicated together with the settling test results. Generally the variation within the flocculation volume at the time when samples were taken was not greater than 0,1 pH-unit. When sets of settling analyses are compared to each other (as in the figures 4-24 to 4-26), the total variation can be larger: up to about 0.25 pH-units.

In figure 4-23 the power input variations for the different experiments are shown. For comparison, the variation patterns according to Section 4.2.1, used on pilot plant scale have been entered into the figure. The experiments I-III was carried out with the intention that they should as far as possible correspond to the three patterns on pilot plant scale with the highest power input levels (numbered 1, 2 and 3). The power input variations I and II was repeated with an activated silica dose of 3 ppm, then labeled with the Roman numerals VII and VIII.

In the experiments numbered IV, V and VI the power input in the first two flocculation tanks was varied and was kept constant at the lowest possible value in the following tanks.

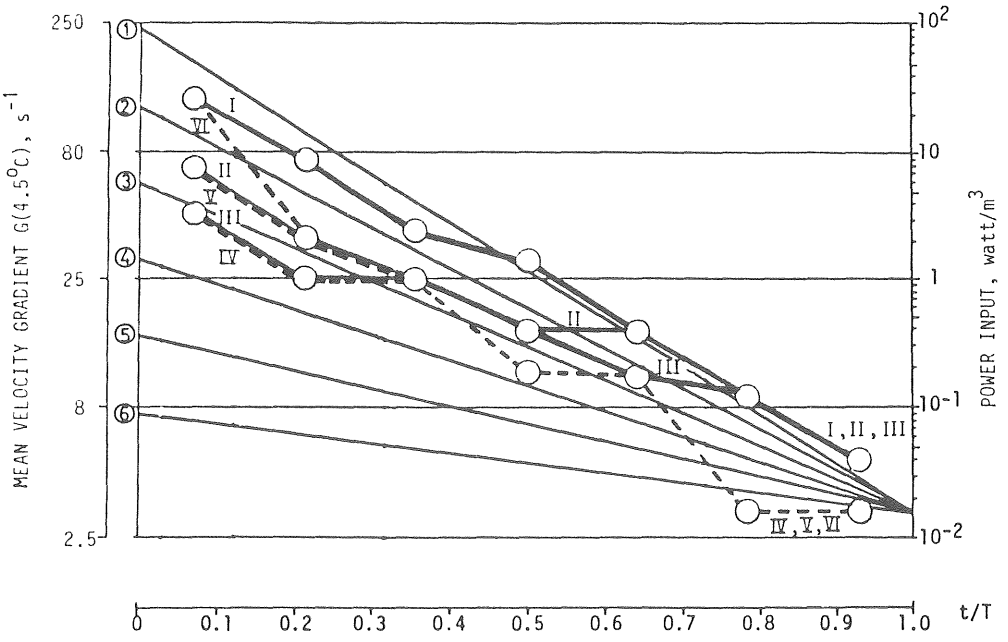

Fig 4-23. Power input variations for the full scale experiments compared to those applied in pilot plant experiments.

Results from the experiments I-III are shown in figure 4-24. The Arabic numbers indicate the flocculation tanks from which the samples are drawn. The general conclusions drawn in Section 4.2.1 seems to be applicable in general terms also for the present results: A higher power input level results in a lower settling velocity standard deviation and a lower mean settling velocity. The latter is earlier reported to be the case provided the power input is higher than that corresponding to the maximum mean settling velocity (see figure 4-2). The results are probably somewhat affected by small pH-changes. During the experiments I and III, consistently pH-values of about 6.0 and 6.2, respectively, was measured. That pH-deviation may cause an exaggregated difference between the two results. Unfortunately, during experiment II a decrease in pH was detected, such that the corresponding pH-values in tank 3 and 7 was 6.1 and slightly below 6.0, respectively.

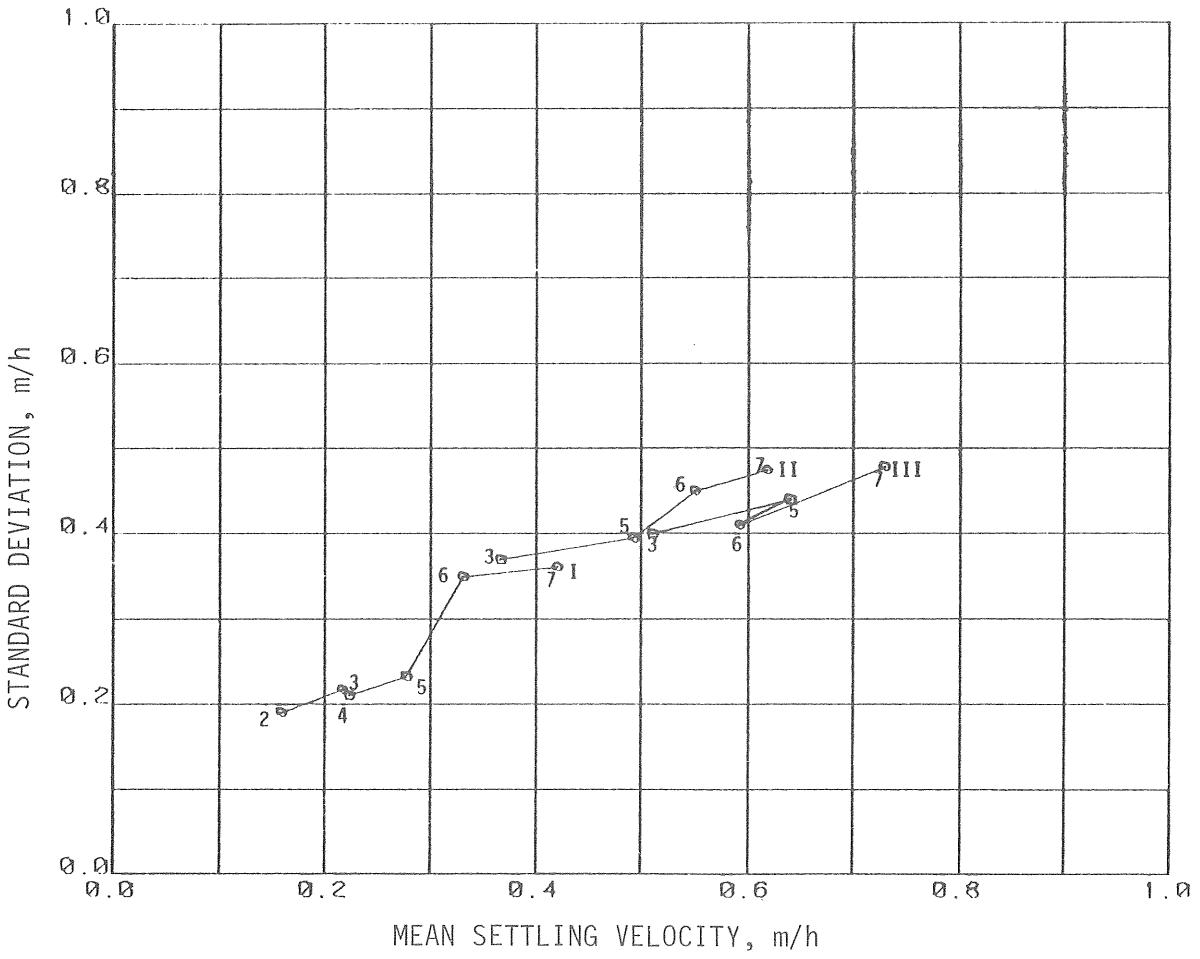

Fig 4-24. Results from settling tests in different flocculation tanks Åmål water treatment plant. Experiments I-III. 35 ppm aluminium sulphate. pH 6.0-6.2. No activated silica. Temperature 4.5°C.

It is obvious that the full scale results are considerably inferior to those reported in Section 4.2.1 (see table 4-8). The v_m and σ values in figure 4-24 are consistenly about half of the values obtained on pilot plant scale. In addition the pilot plant data is obtained at 30 minutes flocculation time and a somewhat lower water temperature (2^oC).

It is evident from the data presented in figure 4-24 that the power input in these experiments was too high. The settling properties of the flocs are consistently improved as the power input level is decreased. This is further confirmed by the results presented in figure 4-25. The curve numbered IV represents settling properties when all stirrers are operating at the lowest possible stirring speed. In the experiments V and VI the stirrers in the first two flocculation tanks where operated at higher speeds. This resulted in a deteriorated floc quality. The difference in settling properties seems to increase in the end of the flocculation process, which is unexpected since the power input is varied only in the first two tanks. Besides experimental errors these results could indicate some irreversible negative effects caused by the high power input in the beginning of the process.

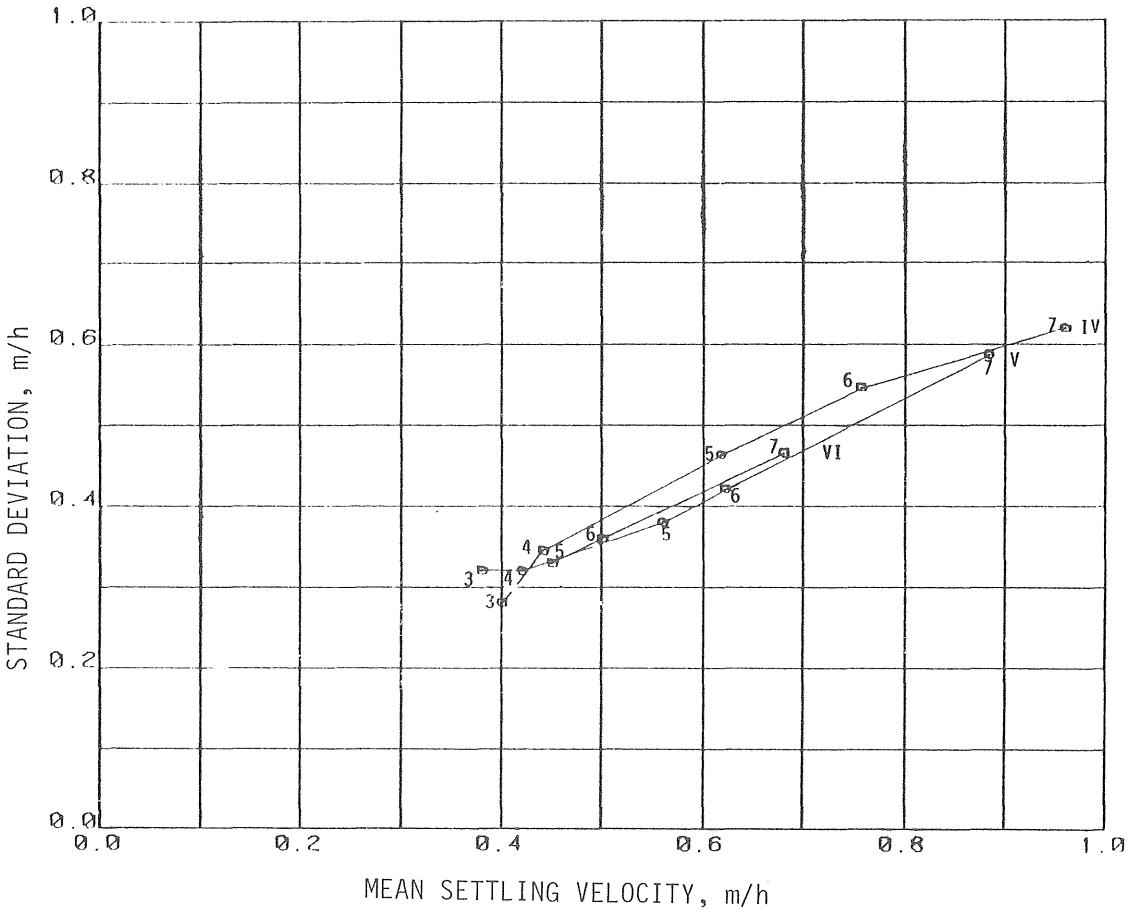

Fig 4-25. Results from settling tests in different flocculation tanks Åmål water treatment plant. Experiments IV, V and VI. 35 ppm aluminium sulphate. pH 6.1-6.2. No activated silica. Temperature 4.5^oC.

The two highest power input levels as represented by the Roman numerals I and II in figure 4-23 were repeated in the experiments VII and VIII, this time with activated silica dosage (3 ppm). In figure 4-26 the results are presented.

With activated silica the results obtained are reasonably close to those obtained on pilot plant scale, as summarized in table 4-9. The flocculation conditions, however, differ in some respects, which make a comparison difficult.

In table 4-9 the power input schemes x = 1 and 2, 2 ppm silica and 30 minutes flocculation time (40 ppm aluminium sulphate is understood) become closest to the present flocculation conditions in experiment VII and VIII respectively. In pilot plant scale the (v_m, σ)-values was found to be (1.55, 1.11) and (1.80, 1.44) which can be compared to the values in the 7th flocculation tank at Åmål: (1.35, 0.80) and (2.1, 1.2) respectively. The floc settling properties in the latter case are slightly better than those reported in table 4-9.

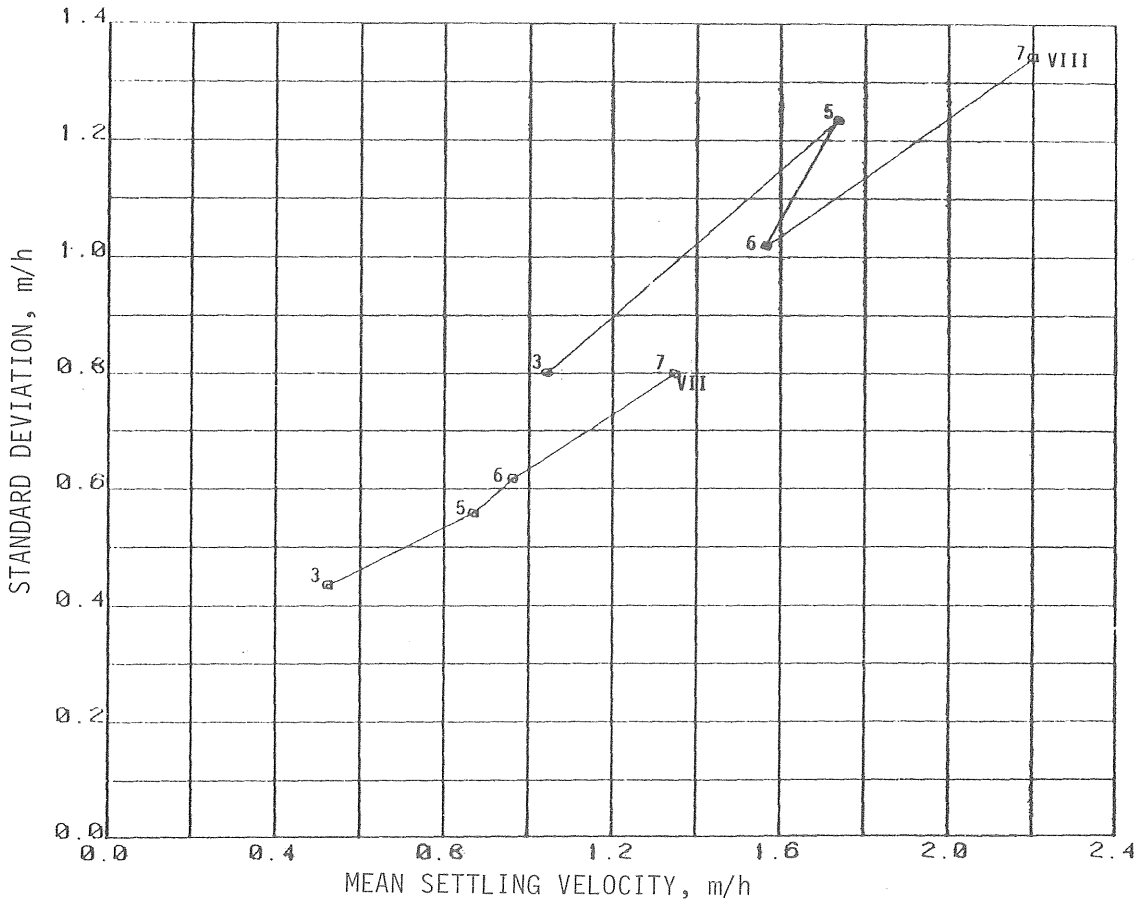

Fig 4-26. Results from settling test in different flocculation tanks. Åmål water treatment plant. Experiments VII and VIII. 35 ppm aluminium sulphate, pH 6.2-6.4. 3 ppm activated silica. Temperature 4,5°C.

4.3.2 Survey on power input and flocculation efficiency at Swedish water treatment plants.

Measurements of floc settling properties at 19 Swedish water works were carried out from March to June 1979. The sum of the yearly water production of the investigated water treatment plants is $105 \cdot 10^6$ m^3/year, ranging from 0.7 to $35 \cdot 10^6$ m^3/year of each plant. The scope of these investigation was to gain experience how the flocculation efficiency varied for different operating conditions and for different raw waters. In table 4-10 the results of these studies are summarized. The data should be considered as a survey of floc quality and operating conditions encountered in Swedish water works rather than experimental results. There are too many variables both measured and not measured, varying at the same time to allow any deeper interpretations evaluation of the results.

In table 4-10 measured floc settling properties are compiled. The measurements were carried out in the final flocculation tank. To simplify comparisons of the sedimentation properties the relative floc residual after sedimentation are calculated for two overflow rates, 0.5 and 1.0 m/h respectively. The calculations are made according to the simplified method described in Section 3.3.6 (see equation 3-86).

Together with the flocculation result some important factors affecting the flocculation process are tabulated.

G-values are calculated according to eqs. (3-97) and (3-91). Hereby, the water co-rotation usually is assumed to be 40% of the paddle speed. If there are stators in the flocculation tank this figure is schematicly reduced to 30%. C_D-values are set to 1.2 for cylindrical and 2.0 for flat paddle shapes. The G-values of Åmål water treatment plant, as an exception, are result from measurements of the power input. If these values are calculated with the schematic method described here the real values are in this case underestimated by about 10%. For more detailed information concerning the design of each flocculation unit it is refered to Hernebring (1980).

Table 4-10. Floc settling properties at 19 Swedish water treatment plants.

	Calculated G-values (s^{-1}) Flocculation tank No							Floc settling properties		Theoretical sedimentation result (% floc residual) at overflow rate		Aluminium sulphate dose, mg/l		pH-value		Activated silica mg/l	Flocculation time (min)	Temp °C
	1	2	3	4	5	6	7	V_m m/h	σ m/h	0.5 m/h	1.0 m/h	Applied	Required	Applied	Required			
Borås	23 20 18 17	14 13 15 11	10 7.5 3.4 9.0	2.8 4.5 4.1 3.0	3.1 2.3			1.0 1.0 1.0 1.1	0.65 0.65 0.65 0.70	13 13 13 11	22 22 22 19	36	40	6.4	6.4	-	60 60 72 77	1.9
Grängesberg	6.8 6.8	3.6 3.6	2.5 2.5	1.5 1.5	1.3 1.3			0.73 0.66	0.85 1.1	29 36	39 44	20	19	6.5	6.2	5	77 85	6.5
Göteborg (Lackarebäck)	15	12	7	4.2	2.7	1.0		1.7	1.5	17	21	38	28	6.2	6.5	2	70	4.0
Helsingborg (Ringsjön)	15	15	7.9	2.8				4.5	2.7	6	7	70	87	7.0	6.5	5	71	2.9
Härnösand	25 25	11 11	5.3 5.3	6.7 6.7	5.6 5.6	2.7 2.7		1.3 0.80	1.3 0.90	22 27	27 37	27	29	5.7	6.5	3	43 41	6.2
Karlshamn	4.1 4.1 4.1	2.2 2.2 2.2	0.90 0.90 0.90					1.3 1.2 1.0	0.90 1.1 0.90	12 19 20	19 26 29	40	30	6.5	6.3	-	79 79 79	2.1
Kramfors	1.9 ~0	1.8 5.7	1.4 4.4	4.0 4.4				1.6 2.4	1.6 2.1	20 15	25 18	31	37	5.7	5.9	6	75 82	14.8
Lidköping	28 28	18 18	12 12	4.8 4.8	4.8 4.8			2.0 2.0	1.2 1.4	7 11	11 14	42	27	6.3	6.3	8	84 82	4.2
Lilla Edet	5.0 5.0	3.2 3.2	2.5 2.5	2.1 2.1	1.5 1.5	1.4 1.4		1.5 1.5	1.6 1.6	22 22	27 27	45	45	5.5	6.5	6	57 57	1.3
Mariestad	13 10 59	9.9 7.9 35	5.8 4.5 14	2.7 2.7 7.7	1.3 1.3 2.7	 1.4		1.3 1.4 1.0	1.4 1.4 0.8	23 21 17	28 26 26	29	24	6.9	6.2	-	81 81 79	5.0
Mjölby	24	9.3	3.6					1.6	1.1	11	16	58	62	6.1	6.2	-	26	11.8
Mölndal	8.6 8.8	3.1 8.8	2.7 4.0	2.7 4.0	 4.0	 2.2		1.4 1.1	1.6 1.1	24 22	29 29	32	21	5.6	6.5	-	110 82	1.1
Mönsterås	15	9.9	4.1	2.2				1.3	0.7	7	13	108	145	5.8	6.5	-	157	5.6
Norrköping	10 5.8	4.6 5.3	4.6 5.3	5.3 3.1	5.3 3.1	1.2 1.3		10 3.9 7.5 6.7 3.4	5.9 2.8 3.6 4.5 2.7	5 10 2 7 12	5 11 3 9 14	56	53	6.5	6.3	-	74 71 68	9.1
Nässjö	35 35	30 30	20 20	8.3 8.3	3.1 3.1	1.8 1.8		2.0 2.0	1.4 1.4	11 11	14 14	38	40	6.1	6.3	-	45 45	2.0
Säffle	7.1 7.1	4.5 4.6	1.2 7.0	0.52 0.65				1.1 1.4	1.8 1.5	32 22	37 27	27	27	6.5	6.4	-	52 61	3.9
Västervik	33 ~0	17 17	13 13	4.8 4.8				2.0 2.5	1.2 1.4	7 5	11 8	27	35	6.3	6.6	5	52 52	4.7
Uddevalla	2.6 2.6	1.9 1.9	1.7 1.7	~0 ~0	0.65 0.65			2.6 3.3	2.9 2.9	21 14	23 17	40	51	6.0	6.7	-	86 86	1.8
Åmål	44	36	24	10	10	3.1	3.1	2.1	1.8	15	19	42	25	6.8	6.3	6	58	1.6

The applied aluminium sulphate dose is shown together with the required dosage, obtained from jar test results (see table 2-4).

Measured pH-values in the flocculation tanks are compared with the optimum pH-value at the required aluminium sulphate dose (table 2-4).

Also tabulated are activated silica dose, mean detention time as determined by tracer experiments in the flocculation unit, and the water temperature.

All these factors have an inpact on the settling properties of the flocs, which makes general conclusions difficult to draw.

As a criterion on a good floc settling quality the theoretical floc residual at a certain the sedimentation overflow rate, e.g. 0.5 m/h can be chosen. A reasonable limit is that at least 85% of the flocs then should be removed. Inserting this value in eq 3-77 and with $K_r = 0.965 \approx 1.0$ (table 3-2) gives:

$$\sigma \leq 1.0 \cdot (v_m - 0.25) \qquad (4\text{-}19)$$

This is not fulfilled at appr half of the treatment plants. This is believed to be caused by a pH-value too far from the optimum at least in four cases. A deviation on the acid side is more detrimental than too high pH-values. The applied G-values are generally low. It is probable that higher G-values in the beginning of the flocculation process in many cases could have improved the floc settling properties. On the other hand the detention time in the flocculation unit in most cases are rather long, which may reduce the importance of a careful choice of power input pattern. Besides the questionable low G-values on plants as Grängesberg, Kramfors, Säffle and Uddevalla the poor settling properties of the flocs may be attributed to a too low coagulant dose. Additional information concerning general aspects of water treatment plant operation is given in Chapter 6.

The extremely good floc settling at the Norrköping treatment plant can not be explained by any of the background variables shown in the table. Neither did the jar test show any strikingly good settling properties on laboratory scale (see figure 2-31).

The only evident aspect in which the operating conditions differed from other places was that the coagulant was mixed into the water in the bottom of the first flocculation tank. The volume of the first flocculation tank was used for oxidation of manganese by means of the addition of potassium permanganate. This would imply poor mixing conditions for the coagulant, thus a floc of poor quality should be excepted. Whether these mixing conditions really are responsible for the measured floc properties should be further investigated. It is also possible that precipitates from the manganese oxidation could improve the floc quality. However, the dose of potassium permanganate was rather low (0.5 mgKM_nO_4/l). The absolute values of v_m and σ in this case are uncertain. The general sampling procedure was deviced to give maximum accuracy for floc suspensions with the mean settling velocity of about 1-2 m/h. The settling test were carried out in three different flocculation systems; in two of them twice. Though great differences in absolute values occur, the extremely good settling is consistent in spite of the fact that no activated silica is added.

5 INTERPRETATION OF SOME EFFECTS THROUGH MATHEMATICAL MODELS FOUNDED ON FLOCCULATION THEORY

5.1 Introduction

In Chapter 4 flocculation results have been treated in a descriptive manner. In the following chapter attempts are made to incorporate the findings into mathematical models. At first, accordance to prevalent flocculation models, based on the residual turbidity concept, is tested. Then more complicated models, which take particle size distribution into account, are used as a means to get closer to an explanation of different floc settling characteristics.

The notation used in the flocculation theories reviewed in Section 3.1 are here changed successively. This is done deliberately, not to confuse the reader, but in order to stress the point that the practical application of the theories demands a number of simplified assumptions to be made. Consequently the theories themselves are not really tested, rather their "translation" in terms of measurable variables.

5.2 Flocculation performance model

The flocculation performance model is concerned with the removal of primary particles from the suspension by their incorporation into flocs. In practice the primary particle content of the fluid is measured by the residual turbidity after a long sedimentation period. Theories for the rate of change in number of primary particles is reviewed in Section 3.1.6. The model as it is presented in, for example, eq. 3-51 can be expressed

$$N_i = \frac{N_{i-1} + F \cdot G^m \cdot T \cdot C2}{1 + F \cdot G \cdot T \cdot C1} \qquad (5\text{-}1)$$

where N_{i-1} is the number concentration of primary particles (measured as residual turbidity) entering the reactor

N_i is the residual turbidity leaving reactor i

F is the floc volume fraction, here measured as the floc turbidity

G (s^{-1}) is the mean velocity gradient

T (s) is the residence time in the reactor

m is a floc breakup exponent

C1 and C2 are constants

Eg. 5-1 implies that the flow conditions in the flocculation tank can be described as those of a completely mixed reactor. These conditions are assumed henceforth. Then the time T becomes equal to the mean residence time in the flocculation tank, i.e. the tank volume divided by the flow.

The constants C1 and C2 will include conversion factors from the originally units used in eq. 3-51 (number of primary particles, floc volume fraction) to the applied measures (relative residual turbidity, floc turbidity). Naturally, the validity of the model depends on whether these conversions are considered correct or not.

The experiments presented in Section 4.1 will be used to test the model. They were carried out with a constant coagulant dose. The floc turbidity is considered to be a constant, F = 4.0 FTU. Consequently F could also be included in the constans C1 and C2. However, this is not done. Nor is the influence of varying F tested.

The data in the tables 4-1, 4-3, 4-4 and 4-5 can be used to determine the flocculation performance at the temperature 2^{o}C for three total flocculation times (10, 20 and 30 minutes), in three concecutive flocculation tanks (no. 2, 3 and 4) for a maximum of six power input levels, and finally with or without the addition of activated silica.

Additional information concerning the influence of a higher temperature is given by table 4-2.

In Section 4.2.3 it was concluded that the three different paddle designs tested caused no great difference in settling characteristics. The results from these tests therefore will be treated here as repeated experiments. The most important independent variable, the power input pattern, is varied in the same way. It is not likely that keeping the three paddle designs separate would result in different calculated values of the constants C1, C2 (and m).

Once the settling characteristics in terms of v_m and σ are known, the theoretical residual turbidity after infinitie sedimentation can be calculated (see Section 3.3.4. eq.3-69):

$$N_i = \Phi \left(- \frac{v_m^i}{\sigma_i}\right) \qquad (5\text{-}2)$$

where Φ is the cumulative settling velocity distribution function, normally distributed with the mean value v_m and the standard deviation σ. The letter "i" denotes the number of the reactor.

The results obtained at 20 min flocculation time comprise six different power input levels. Experiments at 10 and 30 minutes were only carried out at three different power input levels.

The theoretical residual turbidity corresponding to each (v_m, σ)-value was calculated according to eq. 5-2. The values are theoretical in the sense that they are achieved by extrapolation to zero settling velocity from observed values by means of the normal distribution. Values missing in table 4-5 at 10 minutes total flocculation time were replaced by results from separate experiments. 11 additional results were achieved in this way. The total number of residual turbidities used was 143 when the low temperature was considered. In addition experiments at 20°C provided another 36 values.

An important observation of great significance was made after calculations of the theoretical residual turbidities. In spite of the fact that usually substantial improvements in settling properties occured when activated silica was added, the residual turbidity remained essentially the same whether activated silica was added or not (for identical power input conditions). Figure 5-1 illustrates this fact.

Each point represents a pair of experiments with the same power input pattern. The ordinate is the residual turbidity with the activated silica dose 2 mg/l, the abscissa is the corresponding result without activated silica dose. Here, values obtained at $2^{o}C$ as well as results at $20^{o}C$ are included. The values observed for paddle type C in tank 2 are omitted in the figure. The residual turbidities for various conditions can be found in table 5-1.

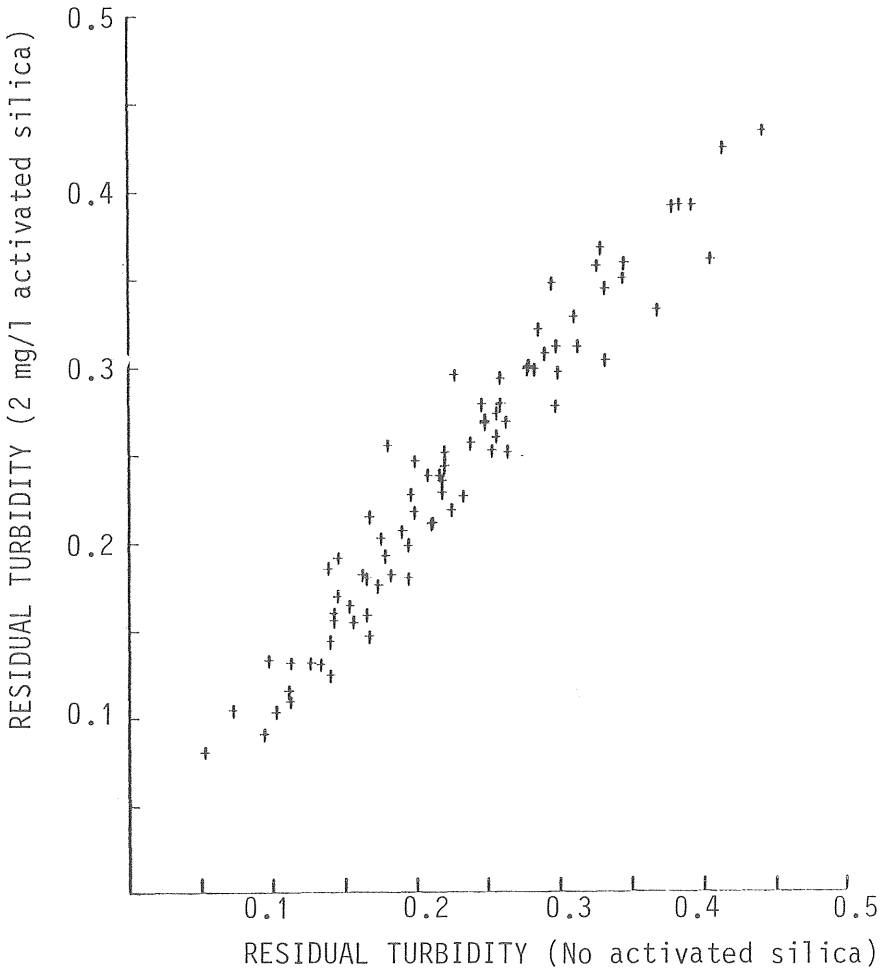

Fig 5-1. Comparison between achieved residual turbidities with and without activated silica.

The number of values in fig 5-1 are 81 and the correlation coefficient 0.97. It can be concluded that activated silica is not effective as a flocculation aid if the flocculation efficiency is measured as the residual turbidity. At the same time a limitation of the residual turbidity parameter is illustrated. In spite of the fact that different floc suspensions have been shown to give the same residual turbidity, we know they represent a great variety of settling characteristics. Consequently the residual turbidity does not provide enough information to evaluate the result of a sedimentation process.

As far as the mathematical model in eq. 5-1 is concerned, these facts are advantageous: the number of duplicate experiments thus are increased and fewer independent variables have to be taken into consideration.

A computer program was designed to determine appropriate values of the constants C1 and C2 and the floc breakup exponent m. Results from experiments carried out at one total flocculation time were treated at each run. An iterative procedure was performed in the following way:

A typical set of data consisted of the residual turbidities after flocculation tanks no. 2, 3 and 4 at a maximum of six power input levels with varying G-value. The value after the first tank was not known. Because eq. 5-1 demands both the input and output residual turbidity to calculate one of the constants (the other being fixed), the output residual turbidity from tank no. 1 had to be given an initial value. The input to the first flocculation tank was set to the relative residual turbidity 1.0.

If the floc breakup is omitted (i.e. C2=0) the constant C1 can be calculated for each flocculation tank. The median of the C1-values thus obtained was chosen as a start value to be fixed in the calculation of C2 for each tank. The median of the latter was then used to correct the initial C1 and assumed residual turbidity from the first tank. The procedure was continued until the corrections were lower than a prescribed value. The interation then was repeated for varying values of the breakup exponent.

Median values were used in the iterations instead of mean values to minimize the influence of gross errors of some calculated constants, and thus increase the tendency towards convergence.

If the data were in perfect accordance with the model the computational process would end up with identical values of the constants. As could be expected this was not the case for any set of data. The constants achieved were thought, however, to represent the best possible fit to the data with a prescribed floc breakup exponent m. If the values of the constants did not coverge towards a certain value or the convergence was very slow, it was taken as a sign of an improper floc breakup exponent.

The floc breakup exponent m was varied stepwise from 1.0 and upwards with the increment 0.05. It was found that the best convergence was achieved for m-values around 1.35.

This is in accordance with results reported by Hedberg and Hernebring (1975), reviewed by Hedberg (1976), where the m-value 4/3 was obtained. The data on which the model was tested, in that case, consisted of the residual turbidity, measured as the turbidity after a shallow-depth sedimentation unit operated at a low overflow rate (around 0.3 m/h). Thus only results after completed flocculation in four flocculation tanks were considered. The G-values applied (calculated according to Camp) varied from 5 to 450 s-1, the flocculation time from 6 to 45 minutes. Results obtained from unequal compartmentalization were shown to be conform with the model. The maximum ratio between detention times in different flocculation tanks was 6.5.

In Section 3.1.4 is mentioned that Argaman and Kaufman (1970) derived an expression with the breakup exponent 2. Experiments confirmed this. Parker *et.al.* (1972) stated the values 2 and 4, depending on the floc size compared to the turbulent microscale.

The experimental results presented by Ødegaard (1975) showed good agreement with a breakup exponent m = 2.

The present data achieved at $2^{o}C$ was found to conform reasonably, though not perfectly, with the model if C1 and C2 were given the values $5.5 \cdot 10^{-5}$ and $2.2 \cdot 10^{-6}$ respectively. In figure 5-2 a visual impression is given of the ability of the model to approximate the measured residual turbidities. The measured and calculated values are indicated as ordinate and abscissa, respectively. The number of values is 143, and the correlation coefficient 0.87. In table 5-1 can be seen where the model fails to give relatively good approximations. On the whole, in the second and third flocculation tanks at low power inputs (i.e. rather high residual turbidity is to be expected) a too high value is calculated. In table 5-2 the applied G-values in each flocculation tank for the various tapered flocculation patterns are given.

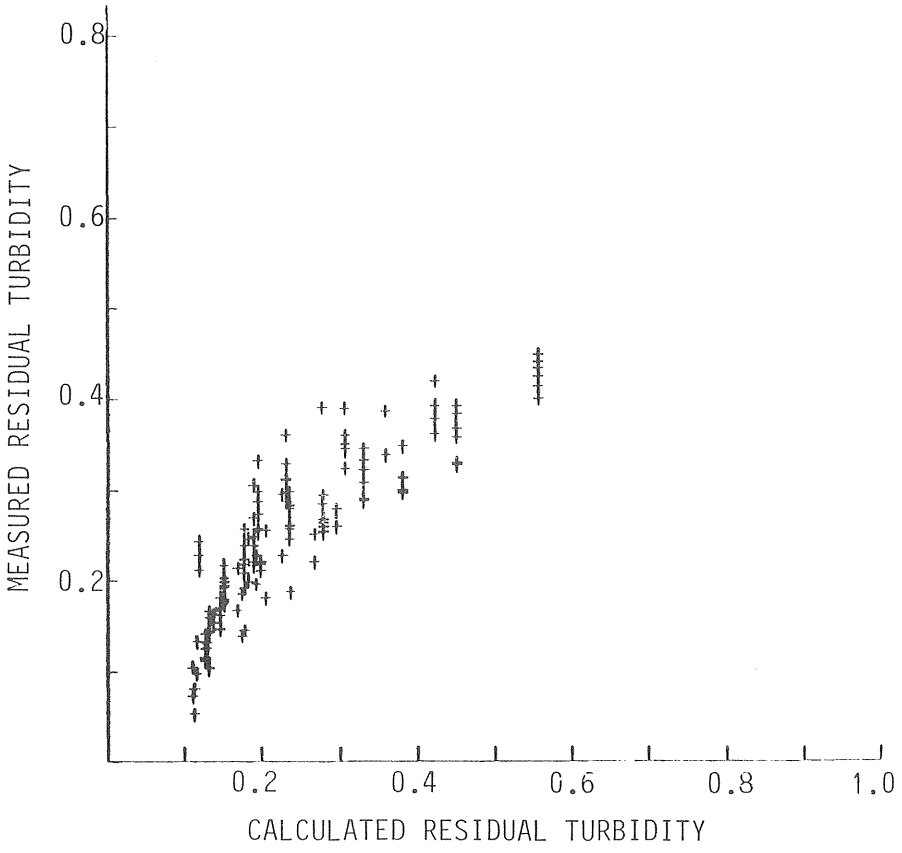

Fig 5-2. Achieved residual turbidities compared to calculated values according to eq. 5-1 with m = 1.35, C1 = $5.5 \cdot 10^{-5}$ and C2 = $2.2 \cdot 10^{-6}$. See data in table 5-1. Temp $2^{o}C$.

Table 5-1. Achieved residual turbidities for different conditions at $2^{o}C$, from data in the tables 4-1, 4-3, 4-4 and 4-5. Values indicated with x are from solitary experiments. The values are compared to the calculated results according eq. 5-1 with m = 1.35, C1 = 5.5.10-5 and C2 = 2.2.10-6. T is the total flocculation time (after four flocculation tanks).

		Stirrer type						
Tank no.	Power input	No act. silica A4	B	C	2 mg/l act. silica A4	B	C	Calculated result
T = 20 minutes								
2	1	0.25	0.22	0.31	0.27	0.24	0.22	0.189
2	2	0.28	0.26	0.33	0.30	0.27	0.25	0.195
2	3	0.31	0.30	0.36	0.33	0.31	0.29	0.231
2	4	0.35	0.34	0.39	0.36	0.35	0.32	0.306
2	5	0.38	0.39	0.42	0.39	0.39	0.36	0.422
2	6	0.41	0.44	0.45	0.42	0.43	0.40	0.556
3	1	0.15	0.16	0.17	0.17	0.18	0.15	0.146
3	2	0.18	0.20	0.19	0.20	0.22	0.18	0.151
3	3	0.21	0.24	0.22	0.24	0.26	0.22	0.177
3	4	0.25	0.28	0.26	0.28	0.30	0.26	0.235
3	5	0.29	0.33	0.29	0.32	0.34	0.31	0.330
3	6	0.33	0.38	0.33	0.37	0.39	0.36	0.450
4	1	0.11	0.11	0.14	0.13	0.12	0.12	0.127
4	2	0.14	0.14	0.17	0.16	0.14	0.16	0.132
4	3	0.18	0.17	0.19	0.19	0.18	0.20	0.152
4	4	0.22	0.21	0.22	0.23	0.21	0.24	0.199
4	5	0.26	0.25	0.26	0.27	0.25	0.29	0.278
4	6	0.31	0.30	0.31	0.31	0.30	0.35	0.380

Tank no.	Power input	Stirrer type: No act. silica A4	B	C	2 mg/l act. silica A4	B	C	Calculated result
T = 10 minutes								
2	1	-			-			0.237
2	2	-			0.28x			0.277
2	3	0.39x			0.34x			0.358
3	1	0.20			0.23x			0.193
3	2	0.23			0.29x			0.226
3	3	0.26			0.28x			0.295
4	1	0.15			0.19x			0.178
4	2	0.18			0.26x			0.205
4	3	0.22			0.25x			0.267
T = 30 minutes								
2	1	0.14			0.19			0.175
2	2	0.17			0.21			0.169
2	3	0.20			0.25			0.183
3	1	0.10			0.10			0.132
3	2	0.13			0.13			0.129
3	3	0.15			0.16			0.137
4	1	0.05			0.08			0.112
4	2	0.07			0.10			0.110
4	3	0.10			0.13			0.116

Table 5-2. Applied G-values (s-1) calculated for 2°C in each flocculation tank at various tapered flocculation patterns "I", see eqs 4-1 and 3-32.

Power Input (I)	G-value (s-1) in flocculation tank no. 1	2	3	4
1	135	46	15	5.2
2	74	29	12	4.7
3	40	19	9.1	4.4
4	22	12	7.0	4.0
5	12	8.0	5.4	3.7
6	6.5	5.2	4.2	3.4

Determination of the constants carried out in the same way as related above, applied on data in table 4-2, (experiments at 20°C) gave C1 = $7.0 \cdot 10^{-5}$ and C2 = $2.8 \cdot 10^{-6}$. In figure 5-3 calculated and measured residual turbidities are indicated. Data is only available from 20 minutes total flocculation time. The number of values is 36 and the correlation coefficient is 0.85. In table 5-3 the values on which figure 5-3 is based are shown. In table 5-4 the G-values valid at 20°C are given. These values differ from those given in table 5-2 by a factor 1.28, according to the difference in viscosity. It can be observed that the ratios between the constants C1 and C2, respectively at the two temperatures are close to the same value. The significance of the latter observation is not quite clear.

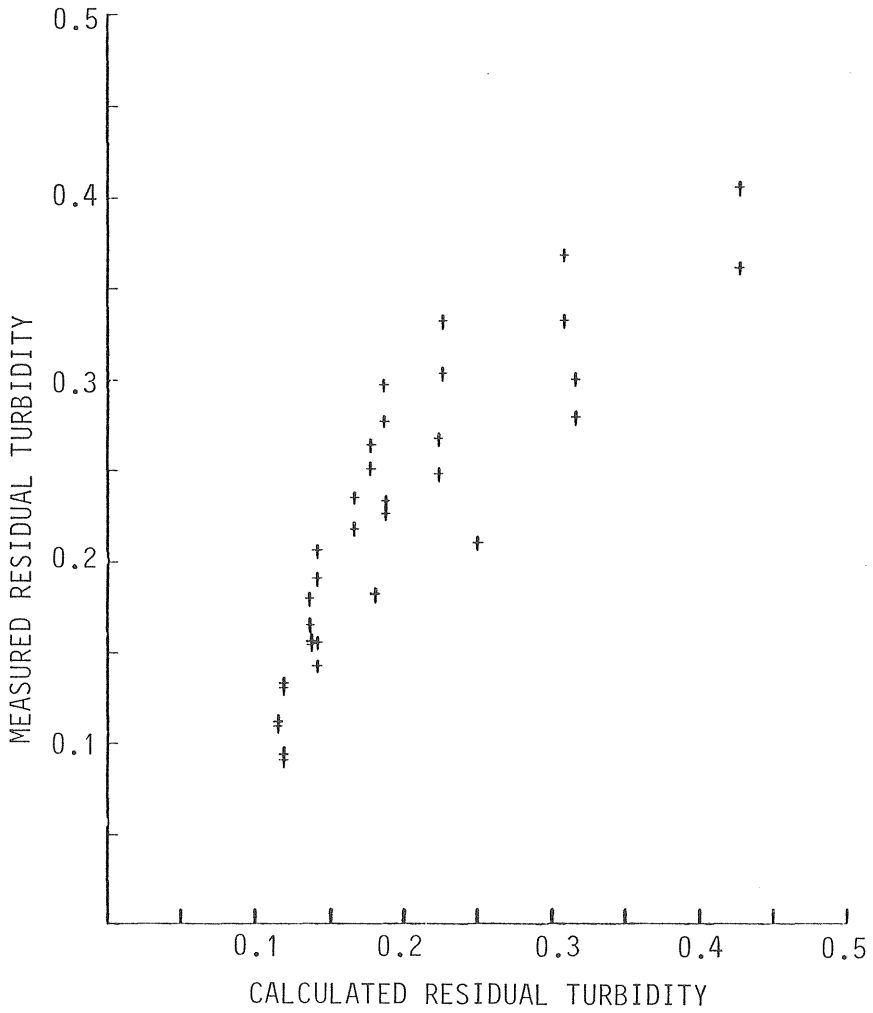

Fig. 5-3. Achieved residual turbidities compared to calculated values according to eq. 5-1 with m = 1.35, C1 = $7.0 \cdot 10^{-5}$ and C2 = $2.8 \cdot 10^{-6}$. See data in table 5-3. Temp 20^{0}C.

Table 5-3. Achieved residual turbidities for different conditions at 20°C, from data in the table 4-2. The values are compared to the calculated results according to eq. 5-1 with m = 1.35, C1 = $7.0 \cdot 10^{-5}$ and C2 = $2.8 \cdot 10^{-6}$. T is the total flocculation time (after four flocculation tanks). Paddle type A4.

Tank no.	Power input	No act. silica	2 mg/l act. silica	Calculated result
T = 20 minutes				
2	1	0.23	0.23	0.187
2	2	0.26	0.25	0.177
2	3	0.30	0.28	0.186
2	4	0.33	0.30	0.206
2	5	0.37	0.33	0.308
2	6	0.41	0.36	0.406
3	1	0.14	0.16	0.141
3	2	0.17	0.18	0.136
3	3	0.19	0.21	0.141
3	4	0.22	0.24	0.166
3	5	0.25	0.27	0.226
3	6	0.28	0.30	0.316
4	1	0.09	0.09	0.119
4	2	0.11	0.11	0.115
4	3	0.13	0.13	0.119
4	4	0.16	0.15	0.137
4	5	0.18	0.18	0.180
4	6	0.21	0.21	0.250

Table 5-4. Applied G-values (s-1) calculated for 20°C in each flocculation tank at various tapered flocculation patterns "I", see eqs 4-1 and 3-32.

Power Input (I)	G-value (s-1) in flocculation tank no. 1	2	3	4
1	173	58	20	6.6
2	94	38	15	6.1
3	52	25	12	5.6
4	28	16	9.0	5.1
5	15	10	7.0	4.7
6	8.4	6.7	5.4	4.3

The experiments with unequal compartmentalization carried out at 2°C, referred to in Section 4.2.5, provide data for an additional test of the model according to eq. 5-1. Settling tests in this case were only carried out in the fourth flocculation tank. The experiments were performed at three different flocculation times (10, 20 and 30 minutes) with and without the addition of activated silica. As three tapered power input patterns were used, 18 residual turbidity values can be compared. In figure 5-4 predicted and measured values are indicated. The correlation coefficient is high (0.89) but the slope of the regression line is appreciably less than 1, indicating that the tendencies of the data are predicted fairly correctly, but the absolute values do not conform appropriately. In table 5-5 can be seen, in more detail, that too high residual turbidities are calculated compared to measured results. Table 5-6 shows the applied G-values, calculated according to eq. 4-1 (and eq. 3-32). In the present case the mean residence time in each succeeding flocculation tank was 6%, 12%, 27% and 55%, respectively.

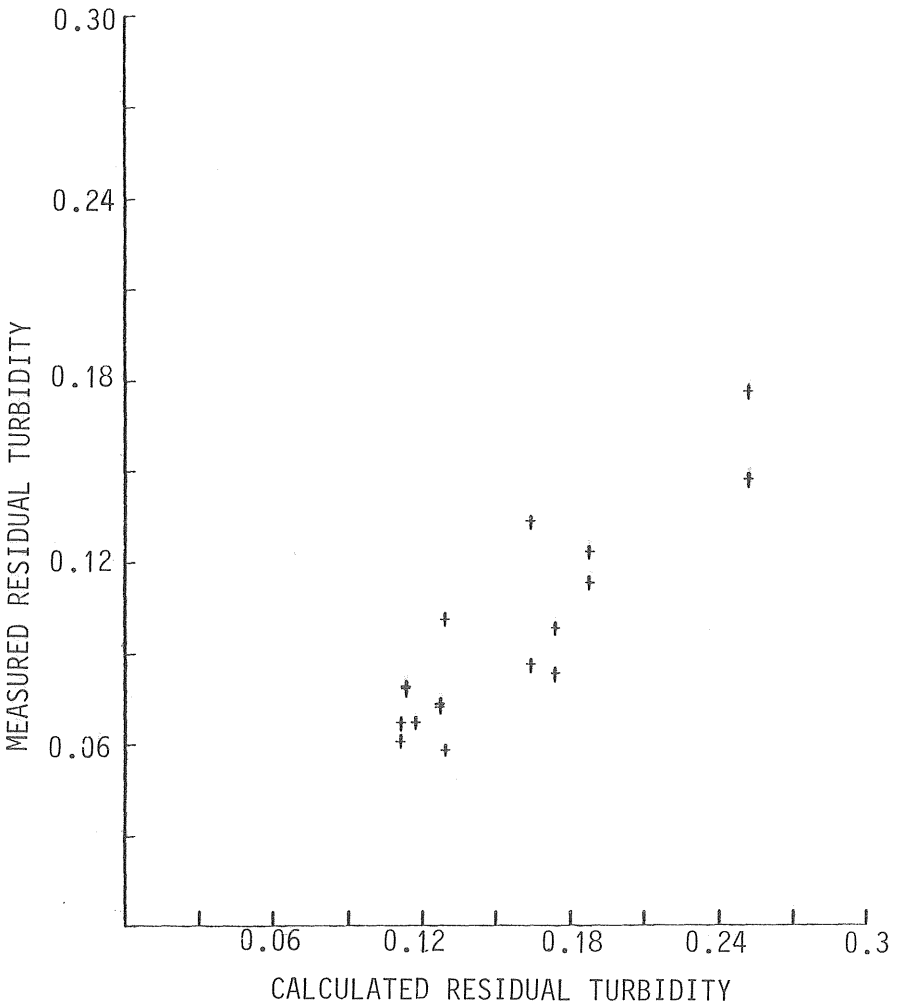

Fig. 5-4. Achieved residual turbidities compared to calculated values according to eq. 5-1 with m = 1.35, $C1 = 5.5 \cdot 10^{-5}$ and $C2 = 2.2 \cdot 10^{-6}$. See data in table 5-5. Temp $2^{o}C$. Unequal compartmentalization. See Section 4.2.5.

Table 5-5. Achieved residual turbidities for unequal compartmentalization at $2^{o}C$, from data in the tables 4-8 and 4-9. The values are compared to the calculated results according eq. 5-1 with m = 1.35, C1 = $5.5 \cdot 10^{-5}$ and C2= $2.2 \cdot 10^{-6}$. T is the total flocculation time (after four flocculation tanks). Paddle types A1, A2, A3 and A4.

Tank no.	Power input	No act. silica	2 mg/l act. silica	Calculated result
T = 10 minutes				
4	1	0.13	0.09	0.164
4	2	0.12	0.11	0.188
4	3	0.15	0.18	0.252
T = 20 minutes				
4	1	0.06	0.09	0.129
4	2	0.07	0.07	0.127
4	3	0.08	0.10	0.174
T = 30 minutes				
4	1	0.07	0.07	0.117
4	2	0.06	0.07	0.111
4	3	0.08	0.08	0.113

Table 5-6. Applied G-values (s-1) calculated for $2^{o}C$ in each flocculation tank at various tapered flocculation patterns "I", see eqs 4-1 and 3-32. Unequal compartmentalization.

Power Input (I)	G-value (s-1) in flocculation tank no. 1	2	3	4
1	203	137	58	9.8
2	104	74	36	8.1
3	53	41	23	6.7

The reason why the mathematical model does not reasonably well conform to the results obtained with the unequal compartmentalization design is difficult to determine.

Inadequacy of the model or insufficient experimental data are, of course possible explanations.

The iterative procedure to compute the values of the constants may have failed in determining the best fit. The calculations were based on the input and output of each tank, which may have caused that small absolute experimental errors was given great relative importance.

It could be argued that the flow conditions in the flocculation tanks were not in accordance with a completely-mixed-flow-reactor, which eq. 5-1 presupposes. However, with the conventional design tracer experiments showed close agreement to such conditions. The cubic form of the tanks is favourable in that respect.

The first three compartments in the unequal design, on the other hand have the height-to-width ratios of 3,3 and 2 respectively, which may have caused some plug flow tendencies. This can be taken into account in the calculation of expected residual turbidities by considering each of these tanks as a number of imaginary tanks in a series. As no tracer experiment was carried out at the first tanks of this design there was no basis to judge a reasonable number. However, if tank 1, 2 and 3 in the calculation was divided into two parts, the calculated residual turbidity in the output from the fourth tank did not change much compared to the values in table 5-5. Some improvement could be seen for the highest power input at 10 minutes flocculation time, which gradually disappeared as the flocculation time was increased. These effects consequently cannot increase the ability of the model to accurately predict the experimental result to any greater extent.

5.3 Particle size distribution model

In Section 5.2 it was shown that the flocculation performance model did not yield enough information to estimate the result after a sedimentation process.

In this section, a theory based on the flocculation rate theories earlier reviewed, which take the particle size distribution into account, will be developed and tested on available experimental data.

Assuming that the flocs are built up by primary particles with the radius r_1, it was shown in Section 3.1.2 that the rate of change of the number n_k of k-particles, consisting of k primary particles, could be written(see eq. 3-18):

$$\frac{dn_k}{dt} = \frac{4}{3} \cdot r_1^3 \cdot G \cdot \left(\frac{1}{2} \sum_{\substack{i=1 \\ j=k-i}}^{l=k-1} n_i \cdot n_j \cdot (i^{1/3} + j^{1/3})^3 - \right. \qquad (5\text{-}3)$$

$$\left. - n_k \cdot \sum_{i=1}^{\infty} n_i \cdot (i^{1/3} + k^{1/3})^3 \right)$$

where n_i, n_j and n_k are the number concentrations of particles within the fractions consisting of i, j or k primary particles, respectively.

This equation neglects floc breakup and presupposes coalescence of the growing flocs (see eq. 3-15).

In order to convert the number of particles into a turbidity measure the following considerations are made.

The total floc volume, regarded as constant throughout the flocculation process, can be written as:

$$\Phi = \sum_{i=1}^{\infty} n_i \cdot \frac{4}{3} \cdot \pi \cdot r_i^3 = \sum_{i=1}^{\infty} n_i \cdot \frac{4}{3} \cdot \pi \cdot i \cdot r_1^3 = r_1^3 \cdot \frac{4}{3} \cdot \pi \cdot \sum_{i=1}^{\infty} n_i \cdot i \qquad (5\text{-}4)$$

The relative floc volume within each size-fraction k, then becomes:

$$\frac{\Phi_k}{\Phi} = \frac{r_1^3 \cdot \frac{4}{3} \cdot \pi \cdot n_k \cdot k}{\Phi} \qquad (5\text{-}5)$$

If turbidity measurements from which information is available concerning the contribution to the turbidity of the particle size fraction k, the relative turbidity for that fraction (f_k) is assumed to express this ratio. Thus:

$$f_k = \frac{\Phi_k}{\Phi} = \frac{r_1^3 \cdot \frac{4}{3} \cdot \pi \cdot n_k \cdot k}{\Phi} \qquad (5\text{-}6)$$

Eq. (5-6) implies:

$$n_k = \frac{\Phi \cdot f_k}{r_1^3 \cdot \frac{4}{3} \cdot \pi \cdot k} \qquad (5\text{-}7)$$

and eq. 5-3 can be rewritten, now in terms of relative turbidities for each size fraction (f_k) instead of numerical concentrations (n_k). Eq. (5-7) inserted in eq. (5-3) yields:

$$\frac{df_k}{dt} = \frac{\Phi \cdot G}{\pi} \cdot k \cdot \left(\frac{1}{2} \cdot \sum_{\substack{i=1 \\ j=k-i}}^{i=k-1} \frac{f_i \cdot f_j}{i \cdot j} \cdot (i^{1/3} + j^{1/3})^3 - \right. \qquad (5\text{-}8)$$

$$\left. - \frac{f_k}{k} \sum_{i=1}^{\infty} \frac{f_i}{i} (i^{1/3} + k^{1/3})^3 \right)$$

For simplicity, this equation will henceforth be written in the form:

$$\frac{df_k}{dt} = \frac{\Phi \cdot G}{\pi} \cdot k \cdot (S1(k) - S2(k)) \qquad (5\text{-}9)$$

where S1(k) denotes the formation of k-particles from sizes less than k, and S2(k) the disappearance of k-particles due to the formation of sizes greater than k.

Because the particle growth process expressed that way comprises transfer of mass from one fraction to another, a summation of eq. 5-9 carried out over all fractions must equal zero, and:

$$\sum_{k=1}^{\infty} k \cdot (S1(k) - S2(k)) = 0 \qquad (5\text{-}10)$$

Besides, it is evident from the definition of f_k in eq. 5-6 that:

$$\sum_{k=1}^{\infty} f_k = 1 \qquad (5\text{-}11)$$

In a completely mixed reactor with the mean residence time T, the change of f_k from the inlet, $f_k(in)$, to the outlet, $f_k(out)$, due to particle aggregation can be expressed as:

$$f_k\,(out) = f_k(in) + \frac{\Phi \cdot G \cdot T}{\pi} \cdot k \cdot (S1(k) - S2(k)) \qquad (5\text{-}12)$$

The sizes of the fractions considered in the summation terms S1 and S2 are representative for the conditions prevailing within the reactor and are consequently the same as those present in the outlet, $f_k(out)$, according to the function of a completely mixed reactor.

It should be remembered that all data are based on turbidity measurements obtained at settling tests, and when e.g. "particle size" and "size distributions" are mentioned in the following, is meant indirect inferences made from measured settling velocity distributions. Because of the way the measurements are carried out, the settling velocity distributions are distributions according to particle mass. The parameter of the floc volume fraction used, the turbidity, is also indirect. Strictly, it is an approximative measure of total particle mass and if e.g. floc density varies with floc size, a constant relationship between floc volume fraction and floc turbidity becomes questionable.

The introduction of the floc breakup into the equations governing the particle size distribution has to be accompanied by a number of assumptions concerning the breakup mechanisms. The present writer will adopt the general view of Spielman (1978), referred to in Section 3.1.6, that a continuous breakup function is more probable than the mechanism of unlimited particle growth until a maximum floc size is reached followed by a sudden disruption.

The simple hypothesis applied here, concerning the tendency of breakup for a size fraction k, can be expressed as:

$$\left(-\frac{dn_k}{dt}\right)_{breakup} = Const \cdot G^m \cdot f(d_k) \cdot n_k = Const \cdot G^m \cdot d_k^n \cdot n_k \qquad (5\text{-}13)$$

This relationship has some support in expressions derived by Tambo and Hozumi (1979): The binding force within a floc with a diameter d was found to increase proportionally to d raised to an exponent of less than 2.0, while the total breakup force increased proportionally to $d^{8/3}$ or d^4, depending on particle size compared to the turbulent microscale.

The other critical point is how the floc fragments from size k caused by the breakup are distributed among the fractions less than k. Here, schematically, three modes are considered:

1 Equal number

A volume of broken k-flocs is distributed into particles sized in such a way that all sizes less than k will increase equally in number of particles.

2 Equal volume

An equal increase in volume of each particle fraction less than k is assumed.

3 Primary particle strip

The breakup mode comprises primary particle strip, i.e. floc fragments will be transferred to the fraction of the smallest particle size (and to the size immediately below the size of the disrupted floc size).

The assumed breakup patterns can be summarized as follows:

$$\left(\frac{df_k}{dt}\right)_{breakup} = - K_2 \cdot G^m \cdot (S3(k) - S4(k)) \qquad (5\text{-}14)$$

where S3(k) denotes the disappearance of disrupted flocs of size k to floc sizes less than k. S4(k) expresses the increase in k-particles due to the breakup of flocs greater than the size k.

The value of S3(k) can, according to eq. 5-13 and 5-7, be calculated as:

$$S3(k) = (\sqrt[3]{k})^n \cdot f_k \qquad , k > 1 \qquad (5\text{-}15)$$

$$S3(1) = 0 \qquad (5\text{-}16)$$

Depending on the breakup mode, S4(k) can be expressed as

1 Equal number

$$S4(k) = k \cdot \sum_{i=k+1}^{\infty} \left((\sqrt[3]{i})^n \cdot f_i \cdot \frac{1}{\sum_{j=1}^{i-1} j} \right) \qquad (5\text{-}17)$$

2 Equal volume

$$S4(k) = \sum_{i=k+1}^{\infty} \left((\sqrt[3]{i})^n \cdot \frac{f_i}{(i-1)} \right) \qquad (5\text{-}18)$$

3 Primary particle strip

$$S4(1) = (\sqrt[3]{2})^n \cdot f_2 + \sum_{i=3}^{\infty} (\sqrt[3]{i})^n \cdot \frac{f_i}{i} \qquad (5\text{-}19)$$

$$k > 1: \quad S4(k) = \frac{k}{k+1} (\sqrt[3]{k+1})^n \cdot f_{k+1} \qquad (5\text{-}20)$$

Also the breakup process implies a transfer of mass from one size fraction to another. Consequently a summation of eq. 5-14, irrespective of breakup mode, yields a net change of f equal to zero, or:

$$\sum_{k=1}^{\infty} S3(k) = \sum_{k=1}^{\infty} S4(k) \qquad (5\text{-}21)$$

Now a complete model for the rate of change of the content in a fraction k can be outlined:

$$\frac{df_k}{dt} = \frac{\Phi \cdot G}{\pi} \cdot k \cdot (S1(k) - S2(k)) - K_2 \cdot G^m \cdot (S3(k) - S4(k)) \qquad (5\text{-}22)$$

Hitherto the number of fractions has been considered infinite. The equations presented therefore cannot be used in any computational procedure if not the number of fractions are reduced in some way. If flocs of 1 mm^3 in order of magnitude are considered as the end product, consisting of primary particles with the diameter 1 μm, still the number of fractions is innumerable: 10^9. As each fraction according to the theory depends on each other fraction the number of calculations to be carried out to compute one of the summation terms is proportional to N^N or N! ($N!=1\cdot2\cdot3\cdot\ldots\cdot N$)if N is the number of fractions. Thus a computer with rather high capacity is needed for these calculations, even if the number of fractions is limited to e.g. 100.

Below is presented one way to simplify the calculations. The method implies that an arbitrary number of fractions can be chosen. The result is not depending on the size of the intervals dividing the particle sizes to any greater extent. Thus essentially the same result will be obtained if very few fractions are considered (e.g. 10) or if the size range is divided into many parts (e.g. 100).

Bacause the settling velocity distributions determined are continuous functions of the settling velocity, an arbitrary settling velocity VMIN can be chosen to be representative of "primary particles".

According to Stokes Law the settling velocity is proportional to the square of the particle diameter. Thus:

$$d_1 \propto \sqrt{VMIN} \tag{5-23}$$

If particles consisting of i dl-particles are considered, the relation between their settling velocity and the settling velocity of the primary particle is:

$$\frac{V_i}{VMIN} = i^{2/3} \tag{5-24}$$

It is assumed that the size relationship can be expressed as:

$$d_i = \sqrt[3]{i} \cdot d_1 \tag{5-25}$$

In that way settling velocities defining limits between each fraction can be determined. It has been chosen to do that in the simplest possible way (eq. 5-24), but it is also possible to incorporate effects of e.g. varying density according to size or differences in viscosity (which affect the settling velocity).

Once the first particle size chosen to represent "elementary particles" is determined, as a consequence the upper limit of the next settling velocity interval sizes, in terms of settling velocities, can be calculated.

The fundamental equation describing the growth kinetics (eq. 5-8) is apparently not affected by the magnitude of size intervals chosen.

However, a few modifications of the equations describing the breakup have to be made so that the breakup rate becomes independent of the initial size interval chosen.

Besides, the equations have to be adopted to a finite number of fractions.

How the practical application of the model is done, will be evident in the following.

If the size distribution in the outlet of the reactor is known, the upper limit of the first settling velocity interval (VMIN) can be used to calculate the required number of intervals (NFRAC). For example can NFRAC be defined to be the number of intervals that contains at least 99 % of all flocs as calculated from the output settling velocity distribution. A larger number of fractions can of course be included, but the content of the additional fractions will be very small and have no significant influence on the calculated result.

The upper limit of each settling velocity interval, VFRAC(K) is calculated according to (compare eq. 5.24):

$$VFRAC(K) = VMIN \cdot K^{VPOT} \qquad (5\text{-}26)$$

Then NFRAC could be determined from the condition

$$\Phi \left(\frac{VMIN \cdot NFRAC^{VPOT} - VMEAN(out)}{SIGMA(out)}\right) > 0.99 \qquad (5\text{-}27)$$

where Φ is the cumulative frequency distribution function, normally distributed (0,1)

VMEAN(out) is the mean settling velocity of the suspension out from the reactor

SIGMA(out) is the standard deviation

The content of each fraction in the inlet, OLDFRC(K), and in the outlet, FRAC(K), is now calculated.

The summation terms S1(K) and S2(K) are determined according to:

$$S1(K) = \frac{1}{2} \sum_{I=1}^{K-1} FRAC(I) \cdot FRAC(K-I) \cdot (I^{RPOT} + (K-I)^{RPOT})^3 / \qquad (5\text{-}28)$$

$$/(I \cdot (K-I))$$

$$S2(K) = \sum_{I=1}^{NFRAC-K} FRAC(K) \cdot FRAC(I) \cdot (I^{RPOT} + K^{RPOT})^3 / (K \cdot I) \qquad (5\text{-}29)$$

where RPOT here, as in eq. 5-25, consistently was set to 1/3.

The upper summation limit in eq. 5-29 is restricted to NFRAC-K because no flocs in intervals greater than NFRAC is considered. Otherwise the condition stated in eq. 5-10 is not fulfilled.

The breakup rate can be written (only disappearance from fraction K is considered):

$$\left(-\frac{df_k}{dt}\right)_{breakup} = Const \cdot G^{GPOT} \cdot \left(\sqrt{VMIN \cdot K^{VPOT}}\right)^{DPOT} \cdot FRAC(K) \qquad (5\text{-}30)$$

where GPOT and DPOT are breakup and size exponents, respectively (see eq. 5-13).

The breakup rate here is stated depending on the absolute particle size within the fraction K (indirectly calculated from the settling velocity), compare the eqs. 5-14 to 5-20. This modification is necessary to make the breakup rate independent of chosen size intervals.

The terms S3(K) and S4(K) then, depending on assumed breakup mode, become:

$$S3(K) = \left(\sqrt{VMIN \cdot K^{VPOT}}\right)^{DPOT} \cdot FRAC(K) \qquad (5\text{-}31)$$

$$S3(1) = 0 \qquad (5\text{-}32)$$

1 Equal number (MODE=1)

$$S4(K) = K \cdot \sum_{I=K+1}^{NFRAC} S3(I) \cdot \frac{1}{\sum_{J=1}^{I-1} J} \qquad (5\text{-}33)$$

$$S4(NFRAC) = 0$$

2 Equal volume (MODE=2)

$$S4(K) = \sum_{I=K+1}^{NFRAC} S3(I) \cdot \frac{1}{(I-1)} \qquad (5\text{-}34)$$

$$S4(NFRAC) = 0$$

3 Primary particle strip (MODE=3)

$$S4(1) = S3(2) + \sum_{I=3}^{NFRAC} S3(I)/I \qquad (5\text{-}35)$$

$$1 < K < NFRAC: \; S4(K) = \frac{K}{K+1} S3(K+1) \qquad (5\text{-}36)$$

$$S4(NFRAC) = 0$$

The general equation governing the particle size distribution in a completely mixed reactor can now be written:

$$FRAC(K) = OLDFRC(K) + GC1 \cdot GVALUE \cdot DTIME \cdot FLTURB \cdot K \cdot$$

$$\cdot (S1(K) - S2(K)) - BC2 \cdot GVALUE^{GPOT} \cdot DTIME \cdot (S3(K) - S4(K)) \qquad (5\text{-}37)$$

where GC1 is a growth constant
BC2 is a breakup constant
FLTURB is the floc volume fraction measured as turbidity (FTU)
DTIME is the mean residence time in the reactor (s)

Eq. 5-37 was used as a basis for the construction of computer programs in order to determine appropriate values of constants and exponents for the model to fit available experimental data. The programs were written in FORTRAN and executed on a NORD-100 computer. The constants to be determined was the growth constant GC1, the breakup constant BC2 and the exponents GPOT and DPOT. However space and time consuming it was found that the most effective way both for computations and in illustration of general issues of the model, was to draw figures containing cumulative settling velocity distributions. It should be stated that, as has been described, the settling analyses performance comprised extraction of samples at times corresponding to the settling velocity interval 0.15-1.8 m/h. Values indicated outside this interval are extrapolated, and within this interval measured values are approximated, in both cases by means of a normal distribution. Thus an apparent accuracy in the following figures sometimes exeeds what can with some certainty be concluded from experimental data.

The testing and calibration of the model demand that the input and output settling velocity distributions are known. Because settling tests have not been performed in the first flocculation tank, the study is at present limited to the third and fourth tanks. Thus the range of G-values for which the validity of the model is tested is limited to appr. 3-15 s^{-1}. No attempts will be made here to make inferences concerning the conditions in the beginning of the flocculation process.

As the output size distribution has to be known in calculation of the terms S1 to S4 in eq. 5-37, the test procedure can be carried out according to one of the following alternatives:

Calculation alternatives

1 The output settling velocity distribution is calculated from eq. 5-37, with the sums S1 to S4 calculated from the known output distribution, and is then compared with the latter.

2 The input settling velocity distribution is calculated from the known output distribution and is then compared with the measured values of the former.

3 An output settling velocity distribution is calculated by an iterative procedure with start values equal to the known output distribution.

4 Calculation of the output velocity distribution by iteration with start values equal to the known input distribution.

All four alternatives have been used. The first two are suitable when rather rapid calculations are required. However, if the calculated size distribution differs to any greater extent from the present reference, a deviation from the "true" calculated result is obtained. That is because the calculation is based on values not conform with the model. Thus a false prognostication is made by the model.

The fourth alternative is naturally the ultimate purpose of a mathematical model, though the most time consuming calculation pattern. Besides, to ascertain convergence towards a probable size distribution some additional features are necessary, as will be seen. The first step in that direction is the third alternative.

In the following the results will be presented in diagrams with the measured input and output cumulative settling velocity distributions represented by continuous lines. Consistently the upper curve is the input and the lower curve the output size distribution. The result calculated from the model is indicated as points at each fraction limit.

The first fraction contains the mass of the particles with settling velocity less than the first fraction limit including that part with settling velocity interpreted as zero (the residual turbidity). Thus the first fraction always will contain more flocs than any other fraction. Besides, the mean settling velocity (and indirectly the particle size) of that fraction will consequently differ more or less

from the middle point of the interval. A discontinuity between the first interval and the second is inevitable to some extent according to the calculation method proposed here. However theoretically unsatisfactory, the practical implications are small, as will be seen.

Data for illustrating some general issues of the model will firstly be taken from eqs. 4-17 and 4-18 and table 4-6. A more comprehensive evaluation is then made with data obtained at one occasion, consisting of the settling velocity response to variations of the power input.

If the mathematical model according to eq. 5-37 gives an accurate description of the floc growth it offers, for example, the possibility to separate the effects of growth and breakup, of different assumed breakup patterns or the floc breakup sensitivity according to size. A great number of calculations were performed from which three important conclusions could be drawn:

1 The sensitivity for disruption of the flocs according to their size can be expressed by the exponent DPOT in eq. 5-30. A value of DPOT of 8 was found to fit the experimental data. This value is applied in the following if nothing else is mentioned.

2 The relation between the floc breakup and the G-value as expressed by the exponent GPOT in eq. 5-30 was described satisfactorily if the exponent was given the value 3.25. This value of the exponent has been used consistently in all calculations presented in the following.

3 The breakup mode 1, i.e. a distribution of floc fragments in such a way that all fractions below the broken size achieve an equal increase in number of particles, was shown to give the closest agreement with measured size distributions.

In the figures 5-5 to 5-13 some effects are illustrated. The measured settling velocity distributions are the same throughout these figures. The result in the third flocculation tank, at the highest applied power input variant, at 20 min total flocculation time and at $2^{o}C$ according to eqs. 4-17 and 4-18 and table 4-6 has been chosen. The corresponding set of data is called: Run T1. The measured variables are as follows:

Run T1

Mean settling velocity (m/h)

in	out
0.33	0.58

Standard deviation (m/h)

in	out
0.42	0.53

G-value: 15.3 s^{-1}

Mean residence time: 300 s

Floc turbidity: 4.0 FTU

The constants GC1 and BC2 was here given the values $0.9 \cdot 10^{-5}$ and $3.6 \cdot 10^{-7}$, respectively. These values are not claimed to be the best to fit the mentioned data. They just represent reasonable approximations, suitable for illustration purposes. The determination of constants, which give the best fit to the data is a laborious task. Besides, that procedure demands a careful evaluation of the reliability of available data. An attempt in that direction is made later on.

In the figures 5-5 to 5-11 the resulting settling velocity distribution is calculated with the known result as a basis for the terms S3 and S4 (calculation alternative 1).

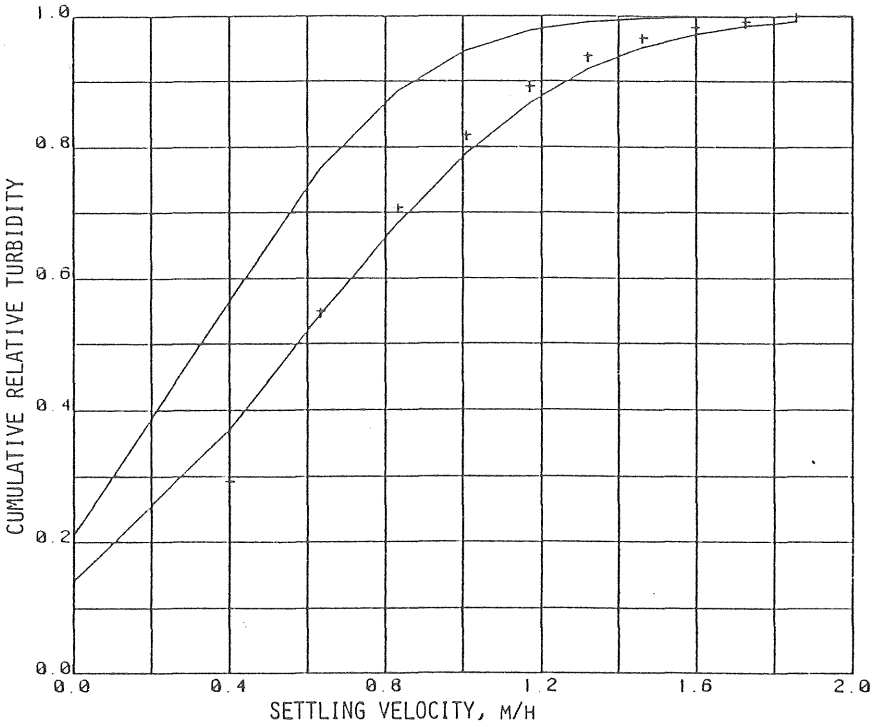

Fig 5-5. Cumulative settling velocity distributions. Measured result compared to calculated result according to eq. 5-37. Run T1.
GC1=0.9 $\cdot 10^{-5}$, BC2=3.6 $\cdot 10^{-7}$, NFRAC=10, VMIN=0.4 m/h.
Floc breakup: MODE=1. Calculation alternative: 1.

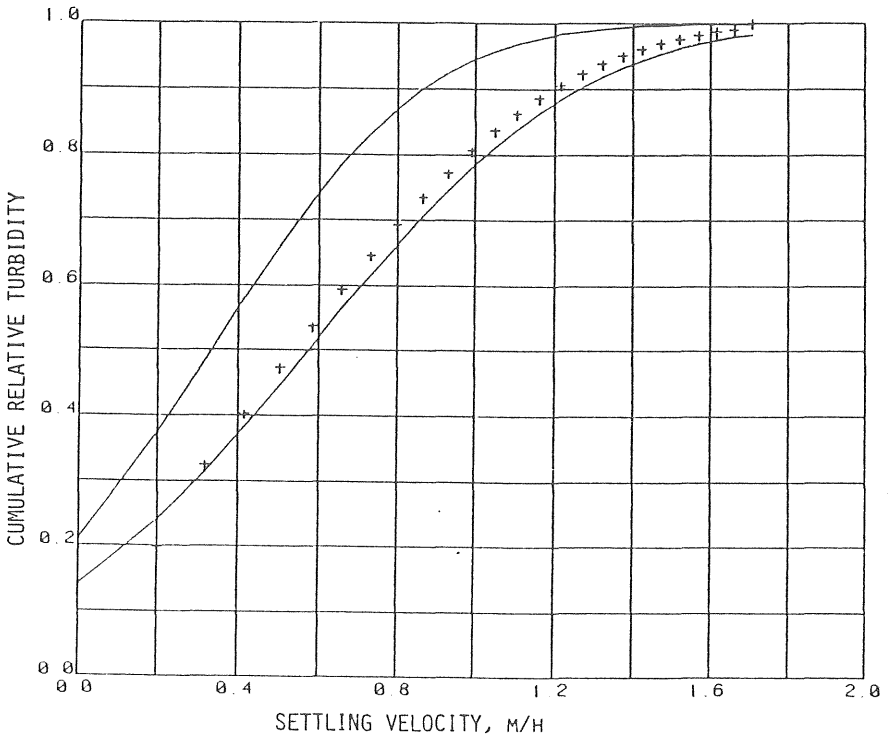

Fig 5-6. Cumulative settling velocity distributions. Measured result compared to calculated result according to eq. 5-37. Run T1.
GC1=0.9 $\cdot 10^{-5}$, BC2=3.6 $\cdot 10^{-7}$, NFRAC=25, VMIN=0.2 m/h.
Floc breakup: MODE=1. Calculation alternative: 1.

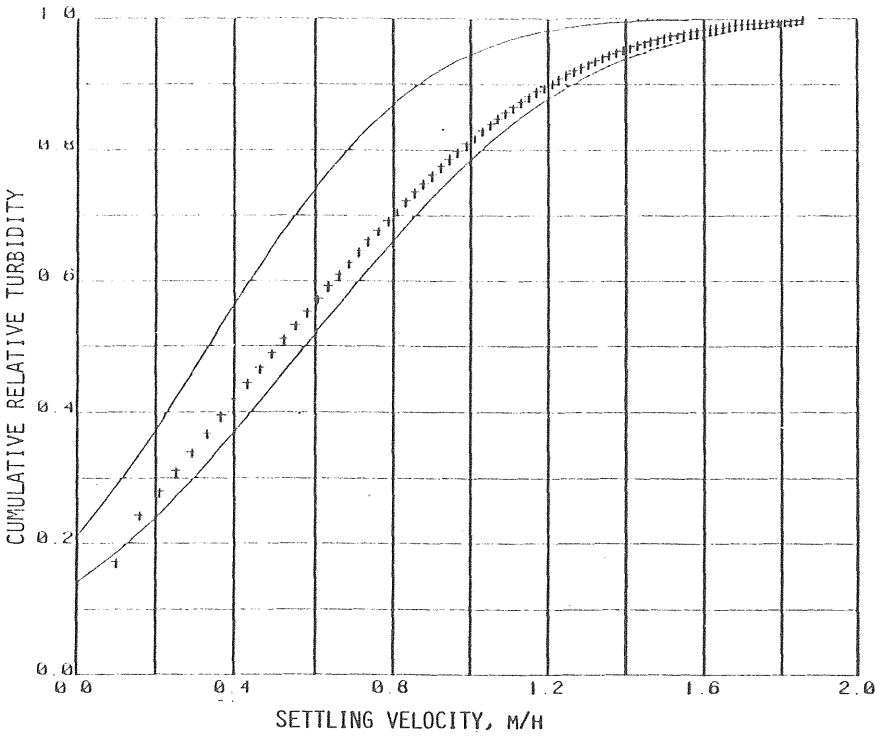

Fig 5-7. Cumulative settling veolicity distributions. Measured result compared to calculated result according to eq. 5-37. Run T1.
GC1=0.9 $\cdot 10^{-5}$, BC2=3.6 $\cdot 10^{-7}$, NFRAC=80, VMIN=0.1 m/h.
Floc breakup: MODE=1. Calculation alternative: 1.

Figure 5-5, 5-6 and 5-7 indicate that the result essentially is not affected by the chosen division of the floc sizes. The numbers of fractions (NFRAC) are 10, 25 and 80. The sizes of the smallest fraction (VMIN) are 0.4, 0.2 and 0.1 m/h, respectively. In these figures the breakup mode is "equal number". (MODE=1).

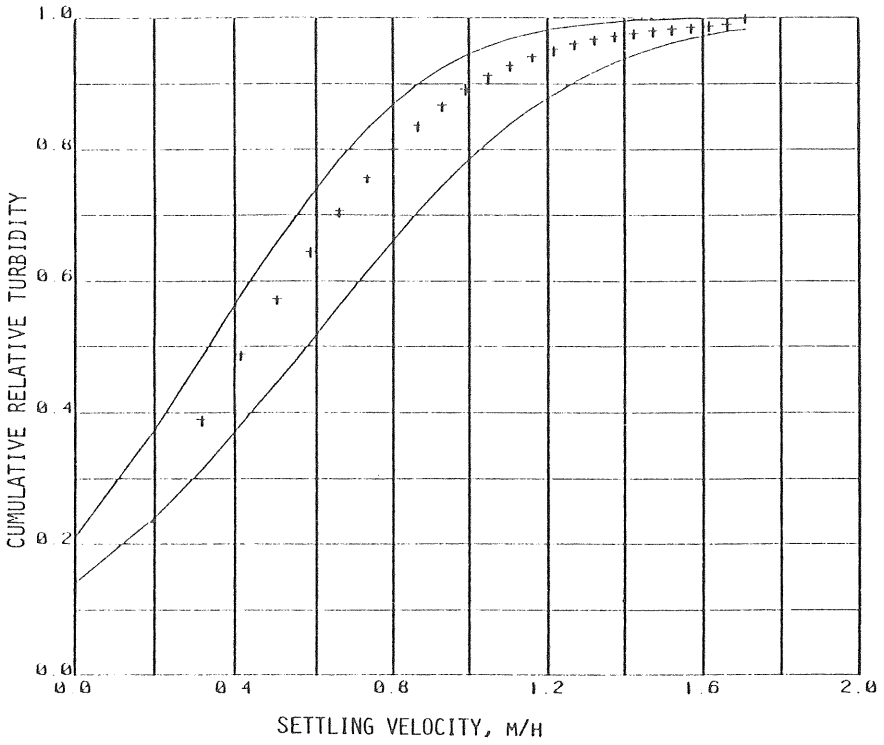

Fig 5-8. Cumulative settling velocity distributions. Measured result compared to calculated result according to eq. 5-37. Run T1.
GCl=0.9 $\cdot 10^{-5}$, BC2=3.6 $\cdot 10^{-7}$, NFRAC=25, VMIN=0.2 m/h.
Floc breakup: MODE=2. Calculation alternative: 1.

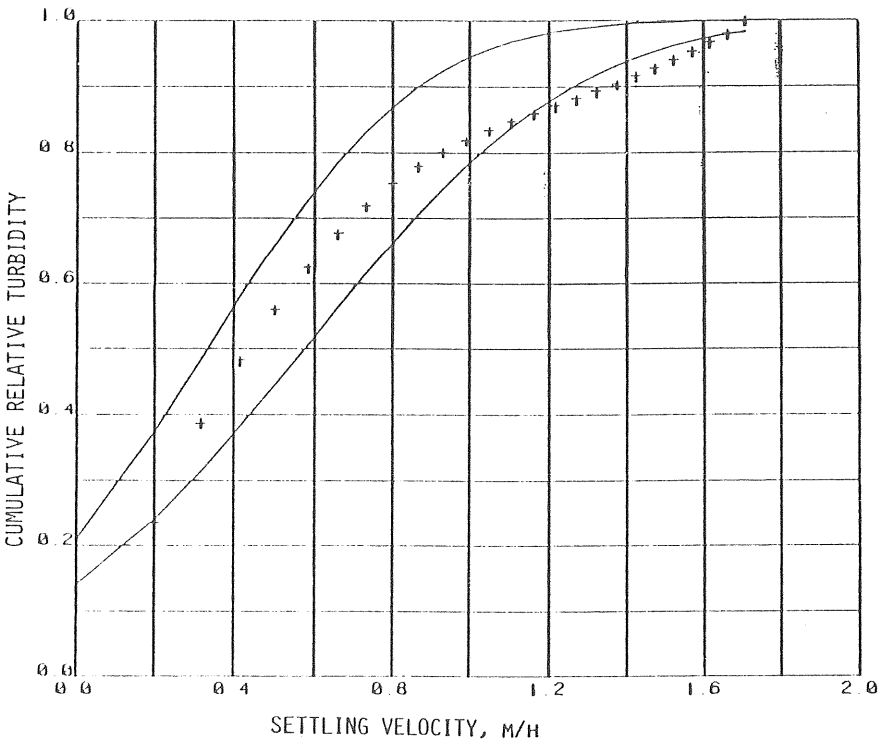

Fig 5-9. Cumulative settling velocity distributions. Measured result compared to calculated result according to eq. 5-37. Run T1.
GCl=0.9 $\cdot 10^{-5}$, BC2=3.6 $\cdot 10^{-7}$, NFRAC=25, VMIN=0.2 m/h, DPOT=6.
Floc breakup: MODE=2. Calculation alternative: 1.

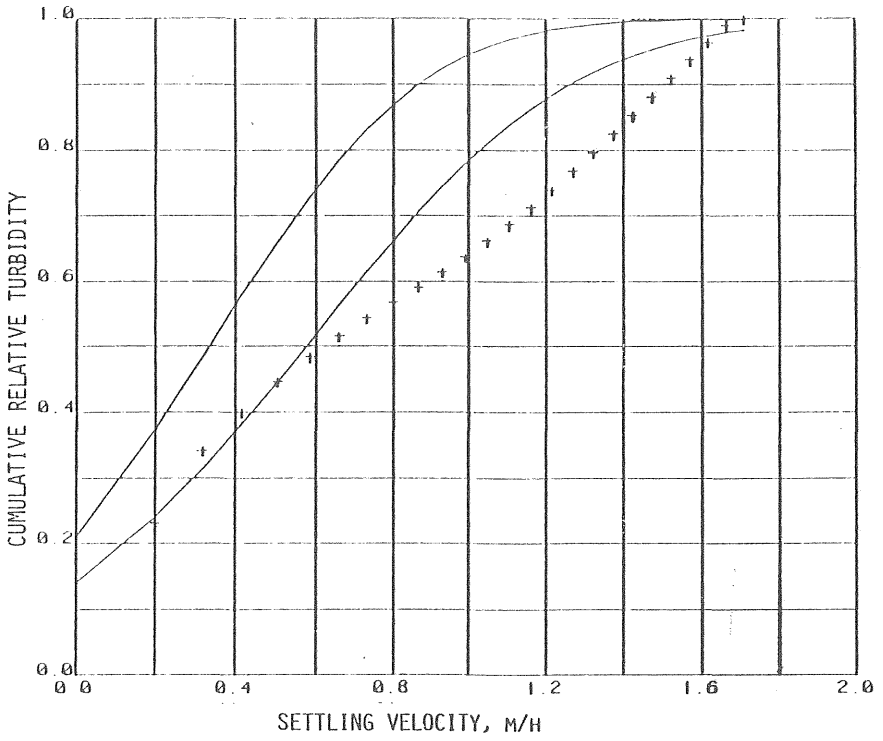

Fig 5-10. Cumulative settling velocity distributions. Measured result compared to calculated result according to eq. 5-37. Run T1.
GC1=0.9 $\cdot 10^{-5}$, BC2=3.6 $\cdot 10^{-7}$, NFRAC=25, VMIN=0.2 m/h.
Floc breakup: MODE=3. Calculation alternative: 1.

In figures 5-8 and 5-9 the breakup mode is "equal volume" (MODE=2), and in figure 5-10 "primary particle strip" (MODE=3). The values of all constants and exponents are the same as in the previous figures, except for DPOT which in figure 5-9 has the value 6 (instead of 8). These figures illustrate that the breakup mode 1 give rise to size distributions of a type closest to the measured ones.

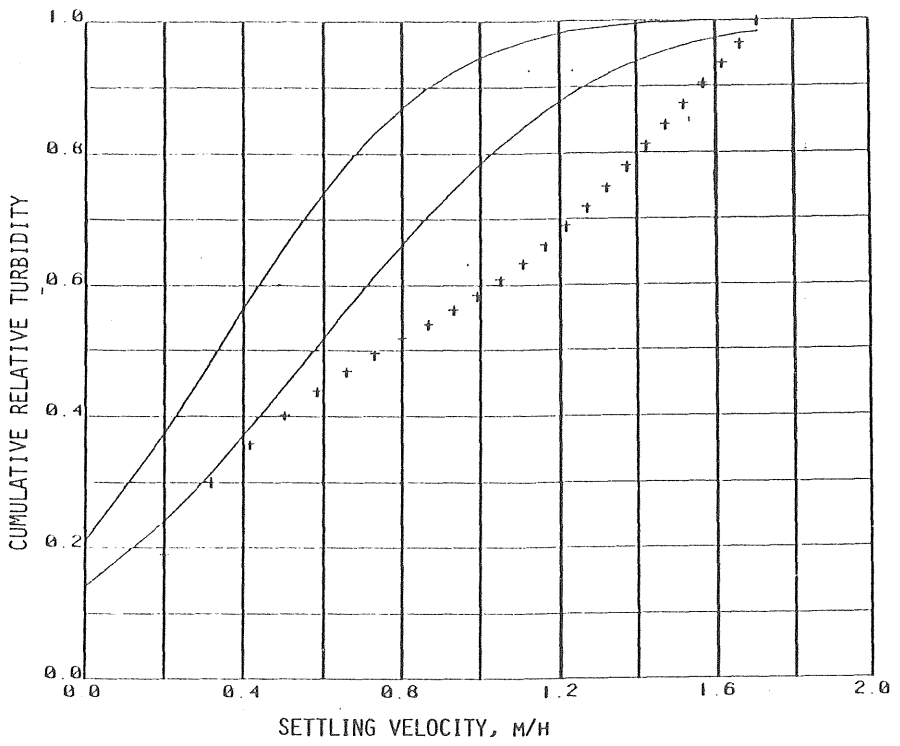

Fig 5-11. Cumulative settling velocity distributions. Measured result compared to calculated result according to eq. 5-37. Run T1.
GC1=0.9 · 10^{-5}, BC2=0, NFRAC=25, VMIN=0.2 m/h.
No floc breakup. Calculation alternative: 1.

Figure 5-11 gives an impression of the effect of the floc breakup. The breakup constant BC2 was here given the value 0. Consequently no transfer of floc fragments due to breakup is calculated. Similar plots made for experiments with lower power input showed, naturally, that a smaller amount of the flocs was redistributed according to the breakup.

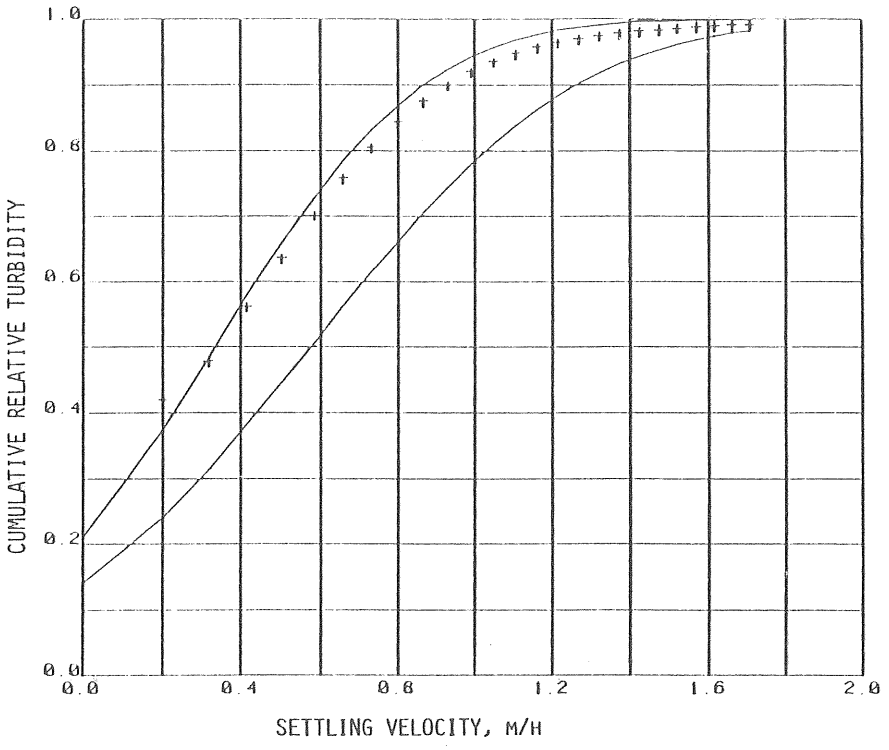

Fig 5-12. Cumulative settling velocity distributions. Measured result compared to calculated result according to eq. 5-37. Run T1.
GC1=0.9 $\cdot 10^{-5}$, BC2=3.6 $\cdot 10^{-7}$, NFRAC=25, VMIN=0.2 m/h.
Floc breakup: MODE=1. Calculation alternative: 2.

In the figure 5-12 the calculation is performed in the opposite direction (calculation alternative 2). The size distribution in the inlet is calculated with the size distribution at the outlet as the only basis. (MODE=1).

In figure 5-13 is shown the result of an iterative procedure. As start values was given the settling velocity distribution in the inlet. The calculations were continued until the content in the first fraction was stabilized around an ultimate value with a prescribed accuracy. The procedure is not very successful. The convergence was slow. A too great prescribed accuracy of the content in the first fraction led to no convergence at all. If the equations governing the calculations are studied, it can be found that a fraction may be calculated to have a negative content. If the number of fractions is low and the start values are far from the ultimate values, this may lead to a divergent calculation pattern. In the present case the content of any fraction was not allowed to be less than zero, but as can be seen there are several fractions that have become just zero content.

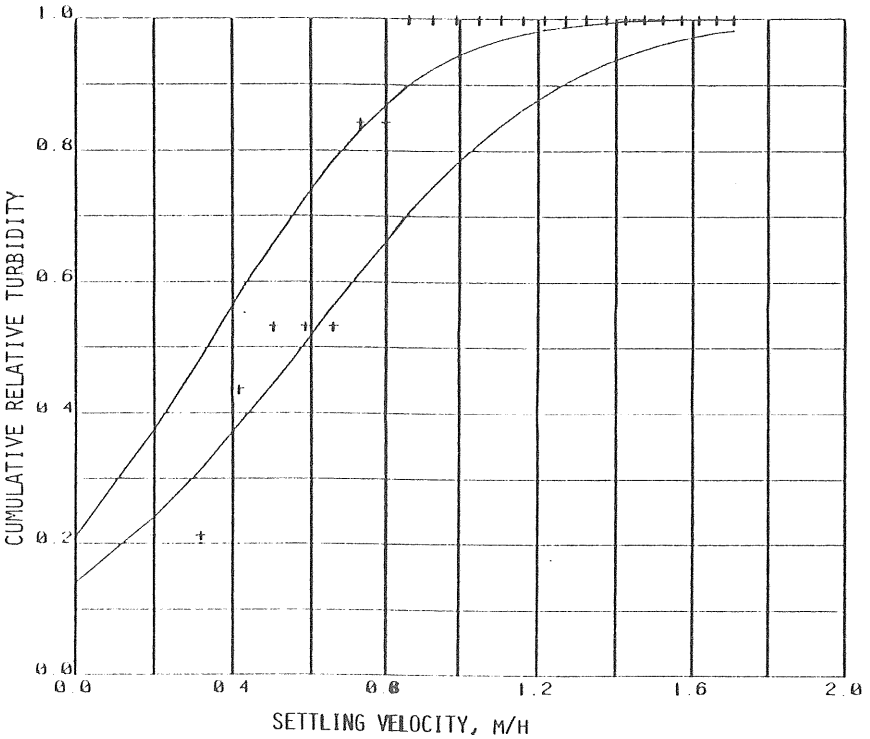

Fig 5-13. Cumulative settling velocity distributions. Measured result compared to calculated result according to eq. 5-37. Run T1. GC1=0.9 $\cdot 10^{-5}$, BC2=3.6 $\cdot 10^{-7}$, NFRAC=25, VMIN=0.2 m/h. Floc breakup: MODE=1. Calculation alternative: 4.

To increase the convergence tendency when calculations were performed according to the fourth calculation alternative, this procedure was modified. After each iterative step the best fit of a continuous size distribution function was used as a means to determine the content of

each fraction to use as a basis for the next step in the calculations. In that way any discontinuity in the calculated size distribution was avoided. The condition that the distribution calculated should be normal (as the measured ones) was convenient for comparison purposes. Thus in the following the size distributions presented as calculated by the model according to calculation alternative 4, are the best fit of continous functions, normally distributed.

The iteration was continued until the difference in size distribution, as expressed by the parameters VMEAN and SIGMA, between two consecutive calculation steps was lower than a prescribed value. As an example, (applied in calculations of which the results are presented in the following figures) the iteration was stopped when both VMEAN and SIGMA differed less than 3% from the previous values. The mean values of the calculated parameters in the last two steps were used as an approximation of the best fitted distribution. A maximum of 16 iterations were performed. Usually if that number was obtained, VMEAN and SIGMA (because a normal distribution then, did not conform to the model accurately enough) were oscillating between two values.
Also in that case the mean values of the parameters in the last two consecutive steps were used to approximate the final size distribution.

It was found that the data summarized in the eqs. 4-17 and 4-18 and in table 4-6 provided a too schematic picture for the present purpose. These data are based on mean values for a great number of experiments. Besides, the assumptions on which this general descriptive model is based, are not in all cases suited for a sufficiently correct description of measured data. Therefore, it was decided to use results from solitary experiments in the following test of the model.

The results obtained with paddle typ A4 (see Appendix 6 and 2) at $2^{o}C$, mainly at the total flocculation time 20 minutes, with and without the addition of activated silica will be used as testing data. In the tables 5-6 and 5-7 results obtained are indicated. Each run is given a label consisting of seven signs (e.g. A4A2031), the first two indicating the paddle type, then a letter A if activated silica is added (E if not). The next two numerals are the total flocculation time in minutes (after four flocculation tanks), followed by the number of the flocculation tank and the power input level ("I").

Table 5-6. Results from six different tapered flocculation patterns in the third and fourth flocculation tank at 20 min total flocculation time, and the corresponding results at 10 and 30 min total flocculation time, respectively, with one of these patterns. Paddle type A4. 2°C. No activated silica added.

Run no.	G-value (s^{-1})	Mean residence time (s)	Settling velocity distribution: Mean settling velocity (m/h) in	Mean settling velocity (m/h) out	Standard deviation (m/h) in	Standard deviation (m/h) out
A4E2031	15.3	300	0.24	0.37	0.36	0.36
A4E2032	11.8	300	0.26	0.43	0.39	0.49
A4E2033	9.1	300	0.24	0.46	0.39	0.48
A4E2034	7.0	300	0.18	0.46	0.59	0.72
A4E2035	5.4	300	0.097	0.30	0.36	0.61
A4E2036	4.2	300	-0.061	0.22	0.48	0.87
A4E2041	5.2	300	0.37	0.70	0.36	0.57
A4E2042	4.7	300	0.43	0.62	0.49	0.60
A4E2043	4.4	300	0.46	0.76	0.48	0.83
A4E2044	4.0	300	0.46	0.68	0.72	0.92
A4E2045	3.7	300	0.30	0.57	0.61	0.76
A4E2046	3.4	300	0.22	0.50	0.87	1.0
A4E1033	9.1	150	0.19	0.35	0.54	0.58
A4E1043	4.4	150	0.35	0.45	0.58	0.76
A4E3041	5.2	450	0.54	1.0	0.37	0.55
A4E3042	4.7	450	0.74	0.96	0.59	0.65

A careful investigation of the data in table 5-6 and comparison with the results calculated by the model, revealed that for an appropriate fit GC1 in eq. 5-37 varied with the applied G-value proportional to G raised to an exponent of -0.65. This is another way to express the fact that the particle growth was found to be proportional, not to the G-value, but approximately to the third root of the G-value. In the following, for eq. 5-37 still to be valid, it will be expressed as the "constant" GC1 (in eq. 5-37) varies with G.

The following figures (5-14 to 5-29) are plottings of the data in table 5-6 compared to calculated result according to eq. 5-37. GC1 and BC2 were given the values $3.0 \cdot 10^{-5}/\text{GVALUE}^{0.65}$ and $1.2 \cdot 10^{-6}$, respectively. The first tvelwe figures represent 20 min total flocculation time, the next two 10 min, followed by two figures with result obtained at 30 min total flocculation time.

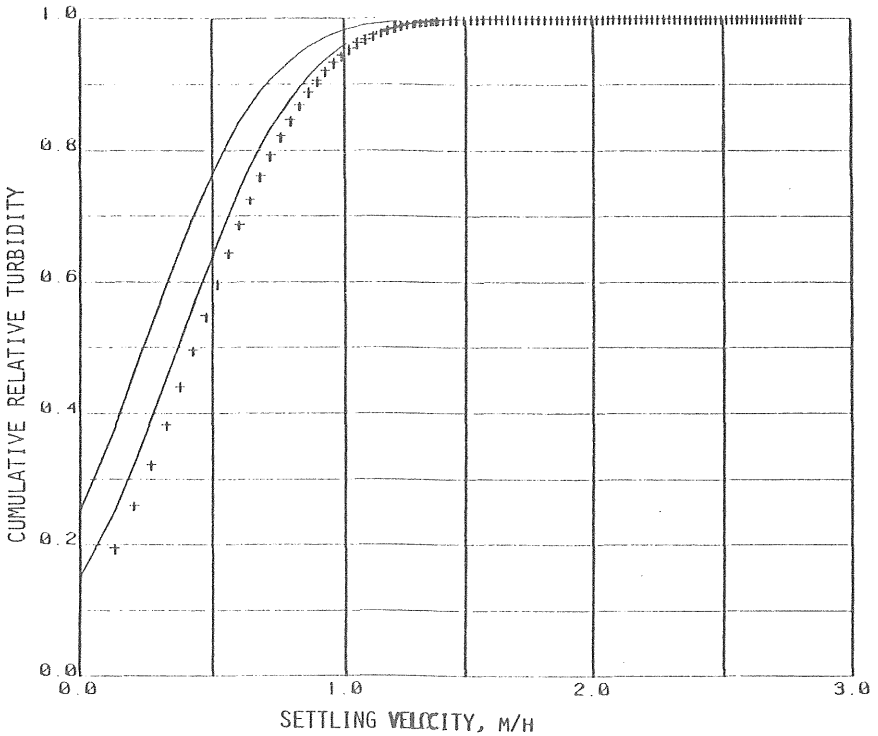

Fig 5-14. Cumulative settling velocity distributions. Measured result compared to calculated result according to eq. 5-37.
Run A4E2031. GC1=$3.9 \cdot 10^{-5}/\text{GVALUE}^{0.65}$, BC2=$1.2 \cdot 10^{-6}$
NFRAC=100, VMIN=0.13 m/h.
Floc breakup: MODE=1. Calculation alternative: 4.

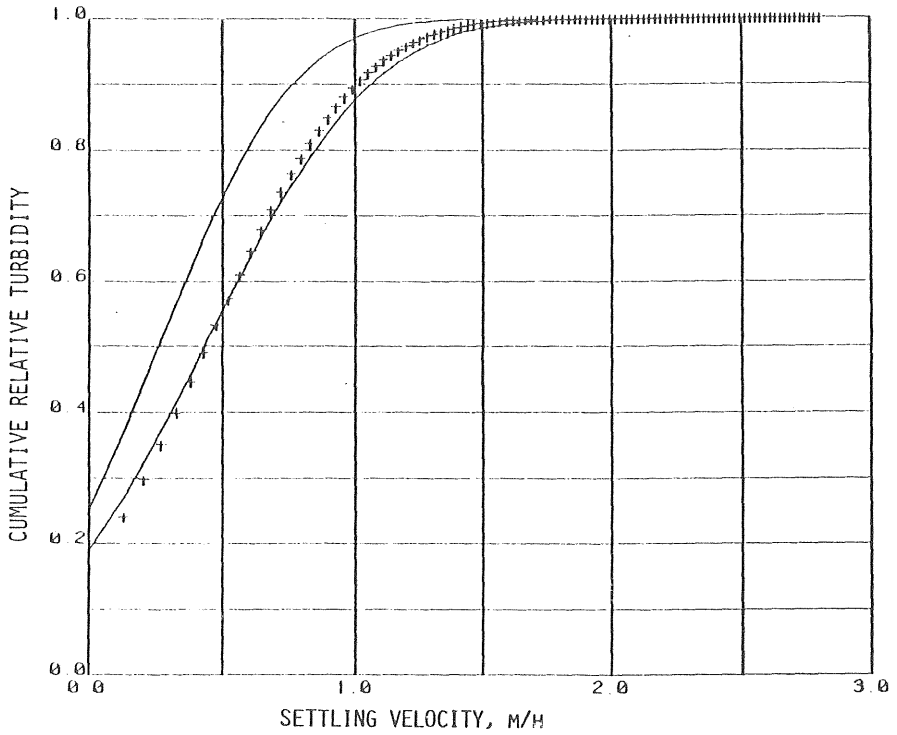

Fig 5-15. Cumulative settling velocity distributions. Measured result compared to calculated result according to eq. 5-37.
Run A4E2032. GC1=3.9 $\cdot 10^{-5}$/GVALUE$^{0.65}$, BC2=1.2 $\cdot 10^{-6}$
NFRAC=100, VMIN=0.13 m/h.
Floc breakup: MODE=1. Calculation alternative: 4.

The iterative procedure did not converge to the prescribed accuracy in the calculations represented in the figures 5-14 and 5-15, that caused an uncertainty especially in the determination of the settling velocity standard deviation calculated by the model.

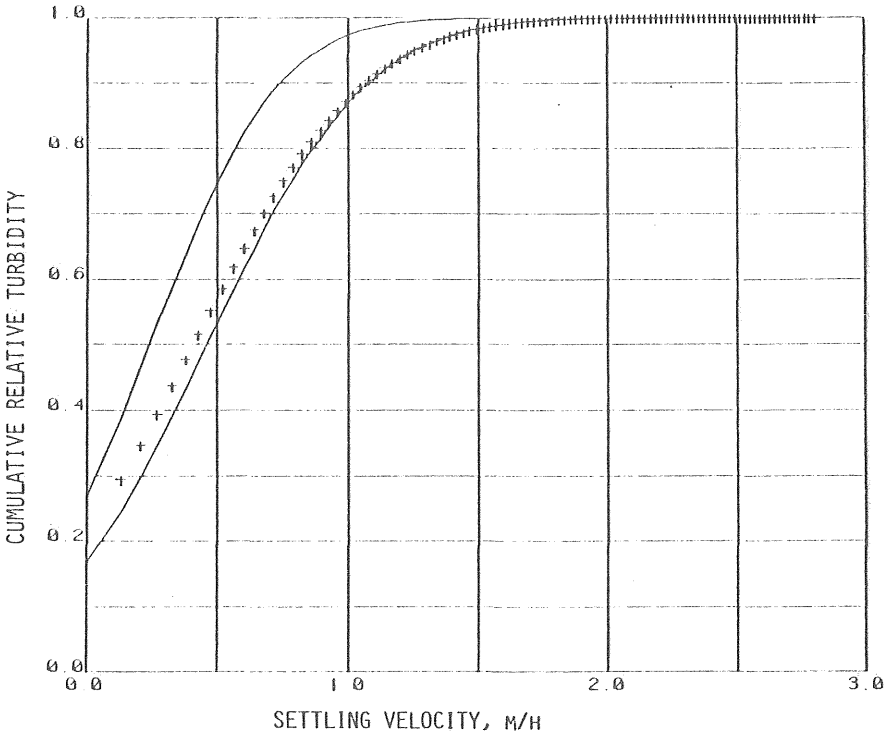

Fig 5-16. Cumulative settling velocity distributions. Measured result compared to calculated result according to eq. 5-37.
Run A4E2033. GC1=3.9 $\cdot 10^{-5}$/GVALUE$^{0.65}$, BC2=1.2 $\cdot 10^{-6}$
NFRAC=100, VMIN=0.13 m/h.
Floc breakup: MODE=1. Calculation alternative: 4.

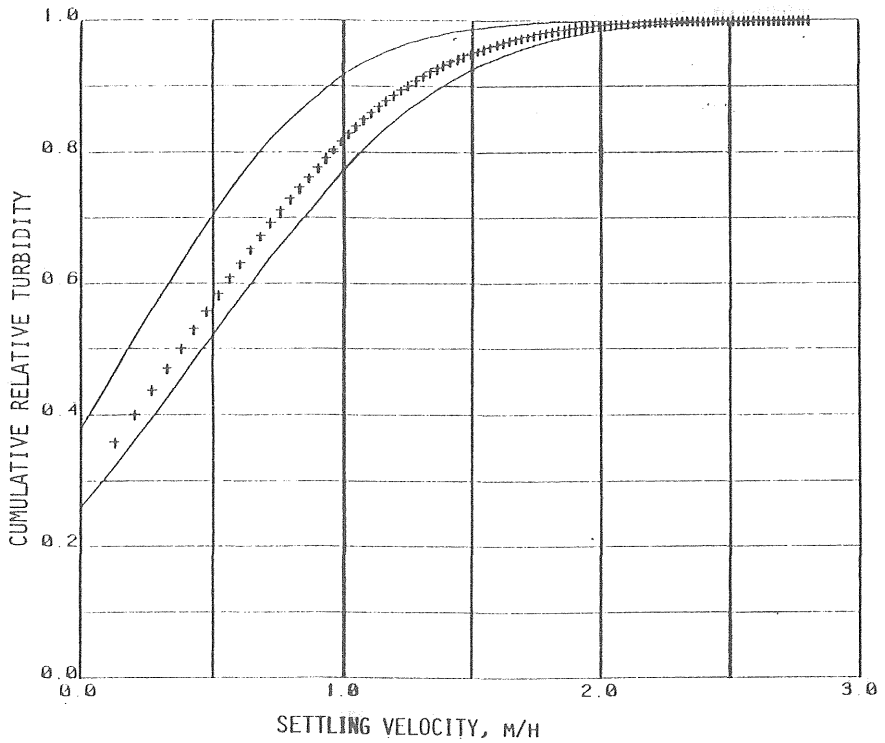

Fig 5-17. Cumulative settling velocity distributions. Measured result compared to calculated result according to eq. 5-37.
Run A4E2034. GC1=3.9 $\cdot 10^{-5}$/GVALUE$^{0.65}$, BC2=1.2 $\cdot 10^{-6}$
NFRAC=100, VMIN=0.13 m/h.
Floc breakup: MODE=1. Calculation alternative: 4.

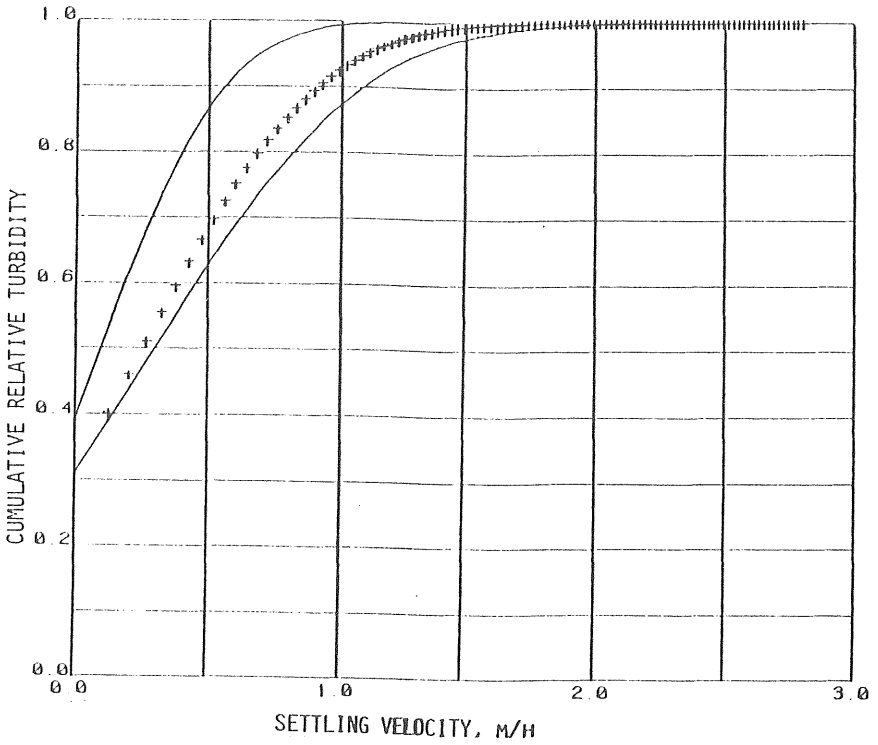

Fig 5-18. Cumulative settling velocity distributions. Measured result compared to calculated result according to eq. 5-37.
Run A4E2035. GC1=3.9 · 10^{-5}/GVALUE$^{0.65}$, BC2=1.2 · 10^{-6}
NFRAC=100, VMIN=0.13 m/h.
Floc breakup: MODE=1. Calculation alternative: 4.

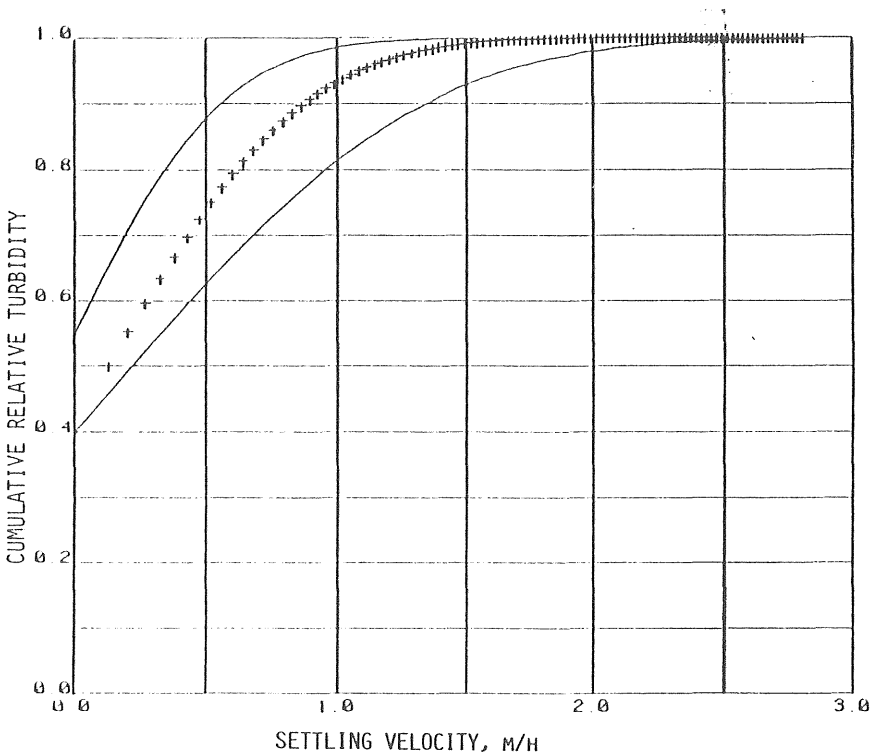

Fig 5-19. Cumulative settling velocity distributions. Measured result compared to calculated result according to eq. 5-37.
Run A4E2036. GC1=3.9 · 10^{-5}/GVALUE$^{0.65}$, BC2=1.2 · 10^{-6}
NFRAC=100, VMIN=0.13 m/h.
Floc breakup: MODE=1. Calculation alternative: 4.

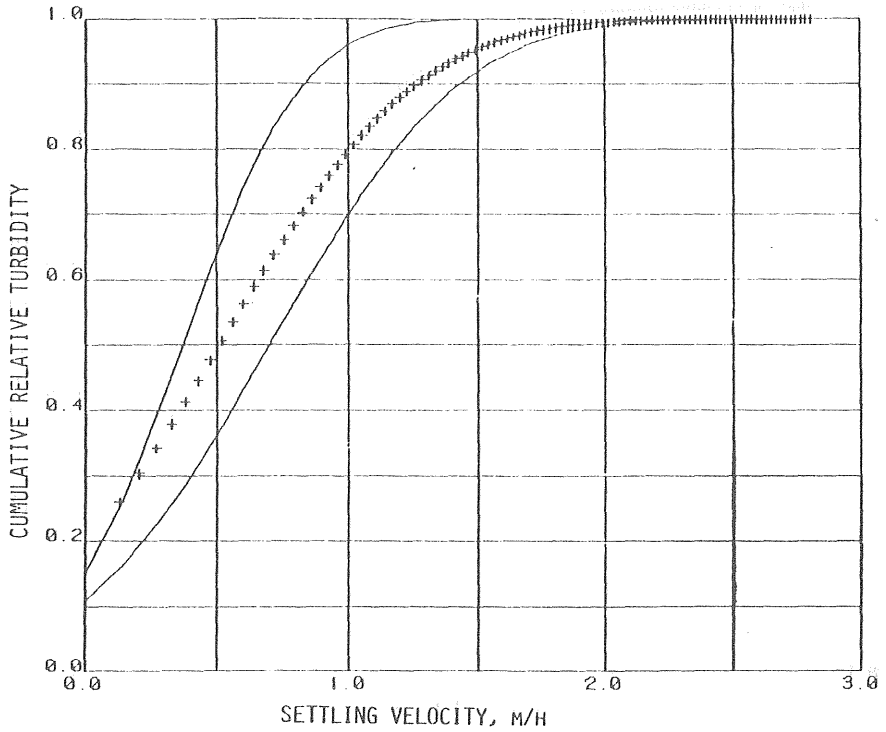

Fig 5-20. Cumulative settling velocity distributions. Measured result compared to calculated result according to eq. 5-37.
Run A4E2041. GC1=3.9 $\cdot 10^{-5}$/GVALUE$^{0.65}$, BC2=1.2 $\cdot 10^{-6}$
NFRAC=100, VMIN=0.13 m/h.
Floc breakup: MODE=1. Calculation alternative: 4.

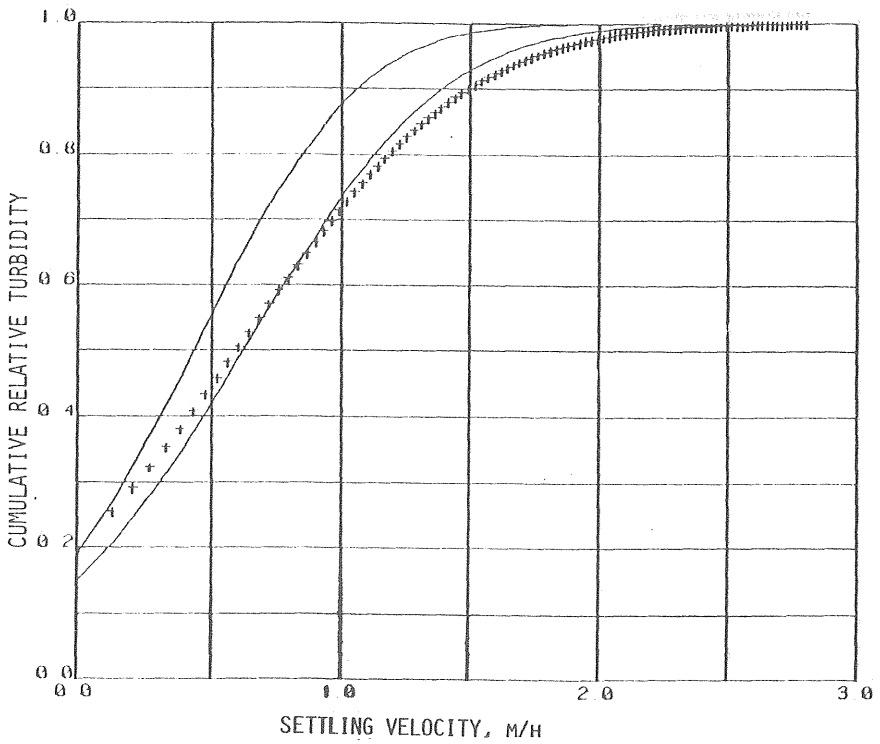

Fig 5-21. Cumulative settling velocity distributions. Measured result compared to calculated result according to eq. 5-37.
Run A4E2042. GC1=3.9 $\cdot 10^{-5}$/GVALUE$^{0.65}$, BC2=1.2 $\cdot 10^{-6}$
NFRAC=100, VMIN=0.13 m/h.
Floc breakup: MODE=1. Calculation alternative: 4.

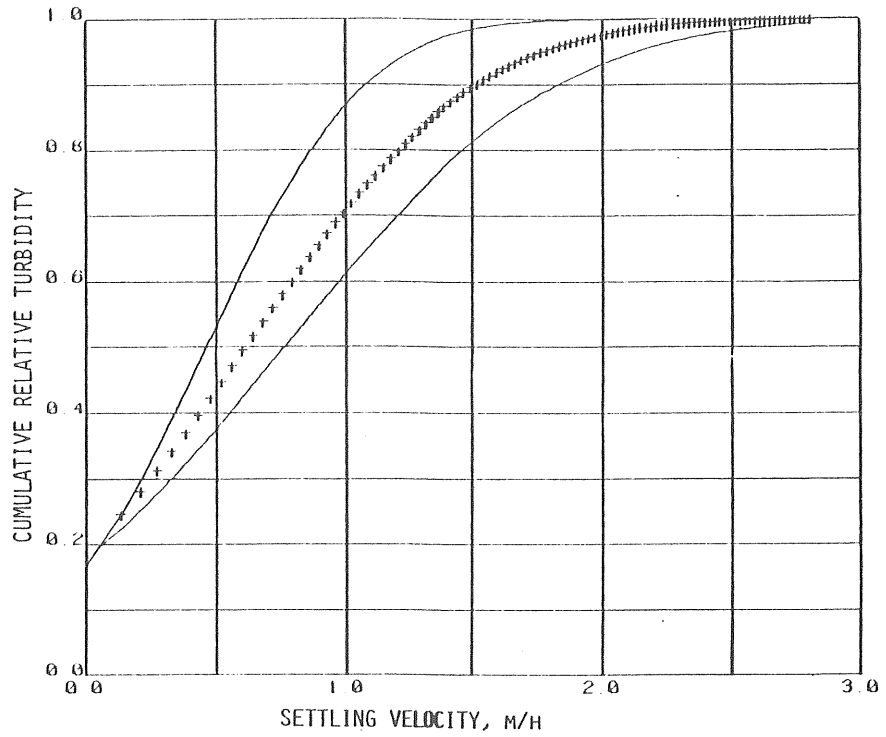

Fig 5-22. Cumulative settling velocity distributions. Measured result compared to calculated result according to eq. 5-37.
Run A4E2043. GC1=3.9 $\cdot 10^{-5}$/GVALUE$^{0.65}$, BC2=1.2 $\cdot 10^{-6}$
NFRAC=100, VMIN=0.13 m/h.
Floc breakup: MODE=100. Calculation alternative: 4.

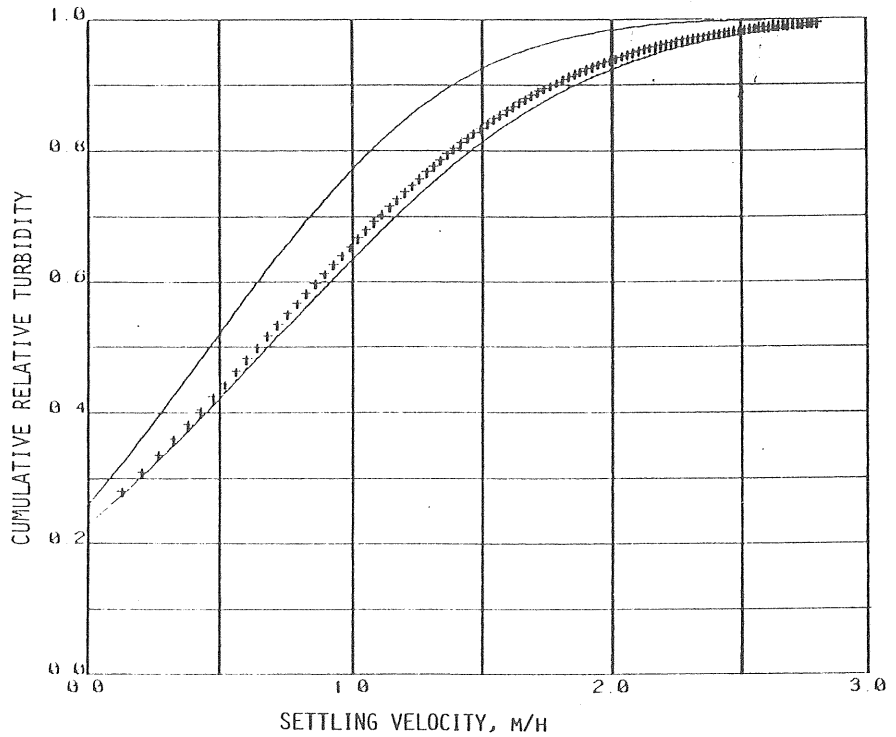

Fig 5-23. Cumulative settling velocity distributions. Measured result compared to calculated result according to eq. 5-37.
Run A4E2044. GC1=3.9 $\cdot 10^{-5}$/GVALUE$^{0.65}$, BC2=1.2 $\cdot 10^{-6}$
NFRAC=100, VMIN=0.13 m/h.
Floc breakup: MODE=1. Calculation alternative: 4.

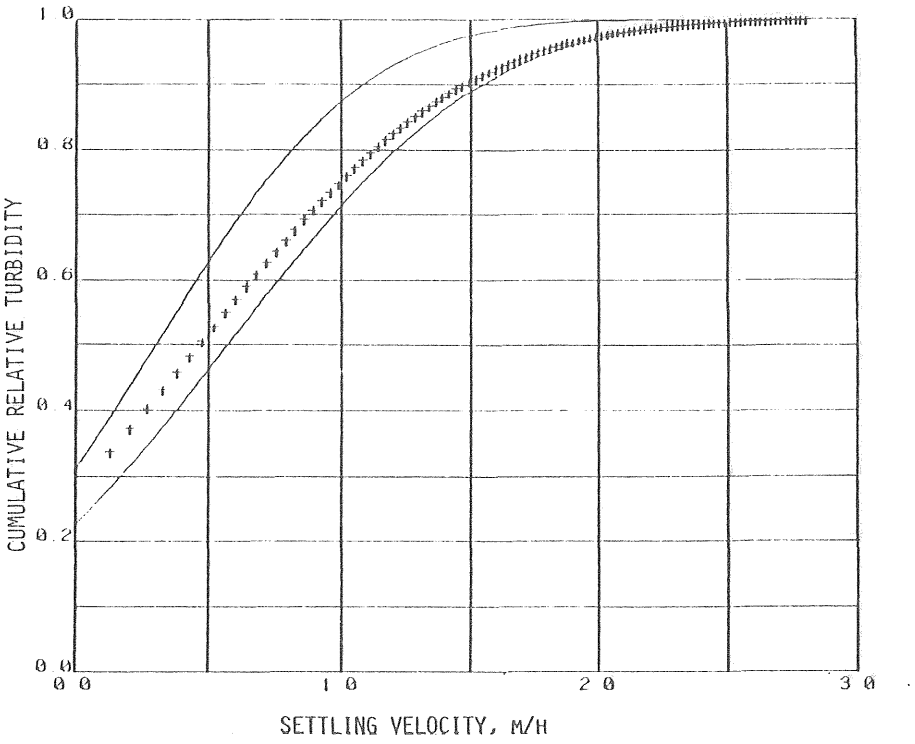

Fig 5-24. Cumulative settling velocity distributions. Measured result compared to calculated result according to eq. 5-37.
Run A4E2045. GC1=3.9 · 10^{-5}/GVALUE$^{0.65}$, BC2=1.2 · 10^{-6}
NFRAC=100, VMIN=0.13 m/h.
Floc breakup: MODE=1. Calculation alternative: 4.

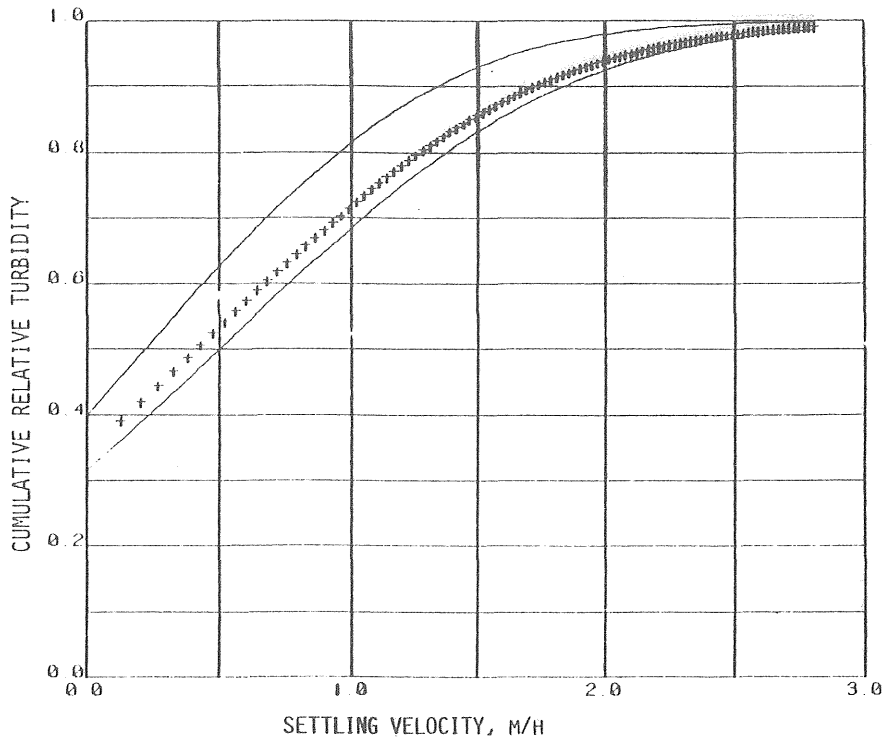

Fig 5-25. Cumulative settling velocity distributions. Measured result compared to calculated result according to eq. 5-37.
Run A4E2046. GC1=3.9 · 10^{-5}/GVALUE$^{0.65}$, BC2=1.2 · 10^{-6}
NFRAC=100, VMIN=0.13 m/h.
Floc breakup: MODE=1. Calculation alternative: 4.

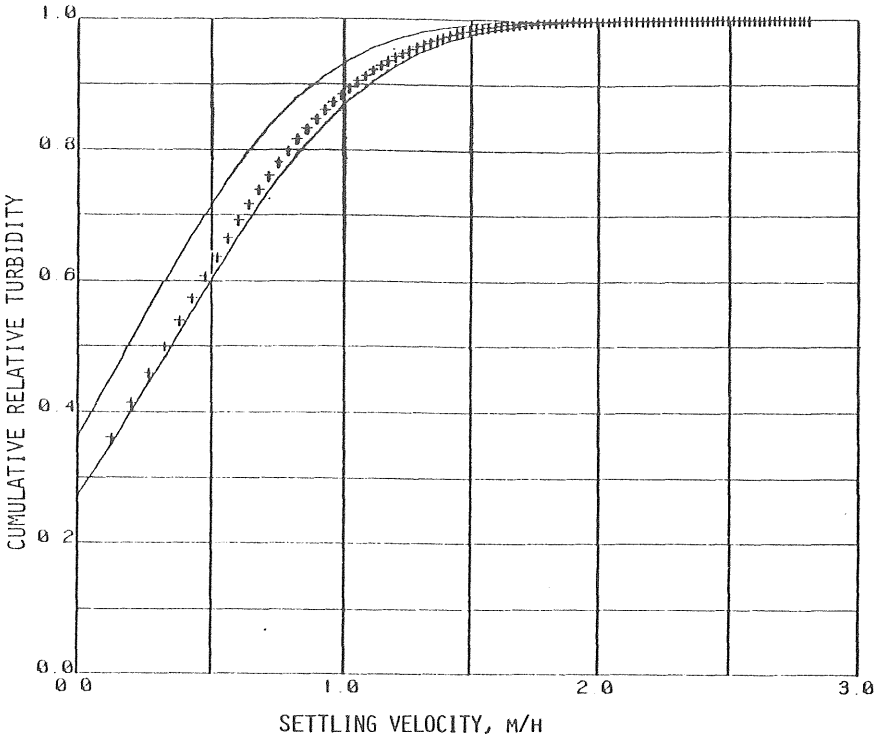

Fig 5-26. Cumulative settling velocity distributions. Measured result compared to calculated result according to eq. 5-37.
Run A4E1033. GC1=3.9 · 10^{-5}/GVALUE$^{0.65}$, BC2=1.2 · 10^{-6}
NFRAC=100, VMIN=0.13 m/h.
Floc breakup: MODE=1. Calculation alternative: 4.

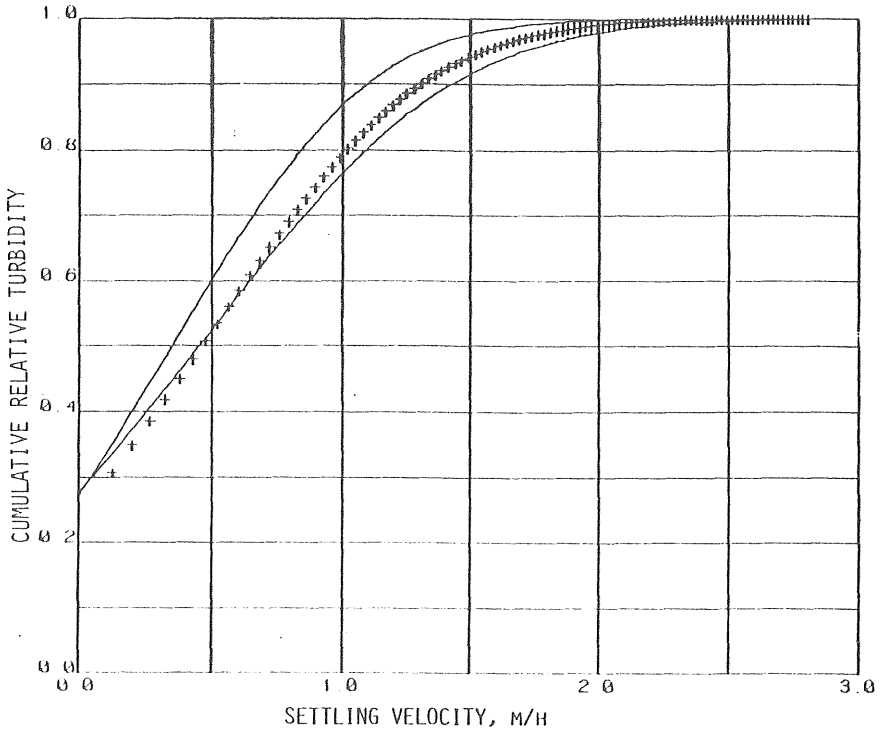

Fig 5-27. Cumulative settling velocity distributions. Measured result compared to calculated result according to eq. 5-37.
Run A4E1043. GC1=3.9 · 10^{-5}/GVALUE$^{0.65}$, BC2=1.2 · 10^{-6}
NFRAC=100, VMIN=0.13 m/h.
Floc breakup: MODE=1. Calculation alternative: 4.

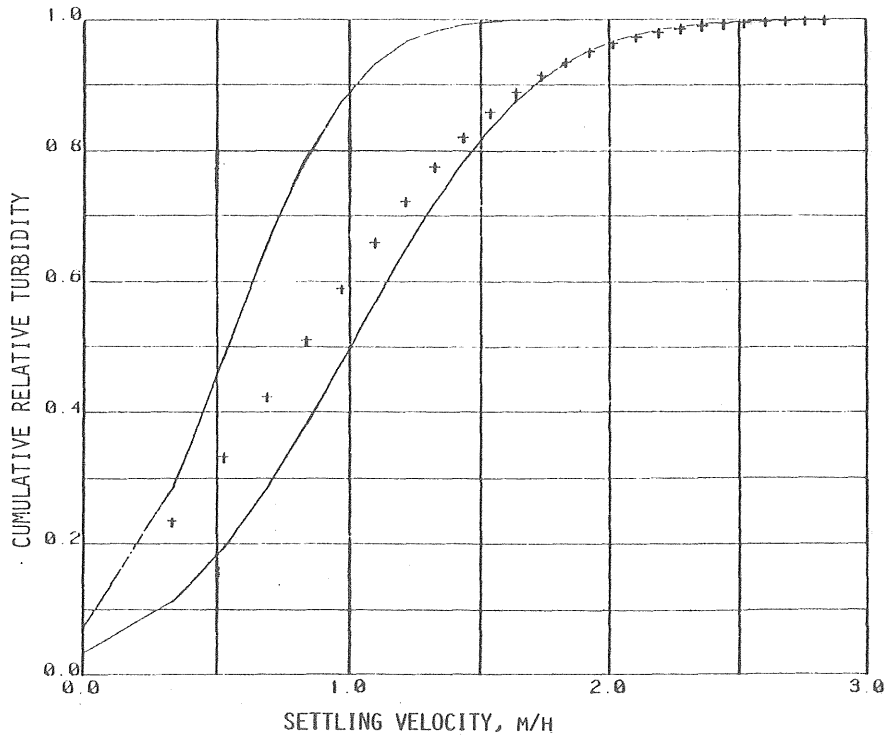

Fig 5-28. Cumulative settling velocity distributions. Measured result compared to calculated result according to eq. 5-37.
Run A4E3044. GC1=3.9 · 10^{-5}/GVALUE$^{0.65}$, BC2=1.2 · 10^{-6}
NFRAC=20, VMIN=0.33 m/h.
Floc breakup: MODE=1. Calculation alternative: 4.

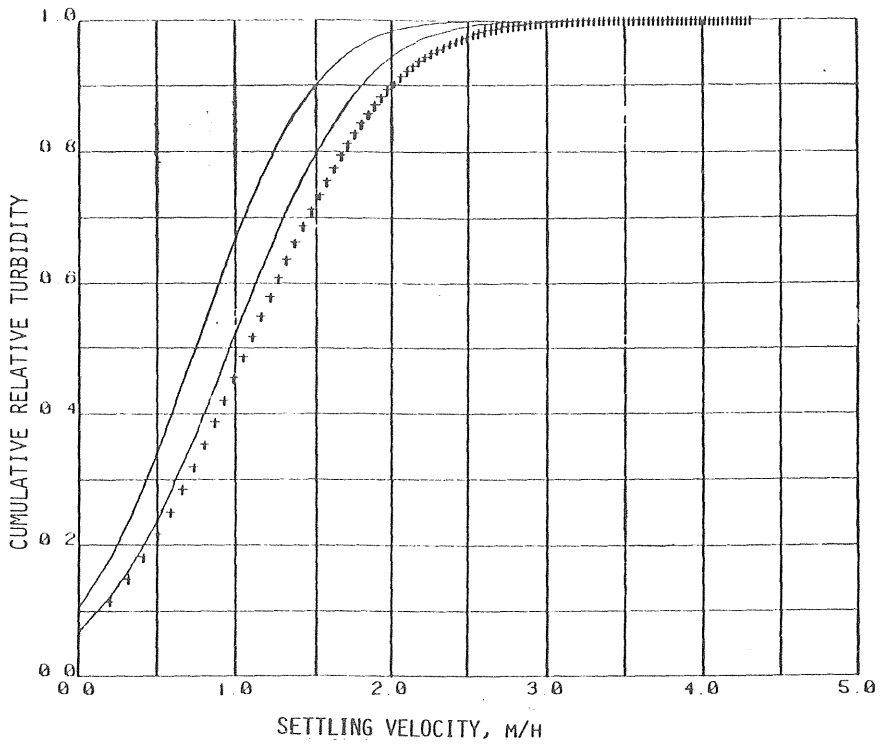

Fig 5-29. Cumulative settling velocity distributions. Measured result compared to calculated result according to eq. 5-37.
Run A4E3042. GC1=$3.9 \cdot 10^{-5}$/GVALUE$^{0.65}$, BC2=$1.2 \cdot 10^{-6}$
NFRAC=100, VMIN=0.13 m/h.
Floc breakup: MODE=1. Calculation alternative: 4.

The figures 5-26 and 5-27 on one hand and the figures 5-28 and 5-29 on the other hand are based on data obtained at 10 and 30 minutes total flocculation time, respectively. These experiments are performed at a different occasion (compared to the 12 previous figures) and there are some indications that the raw water properties have changed and/or the flocculation conditions are slightly different. The proper cause is not known. Nevertheless, the calculations converged rapidly when the model was applied on the data at 10 minutes flocculation time. This was not the case for the calculation result represented in the figures 5-28 and 5-29. A great uncertainty in calculated settling velocity standard deviation remained after 16 calculation steps.

Table 5-7. Results from six different tapered flocculation patterns in the third and fourth flocculation tank at 20 min total flocculation time. Paddle type A4. 2°C. 2 mg/l activated silica added.

Run no.	G-value (s^{-1})	Mean residence time (s)	Settling velocity distribution: Mean settling velocity (m/h) in	Mean settling velocity (m/h) out	Standard deviation (m/h) in	Standard deviation (m/h) out
A4A2031	15.3	300	0.30	0.48	0.64	0.56
A4A2032	11.8	300	0.34	0.67	0.47	0.81
A4A2033	9.1	300	0.36	0.68	0.62	0.98
A4A2034	7.0	300	0.28	0.64	0.85	0.99
A4A2035	5.4	300	0.051	0.41	0.76	1.1
A4A2036	4.2	300	-0.070	0.33	0.63	1.1
A4A2041	5.2	300	0.48	0.89	0.56	0.79
A4A2042	4.7	300	0.67	1.1	0.81	1.1
A4A2043	4.4	300	0.68	1.2	0.98	1.7
A4A2044	4.0	300	0.64	1.0	0.99	1.3
A4A2045	3.7	300	0.41	0.83	1.1	1.4
A4A2046	3.4	300	0.33	0.70	1.1	1.6

In the figures 5-30 to 5-41 the experimental results in table 5-7 (activated silica added) are compared with calculated result according to eq. 5-37. The calculations are carried out the same way as in the figures 5-14 to 5-29 (experiments without activated silica addition). The growth "constant" GC1 is kept the same: $3.9 \cdot 10^{-5}/G^{0.65}$. On the contrary, is the breakup constant BC2 given a lower value: $1.0 \cdot 10^{-7}$. This is in accordance with the expected effect of the activated silica: an increase of the strength of flocs.

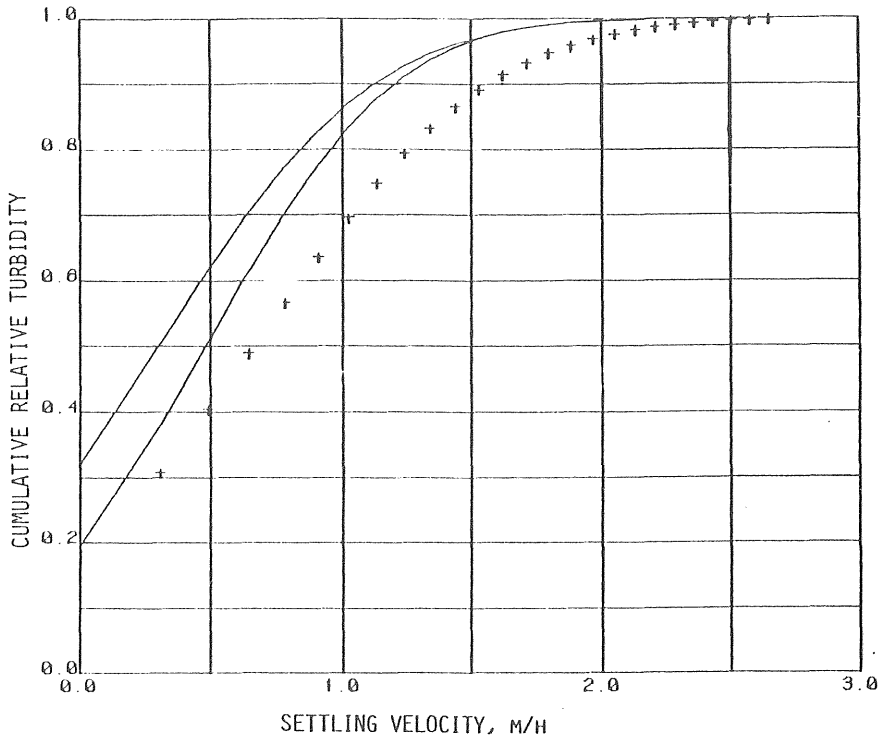

Fig 5-30. Cumulative settling velocity distributions. Measured result compared to calculated result according to eq. 5-37.
Run A4A2031. GC1=3.9 · 10^{-5}/GVALUE$^{0.65}$, BC2=1.0 · 10^{-7}
NFRAC=20. Floc breakup: MODE=1. Calculation alternative: 4.

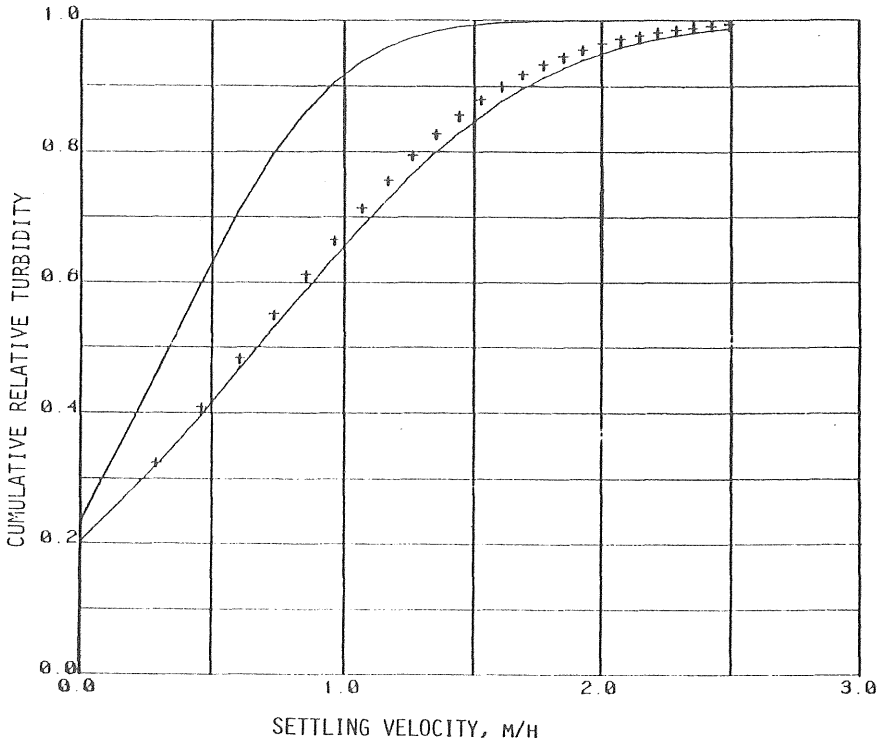

Fig 5-31. Cumultative settling velocity distributions. Measured result compared to calculated result according to eq. 5-37.
Run A4A2032. GC1=3.9 · 10^{-5}/GVALUE$^{0.65}$, BC2=1.0 · 10^{-7}
NFRAC=20. Floc breakup: MODE=1. Calculation alternative: 4.

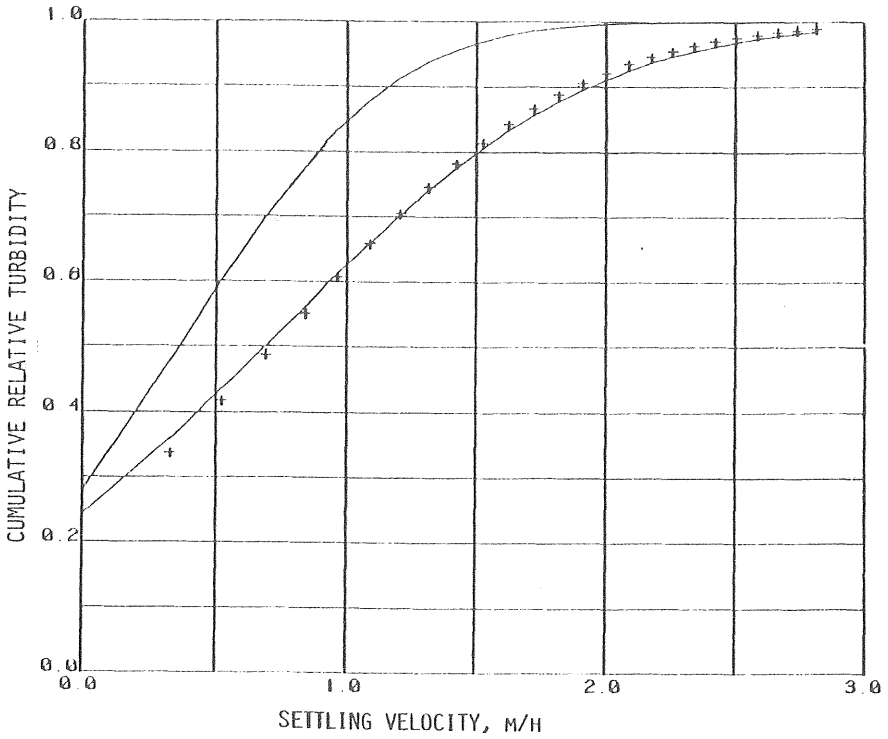

Fig 5-32. Cumulative settling velocity distributions. Measured result compared to calculated result according to eq. 5-37.
Run A4A2033. GC1=3.9 · 10^{-5}/GVALUE$^{0.65}$, BC2=1.0 · 10^{-7}
NFRAC=20. Floc breakup: MODE=1. Calculation alternative: 4.

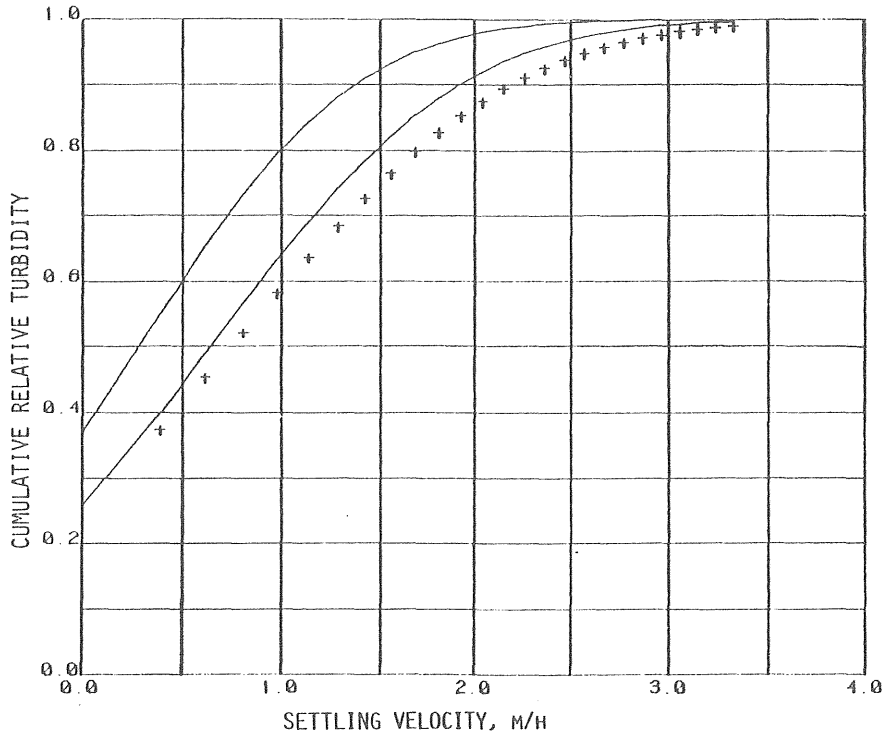

Fig 5-33. Cumultative settling velocity distributions. Measured result compared to calculated result according to eq. 5-37.
Run A4A2034. GC1=3.9 · 10^{-5}/GVALUE$^{0.65}$, BC2=1.0 · 10^{-7}
NFRAC=20. Floc breakup: MODE=1. Calculation alternative: 4.

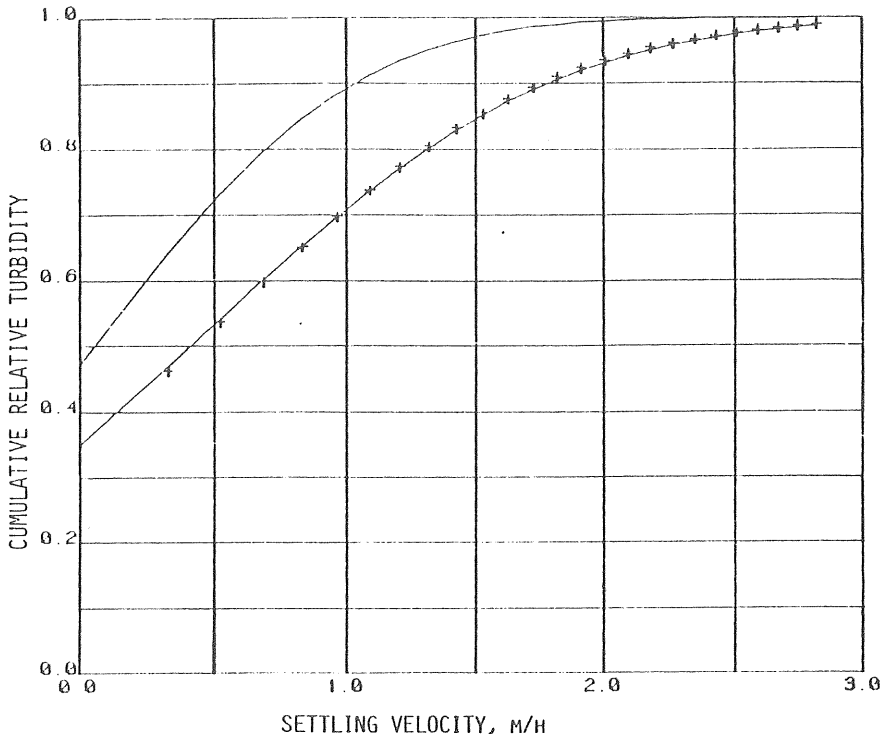

Fig 5-34. Cumulative settling velocity distributions. Measured result compared to calculated result according to eq. 5-37.
Run A4A2035. GC1=3.9 · 10^{-5}/GVALUE$^{0.65}$, BC2=1.0 · 10^{-7}
NFRAC=20. Floc breakup: MODE=1. Calculation alternative: 4.

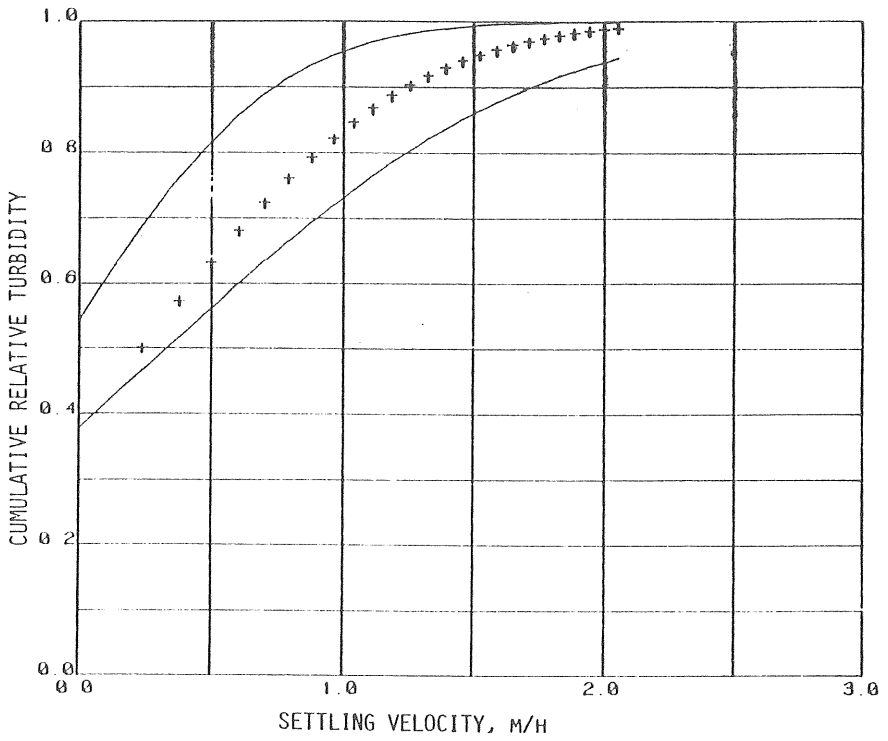

Fig 5-35. Cumulative settling velocity distributions. Measured result compared to calculated result according to eq. 5-37.
Run A4A2036. GC1=3.9 · 10^{-5}/GVALUE$^{0.65}$, BC2=1.0 · 10^{-7}
NFRAC=20. Floc breakup: MODE=1. Calculation alternative: 4.

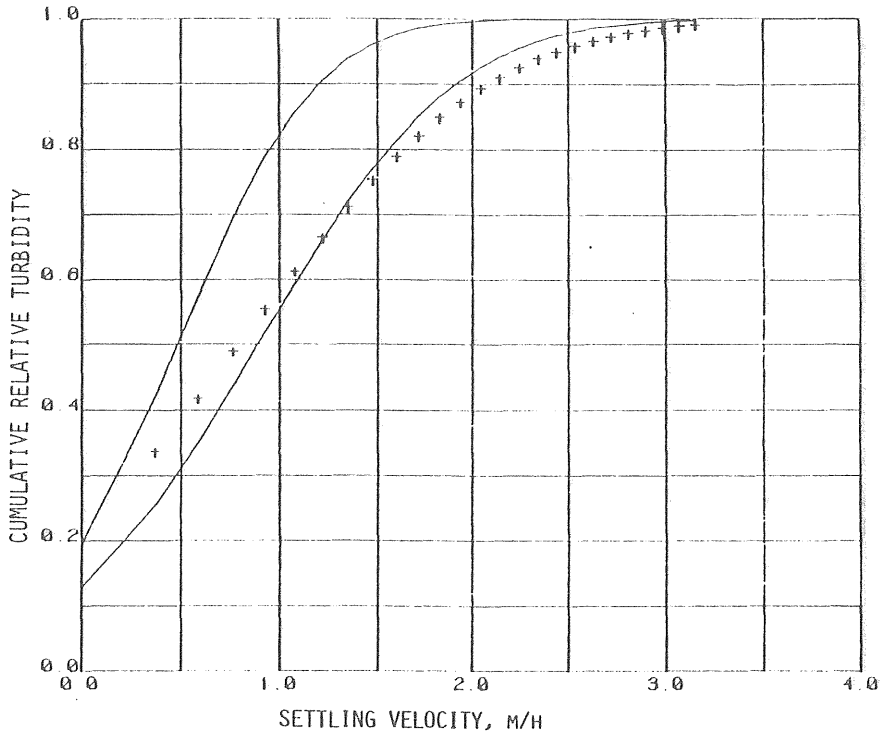

Fig 5-36. Cumulative settling velocity distributions. Measured result compared to calculated result according to eq. 5-37.
Run A4A2041. GC1=3.9 $\cdot 10^{-5}$/GVALUE$^{0.65}$, BC2=1.0 $\cdot 10^{-7}$
NFRAC=20. Floc breakup: MODE=1. Calculation alternative: 4.

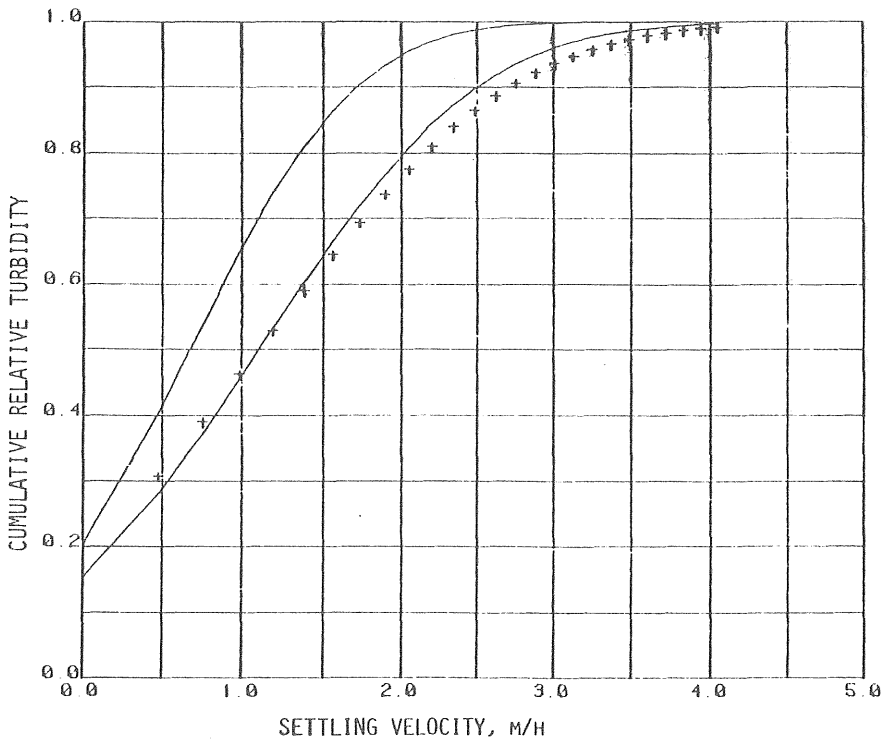

Fig 5-37. Cumultative settling velocity distributions. Measured result compared to calculated result according to eq. 5-37.
Run A4A2042. GC1=3.9 $\cdot 10^{-5}$/GVALUE$^{0.65}$, BC2=1.0 $\cdot 10^{-7}$
NFRAC=20. Floc breakup: MODE=1. Calculation alternative: 4.

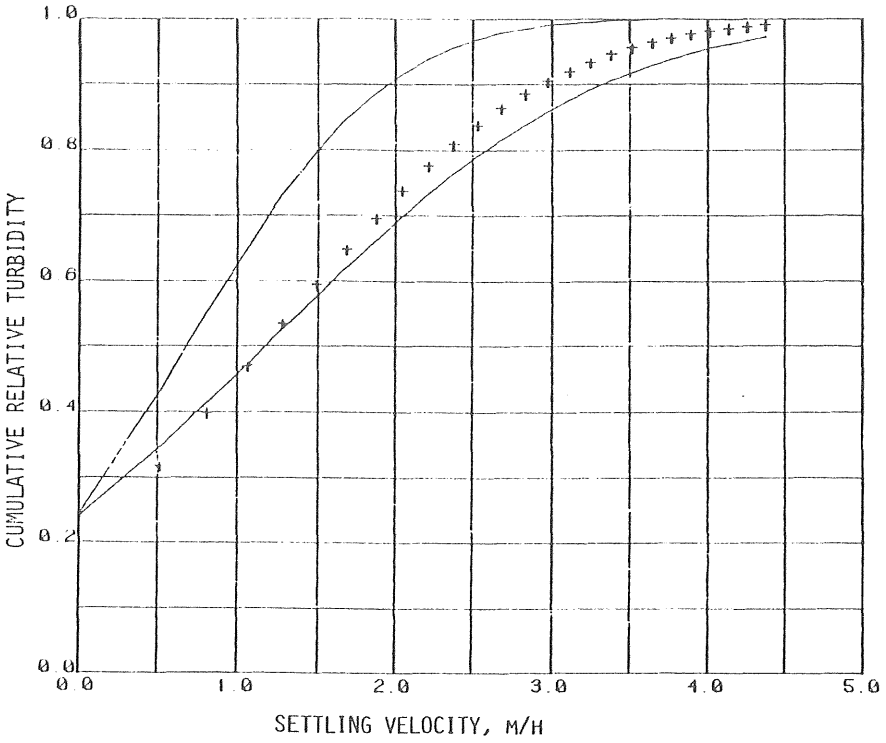

Fig 5-38. Cumulative settling velocity distributions. Measured result compared to calculated result according to eq. 5-37.
Run A4A2043. GC1=3.9 · 10^{-5}/GVALUE$^{0.65}$, BC2=1.0 · 10^{-7}
NFRAC=20. Floc breakup: MODE=1. Calculation alternative: 4.

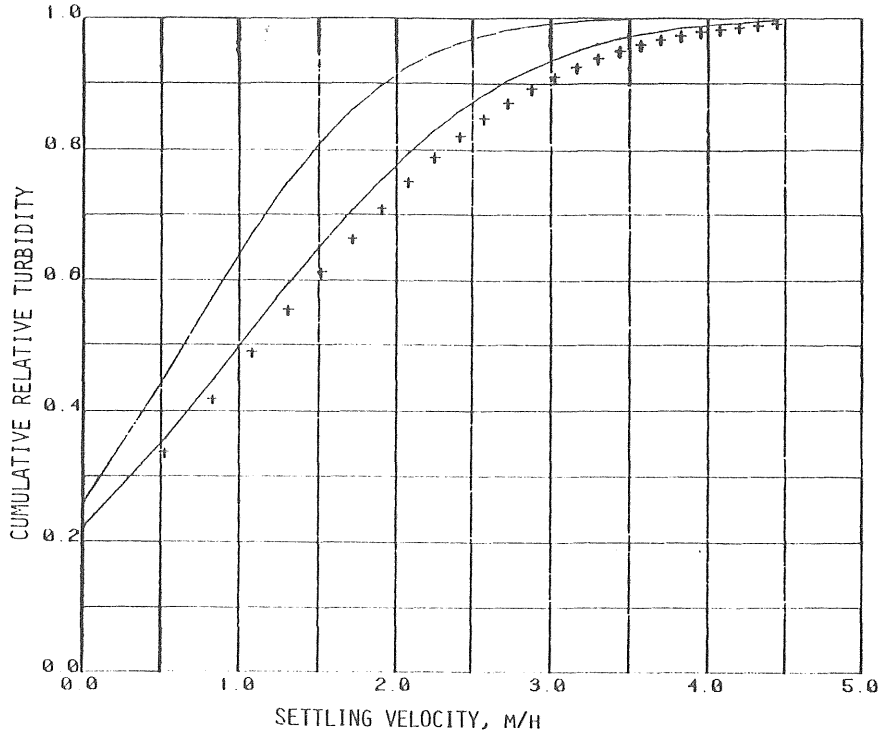

Fig 5-39. Cumultative settling velocity distributions. Measured result compared to calculated result according to eq. 5-37.
Run A4A2044. GC1=3.9 · 10^{-5}/GVALUE$^{0.65}$, BC2=1.0 · 10^{-7}
NFRAC=20. Floc breakup: MODE=1. Calculation alternative: 4.

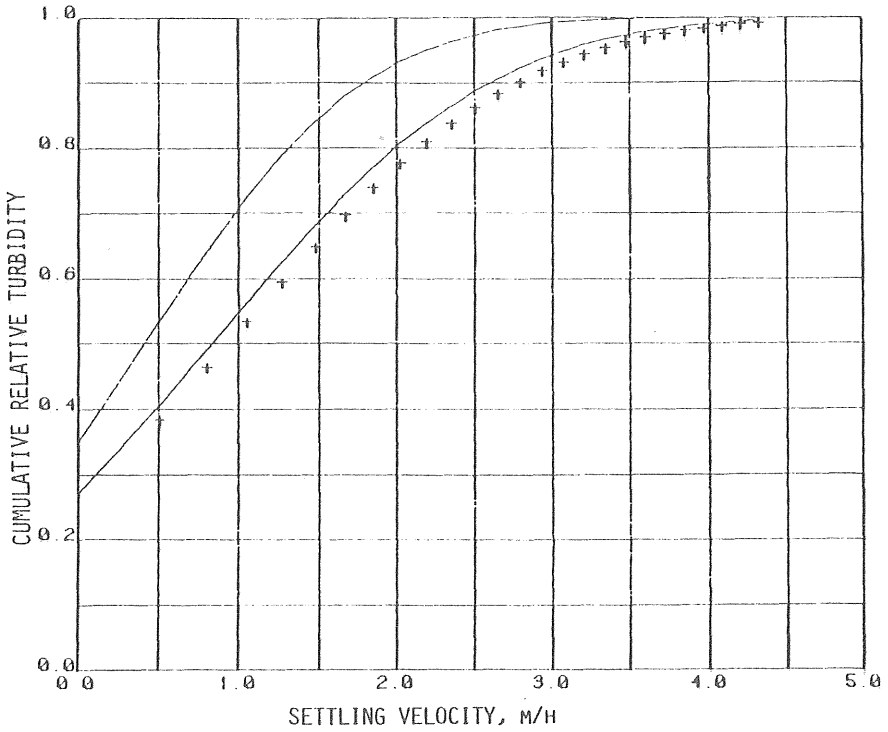

Fig 5-40. Cumulative settling velocity distributions. Measured result compared to calculated result according to eq. 5-37.
Run A4A2045. GC1=3.9 · 10^{-5}/GVALUE$^{0.65}$, BC2=1.0 · 10^{-7}
NFRAC=20. Floc breakup: MODE=1. Calculation alternative: 4.

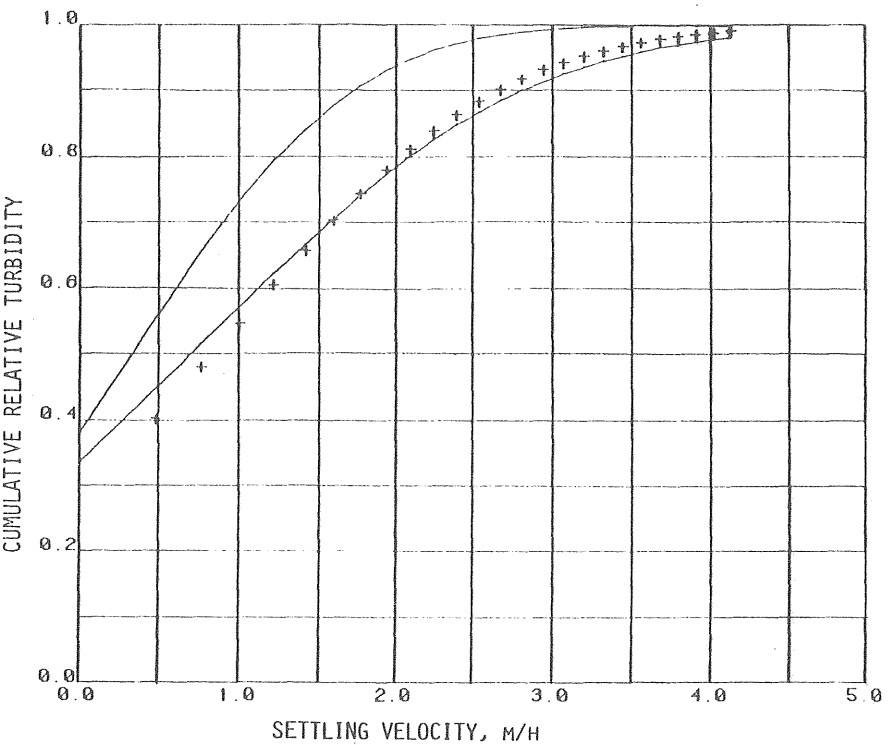

Fig 5-41. Cumultative settling velocity distributions. Measured result compared to calculated result according to eq. 5-37.
Run A4A2046. GC1=3.9 · 10^{-5}/GVALUE$^{0.65}$, BC2=1.0 · 10^{-7}
NFRAC=20. Floc breakup: MODE=1. Calculation alternative: 4.

5.4 Discussion and some consequences of the particle size distribution model

In the previous section a particle size distribution model was developed and was found reasonably well conform to measured data obtained at a variety of flocculation conditions.

The results obtained, when the particle size distribution model was compared to obtained data, can be summarized as follows:

1 The particle growth rate was found proportional, not as was expected to the G-value, but approximately to the G-value raised to the exponent 1/3.

2 The particle breakup rate was found to be proportional to the G-value raised to the exponent 3.25.

3 The sensitivity for disruption of the flocs increased with their diameter raised to the exponent B.

4 A breakup mechanism, where floc fragments are distributed equally in number to sizes less than the broken floc, was shown to be the most appropriate of those tested.

5 The addition of activated silica only affects the breakup rate proportionality constant, the latter can be interpreted as inversely related to the floc strength.

The relatively limited range of G-values for which the model could be tested (3.4-15.3 s^{-1}) has, naturally, some impact when the generality of the findings shall be discussed.

There is some possibility, when the particle growth was found to depend of the G-value to a less extent than was expected, that some other factor is affected at the same time. For example, the residence time distribution is likely to be affected by the mixing intensity in the reactor. An increased G-value then would mean a residence time distribution closer to that of an ideal completely mixed reactor. Such an effect would cause an interpretation of measured data as a less impact on growth rate of the G-value. However, as was stated in Section 5.1, measurements of the residence time distribution for the present tank design did not show any marked effects in that direction. Besides, if a direct proportionality between G-value and growth rate is assumed and GCl is a constant, then T (if the effect of a flow pattern closer to plug-flow is expressed as an increase of the equivalent mean residence time for a completely mixed reactor) in eq. 5-37 has to vary 2.7 times to account for the variations in growth rate from the lowest up to the highest applied G-value, which not seems probable.

There is of course a possibility that the real flocculation pattern is not adequately described by the model, and that the effects interpreted are only apparent. For example, it has been proposed that flocculation only occurs when the flocs to aggregate are relatively equal in size. The possible effect of such a mechanism has not been examined.

The size - disruption relationship stated is concluded from simplified assumptions and the size exponent of B is only apparent. As floc size never was measured a more correct conclusion would be:

The sensitivity for disruption of the flocs increase with their settling velocity raised to the exponent 4. (See eq. 5-30).

In order to illustrate some general features of the particle size distribution model a number of calculations (independent of measured data)were performed. The parameters of an initial settling velocity distribution were chosen to v_m=0.3 m/h and σ = 0.3 m/h. The changes of the settling properties were calculated for varying mean residence times, G-values, and degree of compartmentalization. The calculated result is, naturally, dependent on the initial settling velocity distribution. Therefore, the following figures should only be seen as shematic illustrating pictures.

As start values, moreover, for calculation reasons it is demanded that a settling velocity distribution is given. Hereby difficulties arise when the initial flocculation course is to be calculated. There is no basis to judge what is a reasonable input in the very beginning of the process. One possibility is to perform calculations backwards (see calculation alternative 2) for different experiments. In fact, such computations were performed, but the results were uncertain. Besides, the flocculation pattern description here becomes speculative as the power input usually is appreciably higher than the values for which the model could be tested.

The chosen initial settling characteristics thus can be seen as representative for values occuring in the "middle" of the flocculation process.

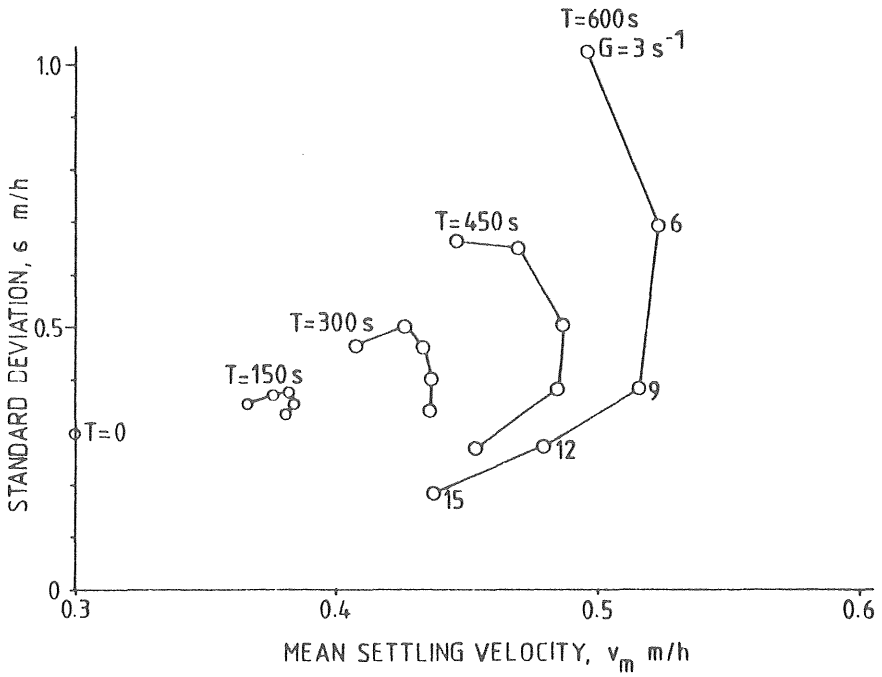

Fig. 5-42 Calculated changes of an initial settling velocity distribution (v_m=0.3 m/h, σ=0.3 m/h) after flocculation in one completely mixed reactor. Varying mean residence time (T,s) and G-value. GC1=3.9·10^{-5}/GVALUE$^{0.65}$, BC2=1.2·10^{-6} NFRAC=50. Floc breakup: MODE=1. Calculation alt.:4

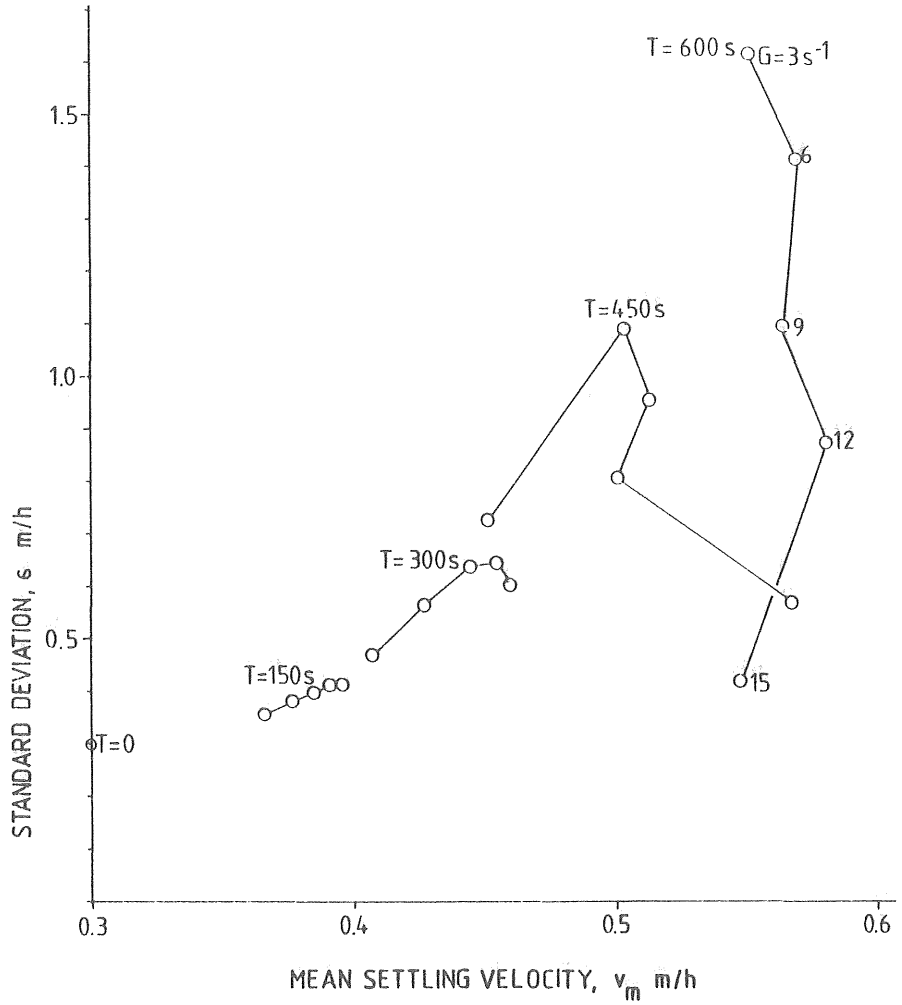

Fig. 5-43 Calculated changes of an initial settling velocity distribution (v_m=0.3 m/h, σ = 0.3 m/h) after flocculation in one completely mixed reactor. Varying mean residence time (T,s) and G-value. GC1=3.9·10^{-5}/GVALUE$^{0.65}$, BC2=1.0·10^{-7}. NFRAC=50. Floc breakup: MODE=1.Calculation alt.: 4.

The figures 5-42 and 5-43 show the calculated performance if the mean residence time T and the G-value are varied in one completely mixed flocculation tank. In order to make the changes more evident, the v_m-axis is drawn to another scale than the σ-axis. The breakup and growth constantsare given the same values as those previously shown valid with and without the addition of activated silica (figs. 5-43 and 5-42, respectively).

The computational result becomes more uncertain (= less convergence tendency) the more the distance to the initial settling properties increases. Consequently, the absolute values corresponding to each point can be questioned. However, the principal tendencies of the calculated result seem to make sense:

As the residence time increases, the maximum attainable mean settling velocity increases. The G-value,which corresponds to the maximum point, is decreased with increasing time. If the changes for a constant G-

value is followed, at first the standard deviation (and the mean settling velocity) increases. Then a maximum dispersion is reached, whereupon it is reduced together with a vanishing growth of the mean settling velocity. The differences between fig. 5-42 and fig. 5-43 reflects the improved strength of flocs caused by the activated silica; in the model expressed as a diminished breakup constant BC2.

A low G-value and a long detention time result in an appreciable increase in the dispersion of floc sizes. The absolute value of that increase, at e.g. G=3 s^{-1}, is questionable. Strictly, the changes in the settling velocity distribution in that case imply a slightly deteriorated floc quality. It is believed intuitively that mixing at low mixing intensities cannot make the floc settling properties to be worse than in the proceeding flocculation tank.

The effect of a compartmentalization of the flocculation volume is illustrated in figs. 5-44 and 5-45. The total flocculation time (300 s) is here kept constant, and the number of completely mixed flocculation tanks in series (N) is varied from 1 to 8. The division of the reactor volume leads to a dramatic improvement of the floc quality, independent of the G-value. The mean settling velocity increases with increased division of the flocculation volume, and most importantly: the standard deviation decreases at the same

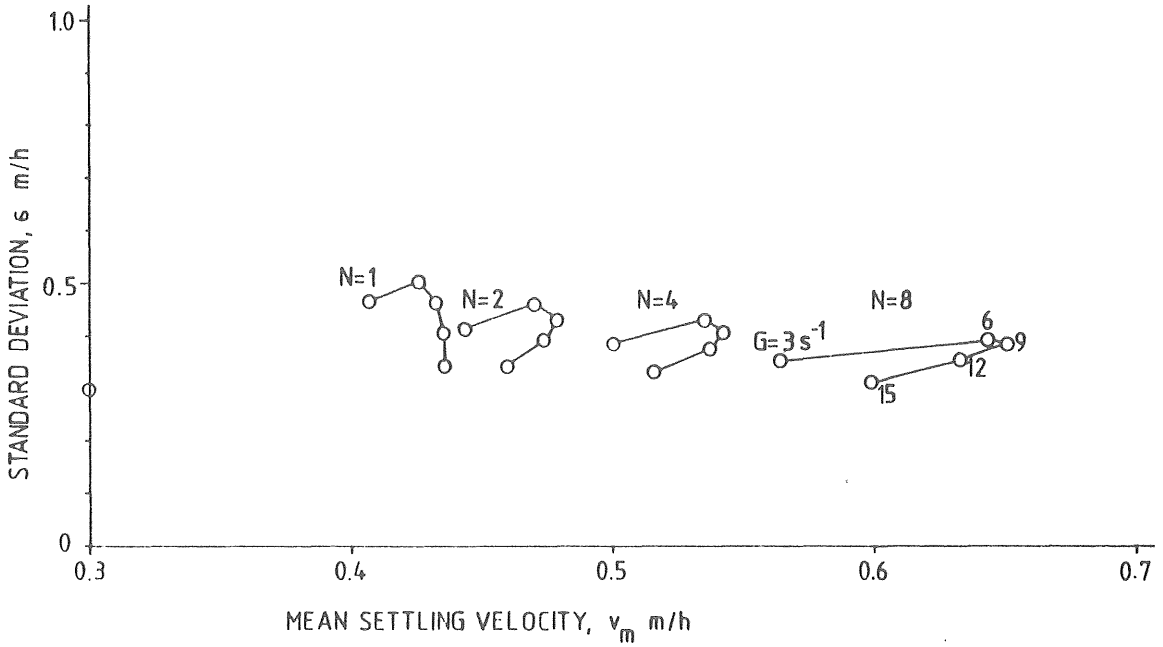

Fig. 5-44 Calculated changes of an initial settling velocity distribution (v_m=0.3 m/h, σ = 0.3 m/h) after flocculation in various number (N) of completely mixed reactors. Total flocculation time T=300 s. GC1=3.9·10^{-5}/GVALUE$^{0.65}$,BC2= 1.2·10^{-6},NFRAC=50.Floc breakup: MODE=1. Calc.alt.:4.

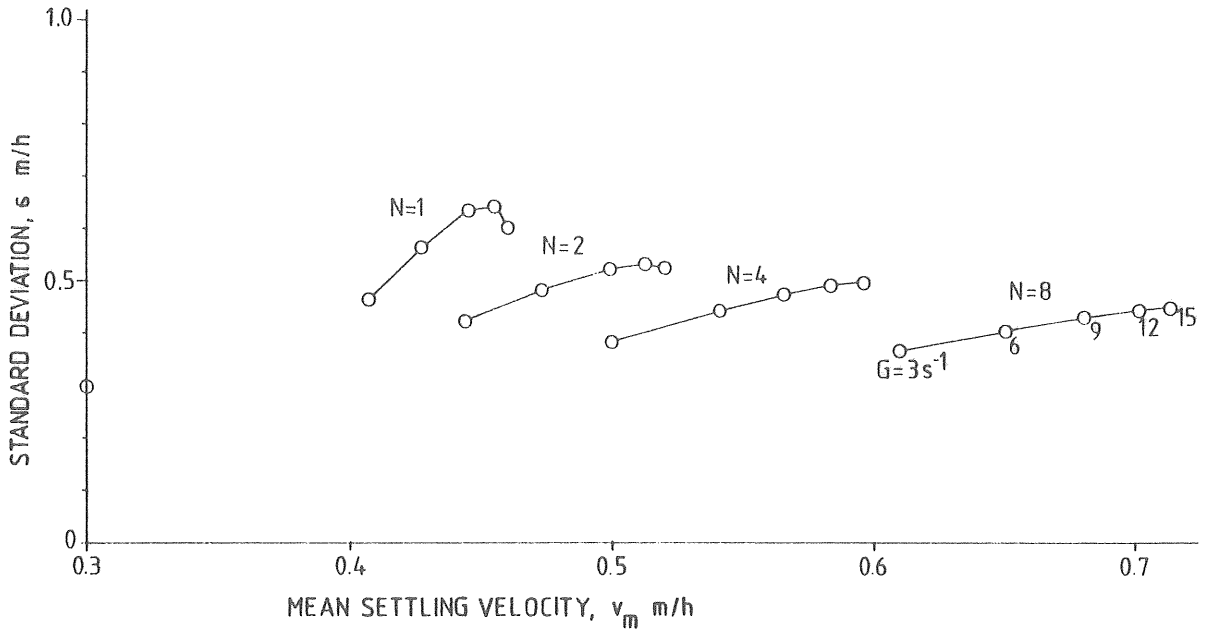

Fig 5-45 Calculated changes of an initial settling velocity distribution (v_m=0.3 m/h, σ = 0.3 m/h) after flocculation in various number (N) of completely mixed reactors. Total flocculation time T=300 s. GC1=$3.9 \cdot 10^{-5}$/GVALUE$^{0.65}$, BC2=$1.0 \cdot 10^{-7}$.NFRAC=50.Floc breakup: MODE=1. Calc.alt.:4.

time. Principally, these effects were expected, but it is striking (in fig. 5-45) that the lowest G-value shows the least dispersion of floc sizes after 8 compartments. The situation is somewhat different in fig. 5-44, where the floc breakup evidently has (and should have) a more accentuated impact on the calculated result. In the figures 5-44 and 5-45 (contrary to the results in figs. 5-42 and 5-43) the results rather become more certain, from a calculation point of view, as the distance to the initial floc properties is increased. It is so because the calculations are performed successively in smaller steps as the number of compartments increases.

6 SOME ASPECTS ON THE OPERATION OF WATER TREATMENT PLANTS

The determination of appropriate power input into the flocculation unit is of little value unless, for example, the required coagulant dose and a correct pH-value are applied. Thus the results referred to in Chapter 4 are only valid if the basic conditions stated in Chapter 2 are fulfilled. Investigations at 20 Swedish water treatment plants revealed that in many cases this was not the case. In Section 4.3.2 more specific information concerning the power input and the floc settling properties found at the plants were given. Here, some general aspects will be mentioned.

The operational problems were often found to be more fundamental than the factors dealed with in Chapter 4, in spite of the fact that chemical treatment of surface waters is considered to be a well known practice.

The dose of the coagulant added, exclusively aluminium sulphate, was on the whole almost the same as the required dosage obtained from jar-tests according to Chapter 2. Figure 6-1 shows the applied dose as a function of the required dose obtained from the laboratory experiments. The deviation from the required dose usually is less than 10%. An overdose with respect to the required dose is more common than the opposite. Hardly any plant applies a dose more than 15% below the required one.

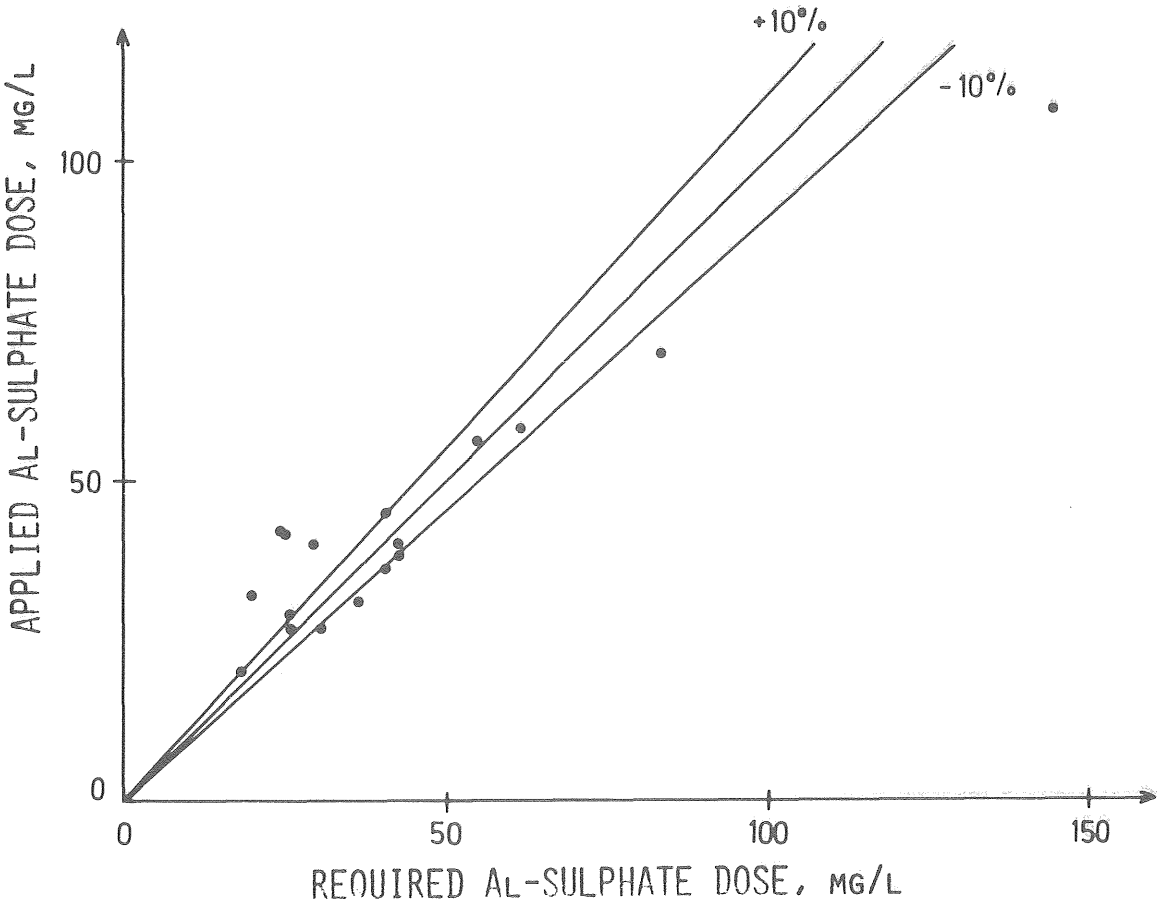

Fig 6-1. Applied aluminium sulphate dose compared to the required dose obtained at jar tests.

The pH-value has a dominating influence on the treatment result achieved. Depending on the coagulant dose in relation to the required dose, the required accuracy varies to some extent. The effect of varying the pH-value on different measured treatment parameters can be seen in detail in the figures 2-2 to 2-41. Insufficient supervision of the pH can to some extent be compensated by an overdose of the coagulant. On the other hand the demands for accurate pH-measurements are increased as the required dose is approached.

The difficulties to obtain an accurately measured pH-value can be great when the water temperature is low and the water is poorly buffered.

The jar-test results made it possible to estimate a favourable pH-interval at the coagulant dose applied at the plant. In figure 6-2 this interval is indicated as ordinate. The width of this interval is among other things depending on the relation between applied and required coagulant dose. As abscissa the measured pH-value at the plant is indicated. A number of samples were measured. The size of this interval is a measure on the process stability, when pH is considered. (Values less than 0.1 pH-units are not indicated).

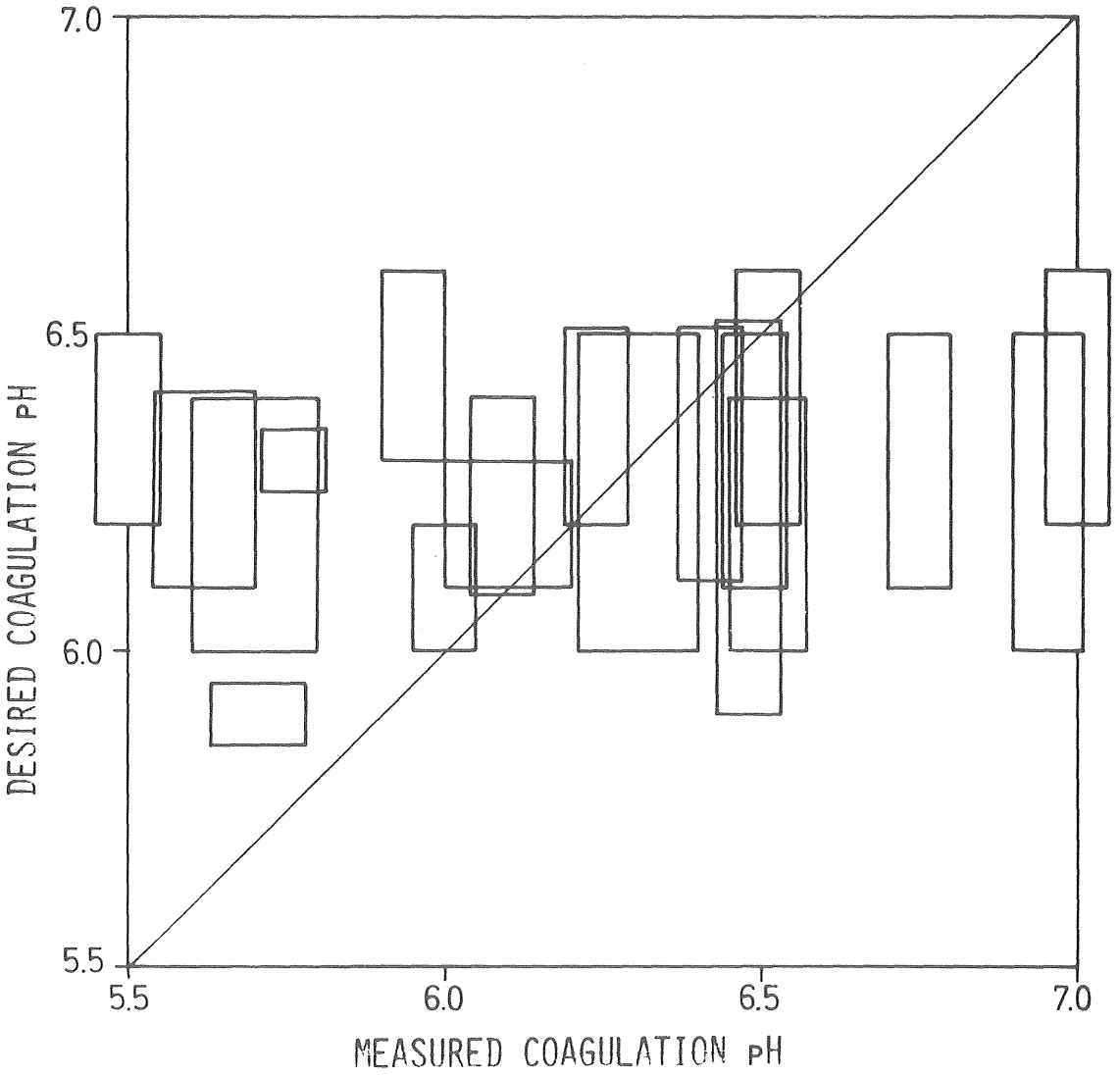

Fig 6-2. Desirable coagulation pH and measured values.

If measured and desirable values coincide, i.e. indicated areas are crossed by the 45^{o}-line, the pH-control works satisfactorily. As can be seen, this is not always the case. At about half of the plants the deviation from the desired value is more than 0.2 pH-units.

These deviations are more evident in figure 6-3, where my pH-values are compared with pH-values recorded by continuous instruments or with analyzes obtained from the plant operator. It can be seen that the coagulation pH, for some reason, is deliberately held at a value differing from the optimum in some cases.

On the vertical axis thus the believed pH-values are indicated, on the horizontal axis the "real" ones. Great efforts were made to minimize systematic errors attributed to the latter value: The measurements, the two point buffering, and the storing of the low temperature electrode, were carried out at the present raw water temperature. The measurements were allowed to take some time. It was shown that the time required (at ca. $2^{o}C$) for the pH-reading to return to an inititial value after an intermediate buffering was at least 10-15 minutes. If there still is some systematical error left, in spite of these efforts, then the pH-values of the presented jar-test experiments should be attributed to an error of the same magnitude, because the measurements were carried out in the same way.

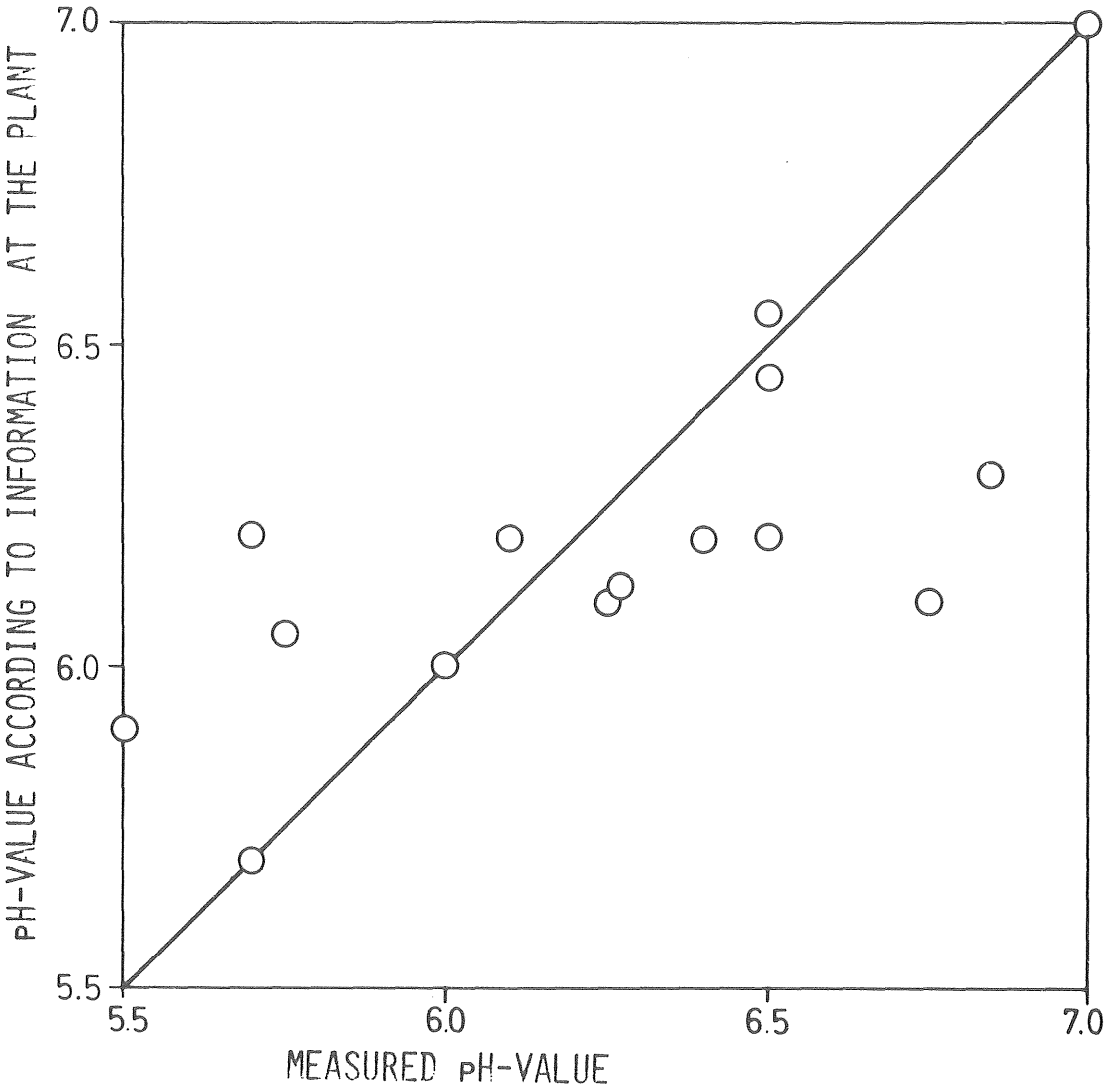

Fig 6-3. Coagulation pH according to information at the plant compared to measured values.

It was concluded in Section 4.3.2 that the power input applied generally is low. In figure 6-4 this is schematically illustrated. Here the theoretical sedimentation result (calculated from settling tests in the last flocculation tank) at the surface load 0.5 m/h is indicated as a function of the maximum G-value encountered during the flocculation. The latter is assumed to be a measure of the power input on the whole, especially in the beginning of the flocculation process. (The highest G-value is in fact usually encountered in the first flocculation tank).

In the figure it has been considered whether the coagulation pH lies within the desired interval and if activated silica is added. A wide distribution of the values can be observed. However, a tendency of improving sedimentation result can be observed with increasing maximum G-values. The effect of the activated silica can be questioned in some cases.

Most water treatment plants are here represented by more than one point because flocculation systems in parallel were measured separately.

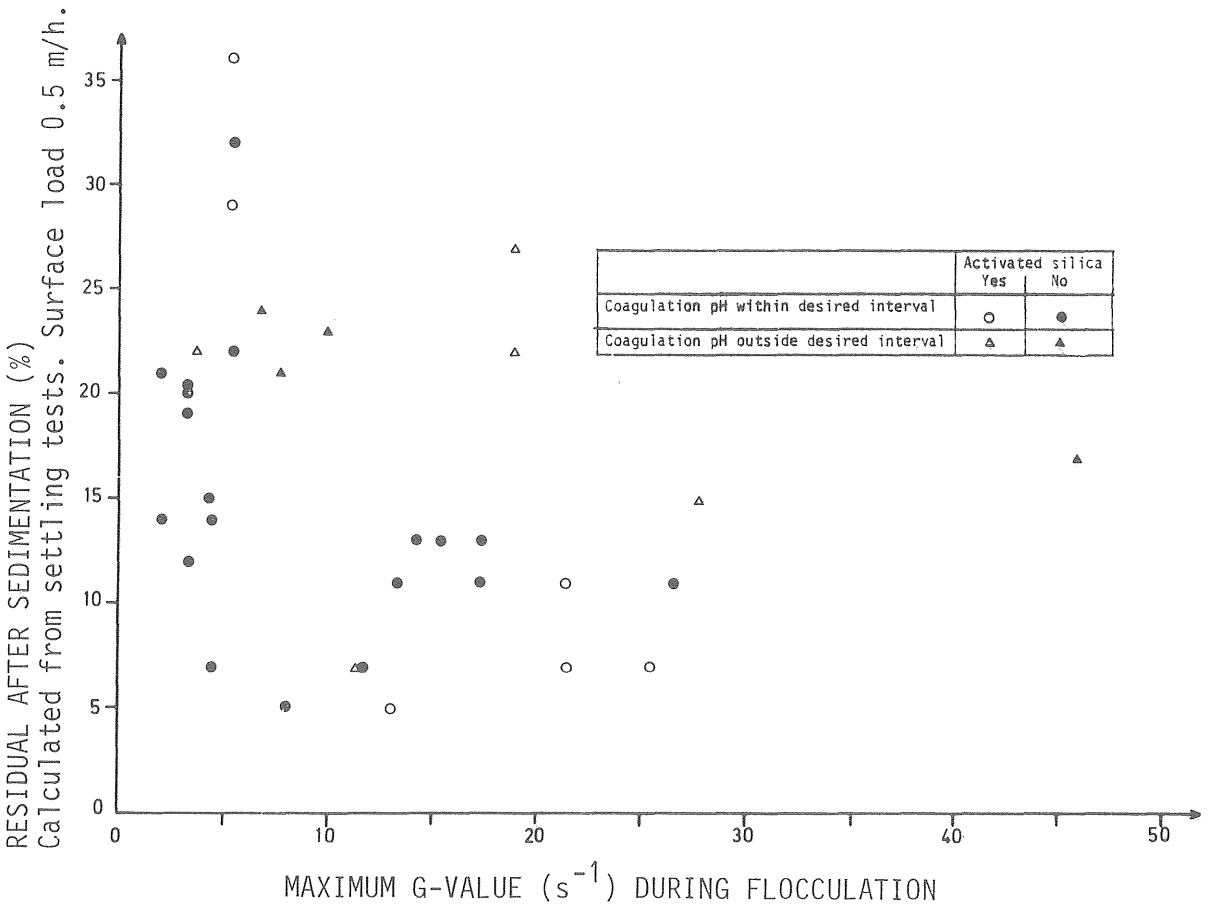

Fig 6-4. Theoretical sedimentation result at a surface load of 0.5 m/h (calculated from settling tests in the last flocculation tank) as a function of maximum G-value encountered during the flocculation.

The performance of the full scale sedimentation basin can be seen in the figure 6-5. The residual amounts of flocs are indicated compared to the applied overflow rate. Extreme variations of the sedimentation efficiency occur: From 3% up to 40% flocs remaining after sedimentation.

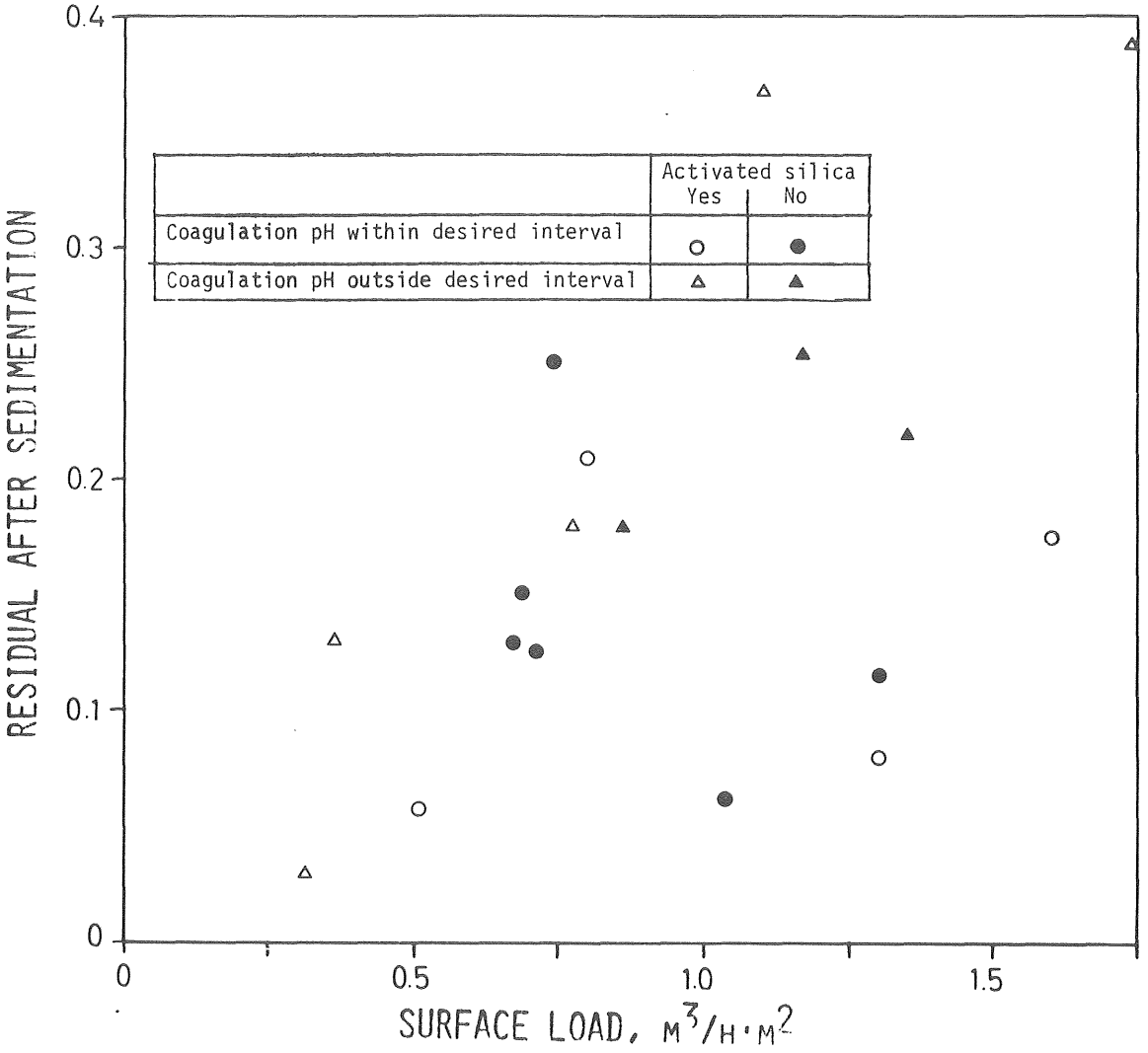

Fig 6-5. Sedimentation efficiency versus overflow rate.

The conditions related above have of course some consequences for the effluent quality from the filter units. These are most evident if the residual aluminium content of the filtrate is analyzed. In the figure 6-6 measured concentrations of aluminium in the filtrates of the treatment plants are indicated as ordinates. When possible, samples were taken from a filter recently back-washed and from that in turn to be cleaned. This gives two values between which the aluminium content of the filtrate is supposed to vary.

On the horizontal axis the results from the laboratory tests are found (with the same coagulant dose as applied at the plant and with optimum coagulation pH). The possible result at the present dose is thus indicated. The Swedish standard for the aluminium content in tap water (denoted as "technically noticeable"), 0.15 mg Al/l, is introduced as a vertical and a horizontal line.

High columns in the diagram indicate too long filter runs before back-washing.

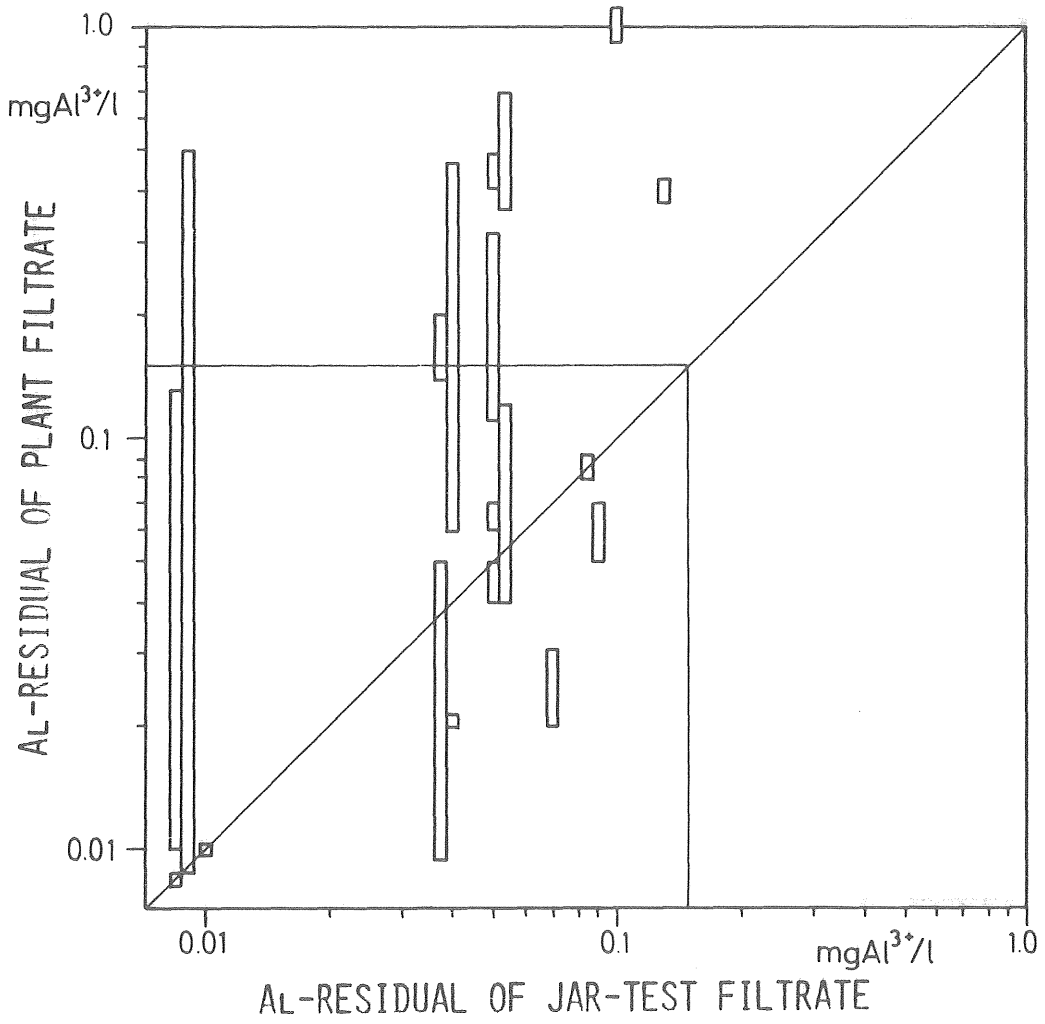

Fig 6-6. Residual aluminium content in the filtrate of water treatment plants compared to laboratory results.

The corresponding diagram, but with respect to organic matter as measured by the permanganate number is found in figure 6-7. The Swedish standard of 20 mg $KMnO_4$/l evidently represents a too low level of ambition. No appreciable difficulties would occur at any water treatment plant to achieve half this value.

The values here are not always quite comparable, because some treatment plants have granulated activated carbon as filter medium. Thus an additional remove of organic matter is obtained during the filter operation by adsorption.

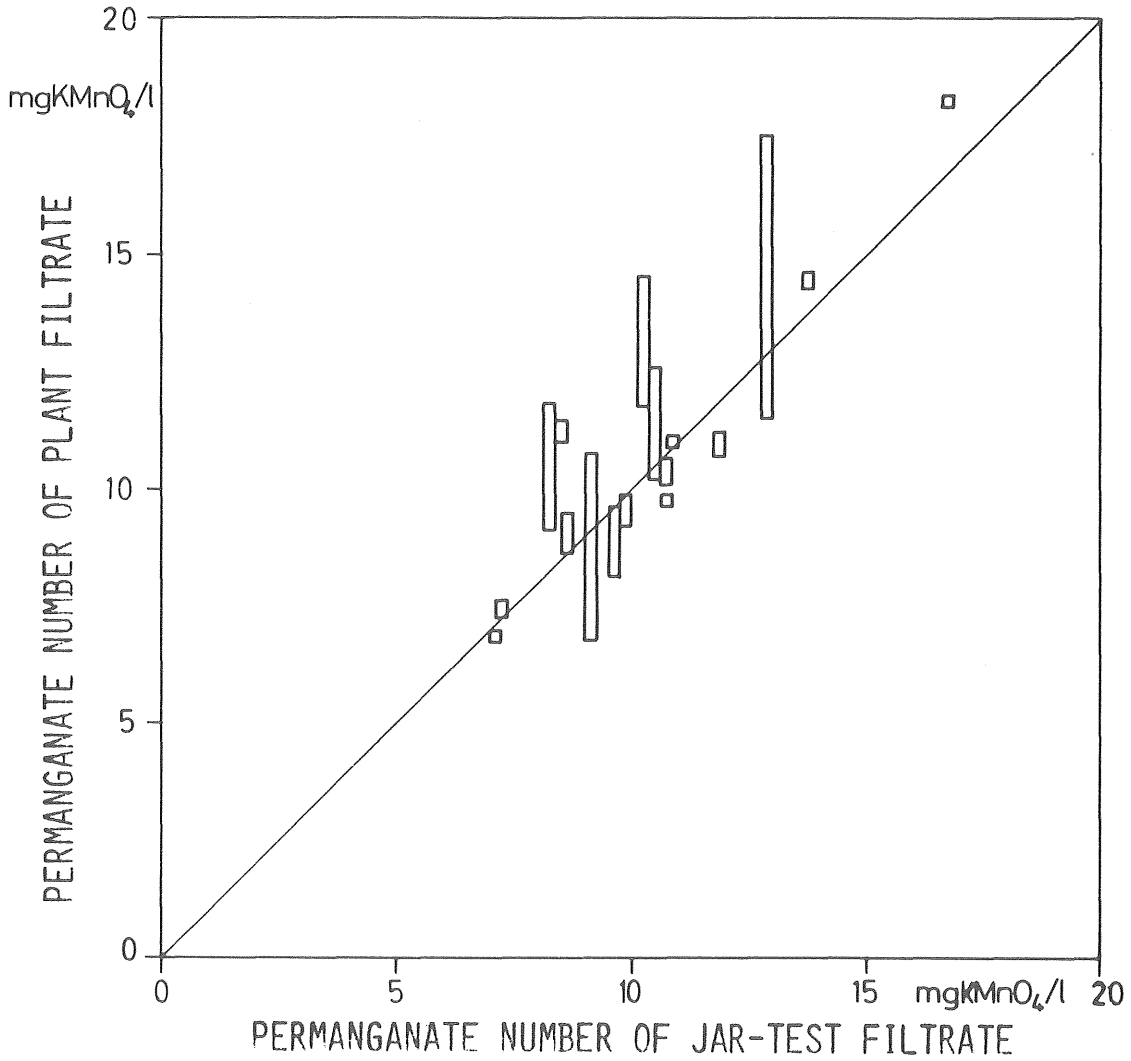

Fig 6-7. Permanganate number of the filtrate in the water treatment plants compared to laboratory results.

As a conclusion rather simple actions would in many cases improve effluent quality considerably.

A basic requirement (apparently not self-evident) for the effective supervision of a treatment process is instruments that provide the operator with correct values of relevant parameters.

Effective measurement and control of the coagulation pH are of greatest importance.

For the supervision of the filter operation a turbidity meter is the most suitable (and also the most simple) instrument.

The head loss over the packed filter bed is sometimes used as an indicator of the time to start back-washing. When a prescribed value is reached (usually 1-1.5 m water pressure) the filter run is stopped. This is not satisfactory for several reasons. Firstly, the head-loss meters often do not work. Secondly, the resistance of the separated matter towards break-through varies considerably with factors such as water temperature, chemicals added and properties of the filter bed. (See e.g. Hedberg, 1976).

Filter back-washings at predetermined time intervals are also common. If the operator is lucky all works well. If the separation efficiency of the sedimentation operation for some reason is low, a filter break-through is likely to occur. Without any measurements of the filtrate quality, which is the rule, the operator has no opportunity to determine if he is successful or not.

The floc settling properties can in many cases be improved by simple measures. This is dealt with to some extent upon in Section 4.3.2. The mean velocity gradient in the beginning of the flocculation process should be about 20 s^{-1} when the total flocculation time is as long as 1 hour. At shorter flocculation times (e.g. 30 min) this value might be doubled.

The effect of so called activated silica in practical operation has in some cases been shown to be questionable. A control of the preparation of the neutralized silica sol seldom occurs.

7 SUMMARY

In this thesis the influence of some important factors affecting the coagulation of surface waters is studied, particularly the flocculation-sedimentation process. The objective of the thesis is to provide data and procedures for an appropriate design and an effective operation of the flocculation stage of a conventional water treatment plant.

In Chapter 2 coagulation of aquatic humus is briefly reviewed. Measurements on a full scale together with laboratory coagulation tests were carried out at 20 Swedish water treatment plants. The jar test results obtained showed good agreement with the treatment result of each water treatment plant, at the corresponding coagulant dose and pH-value. The required coagulant dose was found to be related to the properties of the raw water. However, the relationship between raw water quality and coagulant dose, is not accurate enough to replace the trial-and-error method, the jar test procedure.

In Chapter 3 flocculation theories are reviewed. The problem of measuring "flocculation efficiency" is discussed. It is quite natural when sedimentation is applied for separation, to characterize the floc quality in terms of settling properties. A method is presented how to treat quiescent column settling data to obtain a normally distributed settling velocity distribution characterized by a mean settling velocity and a settling velocity standard deviation. Theoretical considerations and an adjustment to practical results leads to a method useful for computing the result of a continuous sedimentation process from quiescent column settling data. The mean settling velocity and the dispersion of settling velocities as well, have to be considered when optimum floc properties are to be determined. A high mean settling velocity does not necessarily mean a good floc quality. Furthermore, optimum floc settling properties cannot be determined if not the sedimentation operation is considered simultaneously.

Methods to measure and to calculate the power input to a flocculation tank encountered in the literature are critically reviewed. It is shown that an widely used expression, originally developed by Camp, has to be revised. Measurements from laboratory up to a full scale are presented, which show excellent agreement with theory.

In Chapter 4 results from flocculation experiments are presented. The influence of power input, flocculation time, activated silica, water temperature, paddle design, and reactor design is investigated in pilot-plant experiments. A great number of measurements carried out at water treatment plants are also reported. The results can briefly be outlined as follows:

- An exponential tapered power input from varying initial values was applied. If this initial value is increased (at a constant flocculation time) the settling velocity standard deviation is continuously decreased. The mean settling velocity will increase to a certain value. A further increase of the power input reduces the mean settling velocity. The change of the settling properties caused by variations of the power input is described.

- Three different paddle designs were investigated. No important differences in flocculation efficiency were observed at a constant power input level.

- A great number of experiments were carried out at a low water temperature, ca. $2^{o}C$. For a total flocculation time of 20 minutes with 40 mg/l Al-sulphate dose, the maximum attainable mean settling velocity is about 0.7 m/h. The settling velocity standard deviation is of the same magnitude. When activated silica is added the mean settling velocity and the standard deviation are increased to 1.1 m/h and 1.3 m/h, respectively. The corresponding values, if only the flocculation time is altered to 10 or 30 minutes, are (0.5, 0.6) and (1.4, 1.3) respectively. An increase of the temperature to about $20^{o}C$ brings about a mean settling velocity of 1.6 m/h and a standard deviation of 2.3 m/h, if no activated silica is added. With the addition of 2 mg activated silica the corresponding values were 3.5 m/h and 4 m/h, respectively.

ON FLOCCULATION EFFICIENCY IN WATER TREATMENT

by

Claes Hernebring

AKADEMISK AVHANDLING

som för avläggande av teknisk doktorsexamen vid Chalmers tekniska högskola kommer att försvaras offentligt den 10 december 1981 kl. 10.15 i Palmstedtsalen, CTH, Sven Hultins gata 2, Göteborg

Fakultetsopponent: Docent Hallvard Ödegaard

Examinator: Professor Peter Balmér

ON FLOCCULATION EFFICIENCY IN WATER TREATMENT

Claes Hernebring, Department of Sanitary Engineering, Chalmers University of Technology, S-412 96 Göteborg, Sweden

ABSTRACT

This work deals with the preparation of water for consumption by chemical treatment of surface waters. The main object of the study is the flocculation-sedimentation process.The ultimate goal is to develop methods and models for a quantitative description of the effects in terms of sedimentation performance caused by factors affecting the flocculation efficiency.

A method how to carry out quiescent column settling tests and treat the settling data in order to predict the performance of a continuously operated sedimentation tank is presented.

It was found that the optimum floc settling properties have to be determined in a procedure where the flocculation and the sedimentation operations are considered simultaneously.

The influence of power input, water temperature, activated silica, flocculation time, paddle shape and reactor design is described.

Coagulation experiments were carried out on a laboratory scale at 20 Swedish water-treatment plants. The flocculation efficiency at each plant was measured. The jar-test results obtained are compared with the treatment plant performance.

A flocculation model has been developed, which is able to predict the changes of a settling velocity distribution caused by various power input levels in the flocculation tank. The model was tested for a relatively limited range of G-values (3.4 -15.3 s^{-1}). The floc growth rate was found to be proportional to the G-value raised to the exponent 1/3. The floc breakup rate was appr. proportional to G^3. The sensitivity for disruption of the flocs increased with their settling velocity raised to the exponent 4. Thus, a basis is provided for the determination of an optimum operation of the flocculation-sedimentation process in a water treatment plant.

Key words:
Flocculation, Water Treatment, Floc Settling, Sedimentation, Coagulation.

- The design of a flocculation unit, where the size of the reactors gradually is increased, has been tested and compared with the conventional design with a constant reactor size. The results reveal a pronounced additional flocculation efficiency at short flocculation times (10-20 minutes) for the nonuniform system.

In Chapter 5 measured data are tested according to their consistency with prevailing flocculation theories. A satisfactory explanation of the various results was not obtained. The previous models, however, were not able to adequately describe the expected result after a separation process (only sedimentation is considered), and what is most important, how the removal efficiency varies with the applied surface load. A mathematical flocculation model, where the particle size distribution was taken into account, was developed. The accuracy of the model is dependent on assumed breakup patterns. Three different assumptions were made. A breakup mechanism, where floc fragments are distributed equally in number to sizes less than the broken floc, was shown to be the most appropriate of those tested. The model was found to conform reasonably well to measured data obtained at a variety of flocculation conditions. With the model it is possible to calculate the settling properties in the effluent of a flocculation tank, based on an initial settling velocity distribution. The main parameters determining the floc growth process are the power input and the flocculation time. The model could be tested, however, only for a relatively limited range of G-values (3.4 - 15.3 s^{-1}). The results obtained can be summarized as follows:

- The floc growth rate was found to be proportional, not as was expected to the G-value, but approximately to the G-value raised to the exponent 1/3.

- The floc breakup rate was found to be proportional to the G-value raised to the exponent 3.25.

- The sensitivity for disruption of the flocs increased with their equivalent diameter raised to the exponent 8.

8 REFERENCES

Andreu-Villegas R., Letterman R.D. (1976): Optimizing Flocculator Power Input. ASCE J Environ Eng Div 102(1976):EE2 p 251.

Argaman Y., Kaufman W.J. (1970): Turbulence and Flocculation. ASCE J San Eng Div, Proc (1970) p 223.

Baylis J.R. (1937): Coagulation. Part IV. Effect of the Concentration of Alkaline Carbonates and Neutral Salts. Water Works and Sewerage (1937) p 426.

Bates R.L., Fondy P.L., Fenic J.G. (1966): Impeller Characteristics and Power in Mixing. Part I. Ed. Uhl V.W. and Gray J.B., Academic Press 1966, New York.

Bersillon J.L., Brown D.W., Fiessinger F., Hem J.D. (1978): Studies of Hydroxyaluminium Complexes in Aqueous Solution. J Res US Geol Survey 6(1978):3 p 325.

Bhole A.G. (1973a): Mathematics of Flocculation for a Continuous Flow System. J Inst Eng (India)-PH 53(1973) p 43.

Bhole A.G. (1973b): Computer Simulation of Flocculation Process in Water Treatment. J Inst Eng (India)-PH 53(1973) p 47.

Bhole A.G., Dhabadgaonkar S.M., Jarnekar S.G. (1975): Measurement of Power Input in Flocculation. J Inst Eng (India)-PH 55(1975) p 37.

Bhole A.G., Krishna V.M. (1978): Significance of Tapered Flocculation in the Process of Water Treatment. J Inst Eng (India)-EN 58(1978) p 33.

Bhole A.G. (1980): Measuring the Velocity of Water in a Paddled Flocculator. J Am Water Works Assoc 72(1980) p 109.

Black A.P., Singley J.E., Whittle G.P., Moulding J.S. (1963): Stoichiometry of the Coagulation of Color-Causing Organic Compounds with Ferric Sulfate. J Am Water Works Assoc 55(1963) p 1347.

van Breemen A.N. Niejwstad Th.J., van der Meent-Olieman C.G. (1979): The Fate of Fulvic Acids during Water Treatment. Water Res 13(1979) p 771.

Brosset C. (1952): On the Reactions of the Aluminium Zon with Water. Acta Chem Scand 6(1952) p 910.

Brosset C., Biedermann G., Sillén L.G. (1954): Studies on the Hydrolysis of Metal Ions. XI. The Aluminium Ion, Al^{3+} Acta Chem Scand 8(1954):10.

Camp T.R., Stein P.C. (1943): Velocity Gradients and Internal Work in Fluid Motion. J Boston Soc Civ Eng 30(1943):4 p 219.

Camp T.R. (1955): Flocculation and Flocculation Basins. ASCE Trans 120(1955):1.

Camp T.R. (1968): Floc Volume Concentration. J Am Water Works Assoc 60(1968) p 656.

Camp T.R. (1969): Hydraulics of Mixing Tanks. J Boston Soc Civ Eng 56(1969):1 p 1.

Cederwall K., Larsen P. (1976): Hydraulik för väg- och vattenbyggare (Swedish). Liber, Lund (1976).

Chapman D.L. (1913): A Contribution to the Theory of Electrocapillarity. Phil Mag 25(1913) p 475.

Daily J.W., Harleman D.R.F. (1966): Fluid Dynamics. Addison-Wesley Publ C (1966).

Dobbs R.A., Wise R.H., Dean R.B. (1972): The Use of Ultra-Violet Absorbance for Monitoring the Total Organic Carbon Content of Water and Wastewater. Water Res 6(1972) p 1173.

Drobny N.L. (1963): Effect of Paddle Design on Flocculation. ASCE J San Eng Div, Proc (1963) p 17.

Eikebrokk B., Liengen T.E. (1977): Dimensjonering og drift av omrørere i flokkulerinsbasseng. Huvudoppgave (1977), Institutt for vassbygging, Norwegian Institute of Technology, Trondheim (Norway).

Fair G.M., Gemmel R.S. (1964): A Mathematical Model of Coagulation. J Coll Sci 19(1964) p 360.

Fiessinger F. (1976): Coagulation: Former Methods and New Knowledge. Techniques et Sciences Municipales (1976):4.

Fiessinger F. (1978): Coagulation and Flocculation. Part 1: Coagulation. IWSA 12th CONF (1978) Special Subject 3.

Fischerström C.N.H., Larsen I. (1968): Omrörningsarbetets betydelse för flockningsresultatet (Swedish). VBB, Stencil (1968).

Fischerström C.N.H., Larsen I. (1969): Omrörare med alternerande omrörningsriktning (Swedish). VBB, Stencil (1969).

Gjessing E.T. (1976): Physical and Chemical Characteristics of Aquatic Humus. Ann Arbor Science (1976).

Grouy G. (1910): Sur la Fonction Électro capillaire. Ann Phys Lpz 9(1910) p 457.

Grohmann A., Althoff H.W. (1975): Eine Automatische, Schnelle und Genaue Bestimmung des m-Wertes (Alkalinity). Z f Wasser- und Abwasserforschung, 8(1975):5 p 134.

Haberer K., Normann S. (1976): Entfernbarkeit Organischer Stoffe aus Reinwasser durch Fällung und Flockung. Vom Wasser 47(1976) p 399.

Haff J.D. (1978): Removal of Humic Acid using Alum and Synthetic Polymers. J Am Water Works Assoc 70(1978) p 520.

Hahn H.H., Stumm W. (1968): Kinetics of Coagulation with Hydrolyzed Al (III) the Rate Determining Step. J of Colloid and Interface Science 28(1968):1 p 134

Hald A. (1952): Statistical Theory with Engineering Applications. Wiley & Sons (1952).

Hall E.S., Packham R.F. (1965): Coagulation of Organic Color with Hydrolyzing Coagulants. J Am Water Works Assoc 57(1965) p 1149.

Hanna G.P.JR., Rubin A.J. (1970): Effect of Sulfate and other Ions in Coagulation with Aluminium (III). J Am Water Works Assoc 62(1970) p 315.

Hannah S.A., Cohen J.M., Robeck G.G. (1967): Measurement of Floc Strength by Particle Counting. J Am Water Works Assoc 59(1967) p 843.

Hardy W.D. (1900): J Phys Chem 4(1900) p 235.

Harris H.S., Kaufman W.J., Krone R.B. (1966): Orthokinetic Flocculation in Water Purification. ASCE J San Eng Div 92(1966) SA6 p 95.

Hedberg T., Hernebring C. (1974): Studium av flockningsprocessen Del 1: Teoretisk bakgrund (Swedish). Chalmers Univ of Techn, Div of Water Supply and Sewerage, Publ B 74:3.

Hedberg T., Hernebring C. (1975): Studium av flockningsprocessen Del 2: Undersökningar (Swedish, Summary in English). Chalmers Univ of Techn, Div of Water Supply and Sewerage. Publ B 75:3.

Hedberg T. (1976): Flocculation, Sedimentation and Filtration. A Technical and Economic Analysis of Water Treatment. Dissertation, Chalmers Univ of Techn, Dept of Water Supply and Sewerage (1976).

Helenius L. (1972): Jämförande studier av råvattenkvaliteten och reningskostnaderna i Sverige och Finland (Swedish). Chalmers Univ of Techn, Dept Water Supply and Sewerage, Publ B 72:2.

Helmholtz H. von (1879): Studien über Electrische Grenzschichten. Wied Ann 7(1879) p 337.

Hemenway D.R., Keshavan K. (1968): Determination of Optimum Velocity Gradients for Water Coagulated with Polyelectrolytes. Water Sewage Works (1968) p 554.

Hernebring C. (1978): Flockning vid renvattenframställning. Kemisk fällning vid låg vattentemperatur (Swedish, Summary in English). Chalmers Univ of Techn, Div of Water Supply and Sewerage, Publ B 78:2.

Hernebring C. (1980): Driftstudier av vattenverk med kemisk fällning (Swedish). Chalmers Univ of Techn, Div of Water Supply and Sewerage, Publ B 80:1.

Hudson H.E.JR. (1965): Physical Aspects of Flocculation. J Am Water Works Assoc 57(1965) p 885.

Hyde C.G., Ludwig H.F. (1944): Some New Features in the Design of Vertical Flocculation Units. J Am Water Works Assoc 36(1944) p 151.

Ives K.J., Bhole A.G. (1973): Theory of Flocculation for Continuous Flow System. ASCE J Environ Eng Div (1973) p 17.

Ives K.J. (1978a): Introduction in The Scientific Basis of Flocculation. Ed. Ives K.J., Nato Advanced Study Inst Ser E: Appl Sci (1978):27 p 1.

Ives K.J. (1978b): Rate Theories in The Scientific Basis of Flocculation. Ed. Ives K.J., Nato Advanced Study Inst Ser E: Appl Sci (1978):27 p 37.

TeKippe R.J., Ham R.K. (1971): Velocity-Gradient Paths in Coagulation. J Am Water Works Assoc 63(1971) p 439.

Klute R., Neis V., Bantz J. (1979): Untersuchungen zur Kinetik der Flockung mit Polyelektrolyten in Gegenwart von Huminsäure. Vom Wasser 53(1979) p 203.

Lagvankar A.L., Gemmel R.S. (1968): A Size-Density Relationship for Flocs. J Am Water Works Assoc 60(1968) p 1040.

Mc Laughlin R.T. (1959): The Settling Properties of Suspensions. ASCE J Hydr Div, Proc (1959):HY 12 p 9.

Leentvaar J., Ywema T.S.J. (1980): Some Dimensionless Parameters of Impeller Power in Coagulation-Flocculation Processes. Water Res 14(1980) p 135.

Letterman R.D., Tabatabaie M., Ames R.S. (1979): The Effect of the Bicarbonate Ion Concentration on Flocculation with Aluminium Sulfate. J Am Water Works Assoc 71(1979) p 467.

Levich V.G. (1962): Physicochemical Hydrodynamics. Prentice-Hall Inc, 1962.

Licsko I. (1976): Micro Processes in Coagulation. Water Res 10(1976) p 143.

Lyklema J. (1978): Surface Chemistry of Colloids in Connection with Stability in The Scientific Basis of Flocculation. Ed. Ives K.J., Nato Advanced Study Inst Ser E: Appl Sci (1978):27 p 3.

Matijevic E., Mathai K.G., Ottewill R.H., Kerker M. (1961): Detection of Metal Ion Hydrolysis by Coagulation (III) Aluminium. J Phys Chem 65(1961) p 826.

O'Melia C.R. (1972): Coagulation and Flocculation in Physico-chemical Processes for Water Quality Control. Ed. Weber. Wiley-Interscience (1972) p 61.

O'Melia C.R. (1978): Coagulation in Water Treatment Plant Design. Chapt 4. Ed. Sanks R.L. Ann Arbor Science (1978).

La Mer V.K. (1964): Coagulation Symposium Introduction. J Coll Sci 19(1964) p 291.

Narkis N., Rebhun M. (1975): The Mechanism of Flocculation Process in the Presence of Humic Substances. J Am Water Works Assoc 67(1975) p 101.

Narkis N., Rebhun M. (1977): Stoichiometric Relationship between Humic and Fulvic Acids and Flocculants. J Am Water Works Assoc 69(1977) p 325.

Ødegaard H. (1975): Flocculation of Phosphate Precipitates in Wastewater Treatment. Dissertation, Div of Hydraulic Eng, Univ of Trondheim (1975) Norway.

Overath H., Norman S., Haberer (1979): Optimerung der Entnahme Gelöster Organischer Verunreinigungen bei der Flockung von Oberflächenwasser. Vom Wasser 53(1979) p 213.

Packham R.F. (1962): The Theory of the Coagulation Process. A Survey of the Literature.
1. The Stability of Colloids
2. Coagulation as a Water Treatment Process
Soc Water Treatment Exam 11(1962) p 50, 106.

Packham R.F. (1963): The Coagulation Process - A Review of some Recent Investigations. Soc Water Treatment Exam Proc, 12(1963) p 15.

Packham R.F., Sheiham I. (1977): Developments in the Theory of Coagulation and Flocculation. J Inst Water Eng Sci 31(1977):2 p 96.

Parker D.S., Kaufman W.J., Jenkins D. (1972): Floc breakup in Turbulent Flocculation Processes . ASCE J San Eng Div, Proc (1972) p 79.

Pierrou U. Svenska vattenkvalitetskriterier. Organiska ämnen. (Swedish). Statens naturvårdsverk (1977) PM 9:9.

Polasek P. (1979): The Significance of the Root Mean Square Velocity Gradient and its Calculation in Devices for Water Treatment. Water SA 5(1979):4 p 196.

Riddick T.M. (1961): Zeta Potential: New Tool for Water Treatment. Chem Eng (1961):6, :7.

Ritchie A.R. (1956): Theoretical Aspects of Flocculation and Coagulation. Soc Water Treatment Exam Proc, (1956) p 81.

Robinson M. (1964): Flocculation - A Litterature Survey of Theory and Practice. Water and Water Eng (1964) p 96.

Rook J.J. (1974): Formation of Haloforms during Chlorination of Natural Waters. Water Treatment Exam 23(1974) p 234.

Rosén B. (1967): Effekttillförselns inverkan på flockuppbyggnaden. Thesis (Swedish, Summary in English). Chalmers Univ of Techn, Div of Water Supply and Sewerage (1967).

Saatci A.M., Cleasey J.L. (1980): On Measuring the Velocity of Water in a Paddled Flocculator. J Am Water Works Assoc 72(1980):4.

Saffman P.G., Turner J.S. (1956): On the collision of Drops in Turbulent Clouds. J Fluid Mech 1(1956) p 16.

Schilling J. (1975): Die Aufbereitung Stark Huminsäurehaltigen Oberflächenwassers. Ein Beitrag zur Flockung und Adsorption an Makroporösen Ionenaustauschern in der Wasser Technologie. Fortschr -Ber VDI-Z 4(1975):24.

Singley J.E. et al (1971): State of the Art of Coagulation - Mechanisms and Stoichiometry. Committee Report. J Am Water Works Assoc 63(1971) p 99.

von Smoluchowski M. (1918): Versuch einer Mathematischen Theorie der Koagulationskinetik Kolloide Lösungen. Z Phys Chem 92(1918) p 129.

Spielman L.A. (1978): Hydrodynamic Aspects of Flocculation in The Scientific Basis of Flocculation. Ed. Ives K.J. Nato Advanced Study Inst Ser E: Appl Sci 27(1978) p 63.

Stern O. (1924): Zur Theorie der Elektrolytischen Doppelschicht. Z Elektrochem 30(1924) p 508.

Stumm W., O'Melia C.R. (1968): Stoichiometry of Coagulation. J Am Water Works Assoc 60(1968) p 514.

Sullivan J.M. Jr., Singley J.E. (1968): Reactions of Metal Ions in Dilute Aqueous Solution: Hydrolysis of Aluminium. J Am Water Works Assoc 60(1968) p 1280.

Swift D.L., Friedlander S.K. (1964): The Coagulation of Hydrosols by Brownian Motion and Laminar Shear Flow. J Coll Sci 19(1964) p 621.

Tambo N., Watanabe Y, Hozumi H. (1979): Physical Charateristics of Flocs
I The Floc Density Function and Aluminium Floc (1979a)
II Strength of Floc (1979b)
Physical Aspects of Flocculation Process
I Fundamental Treatise (1979c)
II Contact Flocculation (1979d)
Water Res 13(1979) p 409.

Tolman S.L. (1942): Water Conditioning by Flocculation. J Am Water Works Assoc 34(1942):3 p 404.

Tolman S.L. (1949): Use of Models in Solving Flocculation Problems. J Am Water Works Assoc 41(1949) p 641.

Tryland Ø. (1977): Metode for målning av sedimenteringsegenskaper til suspensjoner. NIVA, Publ XK-22 (1977) Norway.

Tryland Ø. (1978): Sedimenteringshastighet til suspensjoner. NIVA, Publ D1-04 (1978) Norway.

Villemonte J.R., Rohlich G.A., Wallace A.T. (1966): Hydraulic and Removal Efficiencies in Sedimentation Basins. Third Int Conf on Water Poll Research WPCF Sect II 16(1966).

Vold M.J. (1963): Computer Simulation of Floc Formation in a Colloid Suspension. J Coll Sci 18(1963) p 684.

Vråle L., Jordan R.M. (1971): Rapid mixing in water treatment. J Am Water Works Assoc 63(1971) p 52.

Weijman-Hane G. (1963): Koagulering, sedimentering och filtrering. Försök med lamellsedimentering (Swedish). Chalmers Univ of Techn, Div of Water Supply and Sewerage, Publ B63:3.

9 NOTATION

Symbol	Definition	Dimensions	First appearance in eq.
A	number of acid equivalents added with the aluminium sulphate dose	meqv H^+/l	(2-13)
A	particle growth proportionality constant	$m^3 \cdot s^{-1}$	(3-48)
A	constant		(3-66)
A	sedimentation area	m^2	(3-78)
A	dimensionless work parameter		(3-112)
A_p	paddle area	m^2	(3-93)
a	coefficient in expression for the effective density according to floc size	$kg \cdot m^{-3}$	(3-46)
B	raw water alkalinity	meqv H^+/l	(fig. 2-1)
B	breakup constant	$s \cdot m^{-2}$	(3-38)
$B(v,\tilde{v})$	breakup function	$m^{-3} \cdot s^{-1}$	(3-58)
B	constant		(3-66)
B	dimensionless work parameter	(-)	(3-112)
b_1	regression coefficient		(4-14)
BC2	floc breakup constant		(5-37)
C	concentration of a substance after coagulation		(2-14)
C	dimensionless work parameter		(3-112)
C,C1,C2	constants		
C_o	concentration of a substance in the raw water		(2-14)
C_m,C_{min}	minimum observed concentration after coagulation at a certain coagulant dose		(2-14)
C_D	coefficient of drag	dimensionless	(3-93)
C_t	turbulent gross drag coefficient	"	(3-111)
COD_{Mn}	Chemical oxygen demand, potassium permanganate as oxidizing agent	mg $KMnO_4$/l	
D	required coagulant dose	mg Al-sulphate/l	(2-10)
D,D_{ij}	diffusion coefficients	$m^2 \cdot s^{-1}$	(3-2)
d	paddle width	m	(3-105)
d_1,d_2	particle diameters	m	(3-6)
d_s	stable floc size	m	(3-41)

d_k	floc diameter in size fraction k		(5-13)
DPOT	floc size exponent, breakup		(5-31)
DTIME	mean residence time in a reactor	s	(5-37)
E_{254}^{4cm}	absorbance at 254 nm, 4 cm cell	(-)	(2-6)
E_{436}^{4cm}	" " 436 " , " " "	(-)	(2-4)
FTU	Formazin turbidity unit		(2-5)
F(v)	cumulative settling velocity distribution	(-)	(3-60)
f(v)	settling velocity distribution	(-)	(3-61)
F_D	drag force on a paddle	N	(3-93)
f	Weissbach-Darcy friction factor	(-)	(3-112)
F	floc turbidity	FTU	(5-1)
FLTURB	" "	"	(5-37)
f_k	relative turbidity of size fraction k	(-)	(5-6)
f_k(in)	into a reactor	(-)	(5-12)
FRAC(K)	" " "	(-)	(5-37)
f_k(out)	out from a reactor	(-)	(5-12)
OLDFRC(K)	" " " "	(-)	(5-37)
G	mean velocity gradient	s^{-1}	(3-8)
GVALUE	" " "	"	(5-37)
GPOT	breakup exponent		(5-30)
GC1	floc growth constant		(5-37)
H	pH-value		(2-14)
H_o	pH-value corresponding minimum concentration (fitted curves)		(2-14)
H_m	pH-value corresponding minimum concentration (observed data)		
h	heigth, depth	m	(3-62)
h_{tot}	total settling column depth	"	(3-62)
h_o	sedimentation basin depth	"	(3-78)
JTU	Jackson turbidity unit		(2-6)
K, K_1, K_2	constants		
k	Boltzmanns constant	$J \cdot K^{-1}$	(3-1)
K_s	proportionality coefficient, particle growth	$s \cdot m^{-2}$	(3-32)

K_p	constant characterizing the stirring equipment	$m^2 \cdot s^{-1}$	(3-33)
K_ρ	floc size exponent in a size-density relationship	(-)	(3-46)
K_r	σ/v_m - ratio for constant residual turbidity	(-)	(3-77)
K_{lam}	coefficient related to the removal efficiency of a shallow depth sedimentation unit	(-)	(3-89)
k	water co-rotation coefficient	(-)	(3-94)
L	dose of pH-adjusting chemical	meqv OH^-/l	(fig. 2-1)
L	lamella length in a shallow depth sedimentation unit	m	(3-79)
m	floc breakup exponent		(3-49)
m	dimensionless time variable		(3-57)
m_1, m_2, m_3	regression coefficients		(4-14,4-15,4-16)
MODE	floc breakup mode		(eqs. 5-17 to 5-20)
$n_i, n_j, n_1, n_2, n_k, n_F$	number concentrations	m^{-3}	(3-1)
n(v),n(v,t)	number concentration distributions	m^{-6}	
n_t	total number of particles per unit of volume	m^{-3}	(3-5)
n	stable floc size exponent		(3-42)
n	collision-agglomeration exponent		(3-56)
n	paddle shaft rotational speed	rps,rpm	(3-94)
N	number of compartments in series		(3-52)
N_i	dimensionless number concentration		(3-57)
N_i	number concentration of primary particles after the i-th compartment		(5-1)
NFRAC	total number of floc size fractions		(5-27)
OLDFRC(K)	see f_k(in)		
pH_o	raw water pH		(fig 2-1)
pH_s	desired coagulation pH		(" ")
p	constant		(3-98)
q	flow	$m^3 \cdot s^{-1}$	(3-50)
Q	"	$m^3 \cdot s^{-1}$	(3-78)
q	rotational speed exponent		(3-99)
r	paddle distance from the shaft	m	(3-94)
r, r_i, r_j	particle radii	m	(3-1)

R_f	raw water colour	mg Pt/l	(2-8)
R_k	raw water COD_{Mn}	mg $KMnO_4$/l	(2-7)
R_s	raw water turbidity	mg SiO_2/l	(2-8)
R_{ij}	collision radius	m	(3-3)
r_F	floc radius	m	(3-32)
r_i	part of the total residence time in the i-th compartment	(-)	(3-53)
Re	Reynolds number	(-)	(3-106)
RPOT	floc size exponent		(5-28)
S	maximum floc size	(-)	(3-56)
s	horizontal lamella distance in a shallow depth sedimentation unit	m	(3-79)
S1(K),S2(K)	Summation terms, floc growth		(5-12)
S3(K),S4(K)	" " , breakup		(5-14)
SIGMA	see σ	$m \cdot h^{-1}$	
t	time	s	(3-1)
T	mean residence time	s,min	(3-51)
T	absolute temperature	K	(3-1)
T	torque	Nm	(3-95)
T	total flocculation time	s, min	(4-1)
t/T	relative flocculation time		(4-1)
$\overline{u^2}$	turbulent mean square velocity fluctuation	$m^2 \cdot s^{-2}$	(3-32)
v	flow velocity	$m \cdot s^{-1}$	(3-6)
V,V_i,v	volume	m^3	(3-15)
v	settling velocity	$m \cdot h^{-1}$	(3-66)
v_m	mean settling velocity	$m \cdot h^{-1}$	(3-68)
VMEAN	" " "	$m \cdot h^{-1}$	(5-27)
v_F	sedimentation overflow rate	$m \cdot h^{-1}$	(3-78)
v_{rel}	paddle velocity relative to the water	$m \cdot s^{-1}$	(3-93)
v_m^{max}	maximum mean settling velocity obtained at a certain flocculation time	$m \cdot h^{-1}$	(4-2)
v_m^i	mean settling velocity in the outlet from the i-th compartment	$m \cdot h^{-1}$	(5-2)
VMIN	settling velocity determining the smallest floc size interval	$m \cdot h^{-1}$	(5-23)
VFRAC(K)	upper limit of settling velocity interval K	$m \cdot h^{-1}$	(5-26)
VPOT	size - settling velocity exponent		(5-26)

V_i	settling velocity of a floc consisting of i primary particles	m/h	(5-24)
W	power input	watt/m^3	(3-40)
$W_i(t/T)$	variation of the power input with relative flocculation time	watt/m^3	(4-1)
w_i	weighing factor	(-)	(2-17)
x	standardized normal distribution variable	(-)	(3-66)
X	number defining power input variation	(-)	(4-3)
X_o	" " " " " corresponding to v_m^{max}	(-)	(4-5)
X_{opt}	optimum power input variation	(-)	(4-13)
Y_i	filtrate residual, substance i		(2-17)
$Y_{k,i}$	comparison value for filtrate quality, substance i		(2-17)
Y_a	flow divided by surface area of a shallow depth sedimentation unit	$m^3/(h \cdot m^2)$	(3-78)
α	collision efficiency factor	(-)	(3-9)
α	inclination angle of lamellae in a shallow depth sedimentation unit	(-)	(3-79)
α_k	collision-agglomeration factor depending on floc size	(-)	(3-56)
α_o	constant	(-)	(3-56)
$\beta(v,\tilde{v})$	aggregation coefficient	$m^3 \cdot s^{-1}$	(3-29)
β	particle growth constant	(-)	(3-34)
$\dot{\gamma}$	rate of angular distortion	s^{-1}	(3-92)
δ	size distribution function	(-)	(3-22)
ε_o	mean rate of energy dissipation effective for flocculation	watt/m^3	(3-34)
Φ	floc volume fraction	(-)	
$\Phi(x)$	standardized cumulative normal distribution	(-)	(3-69)
Φ^{-1}	inverse function of Φ (x)	(-)	(3-73)
$\varphi(x)$	standardized normal distribution	(-)	(3-70)
Φ_k	floc volume fraction of size fraction k	(-)	(5-5)

μ	fluid dynamic viscosity	Ns/m^2	(3-1)
ν	fluid kinematic viscosity	m^2/s	(3-40)
ρ_e	effective floc density	kg/m^3	(3-45)
ρ_f	floc density	"	(3-45)
ρ_w	water density	"	(3-45)
ω	rate of angular displacement of a paddle shaft	s^{-1}	(3-95)
σ	settling velocity standard deviation	m/h	(3-67)
SIGMA	" " " "	"	(5-27)
σ_o	" " " " corresponding v_m^{max}	"	(4-2)
σ^i	settling velocity standard deviation in the outlet from compartment i	"	(5-2)
τ	shear stress	N/m^2	(3-92)
Ψ_1	self-preserving size distribution function	(-)	(3-31)
η	Kolmogoroff turbulent microscale	m	(3-40)

10 APPENDICES

APPENDIX 1

PILOT PLANT DESCRIPTION

The experiments on pilot plant scale were carried out in a flocculation tank with a total volume of 6.9 m^3. The tank design provided the possibility to vary the division of the tank volume by movable partition walls. Usually the flocculation volume was divided into four equal compartments. In parallel with the pilot plant a reference plant was operated with constant flocculation conditions. Thus the effect of uncontrolled factors, such as varying raw water quality, could be recorded. Additional information concerning the design of paddles is given in Sections 3.4.3.2 and 4.2.3.

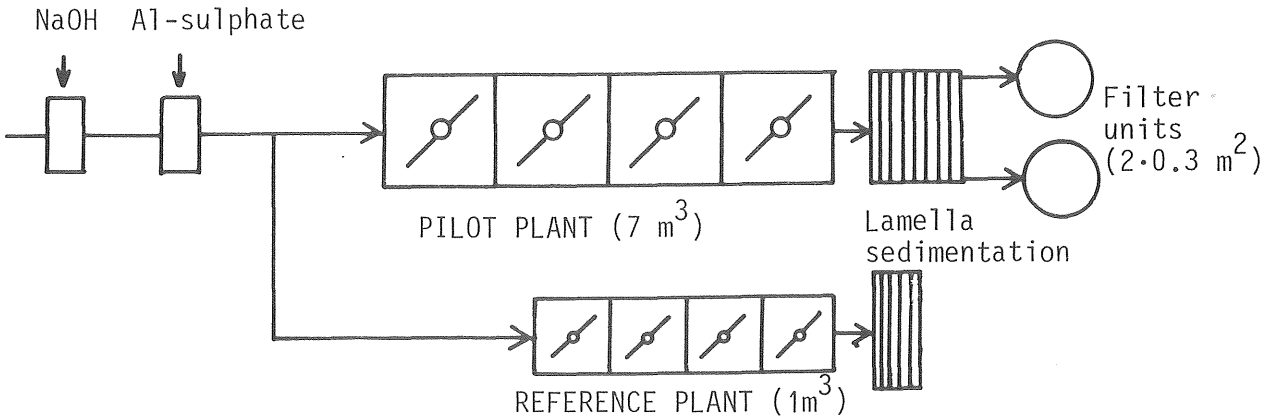

Fig. A.1. Sketch of the pilot plant

The lamella sedimentation unit of the pilot plant is characterized by the following data:

Horizontal water surface area: 1 m^2
Horizontal lamella distance: 0.1 m
Lamella length: 1.9 m
Lamella inclination angle: 55^o

Two filter units with sand and sand-anthracite, respectively, received water from the pilot plant sedimentation unit. No results from the filter operation are reported in this treatise (see Hernebring, 1978).

As a coagulant, aluminium sulphate was used (Boliden, 17-18% Al_2O_3). A feed solution, 5% by weight, was continuously extracted from the water treatment plant at Lackarebäck, Göteborg. The solution was filtered before addition to the water to prevent operating problems in the regulation equipment, consisting of a needle valve and a flow meter. In all pilot plant experiments 40 mg Al-sulphate/l was dosed, corresponding to 0.13-0.14 mmoles Al^{3+}/l. For pH-adjusting, NaOH (45% or 25%) was added by means of a gear pump.

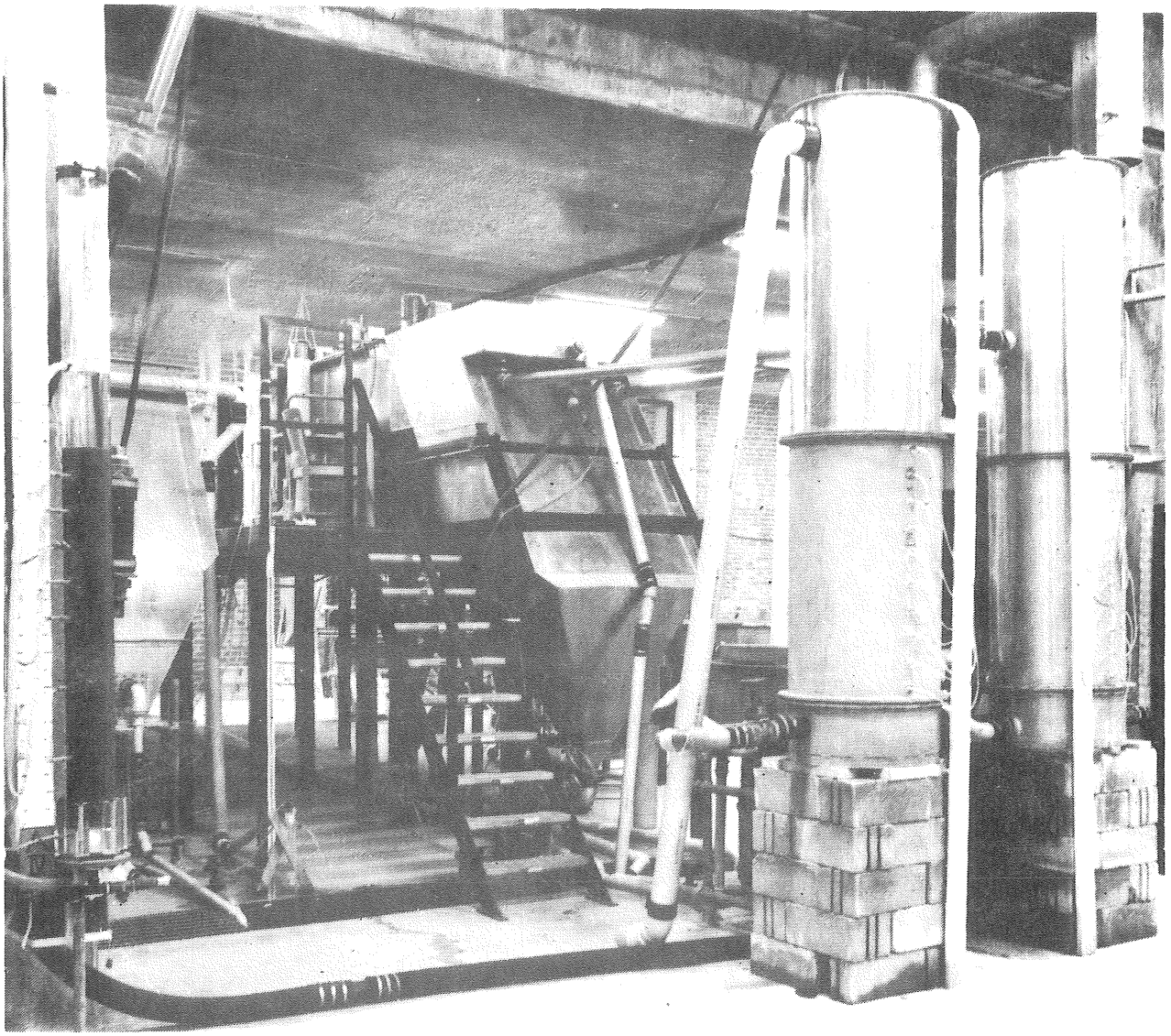

Fig. A.2. Photograph of the pilot plant

The alum solution and the pH-adjusting chemical were added to the water in the raw water pipe before the pilot plant. Turbulence was generated by the mixing device shown in figure A.3. The openings in the metal plates were varied according to the flow. Two mixing units were placed at a distance of ca. 8 m in the raw water pipe with the diameter 100 mm. NaOH was dosed at the first mixing point in all experiments reported.

The neutralized silica sol solution (activated silica) as well, was extracted from the Lackarebäck water treatment plant. The preparation of the activated silica is made by adding aluminium sulphate to a sodium silicate solution. The sodium silicate, trade mark Aurosil N31 (Alsell&Ågren), with appr. 28% SiO_2 is diluted and mixed with aluminium sulphate in a reactor, where the formation of polysilicates takes place. The polymerization is stopped by dilution after appr. 0.5 h mean residence time in the reactor. The concentrations in the reactor are ca. 1.6% of both alum and SiO_2. The final dilution makes the activated silica solution to contain 2 g Aurosil N31/l. During the experiments pH for the solution in the reactor varied from 8.1 to 9.3, the alkalinity 55-76 meqv/l, and the gel time from 70 to 110 minutes. The dosage of activated silica is in this treatise given in terms of the commercial product, Aurosil N31. In the pilot plant experiments the dose was 2 mg/l, corresponding to ca. 0.6 mg SiO_2/l. The activated silica solution was added in the first flocculation tank.

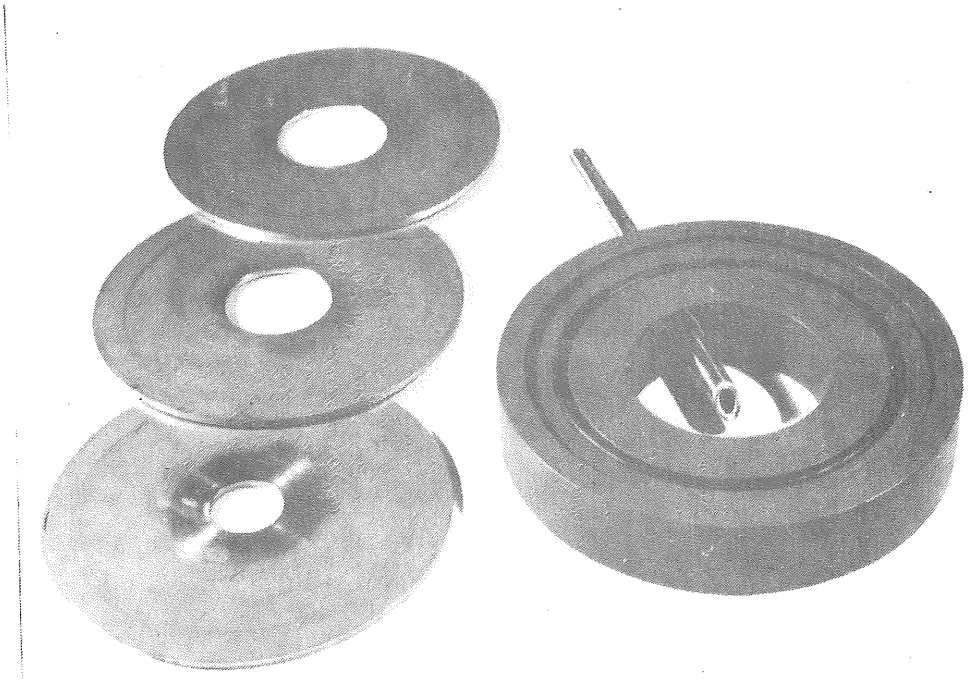

Fig. A.3. Mixing device

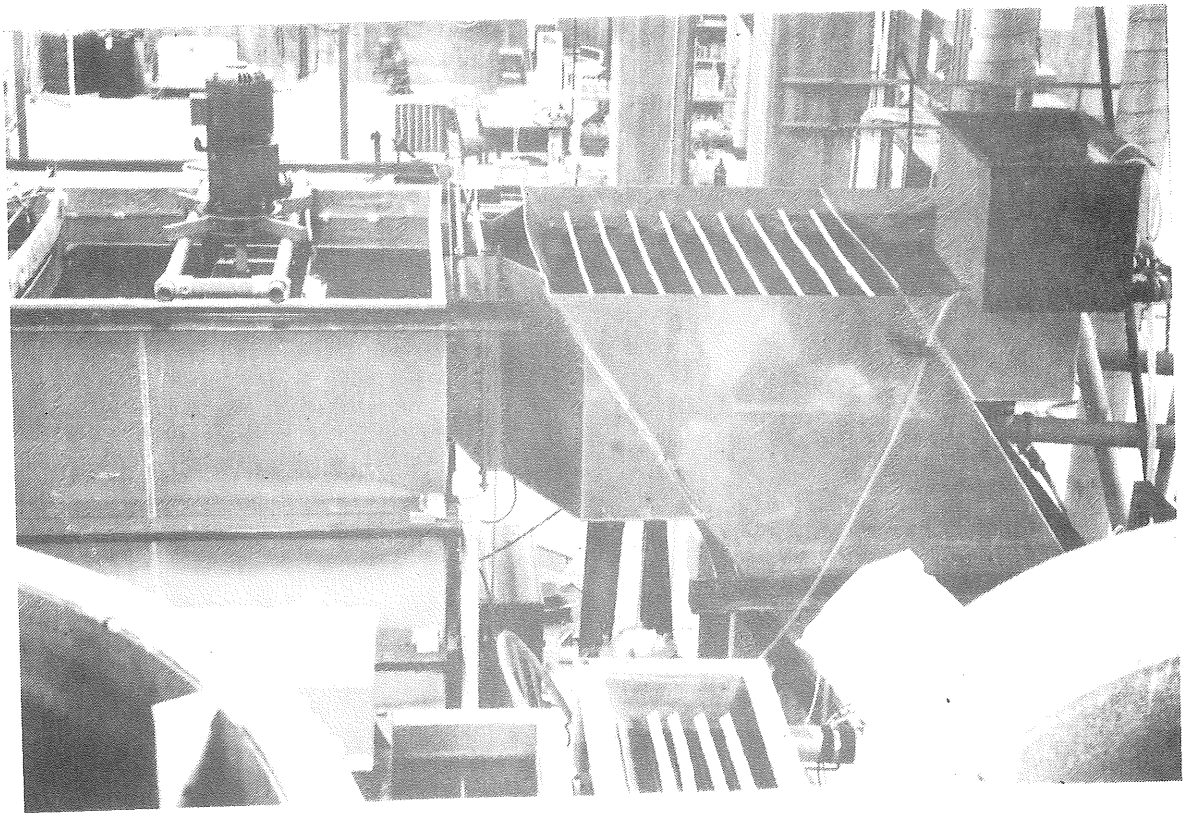

Fig. A.4. Photograph of the pilot plant

APPENDIX 2

RESULTS FROM PILOT PLANT EXPERIMENTS
DATE: 2/2 1976 to 6/3 1976

FLOCCULATION CONDITIONS

Run no.	1	2	3	4	5	6	7	8	9	10	11	12	13	14	15	16	17	18
Total flocculation time (min)	10	10	10	10	10	10	20	20	20	20	20	20	30	30	30	30	30	30
Power input I (see eq. 4-1)	3	2	1	3	2	1	3	2	1	3	2	1	3	2	1	3	2	1
2 ppm activated silica	X	X	X	-	-	-	X	X	X	-	-	-	X	X	X	-	-	-

Coagulant dose: 40 mg Al-sulphate/l
Coagulation pH: 6.5
Paddle type: A4 (see fig. 3.32)
Uniform compartmentalization

SOME CHARACTERISTIC RAW WATER ANALYSES
Temperature: 1.7-2.3 ^{o}C
Turbidity: 1.2-2.1 FTU
Alkalinity: 11-12 mg HCO_3^-
Permanganate number: 32 mg $KMnO_4$/l
Colour: 30 mg Pt/l
pH: 6.8-7.0
Conductivity: 12.5 mS/m

RESULTS FROM SETTLING TESTS
VM and SIGMA are mean settling velocity and settling velocity standard deviation, respectively, calculated from settling test data (see Section 3.3). Normal distribution is assumed.

Run no.	Tank no.	Turbidity (FTU) at sample depth 30 cm after sedimentation time (min) 0	10	20	40	60	120	VM m/h	SIGMA m/h
1	2	4.0	4.2	4.1	2.8	3.1	-	0.31	0.35
	3	4.2	3.9	3.6	2.5	2.5	-	0.34	0.58
	4	4.7	4.1	3.0	2.0	2.5	-	0.51	0.76
2	2	3.6	3.7	3.4	2.2	2.0	1.6	0.25	0.44
	3	3.6	3.6	3.0	2.0	1.8	1.8	0.33	0.61
	4	3.7	3.6	2.2	1.6	1.3	1.1	1.44	0.95
3	2	3.7	3.3	3.3	2.3	1.9	1.8	0.24	0.57
	3	3.7	3.2	2.5	1.5	1.2	1.1	0.60	0.80
	4	3.8	3.2	1.8	1.2	1.1	1.0	0.84	0.96
4	2	3.6	3.5	3.3	2.5	2.6	1.7	0.19	0.54
	3	3.5	3.5	3.0	2.1	1.7	1.3	0.35	0.58
	4	3.8	3.5	2.8	1.7	1.5	1.3	0.45	0.76

Run no.	Tank no.	Turbidity (FTU) at sample depth 30 cm after sedimentation time (min) 0	10	20	40	60	120	VM m/h	SIGMA m/h
5	2	3.5	3.5	3.6	2.7	2.6	1.8	0.12	0.41
	3	3.5	3.5	3.2	1.8	1.7	1.2	0.35	0.44
	4	3.6	3.4	2.5	1.4	1.3	1.2	0.53	0.72
6	2	3.6	3.7	3.6	2.4	2.2	1.8	-	-
	3	3.6	3.7	3.5	2.0	1.6	1.2	-	-
	4	3.6	3.6	3.2	2.0	1.6	1.2	0.47	0.37
7	2	3.3	3.1	2.3	2.1	1.7	1.4	0.17	1.0
	3	3.0	2.5	1.6	1.1	0.98	0.93	0.83	1.2
	4	3.0	2.0	1.1	0.85	0.78	0.78	1.3	1.5
8	2	3.3	3.3	2.5	2.0	1.6	1.3	0.34	0.72
	3	3.3	3.2	2.0	1.2	1.1	0.89	0.64	0.69
	4	3.4	2.8	1.2	0.75	0.70	0.67	1.0	0.87
9	2	3.3	3.3	2.2	2.0	1.2	1.1	0.49	0.86
	3	3.4	3.1	1.4	0.82	0.73	0.68	0.88	0.72
	4	3.4	2.4	0.89	0.62	0.53	0.52	1.3	1.0
10	2	3.5	3.5	3.6	2.2	1.5	1.4	0.32	0.52
	3	3.6	3.3	2.6	1.4	1.3	0.92	0.57	0.74
	4	3.4	3.2	1.9	1.1	0.85	0.81	0.79	0.76
11	2	3.5	3.5	3.2	2.1	1.6	1.3	0.31	0.41
	3	3.4	3.4	2.9	1.4	1.0	0.85	0.49	0.45
	4	3.5	3.2	1.9	1.2	0.90	0.65	0.77	0.71
12	2	3.5	3.5	3.5	3.3	2.1	1.5	0.21	0.18
	3	3.5	3.5	3.3	1.8	1.4	0.85	0.42	0.37
	4	3.7	3.6	2.4	1.4	1.0	0.67	0.63	0.57
13	2	3.6	3.5	1.9	1.4	1.2	1.1	0.79	1.3
	3	3.4	2.5	1.2	0.95	0.72	0.70	1.2	1.2
	4	3.6	1.5	0.75	0.66	0.62	0.59	2.3	2.1
14	2	3.5	3.7	2.3	1.3	1.1	0.89	0.69	0.73
	3	3.8	2.8	1.5	0.94	0.65	0.53	1.1	0.94
	4	3.8	2.0	0.74	0.60	0.55	0.45	1.8	1.3
15	2	4.3	4.1	2.7	1.9	1.2	0.98	0.70	0.75
	3	4.4	3.8	2.0	1.1	0.67	0.57	1.0	0.74
	4	4.6	2.2	0.78	0.53	0.50	0.44	1.9	1.3
16	2	4.4	4.5	2.6	1.7	1.4	1.2	0.69	0.88
	3	4.3	4.0	1.8	1.2	0.92	0.78	1.0	0.95
	4	4.4	3.0	1.3	0.73	0.63	0.63	1.4	1.0
17	2	4.8	4.8	4.2	1.9	1.6	1.2	0.47	0.40
	3	4.8	4.6	3.3	1.5	0.94	0.72	0.74	0.59
	4	4.9	4.7	2.2	1.1	0.65	0.56	0.96	0.65
18	2	4.7	4.8	4.6	2.2	1.6	1.2	0.40	0.28
	3	4.7	4.7	4.0	1.7	1.3	0.77	0.54	0.37
	4	4.8	4.5	2.8	1.0	0.69	0.51	1.0	0.55

APPENDIX 3

RESULTS FROM PILOT PLANT EXPERIMENTS
DATE: 10/3 1976 to 1/4 1976

FLOCCULATION CONDITIONS

Run no.	31	32	33	34	35	36	37	38	39	40	41	42	43	44	45	46	47	48
Total flocculation time (min)	10	10	10	10	10	10	20	20	20	20	20	20	30	30	30	30	30	30
Power input I (see eq. 4-1)	3	2	1	3	2	1	3	2	1	3	2	1	3	2	1	3	2	1
2 ppm activated silica	X	X	X	-	-	-	X	X	X	-	-	-	X	X	X	-	-	-

Coagulant dose: 40 mg Al-sulphate/l
Coagulation pH: 6.5
Paddle type: A1,A2,A3 and A4 (see fig. 3.32)
Non-uniform compartmentalization

SOME CHARACTERISTIC RAW WATER ANALYSES
Temperature: 2.4-2.9 ^{o}C
Turbidity: 2.0-2.4 FTU
Alkalinity: 12 mg HCO_3^-
Permanganate number: 33 mg $KMnO_4$/l
Colour: 30 mg Pt/l
pH: 6.9
Conductivity: 12.5 mS/m

RESULTS FROM SETTLING TESTS

Run no.	Tank no.	Turbidity (FTU) at sample depth 30 cm after sedimentation time (min) 0	10	20	40	60	120	VM m/h	SIGMA m/h
31	4	5.0	3.3	1.7	1.4	1.2	1.1	1.3	1.4
32	4	5.2	2.8	1.2	0.89	0.80	0.71	1.7	1.4
33	4	4.4	3.2	1.4	0.87	0.68	0.57	1.3	0.95
34	4	4.9	4.3	3.0	1.5	1.1	0.98	0.83	0.79
35	4	4.5	4.5	2.6	1.3	0.98	0.87	0.79	0.68
36	4	4.7	4.5	3.2	1.7	1.3	0.77	0.69	0.62
37	4	5.0	2.0	1.2	0.80	0.62	0.60	2.2	1.7
38	4	4.8	2.8	1.4	0.78	0.56	0.47	1.6	1.1
39	4	4.7	3.8	1.8	1.3	0.95	0.60	1.1	0.86
40	4	5.0	4.1	2.0	0.87	0.85	0.69	1.1	0.78
41	4	5.0	5.0	2.8	1.2	0.89	0.58	0.82	0.56
42	4	4.8	4.6	4.0	1.3	1.2	0.70	0.58	0.37
43	4	5.1	2.7	1.2	0.80	0.62	0.53	1.7	1.2
44	4	5.4	4.0	2.1	0.93	0.57	0.47	1.2	0.80
45	4	5.1	3.9	2.3	0.79	0.63	0.51	1.2	0.80
46	4	5.2	5.2	3.0	0.88	0.83	0.65	0.79	0.56
47	4	5.5	5.3	4.7	2.2	1.1	0.86	0.54	0.35
48	4	5.4	5.2	3.8	1.9	1.1	0.67	0.66	0.44

APPENDIX 4

RESULTS FROM PILOT PLANT EXPERIMENTS
DATE: 15/6 1976 to 29/6 1976

FLOCCULATION CONDITIONS

Run no.	P1	P2	P3	P4	P5	P6
Total flocculation time (min)	20	20	20	20	20	20
Power input I (see eq. 4-1)	2	2	2	2	2	2
2 ppm activated silica	X	-	X	-	X	-
Paddle type:	A4	A4	C	C	B	B

Coagulant dose: 40 mg Al-sulphate/l
Coagulation pH: 6.3
Uniform compartmentalization

SOME CHARACTERISTIC RAW WATER ANALYSES
Temperature: 15.1-16.4 ^{o}C
Turbidity: 1.0-1.2 FTU
Alkalinity: 12-14 mg HCO_3^-
Permanganate number: 31 mg $KMnO_4$/l
Colour: 30 mg Pt/l
pH: 7.0-7.2
Conductivity: 11.8 mS/m

RESULTS FROM SETTLING TESTS

Run no.	Tank no.	Turbidity (FTU) at sample depth 30 cm after sedimentation time (min) 0	10	20	40	60	120	VM m/h	SIGMA m/h
P1	2	4.1	3.4	2.0	1.2	1.2	1.3	0.91	0.87
	3	4.0	3.0	1.7	1.0	0.67	0.59	1.1	0.95
	4	4.0	2.2	1.1	0.54	0.50	0.48	1.7	1.2
P2	2	4.2	4.1	2.3	1.6	1.4	1.1	0.75	0.99
	3	4.1	3.8	2.2	1.3	1.1	0.80	0.79	0.73
	4	4.1	2.6	1.4	0.88	0.70	0.58	1.4	1.2
P3	2	3.8	2.8	1.8	1.0	0.86	0.73	1.1	1.1
	3	3.8	2.2	1.3	0.84	0.67	0.58	1.5	1.3
	4	3.8	1.5	0.77	0.59	0.49	0.47	2.3	1.8
P4	2	4.0	4.2	2.6	1.6	1.3	1.1	0.63	0.75
	3	4.0	3.5	1.7	1.3	0.97	0.75	0.91	0.84
	4	4.1	2.7	1.3	0.83	0.73	0.58	1.4	1.1
P5	2	4.2	3.8	2.5	1.5	1.3	1.1	0.70	0.78
	3	4.2	3.2	1.8	1.3	0.88	0.67	1.1	0.97
	4	4.0	1.8	1.3	0.72	0.65	0.48	2.0	1.6
P6	2	4.2	4.3	3.0	1.4	1.4	1.2	0.61	0.60
	3	4.1	4.2	2.6	1.2	1.2	0.82	0.74	0.66
	4	4.2	3.3	1.6	0.95	0.74	0.60	1.1	0.87

APPENDIX 5

RESULTS FROM PILOT PLANT EXPERIMENTS
DATE: 8/7 1976 to 15/7 1976

FLOCCULATION CONDITIONS

Run no.	G1	G2	G3	G4	G5	G6	G7	G8	G9	G10	G11
Total flocculation time (min)	20	20	20	20	20	20	20	20	20	20	20
Power input I (see eq. 4-1)	1	2	3	4	5	6	1	2	3	4	5
2 ppm activated silica	-	-	-	-	-	-	X	X	X	X	X

Coagulant dose: 40 mg Al-sulphate/l
Coagulation pH: 6.3
Paddle type: A4 (see fig. 3.32)
Uniform compartmentalization

SOME CHARACTERISTIC RAW WATER ANALYSES
Temperature: 18.5-20.0 ^{o}C
Turbidity: 0.75 FTU
Alkalinity: 13-14 mg HCO_3^-
Permanganate number: 30 mg $KMnO_4$/l
Colour: 29 mg Pt/l
pH: 7.2
Conductivity: 11.9 mS/m

RESULTS FROM SETTLING TESTS

Run no.	Tank no.	Turbidity (FTU) at sample depth 30 cm after sedimentation time (min) 0	10	20	40	60	120	VM m/h	SIGMA m/h
G1	2	4.6	4.6	4.1	2.3	2.1	1.7	0.35	0.46
	3	4.5	4.4	3.0	1.8	1.5	1.3	0.60	0.68
	4	4.6	3.7	1.8	1.1	0.93	0.78	1.1	0.89
G2	2	4.5	4.6	3.2	1.6	1.5	1.3	0.62	0.69
	3	4.7	4.5	2.8	1.7	1.3	0.89	0.67	0.59
	4	4.6	3.6	1.7	1.3	0.81	0.76	1.1	0.96
G3	2	4.5	4.4	3.0	2.0	2.0	1.7	0.47	1.0
	3	4.3	4.2	2.5	1.7	1.6	1.3	0.63	0.73
	4	4.4	3.2	1.7	1.5	1.3	1.1	1.1	1.4
G4	2	4.4	4.2	3.2	2.1	1.9	1.8	0.44	0.80
	3	4.3	3.7	2.2	1.6	1.4	1.3	0.81	1.1
	4	4.5	2.8	1.6	1.2	0.98	0.91	1.3	1.4
G5	2	4.3	4.1	2.8	2.6	1.9	1.9	0.36	0.84
	3	4.3	3.4	2.3	1.5	1.3	1.3	0.84	1.2
	4	4.2	2.8	1.4	1.2	1.1	1.0	1.3	1.5

Run no.	Tank no.	Turbidity (FTU) at sample depth 30 cm after sedimentation time (min) 0	10	20	40	60	120	VM m/h	SIGMA m/h
G6	2	4.4	4.1	3.2	2.7	2.4	2.5	0.10	1.0
	3	4.2	3.2	2.0	1.7	1.5	1.4	0.87	1.5
	4	4.3	2.3	1.5	1.3	1.2	1.2	1.6	2.4
G7	2	4.5	3.7	2.0	1.4	1.2	1.3	0.90	1.0
	3	4.4	2.6	1.4	1.1	0.75	0.98	1.5	1.4
	4	4.6	2.0	0.80	0.66	0.62	0.64	2.2	1.7
G8	2	4.6	3.0	1.9	1.6	1.3	1.4	1.2	1.7
	3	4.6	2.5	1.5	1.2	0.82	0.77	1.6	1.6
	4	4.7	1.6	0.82	0.85	0.62	0.63	2.8	2.4
G9	2	4.7	3.6	2.2	1.7	1.6	1.5	0.80	1.3
	3	4.7	2.8	1.8	1.5	1.3	1.2	1.3	1.7
	4	4.2	2.0	1.3	1.2	0.97	0.77	2.1	2.3
G10	2	4.6	3.7	2.1	1.8	1.7	1.6	0.79	1.3
	3	4.6	2.6	1.8	1.2	1.3	1.2	1.5	2.0
	4	4.6	1.6	1.3	0.93	0.87	0.90	3.0	3.2
G11	2	4.5	2.8	2.3	2.0	1.9	2.0	0.71	3.1
	3	4.1	2.2	1.7	1.6	1.4	1.4	1.8	3.4
	4	4.5	1.5	1.3	1.0	0.92	0.92	3.5	4.1

APPENDIX 6

RESULTS FROM PILOT PLANT EXPERIMENTS
DATE: 7/2 1977 to 10/2 1977

FLOCCULATION CONDITIONS

Run no.	A11	A12	A13	A14	A15	A16	A21	A22	A23	A24	A25	A26
Total flocculation time (min)	20	20	20	20	20	20	20	20	20	20	20	20
Power input J (see eq. 4-1)	1	2	3	4	5	6	1	2	3	4	5	6
2 ppm activated silica	-	-	-	-	-	-	X	X	X	X	X	X

Coagulant dose: 40 mg Al-sulphate/l
Coagulation pH: 6.5
Paddle type: A4 (see fig. 3.32)
Uniform compartmentalization

SOME CHARACTERISTIC RAW WATER ANALYSES
Temperature: 1.5 ^{o}C
Turbidity: 3.0-3.2 FTU
Alkalinity: 12 mg HCO_3^-
Permanganate number: 33 mg $KMnO_4/l$
Colour: 36 mg Pt/l
pH: 6.6
Conductivity: 14.8 mS/m

RESULTS FROM SETTLING TESTS

Run no.	Tank no.	Turbidity (FTU) at sample depth 30 cm after sedimentation time (min) 0	10	20	40	60	120	VM m/h	SIGMA m/h
A11	2	5.3	5.7	5.2	3.7	3.0	2.3	0.24	0.36
	3	5.3	5.4	5.0	3.3	1.9	1.7	0.37	0.36
	4	5.5	5.2	3.8	1.3	1.3	1.1	0.70	0.57
A12	2	5.4	5.6	5.2	3.2	2.9	2.5	0.26	0.39
	3	5.4	5.4	4.6	2.6	2.3	1.6	0.43	0.49
	4	5.5	5.3	3.3	2.2	1.6	1.3	0.62	0.60
A13	2	5.4	5.4	5.1	3.9	2.7	2.3	0.24	0.39
	3	5.4	5.3	4.5	2.3	1.8	1.7	0.46	0.48
	4	5.4	5.5	3.1	1.8	1.6	1.3	0.76	0.83
A14	2	5.4	5.5	4.9	3.4	3.1	2.8	0.18	0.59
	3	5.4	5.2	4.3	2.5	2.1	1.9	0.46	0.72
	4	5.5	5.4	3.3	2.0	1.7	1.7	0.68	0.92
A15	2	5.4	5.5	5.4	4.5	3.9	3.0	0.10	0.36
	3	5.3	5.3	4.5	3.3	2.5	2.3	0.30	0.61
	4	5.5	5.2	3.2	2.2	2.0	1.8	0.57	0.76

Run no.	Tank no.	Turbidity (FTU) at sample depth 30 cm after sedimentation time (min) 0	10	20	40	60	120	VM m/h	SIGMA m/h
A16	2	5.4	5.4	5.3	4.8	4.2	3.5	-0.06	0.48
	3	5.4	5.2	4.2	3.5	2.9	2.4	0.22	0.87
	4	5.5	5.1	3.3	2.8	2.3	1.9	0.50	1.0
A21	2	5.4	5.3	4.5	3.3	2.7	2.2	0.30	0.64
	3	5.4	5.2	4.2	1.7	2.0	1.5	0.48	0.56
	4	5.5	4.8	2.7	1.3	1.2	1.2	0.89	0.79
A22	2	5.7	5.7	5.1	3.0	2.6	2.2	0.34	0.47
	3	5.6	5.2	3.7	1.9	1.8	1.7	0.67	0.81
	4	5.8	4.4	2.1	1.5	1.4	1.2	1.1	1.1
A23	2	5.6	5.5	4.5	2.8	2.5	2.2	0.36	0.62
	3	5.5	4.8	3.3	2.1	1.9	1.8	0.68	0.98
	4	5.4	5.1	2.4	1.8	1.7	1.5	1.2	1.7
A24	2	5.4	5.2	4.1	2.9	2.8	2.4	0.28	0.85
	3	5.3	4.7	2.9	2.2	1.9	1.9	0.64	0.99
	4	5.2	4.0	2.2	1.8	1.7	1.5	1.0	1.3
A25	2	5.2	5.2	4.6	3.5	3.4	3.0	0.05	0.76
	3	5.2	4.8	3.4	2.8	2.4	2.3	0.41	1.1
	4	5.5	4.1	2.4	2.2	1.9	1.8	0.83	1.4
A26	2	5.3	5.4	5.0	4.2	3.8	3.5	-0.07	0.63
	3	5.4	4.8	3.4	2.8	2.9	2.4	0.33	1.1
	4	5.4	3.8	3.0	2.3	2.2	2.0	0.70	1.6

APPENDIX 7

RESULTS FROM PILOT PLANT EXPERIMENTS
DATE: 14/2 1977 to 17/2 1977

FLOCCULATION CONDITIONS

Run no.	C11	C12	C13	C14	C15	C16	C21	C22	C23	C24	C25	C26
Total flocculation time (min)	20	20	20	20	20	20	20	20	20	20	20	20
Power input I (see eq. 4-1)	1	2	3	4	5	6	1	2	3	4	5	6
2 ppm activated silica	-	-	-	-	-	-	X	X	X	X	X	X

Coagulant dose: 40 mg Al-sulphate/l
Coagulation pH: 6.5
Paddle type: C (see fig. 3.32)
Uniform compartmentalization

SOME CHARACTERISTIC RAW WATER ANALYSES
Temperature: 1.5 ^{o}C
Turbidity: 2.9-3.1 FTU
Alkalinity: 12 mg HCO_3^-
Permanganate number: 33 mg $KMnO_4$/l
Colour: 33 mg Pt/l
pH: 6.6-6.8
Conductivity: 14.8 mS/m

RESULTS FROM SETTLING TESTS

Run no.	Tank no.	Turbidity (FTU) at sample depth 30 cm after sedimentation time (min) 0	10	20	40	60	120	VM m/h	SIGMA m/h
C11	2	5.3	5.2	4.9	4.7	3.4	2.5	0.18	0.23
	3	5.2	5.2	4.8	2.8	1.8	1.4	0.41	0.37
	4	5.2	5.1	3.9	1.7	1.6	1.2	0.61	0.58
C12	2	5.4	5.7	5.5	3.8	3.0	2.5	0.20	0.47
	3	5.3	5.3	4.7	2.6	2.1	1.9	0.40	0.46
	4	5.4	5.4	3.4	1.8	1.5	1.4	0.70	0.74
C13	2	5.6	5.7	5.5	3.6	3.3	2.4	0.20	0.53
	3	5.4	-	-	-	2.3	1.8	-	-
	4	5.4	5.2	2.5	1.8	1.7	1.4	1.1	1.4
C14	2	5.3	5.3	5.0	3.3	2.9	2.4	0.25	0.44
	3	5.3	5.0	4.2	2.9	2.2	1.8	0.41	0.61
	4	5.4	5.2	2.9	2.0	1.8	1.7	0.82	1.2
C15	2	5.9	5.8	5.4	4.2	3.6	3.2	0.12	0.52
	3	5.7	5.7	4.0	3.0	2.6	2.2	0.42	0.71
	4	5.8	5.2	3.1	2.2	2.1	1.8	0.69	0.93

Run no.	Tank no.	Turbidity (FTU) at sample depth 30 cm after sedimentation time (min) 0	10	20	40	60	120	VM m/h	SIGMA m/h
C16	2	5.5	5.6	5.4	4.8	3.9	3.2	0.05	0.43
	3	5.4	5.5	3.9	3.0	3.8	2.3	0.35	1.0
	4	5.8	5.2	3.2	2.7	2.2	1.9	0.62	1.3
C21	2	5.3	5.2	4.7	3.6	2.4	1.9	0.32	0.47
	3	5.2	5.2	3.7	2.0	1.4	1.4	0.61	0.59
	4	5.4	4.5	1.6	1.3	1.1	1.1	1.1	0.88
C22	2	5.3	5.5	4.7	2.7	2.3	2.0	0.41	0.50
	3	5.3	5.3	3.3	1.8	1.6	1.5	0.63	0.61
	4	5.5	4.3	1.7	1.3	1.3	1.3	1.1	1.0
C23	2	5.3	5.6	4.3	2.8	2.5	2.3	0.33	0.68
	3	5.3	5.2	3.2	2.1	1.9	1.7	0.67	1.0
	4	5.4	4.3	1.9	1.7	1.6	1.5	0.98	1.2
C24	2	5.3	5.3	3.3	2.9	2.7	2.5	0.27	-
	3	5.1	5.1	3.1	2.1	2.1	2.1	0.55	-
	4	5.6	3.7	2.0	1.7	1.7	1.6	1.1	1.4
C25	2	5.3	5.5	4.8	3.3	2.8	2.7	0.20	0.55
	3	5.1	4.8	3.0	2.4	2.2	2.2	0.52	1.1
	4	5.5	3.9	2.3	1.9	1.8	1.8	0.94	1.5
C26	2	5.7	5.9	5.6	4.6	4.1	3.5	0.0	0.46
	3	5.4	5.7	3.9	3.1	2.8	2.6	0.27	1.2
	4	5.5	4.4	3.0	2.4	2.3	2.1	0.66	1.4

APPENDIX 8

RESULTS FROM PILOT PLANT EXPERIMENTS
DATE: 21/2 1977 to 24/2 1977

FLOCCULATION CONDITIONS

Run no.	B11	B12	B13	B14	B15	B16	B21	B22	B23	B24	B25	B26
Total flocculation time (min)	20	20	20	20	20	20	20	20	20	20	20	20
Power input I (see eq. 4-1)	1	2	3	4	5	6	1	2	3	4	5	6
2 ppm activated silica	-	-	-	-	-	-	X	X	X	X	X	X

Coagulant dose: 40 mg Al-sulphate/l
Coagulation pH: 6.5
Paddle type: B (see fig. 3.32)
Uniform compartmentalization

SOME CHARACTERISTIC RAW WATER ANALYSES
Temperature: 1.5 ^{o}C
Turbidity: 2.6-2.7 FTU
Alkalinity: 12 mg HCO_3^-
Permanganate number: 33 mg $KMnO_4$/l
Colour: 34 mg Pt/l
pH: 6.6
Conductivity: 14.8 mS/m

RESULTS FROM SETTLING TESTS

Run no.	Tank no.	Turbidity (FTU) at sample depth 30 cm after sedimentation time (min) 0	10	20	40	60	120	VM m/h	SIGMA m/h
B11	2	5.2	5.3	5.0	3.2	2.6	2.1	0.29	0.37
	3	5.2	5.2	4.9	2.8	2.0	1.5	0.42	0.42
	4	5.3	5.4	4.2	1.7	1.4	1.2	0.56	0.44
B12	2	5.1	5.1	4.7	3.2	2.5	2.0	0.30	0.44
	3	5.1	5.5	4.6	2.9	2.2	1.6	0.38	0.43
	4	5.2	4.9	3.2	1.8	1.5	1.2	0.67	0.67
B13	2	5.3	5.2	5.0	3.1	2.5	2.2	0.30	0.38
	3	5.2	5.0	4.2	2.7	1.9	1.7	0.45	0.55
	4	5.3	5.2	3.4	1.9	1.8	1.4	0.64	0.73
B14	2	5.0	5.0	5.1	3.1	3.0	2.6	0.20	0.31
	3	4.9	4.9	4.2	2.5	2.1	1.7	0.40	0.65
	4	5.0	5.1	3.2	1.9	1.7	1.4	0.64	0.80
B15	2	5.1	5.2	5.1	3.6	3.3	2.8	0.07	0.67
	3	4.9	5.1	4.3	2.5	2.5	2.2	0.33	0.63
	4	5.3	5.2	3.2	2.0	1.9	1.6	0.63	0.91